

Carol A. Wise · Jonathan J. Rios *Editors*

# Molecular Genetics of Pediatric Orthopaedic Disorders

 Springer

# **Molecular Genetics of Pediatric Orthopaedic Disorders**

Carol A. Wise • Jonathan J. Rios  
Editors

# Molecular Genetics of Pediatric Orthopaedic Disorders

 Springer

*Editors*

Carol A. Wise  
Sarah M. and Charles E. Seay Center for  
Musculoskeletal Research  
Texas Scottish Rite Hospital for Children  
Dallas  
Texas  
USA

Jonathan J. Rios  
Sarah M. and Charles E. Seay Center for  
Musculoskeletal Research  
Texas Scottish Rite Hospital for Children  
Dallas  
Texas  
USA

ISBN 978-1-4939-2168-3

ISBN 978-1-4939-2169-0 (eBook)

DOI 10.1007/978-1-4939-2169-0

Library of Congress Control Number: 2015930329

Springer New York Heidelberg Dordrecht London  
© Springer Science+Business Media New York 2015

This work is subject to copyright. All rights are reserved by the Publisher, whether the whole or part of the material is concerned, specifically the rights of translation, reprinting, reuse of illustrations, recitation, broadcasting, reproduction on microfilms or in any other physical way, and transmission or information storage and retrieval, electronic adaptation, computer software, or by similar or dissimilar methodology now known or hereafter developed.

The use of general descriptive names, registered names, trademarks, service marks, etc. in this publication does not imply, even in the absence of a specific statement, that such names are exempt from the relevant protective laws and regulations and therefore free for general use.

The publisher, the authors and the editors are safe to assume that the advice and information in this book are believed to be true and accurate at the date of publication. Neither the publisher nor the authors or the editors give a warranty, express or implied, with respect to the material contained herein or for any errors or omissions that may have been made.

Printed on acid-free paper

Springer is part of Springer Science+Business Media ([www.springer.com](http://www.springer.com))

*The editors thank the patients and families with pediatric orthopaedic disorders who have participated in research studies and furthered our understanding of their conditions.*

# Preface

Pediatric orthopaedic practice typically centers around a diverse array of heritable disorders. At one extreme end of the heritability spectrum are completely penetrant Mendelian disorders such as brachydactyly, where unaffected parents never have affected offspring. Described by Farabee in 1905, brachydactyly was the first published description of autosomal dominant inheritance of a human malformation (1). Even earlier, however, Galton described the concept of traits such as height that, although often lacking a clear transmission pattern in families, are still heritable to some degree (2). We of course now appreciate that there are significant genetic underpinnings in many non-traumatic childhood orthopaedic disorders, such as idiopathic scoliosis and talipes equinovarus (clubfoot), and that the care of such complex diseases typically represents the majority of pediatric orthopaedic practice. Finally, at the other extreme of the heritability spectrum is the startling discovery that completely non-heritable malformations such as macrodactyly, paradoxically, have genetic origins. Disease gene discovery for these disorders began, for all practical purposes, in the late 1980's and has since moved ahead with dizzying speed, driven in large part by technological advances. Such discoveries are enabling a new biochemical understanding of disease processes and, more importantly, informing the design of new treatments, as for example therapies that target the signaling pathways causing the troubling manifestations in neurofibromatosis (3).

The purpose of this volume is to update the pediatric orthopaedic community—clinicians, surgeons, geneticists, and researchers—on recent genetic developments relevant to the diverse presentations in these patients. We begin with an introduction to “next-generation” technologies that are enabling rapid gene discovery. We also present chapters describing post-gene discovery advancements for neurofibromatosis, various disorders of the joints, and basic bone development. Almost half of the volume is devoted to the complex disorders scoliosis and clubfoot and describes their classification, genetic contributions, and the exciting breakthrough in understanding genetic and environmental interactions. Finally we present the very recent discoveries of the mutations causing somatic, non-heritable, and all too devastating overgrowth malformations.

New insights into each of these areas are no doubt waiting in the wings, given the pace of discovery today. Our goal in this volume is to provide pediatric clinicians,

surgeons, geneticists, and researchers with a resource for understanding these emerging new developments as a means to advance the care of affected children.

## References

1. Farabee. Inheritance of digital malformations in man. Papers of the peabody museum for American archeology and ethnology. (Harvard University) 1905;3:69.
2. Galton F. Hereditary talent and character. Macmillan's Mag. 1865;12:157.
3. Kalamarides MI, Acosta MT, Babovic-Vuksanovic D, Carpen O, Cichowski K, Evans DG, Giancotti F, Hanemann CO, Ingram D, Lloyd AC, Mayes DA, Messiaen L, Morrison H, North K, Packer R, Pan D, Stemmer-Rachamimov A, Upadhyaya M, Viskochil D, Wallace MR, Hunter-Schaedle K, Ratner N. Neurofibromatosis 2011: a report of the children's tumor foundation annual meeting. *Acta Neuropathol.* 2012;123(3):369–80.

# Contents

<b>1 Overview of Next Generation, High-Throughput Molecular Genetic Methods.....</b>	<b>1</b>
Jonathan J. Rios	
<b>2 Neurofibromin in Skeletal Development.....</b>	<b>17</b>
Mateusz Kolanczyk and David A. Stevenson	
<b>3 Molecular Genetics of Congenital Multiple Large Joint Dislocation....</b>	<b>39</b>
Stephen P. Robertson	
<b>4 DMP-1 in Postnatal Bone Development.....</b>	<b>57</b>
Shuxian Lin and Jerry Jian Q. Feng	
<b>5 The Genetic Architecture of Idiopathic Scoliosis.....</b>	<b>71</b>
Carol A. Wise	
<b>6 Insights into the Genetics of Clubfoot.....</b>	<b>91</b>
Katelyn S. Weymouth, Susan H. Blanton and Jacqueline T. Hecht	
<b>7 Classification and Etiologic Dissection of Vertebral Segmentation Anomalies .....</b>	<b>105</b>
Peter D. Turnpenny	
<b>8 Genetic and Environmental Interaction in Malformation of the Vertebral Column.....</b>	<b>131</b>
Sally L. Dunwoodie and Duncan B. Sparrow	
<b>9 Somatic Mutations in Overgrowth Syndromes.....</b>	<b>153</b>
Jonathan J. Rios and Marybeth Ezaki	
<b>Index.....</b>	<b>167</b>

# Contributors

**Susan H. Blanton** Department of Human Genetics, University of Miami, Miami, FL, USA

**Sally L. Dunwoodie** Developmental and Stem Cell Biology, Victor Chang Cardiac Research Institute, Sydney, NSW, Australia

**Marybeth Ezaki** Department of Orthopaedics, Texas Scottish Rite Hospital for Children, Dallas, TX, USA

**Jerry Jian Q. Feng** Biomedical Sciences, Baylor College of Dentistry, Dallas, TX, USA

**Jacqueline T. Hecht** Department of Pediatrics, University of Texas Health Science Center—Medical School and School of Dentistry, Houston, TX, USA

**Mateusz Kolanczyk** Campus Virchow Institut für Medizinische Genetik und Humangenetik, Neurofibromin in Skeletal Development, Charité Universitätsmedizin, Berlin, Germany

**Shuxian Lin** Biomedical Sciences, Baylor College of Dentistry, Dallas, TX, USA

**Jonathan J. Rios** Sarah M. and Charles E. Seay Center for Musculoskeletal Research, Texas Scottish Rite Hospital for Children, Dallas, TX, USA

**Stephen P. Robertson** Department of Women’s and Children’s Health, Dunedin School of Medicine, University of Otago, Dunedin, New Zealand

**Duncan B. Sparrow** Developmental and Stem Cell Biology, Victor Chang Cardiac Research Institute, Sydney, NSW, Australia

**David A. Stevenson** Department of Pediatrics, Division of Medical Genetics, University of Utah, Salt Lake City, UT, USA

**Peter D. Turnpenny** Clinical Genetics, Royal Devon & Exeter Hospital, Exeter, UK

**Katelyn S. Weymouth** Department of Pediatrics, University of Texas Medical School, Houston, TX, USA

**Carol A. Wise** Sarah M. and Charles E. Seay Center for Musculoskeletal Research, Texas Scottish Rite Hospital for Children, Dallas, TX, USA

Departments of Orthopaedic Surgery, Pediatrics, and McDermott Center for Human Growth and Development, University of Texas Southwestern Medical Center, Dallas, TX, USA

# Chapter 1

## Overview of Next Generation, High-Throughput Molecular Genetic Methods

Jonathan J. Rios

**Abstract** Recent advances in genome-wide technologies have revolutionized how researchers identify disease-causing genes. Both microarray-based genotyping analysis for copy number variations and high-throughput next-generation sequencing (NGS) for sequence variations have enabled a surge in the discovery of genes associated with disease. Application of these technologies in large population studies has shown the extent of sequence and copy-number variations throughout the genome and their contributions to human quantitative traits and diseases. This chapter will highlight both technologies and will provide examples of how each has been used to identify genes causing pediatric orthopaedic disorders.

**Keywords** Exome · Next-generation sequencing · Microarray · Genotyping · Copy number variation

### Introduction

*Genomics* is a term generally used to describe methods of studying genomes, or the genetic makeup of an organism. The evolution of genome studies has largely been driven by technology advancements, including whole-genome microarray-based genotyping and high-throughput massively parallel next-generation sequencing. Whole-genome microarrays are typically used in two ways. The first is for genotyping single nucleotide polymorphisms (SNPs) for genome-wide association studies (GWAS). GWAS have identified a number of genetic associations with orthopaedic diseases, a subject that will not be covered in this chapter. For more information the reader is pointed to a recent review detailing GWAS for orthopaedic diseases [1]. The second application of microarray-based genotyping is the detection of copy number variation (CNV) and regions of homozygosity (ROH). CNVs are gains and losses of genetic material (genes) resulting in either too few (deletion) or too many

---

J. J. Rios (✉)

Sarah M. and Charles E. Seay Center for Musculoskeletal Research,  
Texas Scottish Rite Hospital for Children,  
2222 Welborn Street, Dallas, TX 75219, USA  
e-mail: Jonathan.Rios@tsrh.org

© Springer Science+Business Media New York 2015

C. A. Wise, J. J. Rios (eds.), *Molecular Genetics of Pediatric Orthopaedic Disorders*,  
DOI 10.1007/978-1-4939-2169-0\_1

(amplification) copies of the gene. CNVs impact a greater proportion of the genome than do sequence mutations, and advances in microarray technologies are improving the resolution of CNV detection. Regions of homozygosity describe chromosomal segments that lack expected polymorphic variation and that may consequently harbor recessive disease mutations as described in this chapter.

More recently, methods for whole-genome sequencing are driving the discovery of new genes associated with human conditions, including orthopaedic disorders. The first completed genome sequences were of bacteria, fungus (yeast), invertebrate species (worm and fly) and a plant [2]. In 2001, the initial draft of the human genome was reported [3, 4] and subsequently improved upon to provide the first human genome reference sequence [5]. However it was the introduction of so-called massively parallel, next-generation sequencing (NGS) technologies that improved the potential and scope of genomic research. The genome of Dr. James Watson, co-discoverer of the structure of DNA, was the first to be sequenced using high-throughput NGS [6]. The cost at that time (2008) to sequence one genome was ~US\$ 1 million, compared to genome sequencing using traditional Sanger sequencing (~US\$ 100 million), and it was completed in a fraction of the time. Since 2008, whole-exome sequencing (WES) has become a popular alternative to sequencing the entire genome. The *exome* refers to the ~1% of the genome that corresponds to protein-coding genes. As described in this chapter, WES has been an exceptionally successful strategy for identifying new genes causing human disorders.

Microarray-based genotyping and NGS techniques have the potential to revolutionize our understanding of the biological causes of orthopaedic disease. Ultimately, these genomic technologies will impact patient care by improving genetic diagnoses and pioneering new research initiatives toward alternative treatment paradigms. In this chapter, we will discuss each research method and how it has been applied to studies of orthopaedic conditions.

## Microarray-Based Genotyping and Analysis

The normal human karyotype (male, 46XY; female 46XX) consists of two copies of each autosome (chromosome 1–22) and two sex-chromosomes; 2 copies of the X chromosome in females and one copy each of the X and Y chromosomes in males. Differences in genomic content can include entire chromosomes (monosomy, trisomy, aneuploidy) or submicroscopic regions (1 kilobase to several megabases). Early genome-wide CNV analyses of normal individuals showed copy number gains (amplifications) and losses (deletions) can affect ~12% of the human genome, ranging from 9–19% of individual chromosomes, and impact ~14% of known disease-causing genes annotated in the NCBI Online Mendelian Inheritance in Man (OMIM) database [7]. The role of common and rare CNVs in human disease, particularly neurodevelopmental disorders, has been reviewed elsewhere [8].

As noted, SNPs are single base mutations that occur throughout the genome. Each genome contains millions of SNPs that serve as useful markers across the

genome (Fig. 1.1a). A single microarray makes two independent measurements simultaneously at millions of SNP positions. The first is the SNP genotype, that is, whether an individual is homozygous or heterozygous for each SNP, as shown by the fluorescent color. The second measurement is the fluorescent intensity of the signal. As described below, signal intensity and genotype are used to identify CNVs and ROH, respectively.

## ***Copy Number Variation***

CNV microarrays contain millions of probes that use fluorescent detection methods to determine the patient's genotype at millions of SNPs throughout the genome (Fig. 1.1a). Briefly, DNA is hybridized to the microarray and the genotype of each SNP is detected using fluorescent probes. The signal intensity correlates with the amount of DNA present in the sample. Therefore, regions of the genome with lower than expected signal intensities are designated as deletions and regions with higher than expected signal intensities are designated as amplifications. Individual probe data can be visualized using log-ratio plots. Each SNP probe marker is plotted along the chromosome to show the log-scaled ratio ( $\log R$ ) of the patient's probe intensity compared to the expected intensity (Fig. 1.1b). For a normal copy number ( $N=2$ ), the  $\log R$  is equal to 0. The  $\log R$  ratio increases and decreases in the presence of amplifications and deletions, respectively. Multiple computational programs are available to identify CNVs from the individual probe-level data, and CNVs may be plotted alongside the human ideogram (Fig. 1.1c).

## ***CNVs Associated with Orthopaedic Disorders***

Charcot-Marie-Tooth (CMT) 1 is a class of hereditary demyelinating neuropathies characterized by decreases in nerve conduction with secondary foot and ankle difficulties caused by muscle weakness, hip dysplasia and spinal deformities, including scoliosis, kyphoscoliosis and thoracic kyphosis [9]. CMT type 1A, often seen in orthopaedic clinics, was one of the first diseases associated with a submicroscopic duplication [10, 11]. Specifically, a 1.5 Megabase (Mb) duplication of chromosome 17p11.2 harboring the *PMP22* gene is the primary cause of CMT1 and was reported in majority of CMT1 patients [12]. It is worth noting that the discovery of the CMT1A duplication inspired a new term, "genomic disorder", to describe genetic diseases arising not from simple sequence changes but from complex rearrangements of the genome [13]. Today, molecular genetic clinical testing for the 17p11.2 duplication is widely available and provides a definitive diagnosis of CMT1A.

Recently, a genome-wide CNV study in individuals with idiopathic clubfoot identified a microduplication of the *TBX4* gene in multiple cases [14], and together with copy number variation of the *PITX1* gene [15], these CNVs implicate the intricate processes of hindlimb development in idiopathic clubfoot [16]. The

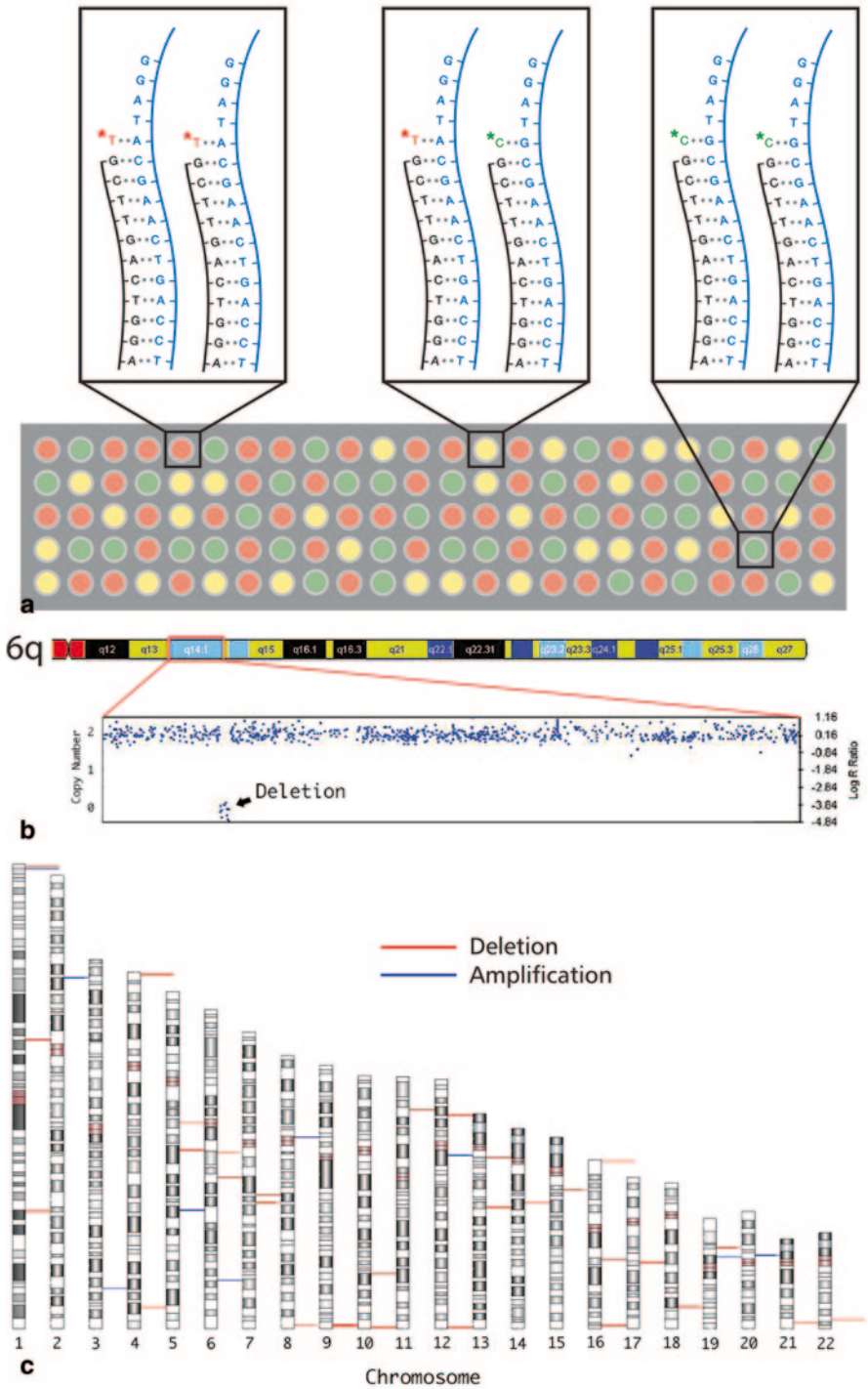


**Fig. 1.1** Microarray SNP genotyping and copy number analysis. **a** Individual SNP genotypes are determined by the fluorescent color emitted when allele-specific probes (shown in black) are hybridized to the sample DNA (shown in blue). Each allele is assigned a color (red or green). Homozygous

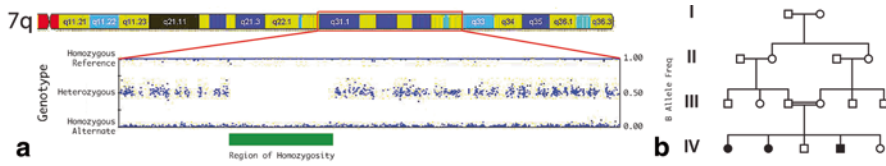


**Fig. 1.2** Regions of homozygosity in consanguineous families. **a** Microarray SNP genotypes are plotted along the chromosome using the B-allele frequency. The B-allele frequency is the measured intensity of the “B” allele divided by the total signal intensity of the SNP (either homozygous AA & BB or heterozygous AB). Homozygous SNP B-allele frequencies are near 0 and 1, and heterozygous SNPs are near 0.5. When plotted along the chromosome, large regions of homozygosity can be easily identified (shown by *green bar*). **b** Regions of homozygosity occur frequently in consanguineous families and result in a higher occurrence of rare recessive disorders. Children from a first-cousin mating may present with increased incidence of a disorder (*filled symbols*) than would be expected by chance.

developmental processes leading to proper bone formation, including proper morphology of supporting structures (muscles, tendons), involve complex regulatory mechanisms with precise spatio-temporal expression of a multitude of genes. The effect of CNVs on gene expression has been well documented [17]. Therefore, it is plausible that CNVs play a substantial role in conditions commonly ascertained in orthopaedic clinics.

## Homozygosity Mapping

SNP genotypes from microarray experiments can also be analyzed to identify regions of homozygosity (ROH), that is, parts of the genome that are devoid of typical genetic variation (Fig. 1.2a). ROH regions result when both copies of the chromosome are identical and every SNP in the region is homozygous. Rarely does the human genome contain long stretches of homozygosity; ROH up to ~3 Mb in length occur naturally in the general population [18]. The primary cause of extended ROH (>3 Mb) in a patient is consanguinity; generational inbreeding decreases the amount of total variation in a person’s genome and increases the amount of homozygosity in the genome (Fig. 1.2b). Because consanguineous parents share a common ancestor, regions of their genome are the same. Therefore, those same regions will be identical in their children. All SNPs in those regions will be homozygous; thus, as the parents are more closely related (or as generational inbreeding continues), ROH regions expand further across the genome. The lack of genetic variation within a consanguineous family or population leads to a higher occurrence of rare recessive disease. Therefore, disease-gene mapping in consanguineous families focuses on

genotypes fluoresce the color of the respective allele, while heterozygous genotypes fluoresce *yellow*. Millions of SNPs can be genotyped simultaneously on a single microarray. **b** Copy number is determined from the intensity of the fluorescent probes. Signal intensity is plotted as the logR ratio, which is the log-scale of the sample’s intensity divided by the expected signal intensity. Higher logR denotes copy number gains or amplifications, while drops in logR signal deletions (shown). **c** Copy number variations can be summarized and plotted for all chromosomes with the chromosome ideogram.

identifying large ROH regions, and, probabilistically, disease-causing homozygous mutations frequently occur in the largest ROH region. Homozygosity mapping is a powerful method for identifying disease genes in consanguineous families/populations and is easily detected using commercial SNP microarrays.

### ***Homozygosity Mapping in Orthopaedic Disorders***

The gene causing autosomal recessive Horizontal Gaze Palsy with Progressive Scoliosis (HGPPS) was identified using homozygosity mapping in consanguineous families. Homozygosity mapping in two consanguineous families initially narrowed the disease locus to chromosome 11q23–25, as it was the only region homozygous in all affected individuals in both families and not homozygous in the unaffected family members [19]. Subsequently, ten HGPPS consanguineous families with homozygosity at the chromosome 11q23–25 region were studied to refine the candidate gene region and identify the disease-causing gene [20]. Sequence analysis identified rare homozygous mutations in the *ROBO3* gene in all families. All homozygous mutations identified in affected family members were not present in control subjects; therefore, the likelihood of these mutations being homozygous in the general population is very low. This study of HGPPS families highlights the power of homozygosity mapping in consanguineous families with rare recessive disease.

In another example, ROH mapping in consanguineous families was used to identify homozygous mutations causing CMT type 4C (CMT4C) [21]. This study identified a region on chromosome 5 that was homozygous in affected individuals from two consanguineous Turkish families. A candidate region was identified as homozygous only in affected individuals and heterozygous in the unaffected siblings, and mutation analysis identified seven different homozygous mutations in the *SH3TC2* gene in nine consanguineous families with CMT4C.

Recessive diseases require mutations in both copies (alleles) of the gene. Thus, mutations are inherited from *both* unaffected parents, and because consanguineous parents share a common ancestor, both parents share the same disease-causing mutation. Recessive diseases are generally caused by sequence variants that render the encoded protein non-functional, so called “loss-of-function” variants. Loss-of-function changes may be frameshift, nonsense, or splice-site mutations that change the amino acid sequence of the protein (frameshift), prematurely truncate the protein (nonsense) or cause entire regions of the protein to be removed (splice-site) (Fig. 1.3). Notably, because of their highly deleterious effects, these mutations occur less frequently in the genome compared to other types of mutations (e.g. synonymous mutations that do not change the protein sequence or missense mutations that change only a single amino acid), have a lower population frequency (are rare) and are more frequently associated with disease [22]. In the CMT4C study for example, five of the seven (71 %) mutations were either frameshift mutations or splice-site mutations [21]. Other mutations were missense mutations that changed single amino acids in the protein, but the consequences of these mutations on protein function were not immediately obvious.

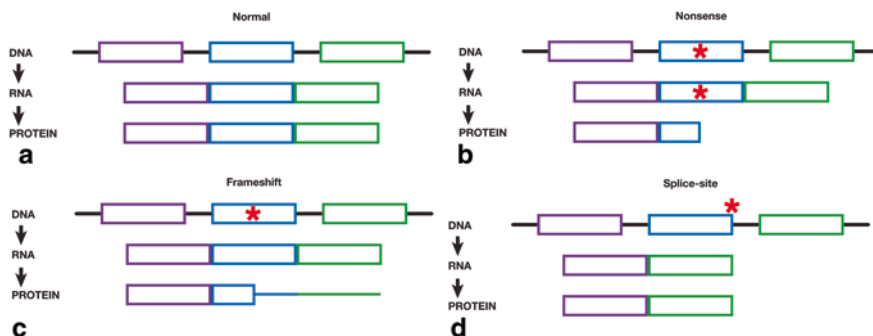


**Fig. 1.3** Schematic diagram showing the effect of mutations on RNA splicing and changes to the resultant protein. **a** DNA consists of exons (colored sections) and introns (*black bars*). Exons are transcribed into RNA and the introns are excluded. Finally, each exon is translated into the final protein, with each exon corresponding to a specific region of the protein. The full protein is represented by all exons being transcribed and translated fully (represented by boxes). **b** Nonsense mutations (*red star*) result in a truncated protein. All exons are fully transcribed; however, translation is prematurely halted and the protein is shortened. All protein sequence after the mutation is lost. **c** Frameshift mutations (*red star*) affect the translation of the protein. All protein sequence prior to the mutation is normal (shown as boxes); however, the sequence after the frameshift mutation is different and results in a protein with different sequence and length (shown by *colored bars*). **d** Splice mutations (*red star*) occur at the beginning or end of introns and results in entire exons being skipped during transcription. When an exon is skipped during transcription, the same exon is not translated into the protein. Thus, the entire region of the protein is lost.

## Next-Generation Sequencing

Next-generation sequencing, or NGS, has revolutionized genomics research by providing a lower-cost and faster alternative to traditional sequencing methods, enabling high-throughput whole-genome and whole-exome sequencing. Because of this new and efficient technology, the 1000 Genomes (1000G) Project set out to catalogue normal sequence variation with at least a 1% frequency in many worldwide populations [23]. The resulting 1000G database (<http://browser.1000genomes.org/index.html>) is an important resource for the genetics community, as it provides the ability to distinguish common benign variation from potentially disease-causing variants. Thus, coupling NGS and public resources like 1000G provides researchers with new opportunities for discovering genes associated with human disease. Beyond research applications, clinical opportunities for NGS are under investigation, as described later in this chapter [24].

## Whole-Exome Sequencing

The *exome* is defined as the protein-coding regions of the genome. The exome corresponds to exons, the parts of genes that encode for RNA and/or protein, and

represents about 1–2% of the entire genome. Whole-exome sequencing (WES) utilizes NGS technology and is an attractive alternative to whole-genome sequencing (WGS); therefore, it is a widely used method to identify genetic causes of rare disease [25]. The goal of WES is to identify disease-causing variants that change the protein sequence (also called nonsynonymous variants) or that alter the function of a RNA molecule. The first WES study to identify new disease-causing variants identified nonsynonymous mutations in the *MYH3* gene in four individuals with dominant Freeman-Sheldon syndrome (FSS), also called distal arthrogryposis type 2A [26]. As detailed below, this study established proof of concept for the power of WES to discover disease-causing variants with relatively few study subjects. This rare-variant analysis strategy has since been used repeatedly to identify pathogenic mutations for many rare human disorders [25, 27]. For a detailed discussion of WES analysis and application to orthopaedic conditions, the readers are directed to a recently published review [28].

### ***Rare Variant Exome Analysis***

In the era preceding WES, disease gene discovery depended on access to extended families with multiple affected individuals, suitable for inheritance mapping. However, because WES examines virtually every gene simultaneously, it has the potential to identify disease-causing genes without the need for large family studies. In this way, WES may identify a single disease-associated gene by studying multiple unrelated individuals with the same rare phenotype. This type of analysis seeks to identify a single, or at least only a small number, of candidate genes (of the ~20,000 in the genome) with rare or novel mutations shared among all affected individuals. Rare mutations are typically defined as those mutations that occur in <1% of the general population, as determined from the 1000G database. Novel mutations are those that are not identified in the 1000G database (or other databases) nor in other control individuals. As a group, rare and novel nonsynonymous mutations occur at evolutionarily conserved amino acids in the protein and, therefore, may be deleterious and alter the protein's function. Thus, they are more frequently associated with human disease [22, 29]. As well, a rare-variant analysis assumes that the same gene is causing the disease in all affected individuals, although the mutation does not need to be identical. Therefore, because the same gene is expected to harbor a rare or novel variant in all affected individuals, the number of candidate genes will decrease as more cases are sequenced. In the proof of concept study by *Bamshad et al.*, four unrelated cases with dominant FSS as well as 8 unrelated control samples were sequenced [25]. Combining WES results from all four cases identified a single gene, *MYH3*, with novel deleterious disease-causing mutations that were absent in controls [26]. In a separate study, rare-variant analysis was applied to WES of four cases with recessive Miller syndrome from three families (two of the cases were siblings). Candidate genes were identified using a recessive model that required two novel mutations. Ultimately, this study identified a single gene, *DHODH*, with novel recessive mutations in all affected individuals [30].

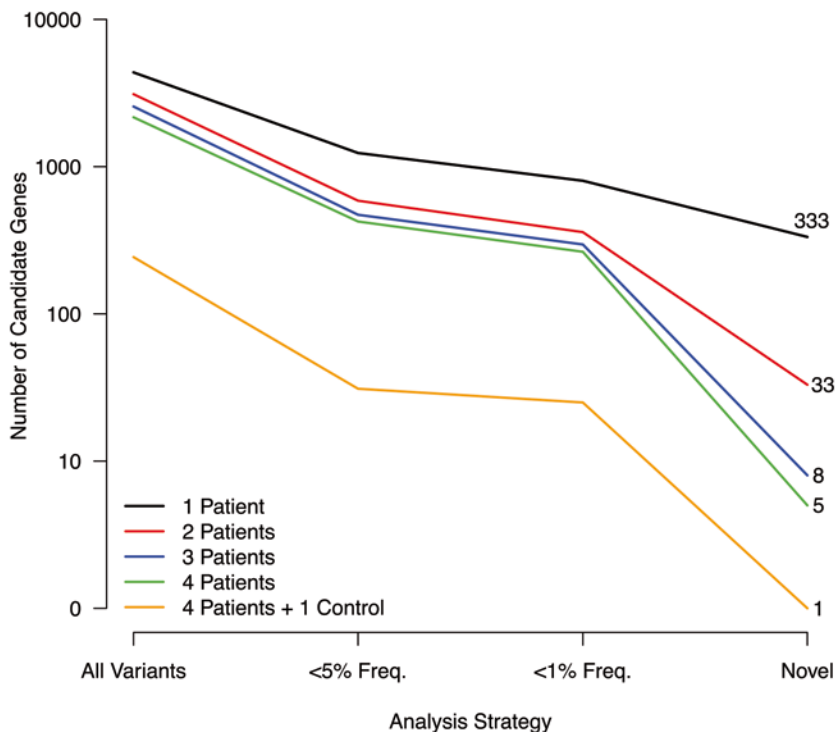


**Fig. 1.4** Number of candidate genes by analysis and number of patients. The number of candidate genes from whole-exome sequencing are shown for different numbers of patients. As the number of patients increases, the number of mutations shared by all patients decreases (*Y-axis*). As well, the number of candidate genes decreases as the analysis strategy includes only rare or novel mutations (*X-axis*). Thus, studies of rare disorders in which multiple patients are sequenced may identify a small number of candidate genes.

These early successes suggested that WES in small cohorts might be sufficient to identify rare or novel nonsynonymous disease-causing mutations. This is critically important for studies of rare orthopaedic disorders, where large numbers of unrelated affected cases are difficult to ascertain. The number of unrelated cases needed to identify a small number of candidate genes is determined, in part, by the frequency of the disease. If the disease is very rare, it is unlikely to be caused by common mutations; therefore, it may be appropriate to apply a WES analysis that considers only novel mutations. If the disease is modestly rare or uncommon, WES analysis may consider a frequency cutoff that only considers novel mutations and mutations with a <1% population frequency. The relationship between the number of resulting candidate genes, analysis strategy and number of cases is shown in Fig. 1.4. For very rare disorders in which only novel variants are considered, sequencing more than one affected individual has a dramatic effect on the number of candidate genes (333 versus 33), and sequencing even more cases further decreases the number of candidate genes, although to a lesser degree (33 versus 5).

The power to identify a small number of candidate genes is greater for recessive compared to dominant disorders because a recessive disorder requires mutations in both copies of the gene. Multiple independent mutations in the same gene occurs much less frequently in the population, and accordingly WES of fewer cases will provide sufficient power to detect fewer candidate genes. This concept was demonstrated using WGS in a single patient with recessive disease [31]. Of >600 genes with novel nonsynonymous mutations, only 42 (~7%) genes had multiple mutations, and only one of the 42 genes had two loss-of-function (nonsense) mutations. This study presumably would have identified the same mutations with WES and demonstrates the power of these technologies to identify recessive disease-causing genes from a small number (or even a single) of affected individuals.

### ***Family-Based Exome Analysis***

Analysis of WES in families is an alternative strategy to sequencing unrelated cases. For families with multiple affected relatives, this analysis method provides multiple advantages compared to the rare-variant approach. First, the possibility of genetic heterogeneity (disease caused by different genes in different individuals) is removed. In the presence of high genetic heterogeneity, the rare-variant analysis strategy has limited power to identify the disease-causing gene(s) in unrelated individuals, as was recently demonstrated in a WES study of Kabuki syndrome [32]. In this study, no single gene harbored novel loss-of-function mutations in all ten cases [32]. However, the gene *MLL2* contained novel loss-of-function mutations in nine of the ten cases. Ultimately, the study identified *MLL2* mutations in 66% of Kabuki cases. Using a family-based approach, all affected relatives are expected to share the same disease mutation, therefore, WES in families provides greater power to overcome genetic heterogeneity.

Second, common diseases may be incompletely penetrant, where an individual carries the disease-causing mutation without manifesting the disease (Fig. 1.5, person III:3). Using the rare-variant strategy, incomplete penetrance may result in the true disease-causing mutation being excluded due to its presence in a control individual or at a very low frequency in the general population. Using a family-based strategy, confounding due to incomplete penetrance in a control population is removed because the analysis only considers related, affected individuals. Only after identifying mutations inherited among all affected family members does the analysis consider population frequency. As illustrated in the family pedigree in Fig. 1.5, the number of rare or novel mutations shared by all affected members in the family will be very small. This strategy removes the need for sequencing unrelated control individuals. And as expected, larger families with more affected individuals (who are distantly related) provides greater power to identify smaller numbers of candidate genes (Fig. 1.5).

In one example of a family-based strategy, WES was used to identify mutations causing dominant axonal CMT type 2 (CMT2) disease in a family with 23 affected members in four generations [33]. In this study, only three distantly related affected

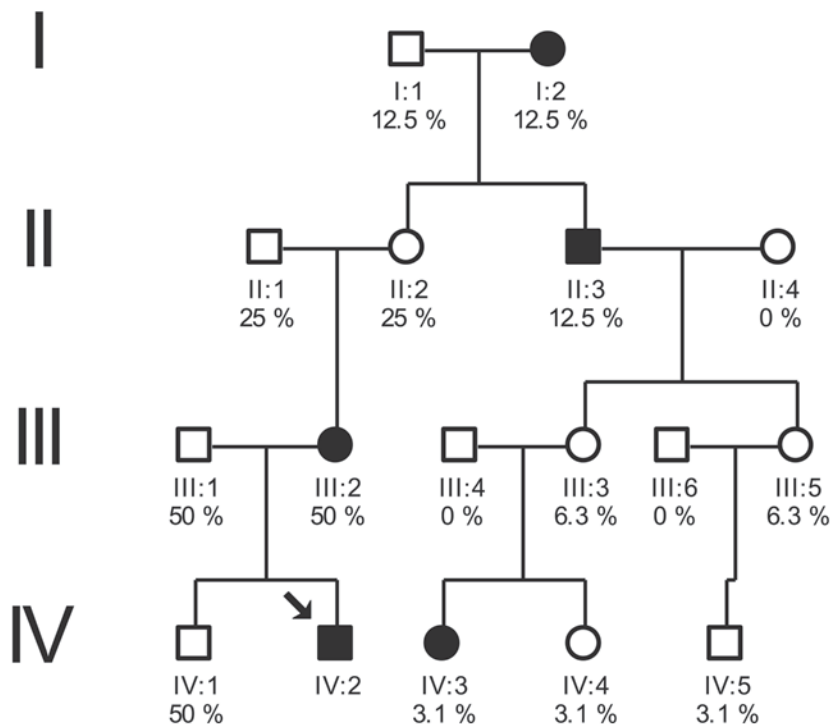


**Fig. 1.5** Family pedigree showing incompletely penetrant disease. The disease is inherited throughout each generation (*filled symbol*); however, some family members (II:2, III:3) are designated as unaffected (*open symbol*) despite an affected parent and affected children. The mutation is presumed to be inherited in these individuals and is described as incompletely penetrant since these two individuals have no signs of disease.

family members were sequenced and WES identified > 170 novel mutations in each patient. However after comparing results, only a single gene, *DYNCH1*, harbored novel nonsynonymous mutations in all affected cases. The mutation was subsequently shown to be inherited by all additional distantly related affected family members.

### ***Exome Analysis in Consanguineous Families***

As discussed earlier, genetic analysis of consanguineous families is a powerful method to identify recessive disease mutations. Whether combined with homozygosity mapping or not, WES has proven particularly useful in this regard. For example, WES of a single affected individual was used to identify the *SERPINF1* gene in a consanguineous family with recessive osteogenesis imperfecta [34]. In this study, the authors identified ROH from WES, an analogous method to microarray-based

genotype analysis. In parallel, WES identified >300 novel nonsynonymous mutations, and after restricting their analysis to only homozygous novel variants, the authors identified seventeen candidate genes. Only the *SERPINF1* gene, located within a 2.99 Mb ROH region, harbored homozygous nonsense mutations. Interestingly, two genes with homozygous missense mutations were located within a very large ~30 Mb ROH region; however, *SERPINF1* was confirmed by the identification of homozygous loss-of-function mutations in additional consanguineous families with osteogenesis imperfecta.

In another example, WES was used in a study of two consanguineous families with multiple orthopaedic manifestations, including congenital joint dislocation, chondrodysplasia, micrognathia and cleft palate [35]. After failing to identify mutations in multiple candidate genes, the authors performed WES in all affected cases with the hypothesis that the same gene was causal in both families. Sequencing three affected cases from the two families yielded on average ~5000 nonsynonymous mutations in each patient. Of these, an average of 136 variants were novel, of which an average of fourteen were homozygous in each person. Only one gene, *IMPAD1*, harbored novel homozygous nonsynonymous mutations in all three individuals. While different homozygous mutations were identified in the families, both occurred at highly conserved amino acids in the *IMPAD1* protein. Follow-up sequencing in a fourth consanguineous patient identified a homozygous splice-site mutation, suggesting the two missense mutations were also loss-of-function and that loss of *IMPAD1* protein is responsible for the skeletal deformities of this disease.

## Clinical Applications of Next-Generation Methods

The explosive success of NGS in disease-gene discovery has propelled efforts to use whole-exome, and even whole-genome, sequencing in clinical practice. Several efforts are underway to determine whether the technical hurdles of these methods can be overcome in clinical settings. For example, optimizing the source of a patient's sample (DNA quality) and generating results in a reasonable amount of time to be clinically actionable are clearly issues that require careful consideration. Current NGS protocols generally require microgram-scale amounts of high-quality DNA that may be challenging to obtain in certain scenarios, for example in sampling fetal DNA for prenatal diagnostic sequencing. However in a recent study, WGS was performed successfully using cell-free DNA from maternal plasma taken at 18.5 weeks gestation to generate fetal sequence [36]. A small percentage of cell-free DNA in maternal plasma is fetal DNA; consequently the genome of the fetus was deduced by sequencing DNA from the father, mother and mother's plasma. In a separate study, DNA from only ~20 cells was used to successfully sequence an entire genome [37]. Continued technological development and improved sequencing accuracy will expand the repertoire of clinical applications of whole-genome

sequencing. Indeed, whole-genome and whole-exome sequencing have been used to provide genetic and clinical diagnoses, and in some cases informed clinical treatment [31, 38–41].

Clinical microarray-based genotyping may improve diagnosis for orthopaedic conditions; however, the full potential for clinical NGS methods, such as whole-genome and whole-exome sequencing, in this arena is as yet unrealized. The spectrum of recently described overgrowth syndromes is an excellent example of how NGS methods uncovered the pathogenesis of a puzzling group of diseases, including Proteus syndrome [42], Cloves syndrome [43], megalencephaly [44, 45], Klippel-Trenaunay syndrome [46] and macrodactyly [47]. These syndromes are discussed in depth in Chap. 5; here, we highlight Type I macrodactyly. Type I macrodactyly is a congenital localized overgrowth commonly affecting digits in the hands and feet. Currently, these children undergo multiple surgeries to de-bulk the overgrowth tissue. Ultimately, the affected digits often require amputation. Comparing WES from overgrowth and normal tissues identified somatic mutations in the *PIK3CA* gene that activate the PI3K/AKT/MTOR cell signaling pathway to promote cell growth [48]; mutations in the same gene were recently described for other overgrowth syndromes (see Chap. 5). These tissue-specific somatic mutations activate the pathway and promote cell growth/proliferation leading to localized overgrowth. Because of the pathway's involvement in multiple cancers, this pathway has been well studied and is the target of several pharmaceuticals designed to limit cell growth. Thus, macrodactyly and other localized overgrowth syndromes are candidates for new, non-surgical treatments as a direct consequence of their association with the PI3K/AKT/MTOR cell signaling pathway. As in this example, NGS methods have great potential to rapidly advance our genetic understanding of orthopaedic disorders. The next challenge in pediatric orthopaedic research is to translate such genetic discoveries and improve patient care.

## References

1. Paria N, Copley LA, Herring JA, Kim HK, Richards BS, Sucato DJ, Rios JJ, Wise CA. The impact of large-scale genomic methods in orthopaedic disorders: insights from genome-wide association studies. *J Bone Joint Surg Am.* 2014;96(5):e38.
2. Lander ES. Initial impact of the sequencing of the human genome. *Nature.* 2011;470(7333):187–97.
3. Venter JC, Adams MD, Myers EW, Li PW, Mural RJ, Sutton GG, Smith HO, Yandell M, Evans CA, Holt RA, et al. The sequence of the human genome. *Science.* 2001;291(5507):1304–51.
4. Lander ES, Linton LM, Birren B, Nusbaum C, Zody MC, Baldwin J, Devon K, Dewar K, Doyle M, FitzHugh W, et al. Initial sequencing and analysis of the human genome. *Nature.* 2001;409(6822):860–921.
5. International Human Genome Sequencing Consortium. Finishing the euchromatic sequence of the human genome. *Nature.* 2004;431(7011):931–45.
6. Wheeler DA, Srinivasan M, Egholm M, Shen Y, Chen L, McGuire A, He W, Chen YJ, Makhijani V, Roth GT, et al. The complete genome of an individual by massively parallel DNA sequencing. *Nature.* 2008;452(7189):872–6.

7. Redon R, Ishikawa S, Fitch KR, Feuk L, Perry GH, Andrews TD, Fiegler H, Shapero MH, Carson AR, Chen W, et al. Global variation in copy number in the human genome. *Nature*. 2006;444(7118):444–54.
8. Girirajan S, Campbell CD, Eichler EE. Human copy number variation and complex genetic disease. *Annu Rev Genet*. 2011;45:203–26.
9. Yagerman SE, Cross MB, Green DW, Scher DM. Pediatric orthopedic conditions in Charcot-Marie-Tooth disease: a literature review. *Curr Opin Pediatr*. 2012;24(1):50–6.
10. Lupski JR, de Oca-Luna RM, Slaugenhaupt S, Pentao L, Guzzetta V, Trask BJ, Saucedo-Cardenas O, Barker DF, Killian JM, Garcia CA, et al. DNA duplication associated with Charcot-Marie-Tooth disease type 1A. *Cell*. 1991;66(2):219–32.
11. Pentao L, Wise CA, Chinault AC, Patel PI, Lupski JR. Charcot-Marie-Tooth type 1A duplication appears to arise from recombination at repeat sequences flanking the 1.5 Mb monomer unit. *Nat Genet*. 1992;2(4):292–300.
12. Boerkoel CF, Takashima H, Garcia CA, Olney RK, Johnson J, Berry K, Russo P, Kennedy S, Teebi AS, Scavina M, et al. Charcot-Marie-Tooth disease and related neuropathies: mutation distribution and genotype-phenotype correlation. *Ann Neurol*. 2002;51(2):190–201.
13. Lupski JR. Genomic disorders: structural features of the genome can lead to DNA rearrangements and human disease traits. *Trends Genet*. 1998;14(10):417–22.
14. Alvarado DM, Aferol H, McCall K, Huang JB, Techy M, Buchan J, Cady J, Gonzales PR, Dobbs MB, Gurnett CA. Familial isolated clubfoot is associated with recurrent chromosome 17q23.1q23.2 microduplications containing TBX4. *Am J Hum Genet*. 2010;87(1):154–60.
15. Alvarado DM, Buchan JG, Frick SL, Herzenberg JE, Dobbs MB, Gurnett CA. Copy number analysis of 413 isolated talipes equinovarus patients suggests role for transcriptional regulators of early limb development. *Eur J Hum Genet*. 2013;21(4):373–80.
16. Duboc V, Logan MP. Regulation of limb bud initiation and limb-type morphology. *Dev Dyn*. 2011;240(5):1017–27.
17. Stranger BE, Forrest MS, Dunning M, Ingle CE, Beazley C, Thorne N, Redon R, Bird CP, de Grassi A, Lee C, et al. Relative impact of nucleotide and copy number variation on gene expression phenotypes. *Science*. 2007;315(5813):848–53.
18. McQuillan R, Leutenegger AL, Abdel-Rahman R, Franklin CS, Pericic M, Barac-Lauc L, Smolej-Narancic N, Janicijevic B, Polasek O, Tenesa A, et al. Runs of homozygosity in European populations. *Am J Hum Genet*. 2008;83(3):359–72.
19. Jen J, Coulin CJ, Bosley TM, Salih MA, Sabatti C, Nelson SF, Baloh RW. Familial horizontal gaze palsy with progressive scoliosis maps to chromosome 11q23–25. *Neurology*. 2002;59(3):432–5.
20. Jen JC, Chan WM, Bosley TM, Wan J, Carr JR, Rub U, Shattuck D, Salamon G, Kudo LC, Ou J, et al. Mutations in a human ROBO gene disrupt hindbrain axon pathway crossing and morphogenesis. *Science*. 2004;304(5676):1509–13.
21. Senderek J, Bergmann C, Stendel C, Kirfel J, Verpoorten N, De Jonghe P, Timmerman V, Chrast R, Verheijen MH, Lemke G, et al. Mutations in a gene encoding a novel SH3/TPR domain protein cause autosomal recessive Charcot-Marie-Tooth type 4C neuropathy. *Am J Hum Genet*. 2003;73(5):1106–19.
22. Kryukov GV, Pennacchio LA, Sunyaev SR. Most rare missense alleles are deleterious in humans: implications for complex disease and association studies. *Am J Hum Genet*. 2007;80(4):727–39.
23. Consortium TGP. A map of human genome variation from population-scale sequencing. *Nature*. 2010;467(7319):1061–73.
24. Biesecker LG, Mullikin JC, Facio FM, Turner C, Cherukuri PF, Blakesley RW, Bouffard GG, Chines PS, Cruz P, Hansen NF, et al. The ClinSeq project: piloting large-scale genome sequencing for research in genomic medicine. *Genome Res*. 2009;19(9):1665–74.
25. Bamshad MJ, Ng SB, Bigham AW, Tabor HK, Emond MJ, Nickerson DA, Shendure J. Exome sequencing as a tool for Mendelian disease gene discovery. *Nat Rev Genet*. 2011;12(11):745–55.

26. Ng SB, Turner EH, Robertson PD, Flygare SD, Bigham AW, Lee C, Shaffer T, Wong M, Bhattacharjee A, Eichler EE, et al. Targeted capture and massively parallel sequencing of 12 human exomes. *Nature*. 2009;461(7261):272–6.
27. Gilissen C, Hoischen A, Brunner HG, Veltman JA. Disease gene identification strategies for exome sequencing. *Eur J Hum Genet*. 2012;20(5):490–7.
28. Paria N, Copley LA, Herring JA, Kim HK, Richards BS, Sucato DJ, Wise CA, Rios JJ. Whole-exome sequencing: discovering genetic causes of orthopaedic disorders. *J Bone Joint Surg Am*. 2013;95(23):e1851–8.
29. Tennessen JA, Bigham AW, O'Connor TD, Fu W, Kenny EE, Gravel S, McGee S, Do R, Liu X, Jun G, et al. Evolution and functional impact of rare coding variation from deep sequencing of human exomes. *Science*. 2012;337(6090):64–9.
30. Ng SB, Buckingham KJ, Lee C, Bigham AW, Tabor HK, Dent KM, Huff CD, Shannon PT, Jabs EW, Nickerson DA, et al. Exome sequencing identifies the cause of a Mendelian disorder. *Nat Genet*. 2010;42(1):30–5.
31. Rios J, Stein E, Shendure J, Hobbs HH, Cohen JC. Identification by whole-genome resequencing of gene defect responsible for severe hypercholesterolemia. *Hum Mol Genet*. 2010;19(22):4313–8.
32. Ng SB, Bigham AW, Buckingham KJ, Hannibal MC, McMillin MJ, Gildersleeve HI, Beck AE, Tabor HK, Cooper GM, Mefford HC, et al. Exome sequencing identifies MLL2 mutations as a cause of Kabuki syndrome. *Nat Genet*. 2010;42(9):790–3.
33. Weedon MN, Hastings R, Caswell R, Xie W, Paszkiewicz K, Antoniadis T, Williams M, King C, Greenhalgh L, Newbury-Ecob R, et al. Exome sequencing identifies a DYNC1H1 mutation in a large pedigree with dominant axonal Charcot-Marie-Tooth disease. *Am J Hum Genet*. 2011;89(2):308–12.
34. Becker J, Semler O, Gilissen C, Li Y, Bolz HJ, Giunta C, Bergmann C, Rohrbach M, Koerber F, Zimmermann K, et al. Exome sequencing identifies truncating mutations in human SERPINF1 in autosomal-recessive osteogenesis imperfecta. *Am J Hum Genet*. 2011;88(3):362–71.
35. Vissers LE, Lausch E, Unger S, Campos-Xavier AB, Gilissen C, Rossi A, Del Rosario M, Venselaar H, Knoll U, Nampoothiri S, et al. Chondrodysplasia and abnormal joint development associated with mutations in IMPAD1, encoding the golgi-resident nucleotide phosphatase, gPAPP. *Am J Hum Genet*. 2011;88(5):608–15.
36. Kitzman JO, Snyder MW, Ventura M, Lewis AP, Qiu R, Simmons LE, Gammill HS, Rubens CE, Santillan DA, Murray JC, et al. Noninvasive whole-genome sequencing of a human fetus. *Sci Transl Med*. 2012;4(137):137ra76.
37. Peters BA, Kermani BG, Sparks AB, Alferov O, Hong P, Alexeev A, Jiang Y, Dahl F, Tang YT, Haas J, et al. Accurate whole-genome sequencing and haplotyping from 10–20 human cells. *Nature*. 2012;487(7406):190–5.
38. Worthey EA, Mayer AN, Syverson GD, Helbling D, Bonacci BB, Decker B, Serpe JM, Dasu T, Tschannen MR, Veith RL, et al. Making a definitive diagnosis: successful clinical application of whole exome sequencing in a child with intractable inflammatory bowel disease. *Genet Med*. 2011;13(3):255–62.
39. Bainbridge MN, Wiszniewski W, Murdock DR, Friedman J, Gonzaga-Jauregui C, Newsham I, Reid JG, Fink JK, Morgan MB, Gingras MC, et al. Whole-genome sequencing for optimized patient management. *Sci Transl Med*. 2011;3(87):87re83.
40. Dixon-Salazar TJ, Silhavy JL, Udpa N, Schroth J, Bielas S, Schaffer AE, Olvera J, Bafna V, Zaki MS, Abdel-Salam GH, et al. Exome sequencing can improve diagnosis and alter patient management. *Sci Transl Med*. 2012;4(138):138ra178.
41. Saunders CJ, Miller NA, Soden SE, Dinwiddie DL, Noll A, Alnadi NA, Andraws N, Patterson ML, Krivohlavek LA, Fellis J, et al. Rapid whole-genome sequencing for genetic disease diagnosis in neonatal intensive care units. *Sci Transl Med*. 2012;4(154):154ra135.
42. Lindhurst MJ, Sapp JC, Teer JK, Johnston JJ, Finn EM, Peters K, Turner J, Cannons JL, Bick D, Blakemore L, et al. A mosaic activating mutation in AKT1 associated with the Proteus syndrome. *New Engl J Med*. 2011;365(7):611–9.

43. Kurek KC, Luks VL, Ayturk UM, Alomari AI, Fishman SJ, Spencer SA, Mulliken JB, Bowen ME, Yamamoto GL, Kozakewich HP, et al. Somatic mosaic activating mutations in PIK3CA cause CLOVES syndrome. *Am J Hum Genet.* 2012;90(6):1108–15.
44. Lee JH, Huynh M, Silhavy JL, Kim S, Dixon-Salazar T, Heiberg A, Scott E, Bafna V, Hill KJ, Collazo A, et al. De novo somatic mutations in components of the PI3K-AKT3-mTOR pathway cause hemimegalencephaly. *Nat Genet.* 2012;44(8):941–5.
45. Riviere JB, Mirzaa GM, O’Roak BJ, Beddaoui M, Alcantara D, Conway RL, St-Onge J, Schwartzenuber JA, Gripp KW, Nikkel SM, et al. De novo germline and postzygotic mutations in AKT3, PIK3R2 and PIK3CA cause a spectrum of related megalencephaly syndromes. *Nat Genet.* 2012;44(8):934–40.
46. Lindhurst MJ, Parker VE, Payne F, Sapp JC, Rudge S, Harris J, Witkowski AM, Zhang Q, Groeneveld MP, Scott CE, et al. Mosaic overgrowth with fibroadipose hyperplasia is caused by somatic activating mutations in PIK3CA. *Nat Genet.* 2012;44(8):928–33.
47. Rios JJ, Paria N, Burns DK, Israel BA, Cornelia R, Wise CA, Ezaki M. Somatic gain-of-function mutations in PIK3CA in patients with macrodactyly. *Hum Mol Genet.* 2012.
48. Rios JJ, Paria N, Burns DK, Israel BA, Cornelia R, Wise CA, Ezaki M. Somatic gain-of-function mutations in PIK3CA in patients with macrodactyly. *Hum Mol Genet.* 2013;22(3):444–51.

# Chapter 2

## Neurofibromin in Skeletal Development

Mateusz Kolanczyk and David A. Stevenson

**Abstract** Skeletal complications are frequent in neurofibromatosis type 1 (NF1). Various skeletal manifestations are observed including generalized osteopenia (low bone mass), scoliosis, long bone bowing, pseudarthrosis, bone lytic lesions, and sphenoid wing dysplasia. Historically, focal skeletal lesions in NF1 were suspected to be caused by nearby localized tumors. However, genetic experiments have brought an entirely new view of NF1 musculoskeletal pathology, illustrating the power of gene discovery and genetic model systems. We now appreciate that neurofibromin is required for normal musculoskeletal system development. We now understand that NF1 bone dysplasia can be caused by loss of function mutations in *NF1*, occurring in the mesenchymal lineage, rather than through tumor influence as previously thought. This is not to say that the presence of tumors has no impact on the bone. It is likely that tumors can impact bone tissue and further exacerbate pathological processes. Here we review the current state of knowledge of neurofibromin in bone and skeletal muscle. We outline mechanisms underlining NF1 musculoskeletal dysplasias derived from both mouse disease models and observations of human NF1 pathology. We also discuss pathways regulated downstream of *NF1* and their potential impact on the musculoskeleton.

**Keywords** NF1 · Nf1Prx1–f1 · Neurofibromatosis · Tibial dysplasia · Bone · Muscle · Cartilage · Low bone mass · Scoliosis

---

M. Kolanczyk (✉)

Campus Virchow Institut für Medizinische Genetik und Humangenetik,  
Neurofibromin in Skeletal Development, Charité Universitätsmedizin,  
Augustenburger Platz 1, Berlin 13353, Germany  
e-mail: mateuszkolanczyk@gmail.com

D. A. Stevenson

Division of Medical Genetics, Stanford University, Lucile Packard Children's Hospital,  
300 Pasteur Drive, H315, Stanford, CA 94305-5208  
e-mail: dasteven@stanford.edu

© Springer Science+Business Media New York 2015

C. A. Wise, J. J. Rios (eds.), *Molecular Genetics of Pediatric Orthopaedic Disorders*,  
DOI 10.1007/978-1-4939-2169-0\_2

## Introduction

Neurofibromatosis type 1 (NF1) is an autosomal dominant disease caused by loss of function mutations in the *NF1* gene that encodes neurofibromin, a GTPase-activating protein. NF1 is a relatively common disorder (1/3000) and is typically diagnosed clinically [1]. Individuals who have two out of the following seven criteria meet clinical diagnostic criteria for NF1: (1.) Six or more café au lait macules (1.5 cm or larger in postpubertal individuals; 0.5 cm or larger in prepubertal individuals); (2.) Two or more neurofibromas of any type or one or more plexiform neurofibromas; (3.) Freckling in the axillary or inguinal region; (4.) Optic glioma; (5.) Two or more Lisch nodules; (6.) A distinctive osseous lesion (e.g. sphenoid bone dysplasia, pseudarthrosis); (7.) First-degree relative with neurofibromatosis type 1 [2]. NF1 can cause various degrees of morbidity. This is especially true in respect to tumor load, which can vary significantly from patient to patient. Although there is significant clinical variability there are relatively few genotype-phenotype correlations [3, 4], and modifier genes are suspected to exist. However, it is likely that somatic second hit mutations or epigenetic factors also contribute to the high clinical variability [5]. The main morbid symptoms of NF1 are related to an increased susceptibility towards neoplastic transformation (e.g. benign cutaneous neurofibromas, plexiform neurofibromas, optic pathway tumors, and aggressive malignant peripheral nerve sheath tumors). Although primarily considered a neurocristopathy, that is, a defect in neural crest development, multiple organ systems are affected in individuals with NF1, including the musculoskeleton. Here we describe the significant musculoskeletal manifestations of NF1 and the underlying role of neurofibromin.

## Bone Development

There are two types of bone development; endochondral and intramembranous ossification (Fig. 2.1). The development of the skeleton is initiated through the process of patterning which is followed by subsequent organogenesis, commencing in the growth of the skeletal elements [6]. Patterning determines spatial arrangement, number and shape of the bone elements. During organogenesis, mesenchymal precursor cells differentiate into chondrocytes (cartilage cells) or osteoblasts (bone cells). During desmal ossification, osteoblasts differentiate directly from mesenchymal cells. Desmal ossification takes place in the bones of skull, parts of the facial skeleton and the collar bone. All other bones develop through the process of endochondral ossification. Here, a cartilaginous system is first formed, which is later replaced by bone. The growth of skeletal elements takes place in a specialized area of long bones called the epiphyseal plate or growth plate. Cartilage differentiation takes place within the growth plate where morphologically distinguished zones are being formed: resting zone, proliferative zone, pre-hypertrophic zone and hypertrophic zone. In the hypertrophic zone, chondrocytes undergo enlargement and eventually apoptosis. In this zone, blood vessels invade the growth plate

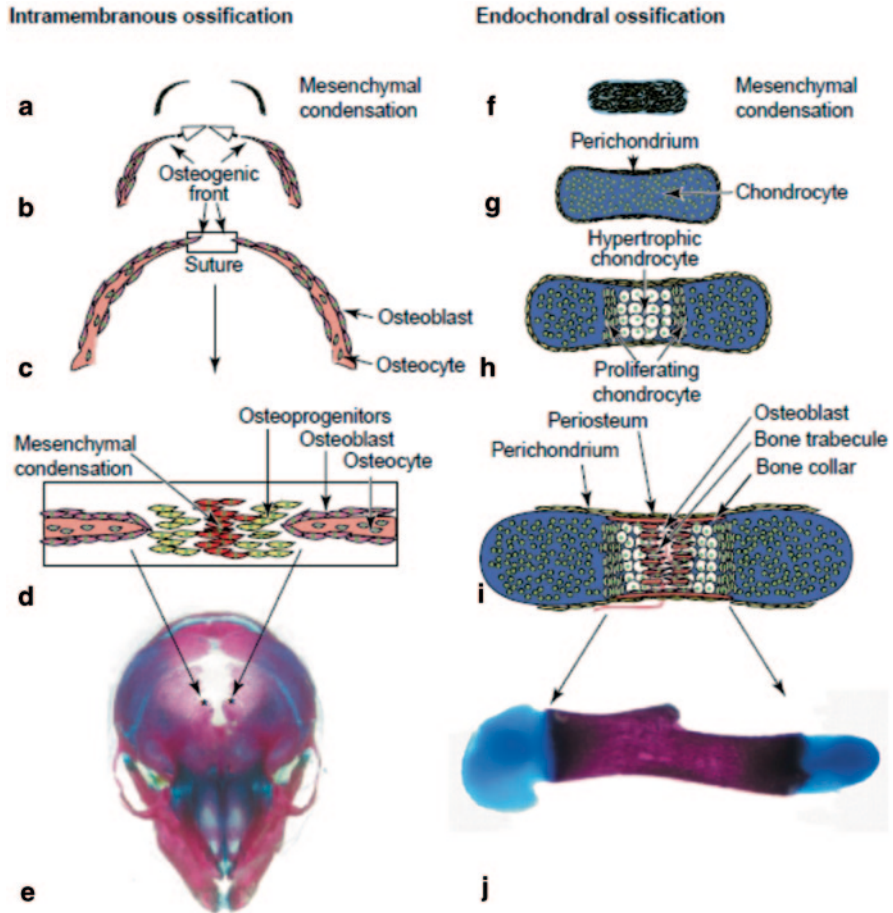


**Fig. 2.1** Bone development cartoon (reprinted from publication title: Transcriptional mechanisms in osteoblast differentiation and bone formation. Trends in Genetics Volume 19, Issue 8, August 2003, Page 459, with permission from Elsevier) Intramembranous ossification and endochondral ossification. **a–d** Craniofacial bones are formed directly from condensations of mesenchymal cells without the formation of a cartilage intermediate, a process described as intramembranous ossification. **a** In mice, formation of frontal bones starts at embryonic day 12.5 (E12.5) in mesenchymal condensations on the lateral side of the head. **b** From the mesenchymal condensation, the cellular mass with osteogenic activity spreads upward toward the top of the skull (arrows). Osteoblasts differentiate from mesenchymal condensation and produce bone matrix at E14.5. **c** At E15.5, the ends of the cellular masses that originate on each side meet at the midline where a suture is formed. **d** In the suture, cells in the mesenchymal condensations differentiate into osteoprogenitor cells. Osteoprogenitor cells then differentiate into osteoblasts that produce bone-matrix molecules. Osteoblasts differentiate into osteocytes, which become embedded within the bone matrix. **e** A schematic frontal view of a mouse skull (E18.5) stained with alizarin red and alcian blue. Asterisks indicate osteogenic fronts of frontal bones. **f–j** By contrast, long bones are formed by endochondral ossification. **f** Development of endochondral bones starts with the formation of mesenchymal condensations. **g** Cells in the mesenchymal condensations then give rise to chondrocytes whereas cells at the periphery of the condensations form a perichondrium. **h** Centrally localized chondrocytes proliferate actively before exiting the cell cycle and differentiating into hypertrophic

and osteoblasts initiate new bone formation in the primary spongiosa. Bone is constantly remodeled through the action of osteoclasts, which are derived from the hematopoietic lineage. In mouse bone the *Nf1* gene is most strongly expressed in the prehypertrophic and hypertrophic zone of the growth plate. It is also expressed in osteoblasts and osteoclasts.

## Bone Complications in NF1

### *Short Growth and Generalized Low Bone Mineral Density*

The most frequent types of skeletal manifestations in NF1 are short stature and generalized osteopenia or osteoporosis. In adults with NF1, 20–30% exhibit height below the 3rd centile [7, 8]. How *NF1* haploinsufficiency causes short stature is currently unknown. It is interesting that *Nf1* heterozygous mice do not show shortening of skeletal elements or reduced bone volume. However, shortening of skeletal elements was observed in conditional mouse mutants that are deficient for *Nf1* in the central nervous system (CNS), including the hypothalamus [9]. In these mice, reduction in pituitary growth hormone synthesis presumably caused a decrease in growth. Reduced growth was also observed in mice in which *Nf1* was doubly inactivated in cartilage [10, 11]. Thus, short stature in NF1 may be related to deficiency in both endocrine and bone growth plate systems. Short stature itself likely does not cause significant morbidity in NF1, and growth remains proportional. However, functional and societal impact of short stature in NF1 has not been adequately investigated.

Decreased bone mineral density (BMD) has been observed in as much as 50% of individuals with NF1 [12–19]. Generalized low bone mass and osteoporosis may be more problematic in these patients, potentially increasing risk of fractures. While literature suggests that children with NF1 have generally low BMD, the sizes of the studied patient groups are small and the clinical consequences are not well known [19]. In one study of 460 NF1 individuals there was a 5.2-fold increased risk of fractures in individuals with NF1 above 41 years of age, a 3.4-fold increased fracture

---

chondrocytes. The sequential differentiation of chondrocytes establishes a unique cellular organization that constitutes the epiphyseal growth plate. At the distal end of the epiphyseal growth plate, hypertrophic chondrocytes further mineralize their own cartilaginous matrix. In parallel to this multistep differentiation pathway, cells from a thin layer of mesenchymal cells, called the periosteum, that envelops the cartilage matrix and invades the zone of hypertrophic chondrocytes in addition to blood vessels and osteoclasts. Whereas osteoclasts degrade the matrix of the zone of hypertrophic chondrocytes, osteoblasts deposit a bone-specific matrix. (i) The partially degraded, mineralized cartilage matrix forms a template for deposition of bone matrix by osteoblasts. Endochondral bone contains an outer envelop of cortical bone (the bone collar) that surrounds the marrow cavity and growth plate. The cortical bone is contiguous with the perichondrium. j A mouse humerus stained with alizarin red and alcian blue

risk in NF1 children, and no increased fracture risk in the age group 17–40 years [20]. In another study of 256 children with NF1 ages 5–20 years, the NF1 individuals without a focal long bone dysplasia did not have a difference in the prevalence of ever having a fracture compared to healthy controls [21]. Thus, it appears that individuals with NF1 have an age-dependent increase of fracture risk. It appears also that individuals with NF1 have generally low vitamin-D concentrations, which could be one of the factors leading to decreased BMD [22, 23]. A small study of bone biopsies from 14 NF1 individuals showed decreased trabecular bone volume and osteoidosis, which coincided with increased osteoblasts and osteoclast number [24]. These observations are similar to the findings in *Nf1Col1<sup>-/-</sup>* mice in which *Nf1* was inactivated in the osteoblast lineage [25]. Inactivation of *Nf1* in osteoblasts causes increased collagen synthesis but inhibits bone mineralization, resulting in the profound osteoidosis. *Nf1Col1<sup>-/-</sup>* mice show osteoblast-mediated increase of osteoclast number. More precisely the *Nf1<sup>-/-</sup>* osteoblasts overproduce RANKL, the receptor activator for nuclear factor kappa-B ligand that triggers osteoclastogenesis. It has been shown that in the *Nf1* deficient osteoblasts, activation of Ras triggers downstream activators ERK1/2, RSK2, PKA as well as ATF4, accelerating collagen synthesis and causing overproduction of RANKL [25]. Defective osteoblast differentiation therefore appears to be one of the main causes of bone pathology in NF1.

### ***FGF Signaling and c-Type Natriuretic Peptide***

Recent research has established a link between short growth in *Nf1Col2<sup>-/-</sup>* mice and increased signaling mediated by the fibroblast growth factor receptor (Fgfr) [26]. These mice lack neurofibromin (*Nf1*) in type II collagen-expressing cells and show a number of phenotypes reminiscent of the ones observed in mice characterized by FGFR gain-of-function mutations. In chondrocyte cultures in-vitro, Fgfr activation by FGF2 pulse-stimulation triggered rapid ERK1/2 phosphorylation in wild type (wt) and *Nf1<sup>-/-</sup>* chondrocytes. However, return to the basal level of ERK activation was delayed in *Nf1<sup>-/-</sup>* cells, suggesting that prolonged ERK signaling is one factor in deficient chondrocyte growth. In separate experiments, *Nf1Col2<sup>-/-</sup>* mice were treated with the NC-2 compound, which is a derivative of c-natriuretic peptide (CNP) [26]. CNP is known to bind to the natriuretic peptide receptor B (N-PRB) and stimulate cGMP synthesis, thus suppressing MAPK activation (Fig. 2.2) [27]. The subcutaneous injections of NC-2 compound at 300 mg/kg per day throughout 18 days from birth on resulted in almost complete rescue of the growth defect in *Nf1Col2* mice, suggesting CNP is a valid candidate compound for the treatment of growth deficiency in NF1. Further studies of CNP in other NF1 mouse models will be helpful to access its potential side effects and determine its suitability for the treatment of other bone manifestations.

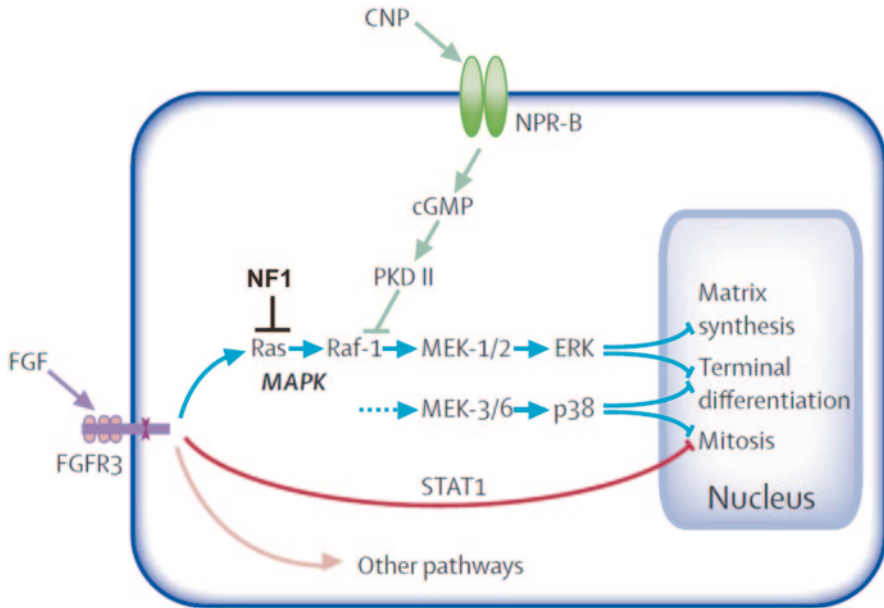


**Fig. 2.2** CNP—MAPK pathway (reprinted with modification from publication title: Achondroplasia, *The Lancet* Vol. 370 July 14, 2007 page 163, with permission from Elsevier). Signalling pathways of FGFR3 most relevant to growth plate chondrocytes FGFR3 signals propagated through STAT1, MAPK-ERK, MAPK-p38, and other pathways inhibit chondrocyte proliferation, post-mitotic matrix synthesis, and terminal (hypertrophic) differentiation. The CNP-NPR-B pathway and NF1 inhibit the MAPK pathways. (Reprinted from *The Lancet*, 370, Horton WA, Hall JG, Hecht JT, Achondroplasia, pp. 162–172, 2007, with permission from Elsevier)

### *Long Bone Dysplasia*

Apart from generalized bone disease, about 3–5% of individuals with NF1 develop a focal skeletal dysplasia of the long bones, predominantly the tibia (Fig. 2.3) [28]. It is currently unknown why the tibia is most often affected. The anterolateral bowing typically is identified in infancy, or even prenatally, and is usually unilateral [28]. This suggests that long bone dysplasia has a prenatal origin. Radiographically, tibial bowing in NF1 prior to fracture usually appears as cortical thickening and medullary canal narrowing at the apex of the convexity, typically near the junction of the middle and distal thirds of the tibia (Fig. 2.3b) [29]. The bowed long bone frequently sustains a fracture that is recalcitrant to union resulting in pseudarthrosis (Fig. 2.3c). Mouse experiments suggest that dystrophic bone changes are caused by complete *NF1* loss-of-function in dividing and multipotent bone cells. Supporting this hypothesis, somatic (i.e. genetic alteration occurring after conception) homozygous inactivation of *NF1* was demonstrated in the pseudarthrosis tissue of one NF1 patient with tibial pseudarthrosis [30]. A mouse model that recapitulates most features of NF1 tibial dysplasia is the *Nf1Prx1<sup>-/-</sup>* mouse (Fig. 2.4), in which *Nf1* was inactivated in the limb bud mesenchyme and head mesenchyme [10]. In these



**Fig. 2.3** Long bone dysplasia in neurofibromatosis type 1 (NF1). **a** Photograph of patient. **b** Radiograph of individual with NF1 with tibial bowing showing characteristic cortical thickening with medullary canal narrowing. **c** Radiograph of pseudarthrosis after long standing fracture of the tibia in an individual with NF1

mice, all cells of mesenchymal origin carry biallelic *Nf1* inactivation, including bone cells, cartilage, muscle, endothelium, fat and connective tissue cells. Although the *Nf1*Prx1<sup>-/-</sup> mouse was generated initially as a model of long bone dysplasia, this model has subsequently provided additional insights that relate to the broad spectrum of NF1 musculoskeletal findings. Some of the important observations from this and other mouse models pertaining to developmental processes controlled by *Nf1* are described below; see also Table 2.1 for review of mouse models and bone fracture related observations.

### Growth Plate Disturbances

*Nf1* deficiency in cartilage causes decreased chondrocyte proliferation and premature growth plate chondrocyte hypertrophy [10]. This is caused by decreased Indian Hedgehog (Ihh) expression in the growth plate and concomitant increase of p21/Waf1 expression that leads to reduced cartilage proliferation and dwarfism of the appendicular skeleton. Reduced Ihh expression is a direct cause of premature hypertrophy and short growth [10].

*Nf1* deficient cartilage strongly expresses the Sox9 transcription factor, which is localized to the nucleus and is responsible for retention of cartilaginous properties. This persistent nuclear localization of Sox9 is observed in the *Nf1*Prx1<sup>-/-</sup> mice in the cartilage anlagen, but also in areas where it should not be expressed (e.g. during hip joint cavitation in joint cavity). Due to persistence of nuclear Sox9 expression, the hip joint cavity retains a cartilaginous phenotype and undergoes fusion with

**Table 2.1** Callus cellular and structural characteristics in *Nf1* mouse models. (Updated and adapted from Stevenson et al. [39])

	<i>Nf1</i> <sup>+/-</sup> Ref [49]	<i>Nf1</i> <sup>ob</sup> <sup>+/-</sup> Refs [11, 25]	<i>Nf1</i> <sup>px</sup> <sup>+/-</sup> Ref [47]	<i>Nf1</i> <sup>ob</sup> <sup>+/-</sup> Ref [25]	<i>Nf1Col2</i> <sup>-/-</sup> Ref [11]	<i>Nf1</i> (flox/-) / AdCre Ref [36]
<i>Nf1</i> genetic setting	+/- (global)	-/- in mature osteoblasts only	-/- in limb mesenchymal osteoprogenitors and progeny (chondrocytes, osteoblasts, endothelial cells, adipocytes, muscles)	+/- (global) -/- in mature osteoblasts only	-/- in mesenchymal osteoprogenitors and progeny (chondrocytes, osteoblasts)	+/- (global) -/- in differentiating callus cells including chondrocytes and osteoblasts
Osteoclast differentiation	Increased (following ovariectomy)	Increased (osteoblast-dependent)	Increased (mechanism ND)	Increased	Increased	Increased
Osteoblast differentiation	Decreased	Normal	Decreased	Decreased	Decreased	Decreased
Mineralization	ND	Delayed	Delayed	Delayed	Delayed	Delayed
Structural properties		Increased callus volume	Cartilaginous remnants	Reduced BV/TV	ND	Reduced closed and open fracture union rates
		Reduced BV/TV	Reduced callus size			Increased fibrotic or undifferentiated tissue at fracture callus
		Increased cortical porosity	Altered BV/TV			
		Cartilaginous remnants	Reduced BMD			

Table 2.1 (continued)

	<i>Nf1</i> <sup>+/-</sup> Ref [49]	<i>Nf1</i> <sup>pkx/-</sup> Refs [11, 25]	<i>Nf1</i> <sup>pkx/-</sup> Ref [47]	<i>Nf1</i> <sup>ob2/-</sup> [25]	<i>Nf1</i> <sup>ob2/-</sup> Ref	<i>Nf1</i> <i>Col2</i> <sup>-/-</sup> Ref [11]	<i>Nf1</i> (flox/-) / AdCre Ref [36]
Callus mechanical properties	ND	Decreased stiffness and maximum force	Reduced torsional stiffness	ND		Reduced vertebral stiffness, yield force, peak force	ND
Callus marrow	Fibrocartilaginous tissue	Normal	Reduced ultimate torque at failure			Reduced femoral rigidity, and bending strength	Fibrocartilaginous tissue

ND not determined, BV<sub>tr</sub> bone volume, TV<sub>tr</sub> trabecular volume

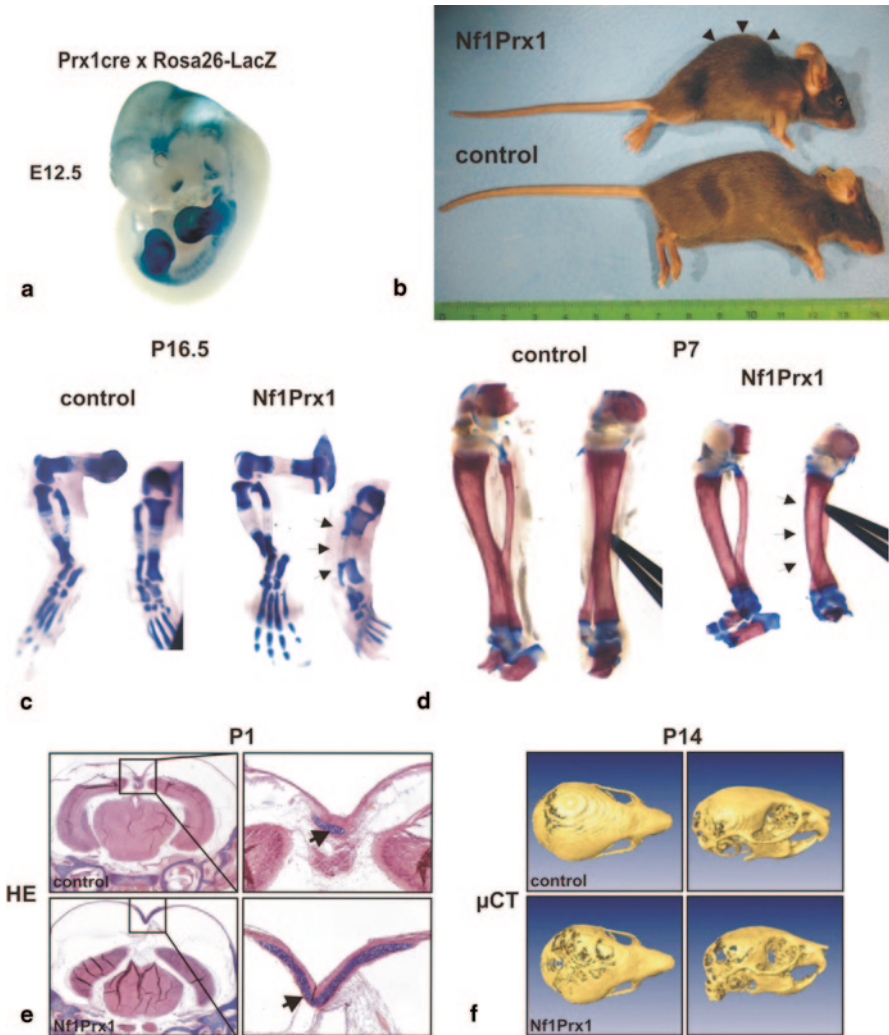


**Fig. 2.4** Gross morphology and skeleton in  $Nf1Prx1^{-/-}$  mice. **a** Whole mount detection of the Cre recombinase activity in the cross of Rosa26-LacZ indicator mouse with Prx1-Cre mice. Note LacZ activity in the limb buds and in the cranial region. **b** A side view of the control and  $Nf1Prx1^{-XE}$  mutant mouse. Note that  $Nf1Prx1^{-mu}$  mutant mice show a profound kyphosis (arrow heads), a phenotype often presented by mice featuring muscle dystrophy. **c, d** Tibia bowing in the prenatal and postnatal development in  $Nf1Prx1^{-T}$  mice. Alcian blue and Alizarin red stained skeletal preparations of E16.5 and P7 mice in side and front view. Note a bowed tibial bone (arrows) visible in the front view of the tibia both at E16.7 and P7 stage indicating a prenatal origin of the phenotype. Note also shortening of the skeletal elements in the mutant mice. **e, f** Delayed mineralization and increased cartilage formation in the  $Nf1Prx1^{-Dc}$  cranium. **e** Hematoxylin-Eosin/Alcian Blue stained transverse sections of the P1 wt and  $Nf1Prx1^{-Bl}$  calvaria. Right panel shows magnification of the sagittal suture with enlarged cartilage area in the  $Nf1Prx1^{-al}$  mouse calvaria (arrows). **f** Delayed mineralization of the calvarial bones in the  $Nf1Prx1^{-XE}$  mice visualized by  $\mu$ CT scan. The top view and the profile view of the skull, with poorly mineralized, transparent areas in the hind cranium of 14 days old  $Nf1Prx1^{-XE}$  mouse

the pelvis [10]. Similarly cartilage is ectopically formed in other regions e.g. in the hind cranium (Fig. 2.4e). It has been proposed that the hip joint fusion phenotype is likely at least partially due to reduced muscle force, which normally initiates joint cavitation. However we note that cases of hip joint fusion have not been observed in individuals with NF1.

Both *Nf1Prx1*<sup>-/-</sup> and *Nf1Col2*<sup>-/-</sup> mice show increased osteopontin (SPP1) expression in *Nf1* deficient growth plate chondrocytes and osteoblasts [26]. The SPP1 gene encodes matrix bone sialoprotein (osteopontin), which is known to attract and stimulate osteoclasts [31, 32]. Thus, not only RANKL expression but also osteopontin expression explains increased numbers of osteoclasts observed in the primary spongiosa in *NF1* deficient mice.

### Disturbances in Muscle Mass

Similar to human NF1 tibial dysplasia cases, *Nf1Prx1*<sup>-/-</sup> mice show tibial bowing even at prenatal stages, suggesting an early embryonic defect in bone and skeletal musculature development. In postnatal stages, *Nf1Prx1*<sup>-/-</sup> mice show decreased skeletal muscle mass in extremities and profound developmental muscle dysplasia, characterized by a decrease of myotube number, increased of connective tissue volume, and increased number of split muscle fibers. This is primarily caused by a defect of late myoblast differentiation during embryogenesis (Fig. 2.5). While muscle progenitor cell migration appears normal, myotube formation was inhibited by *Nf1* ablation, which was associated with increased Ras-MEK1-Erk1/2 signaling and increased proliferation of connective tissue cells [33]. Shortening of the muscles may contribute to tibial bowing, as muscle mass in the lower extremities is unilaterally positioned and exerts force on the tibia which is similar to the force exerted by the chord on a bow. Disproportionate growth of skeletal elements together with shortening of the muscle mass helps explain the bowing phenotype.

### Disturbances in Bone Structural and Material Properties

Bone structural properties are abnormal in NF1. Bone homeostasis is controlled by an interplay of three main bone cell types: osteoblasts, osteocytes and osteoclasts. Osteocytes are the cells that arise at the end stage of osteoblast differentiation and are embedded deep in the mineralized bone matrix, communicating with one another through a network of canaliculi. In both the *Nf1Prx1*<sup>-/-</sup> mouse and NF1 patient cortical bone samples, where functional neurofibromin is confirmed or presumed absent, osteocyte lacunae size is significantly increased (unpublished results—Dr. Jirko Kuehnich). Given that osteocytes constitute ≈90% of living cells in the cortical bone, these enlarged osteocyte lacuna cause significant increase of bone microporosity that may contribute to structural weakening of the *NF1* deficient bone. Also important is macroporosity due to bone demineralization in the proximity of blood vessels. Adult *Nf1Prx1*<sup>-/-</sup> mice have several-fold increased cortical bone

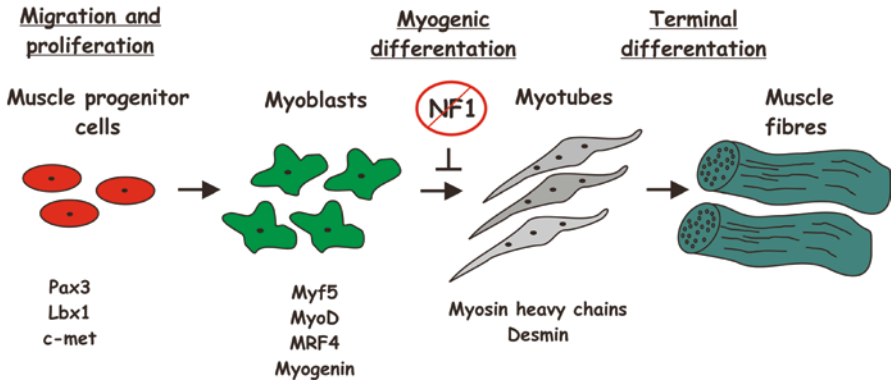


**Fig. 2.5 Muscle development.** (Adopted from Francis-West et al.; *J. Anat.* (2003)**202**, pp. 69–81). The regulation of primary myogenesis in the developing limb. The muscle precursors of the limb initially express the transcription factors *Pax3* and *Lbx1* together with the *c-met* tyrosine kinase receptor for scatter factor. Within the limb field, commitment to myogenic differentiation is marked by the expression of the myogenic regulatory genes (MRFs): *Myf5* is detected first and is soon followed by *MyoD*. *MRF4* is then transiently expressed and this is followed by *myogenin* expression. Subsequently, myoblasts terminally differentiate and express either slow or fast myosin heavy chain (MyHC) isoforms, which determine the muscle fibre type. The MyHC-expressing myoblasts fuse into multinucleate myotubes and assemble to form the muscle fibres. Loss of NF1 inhibits myoblast differentiation and myotube formation. (Reprinted from Journal of Anatomy, Francis-West PH, Antoni L, Anakwe K, Regulation of myogenic differentiation in the developing limb bud, p69–81, 2003, with permission from John Wiley and Sons)

macroporosity associated with the presence of large areas of demineralisation in the proximity of blood vessels penetrating the bone cortex. In mice, ectopic blood vessels were observed in the apex of the bone curve, which seem to predetermine the potential fracture sites. The bone surrounding the blood vessels is likely the primary site of the macroporotic bone structural destabilization in *Nf1Prx1<sup>-/-</sup>* mice (our unpublished observation).

Bone material properties are also abnormal upon loss of neurofibromin. Changes in bone material and bone structure likely play an important role in the etiology of NF1 long bone bowing. *Nf1Prx1<sup>-/-</sup>* mice display softer bone as measured by nanoindentation experiments and contain less calcium than wild-type littermates [10]. In postnatal bones we detected lower bone mineral density and disorganized collagen fiber orientation; consistent with the idea that a significant problem in NF1 is due to defective extracellular matrix (ECM) maturation secondary to osteoblast dysfunction. Delayed osteoblast differentiation and the apparent inability to synthesize mature collagen, especially in the areas of high mechanical load (mid shaft) and in proximity of blood vessels cause focal bone lesions within cortical bone (unpublished results—Dr. Jirko Kuehnisch). A generalized problem is also observed in the form of lower bone mineral content in adult *Nf1Prx1<sup>-/-</sup>* mice. Based on currently available data, the defects of organic matrix maturation and mineralization are important in the etiology of long bone bowing. Thus, multiple converging defects of bone architecture as well as bone organic and mineral phase are responsible for the impairment of bone strength in NF1.

## Disturbances in Blood Vessel Properties

Vascular anomalies have been reported in humans with NF1 (e.g. renal artery stenosis), and analysis of the blood from NF1 patients without vascular disease showed increased concentrations of inflammatory cells and cytokines linked to vascular inflammation [34]. Mouse models also support a role of neurofibromin in blood vessel properties as they are altered in *Nf1* deficient mice. *Nf1*<sup>+/-</sup> mice were shown to have increased neointima formation (i.e. thickened layer) after vascular injury [34]. This was associated with the vascular inflammation. It has also been shown that heterozygous inactivation of *Nf1* in bone marrow derived cells, known to be involved in blood vessel homeostasis, is necessary and sufficient for neointima formation after vascular injury [34]. Thus, bone marrow cells appear to be involved in the inflammatory response in *Nf1* deficient blood vessels, likely including vessels within cortical bone.

## *NF1* in Bone Regeneration

We now understand that neurofibromin is required for normal bone development as well as bone regeneration, but with an important distinction. During development and regeneration, loss of *Nf1* has opposite effects in the early and late osteoblast differentiation. Inactivation in early osteo-progenitor cells *inhibits* osteoblast differentiation, triggers fibrous tissue formation (in context of fracture repair) and diminishes matrix mineralization. This is the case in *Nf1Prx1*<sup>-/-</sup> mice where inactivation occurs in early limb bud mesenchyme and *Nf1Col2*<sup>-/-</sup> mice where inactivation takes place in early osteochondro-progenitor cells. In contrast, *Nf1* inactivation at the osteoblast stage (e.g. in *Nf1Col1*<sup>-/-</sup> mice) leads to increased collagen synthesis and a net *increase* of bone formation. Thus *Nf1Col1*<sup>-/-</sup> mice exhibit both normal development and normal bone regeneration; closed fractures result in normal cartilaginous callus formation and formation of an enlarged, osteoid rich, bony callus [35]. However despite an enlarged callus, the bridging cortices are porous and overall fracture repair is delayed, indicating that late *Nf1* inactivation interferes with normal healing processes. Moreover this model does not recapitulate features of tibial dysplasia-associated pseudarthrosis, and the fractures eventually heal.

Two mouse models, *Nf1* flox/- + Adeno-cre (this mouse model has one allele of NF1 inactivated in germ line and the second alleles floxed, thus second allele can be inactivated with the adenovirally delivered Cre recombinase) [36] and *Nf1Prx1*<sup>-/-</sup> [37], recapitulate pseudarthrosis of the tibia after a forced fracture when *Nf1* is doubly inactivated in the extremity prior to or during fracture. In the first mouse model, *Nf1* flox/- + Adeno-cre, double *Nf1* inactivation is accomplished by local delivery of the adenovirus carrying Cre recombinase gene [36]. Fracture healing in this model was severely delayed, and fracture unions were achieved in less than 50% of tested mice. The fracture site was populated by a highly proliferative fibrous tissue. Additionally, osteoclasts were recruited to the fracture site, and resided both on the

bone and in the fibrous tissue. Importantly, this study has shown that early in-vitro knockout of *Nf1* leads to decreased osteoblast mineralization potential while late osteoblast inactivation did not exert such effect.

The *Nf1Prx1*<sup>-/-</sup> mouse model also closely recapitulates both the developmental processes leading to the long bone dysplasia and the subsequent fracture healing deterioration and pseudarthrosis (development of a non-union after a fracture) [37]. We have shown that loss of *Nf1* in the mesenchymal lineage induces canonical MAPK hyperactivation and interferes with normal programs of osteo-chondro progenitor cell proliferation and differentiation [10]. Experimental induction of closed bone fractures in the femoral bone of *Nf1Prx1*<sup>-/-</sup> mice causes deterioration of the regeneration process [37]. Major histological findings were: (a) diminished cartilaginous callus formation; (b) increased periosteal bone formation in the fractured *Nf1Prx1*<sup>-/-</sup> cortical bone; and (c) accumulation and persistence of the fibrous tissue in the *Nf1Prx1*<sup>-/-</sup> fracture gap with the abundant incidence of smooth muscle actin positive myofibroblasts and TRAP positive osteoclasts. *Nf1* inactivation severely inhibited cartilaginous callus formation while fibrous cells and myofibroblasts populated the fracture site preventing normal healing. This was paralleled by an acceleration of periosteal bone formation, which did not result in fracture bridging. This ossification did not significantly contribute to the overall repair process, as it occurred distant to the fracture gap. The osteoblast mediated matrix mineralization in the fracture gap was defective, and the bone regeneration process did not reestablish functional bone. Thus, among available mouse models, *Nf1Prx1*<sup>-/-</sup> mice appear to resemble most closely the tibial dysplasia and pseudarthrosis situation. Based on this and other models it is suggested that the etiology of tibial dysplasia and pseudarthrosis involves double *NF1* inactivation and is driven by aberrant developmental processes.

### ***Treatment of Long Bone Dysplasia in Mouse Models—The Attempts of Pharmacological Intervention***

The pseudarthrosis of long bones associated with NF1 can cause significant morbidity. Multiple unsuccessful surgeries trying to achieve union are frequent, and ultimately can result in amputation [38]. Poor physical function is still common for individuals with tibial dysplasia that have not developed pseudarthrosis, and those with pseudarthrosis that achieve union after surgical attempts (unpublished observations). Various surgical approaches and combinations of surgical/pharmacologic approaches have been attempted clinically to treat tibial pseudarthrosis. (Reviewed in Stevenson et al. [39].) In brief, procedures include intramedullary rodding, external fixation, vascularized fibula grafting, etc. Pharmacologic adjunctive approaches have been attempted including bisphosphonates and bone morphogenetic proteins (BMPs). However, whether these methods are truly beneficial is not at all clear, as systematic randomized control trials are absent and data are based currently on anecdotal case series. In some instances mouse models have been used to test various pharmacologic agents for NF1 pseudarthrosis.

## Statins

Statins are inhibitors of 3-hydroxy-3-methylglutaryl coenzyme A reductase, broadly used for the reduction of serum cholesterol. As statins inhibit the initial enzyme of the mevalonate pathway, they also reduce prenylation and farnesylation of signaling molecules, such as Ras and Ras-related proteins [40–42]. Further research has shown that statins induce a direct bone anabolic effect, which translates into accelerated bone healing in rats and mice [43, 44]. Statin-induced bone formation is associated with increased osteoblast differentiation as measured by alkaline phosphatase, bone morphogenic protein 2 (BMP-2) and osteocalcin expression [45]. In addition, statins have been shown to inhibit bone resorption by interfering with osteoclast function in a similar way as bisphosphonates [46]. The influence of high dose Lovastatin (0.15 mg/mouse per day) on cortical bone regeneration was tested in the *Nf1Prx1<sup>-/-</sup>* model [47]. Systemic Lovastatin accelerated medullar bone formation and thus enhanced the process of cortical bone regeneration. Also, statins reduced MAPK activation in calvarial bones of *Nf1Prx1<sup>-/-</sup>* mice [47]. Similarly, local lovastatin delivery with microparticles also accelerated bone formation and reduced osteoidosis in *Nf1Col1<sup>-/-</sup>* mice [35]. Thus, delayed bone healing after injury in *Nf1Prx1<sup>-/-</sup>* and *Nf1Col1<sup>-/-</sup>* mice could be accelerated by high dose, systemically delivered lovastatin and low dose locally delivered lovastatin, respectively. Another study of lovastatin in the context of *Nf1* deficiency found that low bone mineral content in the vertebra of *Nf1Col2<sup>-/-</sup>* embryos could be partially reversed by administration of lovastatin microparticles intraperitoneally to the pregnant female mice throughout the second half of pregnancy [11]. These data collectively indicate that mevalonate pathway inhibition is a promising strategy of improving bone formation in NF1. Further translational studies and particularly development of FDA approvable local statin delivery systems are needed to further explore feasibility of statins as pharmacological substances suitable for NF1 pseudarthrosis treatment.

## The TGF Beta Signaling and TβRI Kinase Inhibitor

Increased synthesis of TGF beta by the *Nf1* deficient osteoblasts has been documented in one specific *Nf1* knockout mouse model where one allele of *Nf1* is inactivated in the entire organism and the second allele is inactivated in the osteoblast lineage (*Nf1 flox<sup>-/-</sup>;Col2.3Cre* mice) [48]. This is supported in human studies where increased TGFbeta concentrations were also found in the serum samples from NF1 patients. Interestingly, treatment of *Nf1 flox<sup>-/-</sup>;Col2.3Cre* mice with the TβRI kinase inhibitor, SD-208, rescued bone mass deficits and prevented tibial fracture non-unions. The same inhibitor completely inhibited pSMAD2 activation in pre-osteoclasts in-vitro and dose dependently inhibited osteoclast differentiation and dentin slice resorption in-vitro [48]. From these results, the authors postulated that overproduction of TGF beta by osteoblasts is one of the mechanisms of osteoclast activation and bone loss in *Nf1* deficient mice. This hypothesis is an attractive one and will require further investigation to assess therapeutic efficacy.

## Bisphosphonates and BMPs

Abnormalities in bone formation and resorption have been observed in *Nf1* deficient mice. One study addressed a possibility of combining bisphosphonates and bone morphogenetic proteins for induction of bone formation and inhibition of bone resorption [49]. In this study *Nf1*<sup>+/-</sup> osteoblasts were shown to respond to BMP2 *in vitro* with increased alkaline phosphatase expression and enhanced matrix mineralization. Bone formation was tested in the heterotopic intramuscular BMP2 carboxymethylcellulose carrier implantation model [49]. In this setup *Nf1*<sup>+/+</sup> (wildtype) mice consistently showed less heterotopic bone than *Nf1*<sup>+/-</sup> controls when analyzed 3 and 6 months post implantation. BMP-only treatment resulted in bone formation, which was strongly counter-balanced by the resorption. When mice were dosed twice weekly with 0.02 mg/kg zoledronic acid (ZA) commencing three days postoperatively, ZA treatment produced a striking increase in the radiographic BMD of BMP-2-induced heterotopic bone. ZA-treated mice showed a robust retention of trabecular bone, while bone was almost completely lost in the saline treated mice. Thus, dual treatment with BMPs and bisphosphonates appears to be a promising strategy for future clinical tests in the treatment of tibial dysplasia and pseudarthrosis.

For additional information on the topic of tibial dysplasia and current therapeutic guidance, we refer readers to our recent review [39].

## Scoliosis

Scoliosis is a very frequent musculoskeletal manifestation of NF1 (Fig. 2.6). About 10–30% of NF1 individuals develop scoliosis, and it is estimated that 2% of all childhood scoliosis cases are NF1 patients [28]. Scoliosis in NF1 is traditionally described as “dystrophic” or “non-dystrophic”. The term dystrophic describes a dysplastic type of scoliosis with a rapid course of progression [50].

Non-dystrophic scoliosis is more common in NF1, characterized by slow progression similar to idiopathic adolescent scoliosis. Although non-dystrophic scoliosis in NF1 is also poorly understood, it may arise secondary to muscle weakness, specifically hypotonia and weakness of spinal musculature [51]. It is important to note that defects in dorsal musculature cause a profound kyphosis in *Nf1Prx1*<sup>-/-</sup> mice (Fig. 2.2b) [33]. This phenotype is due to weakness of muscles that normally keep the spine straight (e.g. *m. latissimus dorsi*). Chest wall deformities in NF1 may also be the result of an abnormal muscle phenotype, an idea that derives from the observation that *Nf1Prx1*<sup>-/-</sup> mice develop a profound chest wall deformation (*pectus carinatum*) (data not shown) despite the fact that the chest wall bone and cartilage are not affected by *Nf1* inactivation in this model. Thus, we can postulate a role of spinal and chest musculature in the etiology of this symptom in *Nf1Prx1*<sup>-/-</sup> mice and in chest wall deformities in NF1 patients.

Dystrophic scoliosis is one of the most severe and morbid osseous manifestations occurring in NF1 patients (Fig. 2.3b, c). Dystrophic scoliosis usually manifests in

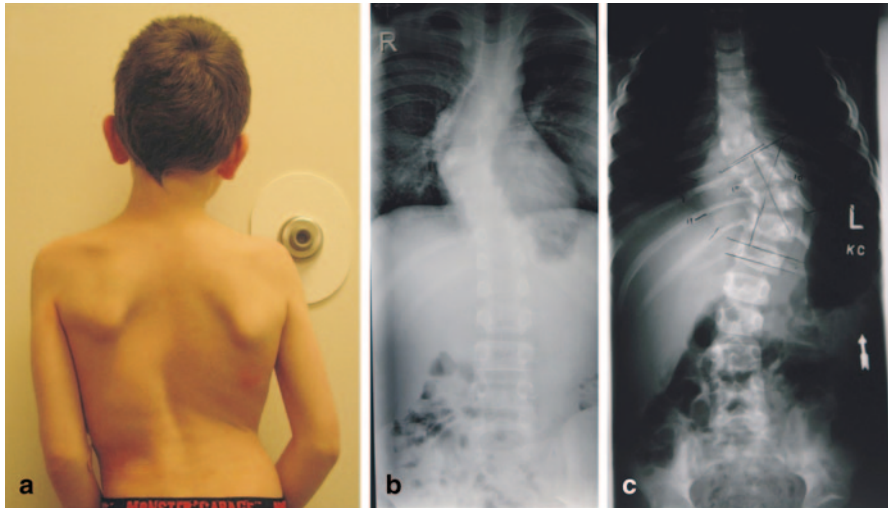


**Fig. 2.6** Scoliosis in neurofibromatosis type 1 (NF1). **a** Child with NF1 and scoliosis. **b, c** Radiographs of individuals with NF1 with dystrophic scoliosis

pre-adolescent NF1 children as a sharp angulated curve along a short segment of the spine, usually 4–6 vertebrae. This kind of scoliosis is typically associated with dysplastic vertebral elements. *Durrani et al.* listed nine radiographic features associated with dystrophic scoliosis (1.) rib penciling, (2.) vertebral rotation, (3.) posterior vertebral scalloping, (4.) anterior vertebral wedging, (5.) lateral vertebral scalloping, (6.) vertebral wedging in either the sagittal or coronal plane, (7.) spindling of the transverse process, (8.) widened interpedicular distance, and (9.) enlarged intervertebral foramina. It has also been noted that in 70% of dystrophic scoliosis cases, nearby tumors could be detected via MRI [28, 52, 53]. The observations that spinal neurofibromas associate with 70% of the cases of dystrophic scoliosis fostered belief that adjacent neurofibromas might cause bone lytic lesions and dystrophic scoliosis. However, in 30% cases there are no spinal neurofibromas in proximity of dystrophic vertebrae, indicating that tumors are not necessary for dystrophic scoliosis to occur [52, 53]. The exact etiology of dystrophic scoliosis is not well understood; however, the role of a local skeletal defect (similar to long bone dysplasia) appears likely. Mouse experiments support this concept [11]. Analysis of the *Nf1Col2<sup>-/-</sup>* mice suggest that dystrophic scoliosis in NF1 might result from a bone cell-autonomous defect. The *Nf1Col2<sup>-/-</sup>* model closely recapitulates vertebral skeletal deterioration observed in NF1 [26]. In *Nf1Col2<sup>-/-</sup>* mice, *Nf1* was doubly inactivated in all chondrogenitor cells of the skeleton, including the vertebrae. Importantly, spinal neurofibromas were not observed in *Nf1Col2<sup>-/-</sup>* mice. In these mice, vertebral fusions were observed at the base of the tail and loss of alignment of vertebral bodies was seen at one month of age. By 3 months of age, scoliosis and kyphosis were observed and by 6 months of age mice developed vertebral fusions and severe loss of BMD in the vertebral column. Indeed, changes in the vertebral

column were so dramatic that parts of the vertebra (*vertebral pedicles*) quasi disappeared. These observations deliver a strong argument for the hypothesis that the vertebral phenotype in mice and possibly vertebral dysplasia in NF1 patients is bone-cell autonomous with a developmental origin.

## Craniofacial Bone Lesions

The most frequent cranial defect in NF1 is sphenoid wing dysplasia (dysplasia of the greater wing of the sphenoid bone in the skull), which has been estimated to occur in  $\approx 10\%$  of NF1 patients [54]. Most cranial defects are associated with plexiform neurofibromas, often with infiltration and decalcification of the bone adjacent to the tumor [55, 56]. Therefore, it is currently thought that sphenoid wing is caused by encroachment of nearby tumors. However it is also possible that neurofibromin has a mesenchymal tissue-autonomous function in cranial bones and that loss of this function is involved in the etiology of sphenoid wing dysplasia. Data from the *Nf1Prx1*<sup>-/-</sup> mouse model support such a notion; inactivation of *Nf1* in the cranial mesenchyme (*Nf1Prx1*<sup>-/-</sup> mice) causes delayed ossification of the flat bones of the hind cranium (Fig. 2.4e, f). In these mice, flat bones of the hind cranium are formed with delay and appear to be initially replaced by the cartilaginous anlagen. Thus, *Nf1Prx1*<sup>-/-</sup> mice show delays of cranial bone formation, an observation suggestive of a possible mesenchymal cell autonomous role of NF1 in the cranial skeleton.

## Muscle Phenotype

The muscle phenotype in individuals with NF1 is not well described but abnormal motor proficiency [57, 58], decreased muscle area [59], and decreased grip strength has been documented in NF1 [60] providing evidence that skeletal muscle is affected in NF1. Mouse studies also suggest that neurofibromin impacts the regulation of myoblast differentiation and various downstream pathways have been implicated [33]. Increased STAT3 signaling was recently shown to characterize cancer associated muscle cachexia [61], and STAT3 is downstream of Ras and potentially contributes to the anti-myogenic phenotype in NF1 [62]. In addition to the dramatic decreased in strength and muscle size in the *Nf1Prx1*<sup>-/-</sup> mice, there were significant muscle abnormalities including lipid droplet apposition within the muscle fibers, and increased adipose tissue between muscle fibers in this mouse model [33]. The c-Jun/JNK pathway is involved in the regulation of fatty acid metabolism [63], and it can be expected that increased JNK signaling due to loss of *NF1* will induce glucose oxidation and decrease cellular nonesterified fatty acid oxidation while promoting conversion to phospholipids and triglycerides. Thus, *NF1* is likely involved in the regulation of glucose and lipid homeostasis in skeletal muscles.

A further in-depth review of the signaling pathways downstream of neurofibromin and their involvement in skeletal muscle development (e.g. cAMP-PKA, MEK1, STAT3, PI3K, mTOR) is beyond the scope of this chapter [64–67]. However, NF1 mouse models in combination with the human NF1 phenotype provide significant evidence that muscle is affected in NF1, and we suggest that the abnormal muscle phenotype contributes significantly to the skeletal abnormalities in NF1.

## Conclusions

As outlined in this chapter, loss of *NF1* negatively affects both skeletal and muscle tissue. We have reviewed current information about the mechanisms behind bony and muscular manifestations in NF1. An important point from these studies is that NF1 is not simply a neoplastic disorder, but also a developmental dysplasia. As recently and most appropriately articulated by Prof. Vincent Riccardi [68], “NF1 is a disorder of dysplasia with importance in distinguishing features, consequences and complications”, and it fully applies to the skeletal and muscle manifestations.

## References

1. Huson SM, Harper PS, Compston DA. Von Recklinghausen neurofibromatosis. A clinical and population study in south-east Wales. *Brain*. 1988;111(Pt 6):1355–81.
2. National Institutes of Health Consensus Development Conference Statement: neurofibromatosis. Bethesda, Md., USA, July 13–15, 1987. *Neurofibromatosis*, 1988;1(3):172–8.
3. Kayes LM, et al. Large de novo DNA deletion in a patient with sporadic neurofibromatosis I, mental retardation, and dysmorphism. *J Med Genet*. 1992;29(10):686–90.
4. Upadhyaya M, et al. An absence of cutaneous neurofibromas associated with a 3-bp inframe deletion in exon 17 of the NF1 gene (c.2970-2972 delAAT): evidence of a clinically significant NF1 genotype-phenotype correlation. *Am J Hum Genet*. 2007;80(1):140–51.
5. Viskochil D. Genetics of neurofibromatosis 1 and the NF1 gene. *J Child Neurol*. 2002;17(8):562–70; (discussion 571–2, 646–51).
6. Mundlos S. Skeletal morphogenesis. *Methods Mol Biol*. 2000;136:61–70.
7. Szudek J, Birch P, Friedman JM. Growth charts for young children with neurofibromatosis 1 (NF1). *Am J Med Genet*. 2000;92(3):224–8.
8. Virdis R, et al. Growth and pubertal disorders in neurofibromatosis type 1. *J Pediatr Endocrinol Metab*. 2003;16(Suppl 2):289–92.
9. Hegedus B, et al. Neurofibromin regulates somatic growth through the hypothalamic-pituitary axis. *Hum Mol Genet*. 2008;17(19):2956–66.
10. Kolanzyk M, et al. Multiple roles for neurofibromin in skeletal development and growth. *Hum Mol Genet*. 2007;16(8):874–86.
11. Wang W, et al. Mice lacking Nf1 in osteochondroprogenitor cells display skeletal dysplasia similar to patients with neurofibromatosis type I. *Hum Mol Genet*. 2011;20(20):3910–24.
12. Illes T, et al. Decreased bone mineral density in neurofibromatosis-1 patients with spinal deformities. *Osteoporos Int*. 2001;12(10):823–7.

13. Kuorilehto T, et al. Decreased bone mineral density and content in neurofibromatosis type 1: lowest local values are located in the load-carrying parts of the body. *Osteoporos Int.* 2005;16(8):928–36.
14. Lammert M, et al. Decreased bone mineral density in patients with neurofibromatosis 1. *Osteoporos Int.* 2005;16(9):1161–6.
15. Dulai S, et al. Decreased bone mineral density in neurofibromatosis type 1: results from a pediatric cohort. *J Pediatr Orthop.* 2007;27(4):472–5.
16. Stevenson DA, et al. Bone mineral density in children and adolescents with neurofibromatosis type 1. *J Pediatr.* 2007;150(1):83–8.
17. Yilmaz K, et al. Bone mineral density in children with neurofibromatosis 1. *Acta Paediatr.* 2007;96(8):1220–2.
18. Duman O, et al. Bone metabolism markers and bone mineral density in children with neurofibromatosis type-1. *Brain Dev.* 2008;30(9):584–8.
19. Brunetti-Pierri N, et al. Generalized metabolic bone disease in Neurofibromatosis type I. *Mol Genet Metab.* 2008;94(1):105–11.
20. Heerva E, et al. A controlled register-based study of 460 neurofibromatosis 1 patients: increased fracture risk in children and adults over 41 years of age. *J Bone Miner Res.* 2012;27(11):2333–7.
21. George-Abraham JK, et al. Fractures in children with neurofibromatosis type 1 from two NF clinics. *Am J Med Genet A.* 2013;161(5):921–6.
22. Stevenson DA, et al. Pediatric 25-hydroxyvitamin D concentrations in neurofibromatosis type 1. *J Pediatr Endocrinol Metab.* 2011;24(3–4):169–74.
23. Lammert M, et al. Vitamin D deficiency associated with number of neurofibromas in neurofibromatosis 1. *J Med Genet.* 2006;43(10):810–3.
24. Seitz S, et al. High bone turnover and accumulation of osteoid in patients with neurofibromatosis 1. *Osteoporos Int.* 2010;21(1):119–27.
25. Elefteriou F, et al. ATF4 mediation of NF1 functions in osteoblast reveals a nutritional basis for congenital skeletal dysplasiae. *Cell Metab.* 2006;4(6):441–51.
26. Ono K, et al. The Ras-GTPase activity of neurofibromin restrains ERK-dependent FGFR signaling during endochondral bone formation. *Hum Mol Genet.* 2013;22(15):3048–62.
27. Ozasa A, et al. Complementary antagonistic actions between C-type natriuretic peptide and the MAPK pathway through FGFR-3 in ATDC5 cells. *Bone.* 2005;36(6):1056–64.
28. Elefteriou F, et al. Skeletal abnormalities in neurofibromatosis type 1: approaches to therapeutic options. *Am J Med Genet A.* 2009;149A(10):2327–38.
29. Stevenson DA, et al. The use of anterolateral bowing of the lower leg in the diagnostic criteria for neurofibromatosis type 1. *Genet Med.* 2007;9(7):409–12.
30. Stevenson DA, et al. Double inactivation of NF1 in tibial pseudarthrosis. *Am J Hum Genet.* 2006;79(1):143–8.
31. Sugatani T, Alvarez U, Hruska KA. PTEN regulates RANKL- and osteopontin-stimulated signal transduction during osteoclast differentiation and cell motility. *J Biol Chem.* 2003;278(7):5001–8.
32. Franzen A, et al. Altered osteoclast development and function in osteopontin deficient mice. *J Orthop Res.* 2008;26(5):721–8.
33. Kossler N, et al. Neurofibromin (Nf1) is required for skeletal muscle development. *Hum Mol Genet.* 2011;20(14):2697–709.
34. Lasater EA, et al. Genetic and cellular evidence of vascular inflammation in neurofibromin-deficient mice and humans. *J Clin Invest.* 2010;120(3):859–70.
35. Wang W, et al. Local low-dose lovastatin delivery improves the bone-healing defect caused by Nf1 loss of function in osteoblasts. *J Bone Miner Res.* 2010;25(7):1658–67.
36. El-Hoss J, et al. A murine model of neurofibromatosis type 1 tibial pseudarthrosis featuring proliferative fibrous tissue and osteoclast-like cells. *J Bone Miner Res.* 2012;27(1):68–78.
37. El Khassawna T, et al. Deterioration of fracture healing in the mouse model of NF1 long bone dysplasia. *Bone.* 2012;51(4):651–60.

38. Stevenson DA, et al. Descriptive analysis of tibial pseudarthrosis in patients with neurofibromatosis 1. *Am J Med Genet.* 1999;84(5):413–9.
39. Stevenson DA, et al. Approaches to treating NF1 tibial pseudarthrosis: consensus from the Children’s Tumor Foundation NF1 bone abnormalities consortium. *J Pediatr Orthop.* 2013;33(3):269–75.
40. Khanzada UK, et al. Potent inhibition of small-cell lung cancer cell growth by simvastatin reveals selective functions of Ras isoforms in growth factor signalling. *Oncogene.* 2006;25(6):877–87.
41. Morgan MA, et al. Combining prenylation inhibitors causes synergistic cytotoxicity, apoptosis and disruption of RAS-to-MAP kinase signalling in multiple myeloma cells. *Br J Haematol.* 2005;130(6):912–25.
42. Ghittoni R, et al. Simvastatin inhibits T-cell activation by selectively impairing the function of Ras superfamily GTPases. *FASEB J.* 2005;19(6):605–7.
43. Garrett IR, et al. Locally delivered lovastatin nanoparticles enhance fracture healing in rats. *J Orthop Res.* 2007;25(10):1351–7.
44. Skoglund B, Aspenberg P. Locally applied Simvastatin improves fracture healing in mice. *BMC Musculoskelet Disord.* 2007;8:98.
45. Ohnaka K, et al. Pitavastatin enhanced BMP-2 and osteocalcin expression by inhibition of Rho-associated kinase in human osteoblasts. *Biochem Biophys Res Commun.* 2001;287(2):337–42.
46. Fisher JE, et al. Alendronate mechanism of action: geranylgeraniol, an intermediate in the mevalonate pathway, prevents inhibition of osteoclast formation, bone resorption, and kinase activation in vitro. *Proc Natl Acad Sci U S A.* 1999;96(1):133–8.
47. Kolanczyk M, et al. Modelling neurofibromatosis type 1 tibial dysplasia and its treatment with lovastatin. *BMC Med.* 2008;6:21.
48. Rhodes SD, et al. Hyperactive transforming growth factor-beta1 signaling potentiates skeletal defects in a neurofibromatosis type 1 mouse model. *J Bone Miner Res.* 2013;28(12):2476–89.
49. Schindeler A, et al. Modeling bone morphogenetic protein and bisphosphonate combination therapy in wild-type and Nf1 haploinsufficient mice. *J Orthop Res.* 2008;26(1):65–74.
50. Durrani AA, et al. Modulation of spinal deformities in patients with neurofibromatosis type 1. *Spine (Phila Pa 1976).* 2000;25(1):69–75.
51. Forst R, et al. Characteristics in the treatment of scoliosis in muscular diseases. *Z Orthop Ihre Grenzgeb.* 1997;135(2):95–105.
52. Khong PL, et al. MR imaging of spinal tumors in children with neurofibromatosis 1. *AJR Am J Roentgenol.* 2003;180(2):413–7.
53. Tsirikos AI, et al. Assessment of vertebral scalloping in neurofibromatosis type 1 with plain radiography and MRI. *Clin Radiol.* 2004;59(11):1009–17.
54. Friedman JM, Birch PH. Type 1 neurofibromatosis: a descriptive analysis of the disorder in 1728 patients. *Am J Med Genet.* 1997;70(2):138–43.
55. Jacquemin C, et al. Reassessment of sphenoid dysplasia associated with neurofibromatosis type 1. *AJNR Am J Neuroradiol.* 2002;23(4):644–8.
56. Jacquemin C, Bosley TM, Svedberg H. Orbit deformities in craniofacial neurofibromatosis type 1. *AJNR Am J Neuroradiol.* 2003;24(8):1678–82.
57. Johnson BA, et al. Motor proficiency in children with neurofibromatosis type 1. *Pediatr Phys Ther.* 2010;22(4):344–8.
58. Johnson BA, et al. Lower extremity strength and hopping and jumping ground reaction forces in children with neurofibromatosis type 1. *Hum Mov Sci.* 2012;31(1):247–54.
59. Stevenson DA, et al. Case-control study of the muscular compartments and osseous strength in neurofibromatosis type 1 using peripheral quantitative computed tomography. *J Musculoskel Neuron Interact.* 2005;5(2):145–9.
60. Stevenson DA, et al. Peripheral muscle weakness in RASopathies. *Muscle Nerve.* 2012;46(3):394–9.
61. Bonetto A, et al. STAT3 activation in skeletal muscle links muscle wasting and the acute phase response in cancer cachexia. *PLoS One.* 2011;6(7):e22538.

62. Hoene M, et al. Interleukin-6 promotes myogenic differentiation of mouse skeletal muscle cells: role of the STAT3 pathway. *Am J Physiol Cell Physiol*. 2013;304(2):C128–36.
63. Vijayvargia R, et al. JNK deficiency enhances fatty acid utilization and diverts glucose from oxidation to glycogen storage in cultured myotubes. *Obesity (Silver Spring)*. 2010;18(9):1701–9.
64. Dang I, De Vries GH. Aberrant cAMP metabolism in NF1 malignant peripheral nerve sheath tumor cells. *Neurochem Res*. 2011;36(9):1697–705.
65. Perry RL, Parker MH, Rudnicki MA. Activated MEK1 binds the nuclear MyoD transcriptional complex to repress transactivation. *Mol Cell*. 2001;8(2):291–301.
66. Banerjee S, et al. The neurofibromatosis type 1 tumor suppressor controls cell growth by regulating signal transducer and activator of transcription-3 activity in vitro and in vivo. *Cancer Res*. 2010;70(4):1356–66.
67. Ma J, et al. Hyperactivation of mTOR critically regulates abnormal osteoclastogenesis in neurofibromatosis Type 1. *J Orthop Res*. 2012;30(1):144–52.
68. Riccardi VM. Neurofibromatosis type 1 is a disorder of dysplasia: the importance of distinguishing features, consequences, and complications. *Birth Defects Res A Clin Mol Teratol*. 2010;88(1):9–14.

# Chapter 3

## Molecular Genetics of Congenital Multiple Large Joint Dislocation

Stephen P. Robertson

**Abstract** As the rate of discovery of loci mutated in monogenic disorders accelerates there has been a rapid increase in the recognition and definition of syndromic conditions characterised by dislocation of the large joints. Assigning a correct clinical diagnosis with corroboration through molecular genetic testing is important because disorders demonstrating both autosomal dominant and autosomal recessive inheritance can be difficult to distinguish from one another in the neonatal period. While the pathogenic mechanisms underlying most of these conditions remains elusive, several conditions have been identified that relate to disturbances of proteoglycan (PG) metabolism and a primary dysfunction of connective tissue in the periarticular joint capsule. In contrast an understanding of the aetiology and pathogenesis of the most common form of non-syndromic joint dislocation, developmental dysplasia of the hip, has remained stubbornly refractory to understanding despite considerable clinical and epidemiological evidence to suggest that genetic factors contribute to the susceptibility to this disorder.

**Keywords** Joint dislocation · Larsen syndrome · Proteoglycan synthesis · Ehlers Danlos syndrome arthrochalasia type · Congenital multiple large joint dislocation

### Definition of Large Joint Dislocation

Congenital joint dislocation is defined here as the disarticulation of a synovial joint structure that is evident at birth. This chapter focuses on genetic conditions that primarily present with dislocation of the large joints—the shoulder, elbow, hip and knee joints—although involvement of smaller joints can be a clinical accompaniment. Many Mendelian conditions have been described in which large joint dislocation is both an infrequent or variable clinical manifestation,

---

S. P. Robertson (✉)  
Department of Women's and Children's Health, Dunedin School of Medicine,  
University of Otago, Dunedin 9054, New Zealand  
e-mail: stephen.robertson@otago.ac.nz

and symptoms and signs in other organ systems primarily guide diagnosis. Some conditions present with primary ligamentous laxity that can predispose to either recurrent joint subluxation or frank dislocation, but presentation with congenital disarticulation of joint structures is rare. For that reason this group of disorders is not considered in detail here. Similarly, those disorders in which joint dislocation is confined to one type of joint—e.g. the hips or radio-humeral joint, are not described in detail.

A large and heterogeneous group of conditions exist which present with multiple joint dislocations as a secondary consequence of neuromuscular disease. Although systematic studies are lacking, as a group they numerically are likely to comprise the commonest cause of congenital multiple large joint dislocation. Several excellent reviews exist that describe the underlying basis for these disorders which is frequently located in molecular abnormalities of the muscle sarcomere or neuromuscular synapse [1, 2]. Since the evaluation of these children is focused on the primary neuromuscular cause, this large group of conditions are not considered in detail here. In this chapter, the major Mendelian disorders characterised by large joint dislocation are described together with what is understood about their molecular pathogenesis. Developmental dysplasia of the hip is briefly reviewed within the final section alongside a broad discussion of the aetiopathogenesis of these conditions as a group.

## **Mendelian Disorders of Congenital Large Joint Dislocation**

There are no accurate prevalence figures for any of the monogenic conditions discussed in this chapter, but most disorders are likely to be present at rates less frequent than 1:100,000 in most populations. Some disorders with autosomal recessive inheritance patterns may exhibit founder effects in some communities although, again, precise estimates of these allele frequencies are not available. Although many Mendelian conditions can exhibit congenital large joint dislocation as a presenting feature, a relatively small number have this sign as a primary and reproducible presenting feature. The latter conditions are the focus of the discussion below with the emphasis placed on clinical and molecular insights into the pathogenesis of joint dysfunction. The list of Mendelian disorders that present primarily with congenital large joint dislocation is presented in Table 3.1. Currently new, predominantly recessive phenotypes are being defined at the molecular genetic level and it is likely that this list will grow substantially in the near future.

**Table 3.1** Mendelian disorders presenting with congenital dislocation of the large joints

	Gene	OMIM number
<i>Autosomal dominant</i>		
Larsen syndrome	<i>FLNB</i>	150250
Ehlers Danlos syndromes, arthrochalasia type	<i>COL1A1, COL1A2</i>	130060
Spondyloepimetaphyseal dysplasia with joint laxity- type 2	<i>KIF22</i>	603546
<i>Autosomal recessive</i>		
Spondyloepimetaphyseal dysplasia with joint laxity type 1	<i>B3GALT6</i>	271640
Multiple joint dislocations—CHST3 type	<i>CHST3</i>	143095
Multiple joint dislocations—B3GAT3 type	<i>B3GAT3</i>	245600
Chondrodysplasia with joint dislocation- GPAPP type	<i>IMPAD1</i>	614078
Desbuquois dysplasia type 1	<i>CANTI</i>	251450
Desbuquois dysplasia type 2	<i>Unknown</i>	251450
Multiple Joint Dislocations—Reunion Island type	<i>Unknown</i>	245600

## Autosomal Dominant Disorders

### *Larsen syndrome (OMIM 150250)*

Larsen syndrome is characterized by a variable combination of congenital dislocations of the large joints (elbows, hips, knees, occasionally shoulders), scoliosis, cleft palate, conductive deafness and cervical kyphosis, which can be associated with cervical spinal cord damage [3]. It exhibits complete penetrance with significantly variable expressivity. The vast majority of individuals in Larsen syndrome (as defined by a phenotype shown to be caused by a mutation in *FLNB*) have dislocations or subluxations of the large joints (80% hip, 80% knee, and 65% elbow) with subluxation of the shoulders being the mildest manifestation (Fig. 3.1a). Clubfoot is also present in 75%. Larsen syndrome is allelic to three other disorders of defective osteogenesis—atelosteogenesis types I and III and Boomerang dysplasia—making up the so-called Larsen syndrome-atelosteogenesis “LS-AO” spectrum disorders. The latter two disorders in the spectrum are invariably lethal in the perinatal period [4]. Despite this link, stature is only mildly affected in Larsen syndrome with the height of the majority of individuals with the condition lying between the 1st and 10th centile. Radiographically evident spinal abnormalities are present in the majority with some degree of cervical spinal dysplasia noted in 50%. Typically this takes the form of subluxation or fusion of the bodies of C2–C4, associated with posterior vertebral arch dysraphism. Individuals with Larsen syndrome and cervical spine dysplasia are at significant risk of cervical cord myelopathy and secondary tetraparesis. Other clinical findings include cleft palate and conductive deafness. Although



**Fig. 3.1** Radiographs of individuals with multiple large joint dislocation syndromes. **a** Larsen syndrome showing disarticulation of the knee and elbow joints, but, with the exception of distal tapering of the humerus, little disturbance to the morphogenesis of the bony structures of the skeleton. **b** Radiographs of the knee joints of an adult individual with CHST3 deficiency show significant erosion and destruction of the joint spaces as a consequence of the epiphyseal dysplasia seen in this condition in the context of chronic joint dislocation. **c** Desbuquois dysplasia demonstrating shortening of the long bones, metaphyseal widening and dislocation of the radial head and advanced bone age. An accessory ossification center is evident proximal to the proximal phalanx of the second digit (*arrowed*)

laryngotracheomalacia has been reported in association with Larsen syndrome, few individuals with confirmed Larsen syndrome are severely affected. Survival into adulthood is the norm, and cognitive functioning is unaffected. Clinical variability can result from the presence of somatic mosaicism for a causative mutation in a mildly affected parent with the associated mutation in the germline leading to a more severe phenotype in the offspring.

Although the primary clinical presenting feature in Larsen syndrome is dislocation of the large joints there are no consistent primary epiphyseal or metaphyseal anomalies present. In some individuals with a clinical diagnosis of Larsen syndrome a tapering distal humerus can be observed, reminiscent of that seen in the allelic disorder atelosteogenesis III. The most characteristic radiological signs are the appearance of supernumerary carpal ossification centres evident from early childhood onwards. A bipartite calcaneal ossification centre is similarly seen but is a less specific diagnostic sign.

Larsen syndrome is caused by missense mutations or small in-frame deletions in the gene encoding the actin binding protein, filamin B [3, 4]. The level of expression of protein is unaffected by these mutations and the phenotypic dissimilarity between LS and the allelic loss of function recessive disorder, spondylocarpotarsal syndrome, has led to the conclusion that mutations leading to LS lead to disease through a gain of function mechanism. All three filamin paralogs (filamin A, B and C) encode a highly homologous tertiary structure with an N-terminal actin binding domain composed of two calponin homology domains, CH1 and CH2 followed by a chain of 24 filamin repeats, each which adopt an immunoglobulin-like barrel structure consisting of seven folded  $\beta$ -strands. The chain of filamin repeats is interrupted by two “hinge” regions between repeats 15 and 16 and repeats 23 and 24. Filamin

B adopts a dimeric structure *in vivo* and *in vitro*, this interaction being mediated by the anti-parallel apposition of repeat 24 from each monomer.

Mutations leading to Larsen syndrome are clustered within exons encoding the actin binding domain or in the region of the gene specifying domains flanking the flexible hinge region of the filamin B protein. To date over 40 mutations have been described with some mutations being highly recurrent as *de novo* events in unrelated individuals (Table 3.2). For pathogenic substitutions occurring in the actin binding domain of the protein, a gain of function of mechanism has been proposed manifested biochemically by enhanced avidity for the binding partner actin [5]. A similar but more pronounced biochemical property is conferred by mutations

**Table 3.2** Mutations in *FLNB* leading to Larsen syndrome

Mutation	Protein	Protein domain
c.362A > T	p.Tyr121Phe	CH2
c.482T > G	p.Phe161Cys	CH2
c.488A > C	p.Gln163Pro	CH2
c.500A > G	p.Asp167Gly	CH2
c.501C > A	p.Asp167Glu	CH2
c.508G > C	p.Ala170Pro	CH2
c.520C > A	p.Leu174Met.	CH2
c.572C > T	p.Pro191Leu	CH2
c.590A > T	p.Asn197Ile	CH2
c.622T > C	p.Trp208Arg	CH2
c.661A > T	p.Ile221Phe	CH2
c.679G > A	p.Glu227Lys	CH2
c.685T > C	p.Ser229Pro	CH2
c.700C > G	p.Leu234Val	CH2
c.719C > T	p.Ala240Val	CH2
c.4292T > G	p.Leu1431Arg	Repeat 13
c.4550C > A	p.Ala1517Asp	Repeat 14
c.4580T > A	p.Leu1527His	Repeat 14
c.4580T > C	p.Leu1527Pro	Repeat 14
c.4621G > C	p.Ala1541Pro	Repeat 14
c.4625T > C	p.Ile1542Thr	Repeat 14
c.4711_4713del	p.1571delAsn	Repeat 14
c.4725_4736del12	p.1576_1579del	Repeat 14
c.4756G > A	p.Gly1586Arg	Repeat 14
c.4769T > C	p.Ile1590Thr	Repeat 14
c.4775T > A	p.Val1592Asp	Repeat 14
c.4781A > C	p.Tyr1594Ser	Repeat 14
c.4795A > T	p.Ile1599Phe	Repeat 14

**Table 3.2** (continued)

Mutation	Protein	Protein domain
c.4805C > A	p.Ser1602Tyr	Repeat 14
c.4808C > T	p.Pro1603Leu	Repeat 14
c.4936G > A	p.Gly1646Ser	Repeat 15
c.5023_5025delTTC	p.1675delPhe	Repeat 15
c.5047A > T	p.Thr1683Ser	Repeat 15
c.5071G > T	p.Gly1691Cys	Repeat 15
c.5071G > A	p.Gly1691Ser	Repeat 15
c.5072G > A	p.Gly1691Asp	Repeat 15
c.5095C > G	p.Pro1699Ala	Repeat 15
c.5706C > A	p.Ser1902Arg	Repeat 17
c.5705C > A	p.Ser1902Ile	Repeat 17

that lead to atelosteogenesis types I and III and Boomerang dysplasia, suggesting that the defect in osteogenesis evident in these disorders might have its subclinical equivalent in individuals with Larsen syndrome. No clear explanation for how the substitutions that cluster around the hinge region confer the phenotype has been offered but these mutations have been shown to lead to a redistribution of filamin protein from a cortical to a perinuclear position [6].

LS and its allelic disorders, atelosteogenesis types 1 and 3 and Boomerang dysplasia, share significant phenotypic similarities to the filaminopathies caused by mutations in the paralogous gene *FLNA*, although notably joint dislocations are not a feature of this group of disorders [7]. Although the differing expression of *FLNB* and *FLNA* over the growth plate may explain some of the differences in the chondrodysplasia seen in the *FLNA*-linked otopalatodigital syndrome spectrum disorders and the LS-AO spectrum [4], the role of *FLNB* in the formation and integrity of the joint capsule, possibly underlying the multiple congenital joint dislocations observed in these conditions, has not been investigated. Within the growth plate of individuals with AO1 there has been the frequent observation of multinucleate giant cells in the context of a relatively cell sparse structure. This suggests that *FLNB* exerts some role in cell proliferation or division, and indeed *FLNB* has been observed lining the cell cleavage furrow of dividing chondrocytes in normal human growth plate [4].

### ***The Ehlers Danlos Syndrome (EDS) Arthrochalasia Type***

The group of conditions broadly subsumed under the term Ehlers Danlos syndromes phenotypically manifest with connective tissue dysfunction leading to fragile, thin or wrinkled skin, joint hypermobility and occasionally fragility of other organ systems such as the vasculature. In the Villefranche classification of EDS [8], six main

descriptive types were substituted for earlier types numbered with Roman numerals. One form in particular, the arthrochalasia type (formally termed EDS VII) is characterised by hip dislocation. This disorder is caused by a genetically determined resistance to enzymatic procollagen maturation. Milder forms of EDS (EDS hypermobility type) and familial joint instability syndrome are more associated with pronounced joint laxity and congenital joint dislocation is uncommon.

EDS, arthrochalasia type, is distinguished clinically from the other types of EDS by the frequency of congenital hip dislocation, extreme joint laxity with recurrent joint subluxations but minimal skin involvement [9, 10]. Dislocation of the knees and other large joints can occasionally be observed [11], the fingers can exhibit swan neck deformities and contractures and inguinal herniae have recurrently been observed. Radiographic manifestations can include calvarial wormian bones and recurrent fractures. EDS, arthrochalasia type, is caused by either monoallelic mutations in *COL1A1* and *COL1A2* [12–15] where they lead to the exclusion of exon 6 which encodes procollagen N-proteinase cleavage site of each respective gene transcript [9]. Interestingly, biallelic mutations in the gene encoding the procollagen protease convertase itself, *ADAMTS2*, cause EDS dermatospraxis type, which is characterised by a severe skin phenotype and joint hypermobility, but only rarely congenital joint dislocation. The presumptive pathogenesis of this disorder presumably relates to the role that collagen 1 plays in the integrity of the articular joint capsule of the large synovial joints.

### ***Spondyloepimetaphyseal Dysplasia with Joint Laxity-2***

The principal clinical characteristics of SEMDJL2 (previously termed SEMD-JL-leptodactylic type or SEMD-JL-Hall type) include generalized ligamentous laxity (especially evident at the knees), short stature, maxillary retrusion and mild spinal deformities [16]. Dislocations can occur at all the large joints but the knees are the most commonly and severely affected joint. Laryngotracheomalacia in infancy and childhood has been reported in a sizable minority of cases [17, 18] and occasionally necessitating tracheostomy placement [19]. Marked intrafamilial phenotypic variability has been observed. Features that are noticeably absent in described cases to date that might aid in differential diagnosis, particularly from Larsen syndrome, include cleft palate, deafness and congenital kyphoscoliosis. Key radiographic findings include small, flattened, irregular and fragmented epiphyses and widened, irregular metaphyses with striations. The dorsal vertebral bodies show posterior decrease in height, vertebral endplate irregularity, and progressive caudal narrowing of the interpedicular distances. The metacarpals are gracile with long slender phalanges and the distal phalangeal tufts are prominent. The carpal bones are small and irregular and progressively erode over adolescence and into adulthood. There is a global epiphyseal delay in ossification, especially evident in the phalanges [20]. The disorder evolves into an epiphyseal dysplasia with the precocious development of osteoarthritis.

SEMD-JL2 is caused by heterozygosity for mutations in *KIF22* which encodes KIF22, a kinesin motor domain-containing protein that has homology to proteins that mediate intracellular transport along microtubular structures [20, 21]. Mutations are exclusively missense, are recurrent and all mutations reported to date occur in exon 4 which encodes highly conserved residues which are adjacent to an ATP binding site within the motor domain of the protein. Notably KIF22 binds to chromosomes and appears to have functions relating to chromosomal segregation during certain phases of mitosis [22, 23]. It is perhaps notable that a cell cycle related function is implicated in the pathogenesis of a joint dislocation disorder, just as some observations relating to the pathogenesis of some of the LS-AO spectrum syndromes also indicate a disturbance in cell division.

## Autosomal Recessive Disorders

### *Spondyloepimetaphyseal Dysplasia with Joint Laxity Type 1*

Originally described in South African families of Afrikaans descent [24], Spondyloepimetaphyseal dysplasia with joint laxity type 1 (SEMDJL1; previously termed SEMDJL-Beighton type) is characterized by the cardinal skeletal findings of vertebral abnormalities and ligamentous laxity. This disorder evolves a progressive severe kyphoscoliosis, often resulting in severe respiratory compromise. Large joint manifestations include dislocation of the radial head and dislocated hips. Clubfeet are commonly observed and a subset of patients can also present with bone fragility [25]. Joint hypermobility is particularly evident in the hands and a dysmorphic facial profile has been proposed (an oval face, with maxillary flattening, prominent eyes and a long philtrum). Cleft palate is commonly observed [24, 26–28]. Accompanying features included skin fragility, delayed wound healing, joint hyperlaxity and contractures and intellectual disability. The progressive kyphoscoliosis associated with this disorder is especially refractory to external bracing and internal fixation is often indicated. Progression can often not only result in cardiorespiratory compromise but also spinal cord compression. Death within the first two decades of life is common although survival into the fourth decade has been reported [29]. The radiological phenotype of this condition consists of the severe scoliosis, ‘bat-like’ splaying of the ilia, dysplastic acetabulae and brachydactyly. In some individuals expanded metaphyses can be present [30, 31].

Bilallelic mutations in *B3GALT6* cause SEMDJL1. *B3GALT6* encodes a glycosyltransferase (B3GALNT6) that is central for the initiation of both chondroitin sulfate and heparin sulfate biosynthesis (Fig. 3.2). These glycosaminoglycans are central components of articular and other forms of cartilage. Their synthesis progresses by the iterative transfer of monosaccharide residues to the lengthening side chains, a process mediated by glycosyl transferases [32]. B3GALNT6 catalyses a priming step in the initial phases of this process, sponsoring the addition of the second galactose unit to the common linker peptide. Functional studies of B3GALT6

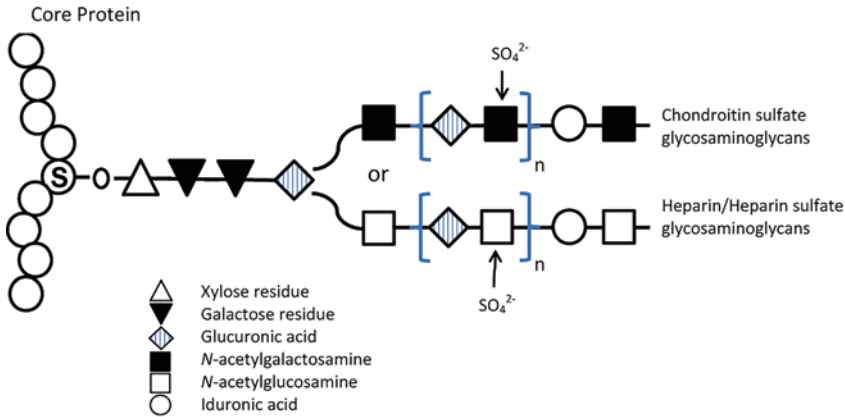


**Fig. 3.2** Diagram of proteoglycan synthesis with the locations of defects leading to congenital large joint dislocation phenotypes. Glycosaminoglycan side chains are added to core proteins through the hydroxyl group of serine residues. A common tetra-saccharide linker region is synthesised first with the sequential addition of a xylose residue followed by two galactose residues and finally a glucuronate residue. Defects in the enzymes adding the second galactose residue and the final glucuronic acid residue to the common linker region lead to SEMD-JL type1 and multiple joint dislocations—B3GAT3 type respectively. Defective generation of nucleoside modified monosaccharide substrates prior to their addition to GAG sidechains, are causative of Desbuquois dysplasia and multiple joint dislocations GPAPP type. Defects in the sulfation of secreted chondroitin sulfate glycosaminoglycans is a hallmark of multiple joint dislocations-CHST3 type

proteins with mutations shown to cause SEMDJL1 showed a loss of function due to either cellular mislocalisation or deficient catalytic activity. Patient fibroblasts exhibit substantially diminished priming of glycosaminoglycan synthesis together with impaired glycanation of the small chondroitin/dermatan sulfate PG decorin. Dermal electron microscopy show abnormalities in collagen fibril organization which may contribute to the ligamentous laxity, cutaneous manifestations, joint hypermobility, osteopenia and bone fragility.

Mutations in *B3GALT6* also cause a progeroid type of Ehlers-Danlos syndrome (EDSP2; OMIM 615349), which shares phenotypic similarities with SEMDJL1 although, notably large joint hypermobility rather than frank congenital joint dislocation is a feature of this latter condition [33]. EDSP exhibits locus heterogeneity with some individuals having mutations in *B4GALT7*, which encodes galactosyl-transferase 1. Mutations underlying SEMDJL1 and EDSP2 both seem to confer loss of enzymatic function and so the explanation of the phenotypic differences resulting from these two allelic disorders is yet to be explained. In a cohort from Asia [33] a disorder with features overlapping SEMDJL1 and the progeroid form of Ehlers-Danlos syndrome (EDSP2) was described indicating a broader than suspected spectrum of phenotypic severity. Adding further to the broad expressivity of conditions associated with biallelic loss of function mutations at this locus, Malfait et al. described another severe spondyloepimetaphyseal dysplasia with bone fragility, multiple early-onset fractures, and severe kyphoscoliosis [25].

### ***Autosomal Recessive Multiple Joint Dislocations—CHST3 Type***

This spondyloepiphyseal dysplasia (SED) is one of the more common autosomal recessive joint dislocation syndromes. Initially described by Cortina et al. [34] and in two large Omani kindreds [35] and labelled alternatively by the names humero-spinal dysostosis and spondyloepiphyseal dysplasia, Omani type, respectively, the clinical features of this condition include near to normal length at birth, short stature (adult height of 110–139 cm) rhizomelic shortening of the upper limbs, childhood onset severe progressive kyphoscoliosis, and an epiphyseal dysplasia that results in arthritic changes with joint dislocations, genu valgum, cubitus valgus, mild and irregular brachydactyly, and camptodactyly. Congenital dislocation of the knees and/or hips is common, as is clubfoot. A dysplasia of the upper cervical spine can result in clinical instability and require stabilisation [36]. Supernumerary carpal and tarsal bones can be observed [36, 37]. Microdontia is an association, intelligence is typically normal [38] but significant valvular heart disease can evolve in this condition [39] (Fig. 3.1b).

Typically during childhood, the dislocations improve, both spontaneously and with surgical treatment, and features of spondyloepiphyseal dysplasia (SED) become apparent, leading to arthritis of the hips and spine with intervertebral disc degeneration, rigid kyphoscoliosis, and trunk shortening by late childhood [38]. The radiologic presentation is one of spondyloepiphyseal dysplasia with minimal metaphyseal involvement. In infancy the vertebral bodies only exhibit endplate irregularity but this progresses with intervertebral space narrowing, intervertebral fusion and the evolution of a kyphoscoliosis. The epiphyses are small and a significant osteoarthropathy usually develops involving both small and large joints.

Biallelic mutations in *CHST3* cause SED-CHST3 type [37, 38, 40, 41]. The biochemical deficit is a specific defect in sulfation of chondroitin sulfate side chains (Fig. 3.2).

### ***Multiple Joint Dislocations—B3GAT3 Type***

Baasanjav et al. [42] defined this condition by linking the autosomal recessive co-inheritance of multiple large joint dislocations with significant and severe congenital heart defects [42]. Heart defects included bicuspid aortic valve with dilation of the aortic root, mitral valve prolapse, and ventricular septal defect. The morphogenic defects in cardiac valvular structures seen in this condition may relate to the significant dependence that these structures have upon PG synthesis. The joint dislocations were limited to dislocations and contractures of the elbow joints as well as talipes equinovarus and/or metatarsus varus in addition to small joint hypermobility. One individual had dislocation of the shoulder and proximal radioulnar joints. The sibs reported by Strisciuglio et al. [43] may have had the same disorder. This condition is caused by biallelic mutations in *B3GAT3* gene. This gene encodes glucuronosyltransferase I, an enzyme that mediates a critical step in PG

linker synthesis—the addition of the final glucuronic acid residue to the terminal part of the common linker region (Fig. 3.2). Accordingly skin fibroblasts from individuals with this condition demonstrate diminished levels of all types of O-linked glycanated PGs: dermatan sulfate, chondroitin sulfate and heparin sulfate.

### ***Desbuquois Dysplasia***

This well-recognised chondrodysplasia has also emerged as a deficiency in PG synthesis, but instead of the lesion being in either the sulfation of GAGs or in linker synthesis, this condition is caused by defective metabolism of monosaccharides within the Golgi compartment of the cell. Desbuquois dysplasia (DBQD) is characterized by prenatal and postnatal growth retardation (stature less than  $-5$  SD), joint laxity leading to dislocations particularly at the hips and knees but also the small joints of the hand, short extremities, and progressive scoliosis. A distinctive facial gestalt has been recognised with a round flat face, prominent eyes, micrognathia, and long upper lip with flat philtrum being features. Glaucoma can be an accompaniment as can renal anomalies such as ureteropelvic dilatation, horseshoe kidney, and renal cysts [44–46]. Radiological examination holds the key to diagnosis—short long bones with metaphyseal widening, a ‘Swedish key’ appearance of the proximal femur and coronal clefting of the vertebrae in early infancy are key diagnostic signs. The carpal and tarsal bone age is advanced. Hand anomalies are a useful diagnostic sign and are the primary clinical discriminator between the two subtypes of this disorder. The presence (type 1) or absence (type 2) of hand anomalies including an extra ossification center proximal to the second proximal phalanx (termed a delta phalanx), bifid distal phalanx on the thumb, and dislocation of the interphalangeal joints define these two subgroupings [45] (Fig. 3.1c). This dichotomy is not absolute however and a hypomorphic phenotype, allelic to DD type 1 has also been described in eastern Asian populations [47–49].

Homozygosity or compound heterozygosity for mutations in *CANTI* cause Desbuquois dysplasia type 1 [50]. *CANTI* encodes for calcium activated nucleotidase 1, an enzyme that acts to hydrolyse nucleotide di- and triphosphates. CANT1 shows highest activity towards UDP, GDP, and UTP, all of which are important in the enzymatic modification of monosaccharides in the Golgi prior to their incorporation into PG side chains. It is likely that all mutations leading to this phenotype confer a loss of function since missense mutations identified in individuals with this disorder cluster in and around the catalytic site of the enzyme substituting highly conserved residues. Truncating mutations in *CANTI* are possibly correlated with early morbidity due to respiratory insufficiency. Accordingly PG production has been shown to be reduced in fibroblasts obtained from individuals with DD [51]. Growth plate cartilage shows dilated cisterns of rough endoplasmic reticulum in reserve zone chondrocytes in individuals with DD.

### ***Chondrodysplasia with Joint Dislocations, GPAPP Type***

This condition has been defined by a single report of four individuals with short stature, a chondrodysplasia with brachydactyly, congenital joint dislocations, micrognathia, cleft palate, and facial dysmorphism [52]. This condition is caused by biallelic mutations in *IMPAD1* which encodes a Golgi resident nucleotide phosphatase, Golgi 3' phosphoadenosine 5' phosphate 3' phosphatase (GPAPP). Although experimental data are lacking to point to a likely pathogenic mechanism leading to this condition, the defect in nucleoside di- and tri- phosphate recycling could lead to a similar limitation in PG biosynthesis as that seen in Desbuquois dysplasia.

### ***Multiple Congenital Joint Dislocations with Short Stature—Reunion Island Type***

A distinctive autosomal recessive multiple large joint dislocation syndrome has been described amongst the residents of the Indian ocean island, La Reunion [53]. The disorder has strong similarities to those conditions caused by other recessive disorders of PG biosynthesis with the phenotype being characterised by short stature (<-4SDS), dysmorphic facies, bilateral dislocations of the elbows, hips, and knees, clubfeet, and short stature, as well as cardiovascular defects. Radiographs demonstrate osteoporosis in the setting of early bone maturation with multiple ossification centers, and metaphyseal enlargement with diaphyseal bowing.

### ***Developmental Dysplasia of the Hips***

Developmental dysplasia of the hip (DDH) is an abnormality of the seating of the femoral head in the acetabulum. Its severity ranges from mild instability of the femoral head with slight capsular laxity, through moderate lateral displacement of the femoral head, without loss of contact of the head with the acetabulum, up to complete dislocation of the femoral head from the acetabulum. It is one of the most common skeletal congenital anomalies, approximating an incidence of 1:1000 in populations with Western European ancestry, although there is a great discrepancy in the frequency of DDH according to geographic and ethnic differences.

A number of lines of evidence point to a genetic predisposition unpinning DDH. In general, DDH is more frequent in whites than in blacks and Chinese [54]. Classical studies estimated sib recurrence rates in the region of 5% [55]. DDH also demonstrates a female preponderance [54]. Much of the thinking underpinning the pathogenesis of the disorder relates to factors that impact upon the laxity of joint capsule on one hand and the degree of acetabular dysplasia on the other [56–58]. A number of apparently monogenic forms of DDH have been described, all of which have yet to have a molecular basis defined, that may illuminate some of these contributory genetic factors [59–62]. Having acknowledged that Mendelian disorders

have much to contribute in terms of understanding the pathogenesis of diseases with multifactorial and complex genetic architecture such as DDH, it is notable that no well powered genome wide association study has been performed to identify some associated loci contributing to the susceptibility to the development of the disorder. The reasons for this lack are unclear but once performed, an informative study is likely to synergise strongly with insights gained in recent years on the aetiopathogenesis of Mendelian syndromes characterised by congenital large joint dislocation.

### ***Overview of the Aetiopathogenesis of Large Joint Dislocation***

New insights into the developmental biology of joint formation has been obtained from the study of genetic joint dislocation syndromes. While the pathogenesis of some conditions is perhaps self-evident—e.g. the protein collagen 1, the genes for which are mutated in EDS arthrochalasia type, is an integral component of the synovial joint capsule—other molecular players such as filamin B and KIF22, mediate enigmatic roles. An unanticipated but consistent theme from the study of Mendelian disorders featuring large joint dislocation is that defects in PG synthesis interfere with joint development. Although PGs are known to be important components of cartilage architecture, the mechanism by which they contribute to the morphogenesis of joint structures is less evident. Recent work has shown that deficiency of the chondroitin sulfate PG versican reduces the interzone space of developing synovial joints in the chick [63] and leads to dislocated small joint structures in the mouse [64]. The expression of this PG is developmentally regulated in early joint morphogenesis and interacts with other molecular factors such as CD44 and hyaluronan which are well established key regulators of the genesis of different joint structures. While it would be premature to implicate this particular PG as the key unitary factor in the pathogenesis of these disorders, it is clear that further research should be redirected to focus on PGs as developmental regulators in joint morphogenesis.

### **References**

1. Kalampokas E, Kalampokas T, Sofoudis C, Deligeoroglou E, Botsis D. Diagnosing arthrogyriposis multiplex congenita: a review. *ISRN Obstet Gynecol.* 2012;2012:264918.
2. Hall JG. Arthrogyriposis multiplex congenita: etiology, genetics, classification, diagnostic approach, and general aspects. *J Pediatr Orthop.* 1997;6:159–66.
3. Bicknell LS, Farrington-Rock C, Shafeghati Y, Rump P, Alanay Y, Alembik Y, Al-Madani N, Firth H, Karimi-Nejad MH, Kim CA, et al. A molecular and clinical study of Larsen syndrome caused by mutations in FLNB. *J Med Genet.* 2007;44:89–98.
4. Krakow D, Robertson SP, King LM, Morgan T, Sebald ET, Bertolotto C, Wachsmann-Hogiu S, Acuna D, Shapiro SS, Takafuta T, et al. Mutations in the gene encoding filamin B disrupt vertebral segmentation, joint formation and skeletogenesis. *Nat Genet.* 2004;36:405–10.
5. Sawyer GM, Clark AR, Robertson SP, Sutherland-Smith AJ. Disease-associated substitutions in the filamin B actin binding domain confer enhanced actin binding affinity in the absence of major structural disturbance: insights from the crystal structures of filamin B actin binding domains. *J Mol Biol.* 2009;390:1030–47.

6. Daniel PB, Morgan T, Alanay Y, Bijlsma E, Cho TJ, Cole T, Collins F, David A, Devriendt K, Faivre L, et al. Disease-associated mutations in the actin-binding domain of filamin B cause cytoplasmic focal accumulations correlating with disease severity. *Hum Mutat.* 2012;33:665–73.
7. Robertson SP, Twigg SR, Sutherland-Smith AJ, Biancalana V, Gorlin RJ, Horn D, Kenwrick SJ, Kim CA, Morava E, Newbury-Ecob R, et al. Localized mutations in the gene encoding the cytoskeletal protein filamin A cause diverse malformations in humans. *Nat Genet.* 2003;33:487–91.
8. Beighton P, De Paepe A, Steinmann B, Tsipouras P, Wenstrup RJ. Ehlers-Danlos syndromes: revised nosology, Villefranche, 1997. Ehlers-Danlos National Foundation (USA) and Ehlers-Danlos Support Group (UK). *Am J Med Genet.* 1998;77:31–7.
9. Byers PH, Duvic M, Atkinson M, Robinow M, Smith LT, Krane SM, Grealley MT, Ludman M, Matalon R, Pauker S, et al. Ehlers-Danlos syndrome type VIIA and VIIB result from splice-junction mutations or genomic deletions that involve exon 6 in the COL1A1 and COL1A2 genes of type I collagen. *Am J Med Genet.* 1997;72:94–105.
10. Giunta C, Superti-Furga A, Spranger S, Cole WG, Steinmann B. Ehlers-Danlos syndrome type VII: clinical features and molecular defects. *J Bone Joint Surg.* 1999;81:225–38.
11. Cole WG, Chan D, Chambers GW, Walker ID, Bateman JF. Deletion of 24 amino acids from the pro-alpha 1(I) chain of type I procollagen in a patient with the Ehlers-Danlos syndrome type VII. *J Biol Chem.* 1986;261:5496–503.
12. Steinmann B, Tuderman L, Peltonen L, Martin GR, McKusick VA, Prockop DJ. Evidence for a structural mutation of procollagen type I in a patient with the Ehlers-Danlos syndrome type VII. *J Biol Chem.* 1980;255:8887–93.
13. Weil D, D'Alessio M, Ramirez F, de Wet W, Cole WG, Chan D, Bateman JF. A base substitution in the exon of a collagen gene causes alternative splicing and generates a structurally abnormal polypeptide in a patient with Ehlers-Danlos syndrome type VII. *EMBO J.* 1989;8:1705–10.
14. Weil D, D'Alessio M, Ramirez F, Eyre DR. Structural and functional characterization of a splicing mutation in the pro-alpha 2(I) collagen gene of an Ehlers-Danlos type VII patient. *J Biol Chem.* 1990;265:16007–11.
15. Weil D, D'Alessio M, Ramirez F, Steinmann B, Wirtz MK, Glanville RW, Hollister DW. Temperature-dependent expression of a collagen splicing defect in the fibroblasts of a patient with Ehlers-Danlos syndrome type VII. *J Biol Chem.* 1989;264:16804–9.
16. Hall CM, Elcioglu NH, Shaw DG. A distinct form of spondyloepimetaphyseal dysplasia with multiple dislocations. *J Med Genet.* 1998;35:566–72.
17. Park SM, Hall CM, Gray R, Firth HV. Persistent upper airway obstruction is a diagnostic feature of spondyloepimetaphyseal dysplasia with multiple dislocations (Hall type) with further evidence for dominant inheritance. *Am J Med Genet.* 2007;143A:2024–8.
18. Holder-Espinasse M, Fayoux P, Morillon S, Fourier C, Dieux-Coeslier A, Manouvrier-Hanu S, Le Merrer M, Hall CM. Spondyloepimetaphyseal dysplasia (Hall type) with laryngeal stenosis: a new diagnostic feature? *Clin Dysmorphol.* 2004;13:133–5.
19. Kim OH, Cho TJ, Song HR, Chung CY, Miyagawa S, Nishimura G, Superti-Furga A, Unger S. A distinct form of spondyloepimetaphyseal dysplasia with joint laxity (SEMDJL)-leptodactylic type: radiological characteristics in seven new patients. *Skeletal Radiol.* 2009;38:803–11.
20. Min BJ, Kim N, Chung T, Kim OH, Nishimura G, Chung CY, Song HR, Kim HW, Lee HR, Kim J, et al. Whole-exome sequencing identifies mutations of KIF22 in spondyloepimetaphyseal dysplasia with joint laxity, leptodactylic type. *Am J Hum Genet.* 2011;89:760–6.
21. Boyden ED, Campos-Xavier AB, Kalamajski S, Cameron TL, Suarez P, Tanackovic G, Andria G, Ballhausen D, Briggs MD, Hartley C, et al. Recurrent dominant mutations affecting two adjacent residues in the motor domain of the monomeric kinesin KIF22 result in skeletal dysplasia and joint laxity. *Am J Hum Genet.* 2011;89:767–72.
22. Tokai N, Fujimoto-Nishiyama A, Toyoshima Y, Yonemura S, Tsukita S, Inoue J, Yamamota T. Kid, a novel kinesin-like DNA binding protein, is localized to chromosomes and the mitotic spindle. *EMBO J.* 1996;15:457–67.

23. Funabiki H, Murray AW. The *Xenopus* chromokinesin Xkid is essential for metaphase chromosome alignment and must be degraded to allow anaphase chromosome movement. *Cell*. 2000;102:411–24.
24. Beighton P. Spondyloepimetaphyseal dysplasia with joint laxity (SEMDJL). *J Med Genet*. 1994;31:136–40.
25. Malfait F, Karimnejad A, Van Damme T, Gauche C, Syx D, Merhi-Soussi F, Gulberti S, Symoens S, Vanhauwaert S, Willaert A, et al. Defective Initiation of Glycosaminoglycan synthesis due to B3GALT6 mutations causes a pleiotropic Ehlers-Danlos-Syndrome-like connective tissue disorder. *Am J Hum Genet*. 2013;92:935–45.
26. Torrington M, Beighton P. The ancestry of spondyloepimetaphyseal dysplasia with joint laxity (SEMDJL) in South Africa. *Clin Genet*. 1991;39:210–3.
27. Beighton P, Gericke G, Kozlowski K, Grobler L. The manifestations and natural history of spondylo-epi-metaphyseal dysplasia with joint laxity. *Clin Genet*. 1984;26:308–17.
28. Beighton P, Kozlowski K, Gericke G, Wallis G, Grobler L. Spondylo-epimetaphyseal dysplasia with joint laxity and severe, progressive kyphoscoliosis. A potentially lethal dwarfing disorder. *S Afr Med J (Suid-Afrikaanse tydskrif vir geneeskunde)*. 1983;64:772–5.
29. Tsirikos AI, Mason DE, Scott CI Jr, Chang WN. Spondyloepimetaphyseal dysplasia with joint laxity (SEMDJL). *Am J Med Genet*. 2003;119A:386–90.
30. Farag TI, Al-Awadi SA, Hunt MC, Satyanath S, Zahran M, Usha R, Uma R. A family with spondyloepimetaphyseal dwarfism: a 'new' dysplasia or Kniest disease with autosomal recessive inheritance? *J Med Genet*. 1987;24:597–601.
31. Bradburn JM, Hall BD. Spondyloepimetaphyseal dysplasia with joint laxity (SEMDJL): clinical and radiological findings in a Guatemalan patient. *Am J Med Genet*. 1995;59:234–7.
32. Bai X, Zhou D, Brown JR, Crawford BE, Hennet T, Esko JD. Biosynthesis of the linkage region of glycosaminoglycans: cloning and activity of galactosyltransferase II, the sixth member of the beta 1,3-galactosyltransferase family (beta 3GalT6). *J Biol Chem*. 2001;276:48189–95.
33. Nakajima M, Mizumoto S, Miyake N, Kogawa R, Iida A, Ito H, Kitoh H, Hirayama A, Mitsubuchi H, Miyazaki O, et al. Mutations in B3GALT6, which encodes a glycosaminoglycan linker region enzyme, cause a spectrum of skeletal and connective tissue disorders. *Am J Hum Genet*. 2013;92:927–34.
34. Cortina H, Vidal J, Vallcanera A, Alberto C, Muro D, Dominguez F. Humero-spinal dysostosis. *Pediatr Radiol*. 1979;8:188–90.
35. Rajab A, Kunze J, Mundlos S. Spondyloepiphyseal dysplasia Omani type: a new recessive type of SED with progressive spinal involvement. *Am J Med Genet*. 2004;126A:413–9.
36. Megarbane A. Osseous dysplasia with severe short stature, multiple dislocations, and delayed bone age: report on a second Lebanese patient. *Am J Med Genet*. 2007;143A:1782–7.
37. van Roij MH, Mizumoto S, Yamada S, Morgan T, Tan-Sindhunata MB, Meijers-Heijboer H, Verbeke JI, Markie D, Sugahara K, Robertson SP. Spondyloepiphyseal dysplasia, Omani type: further definition of the phenotype. *Am J Med Genet*. 2008;146A:2376–84.
38. Unger S, Lausch E, Rossi A, Megarbane A, Sillence D, Alcausin M, Aytes A, Mendoza-Londono R, Nampoothiri S, Afroz B, et al. Phenotypic features of carbohydrate sulfotransferase 3 (CHST3) deficiency in 24 patients: congenital dislocations and vertebral changes as principal diagnostic features. *Am J Med Genet*. 2010;152A:2543–9.
39. Tuysuz B, Mizumoto S, Sugahara K, Celebi A, Mundlos S, Turkmen S. Omani-type spondyloepiphyseal dysplasia with cardiac involvement caused by a missense mutation in CHST3. *Clin Genet*. 2009;75:375–83.
40. Hermanns P, Unger S, Rossi A, Perez-Aytes A, Cortina H, Bonafe L, Boccone L, Setzu V, Dutoit M, Sangiorgi L, et al. Congenital joint dislocations caused by carbohydrate sulfotransferase 3 deficiency in recessive Larsen syndrome and humero-spinal dysostosis. *Am J Hum Genet*. 2008;82:1368–74.
41. Thiele H, Sakano M, Kitagawa H, Sugahara K, Rajab A, Hohne W, Ritter H, Leschik G, Nurnberg P, Mundlos S. Loss of chondroitin 6-O-sulfotransferase-1 function results in severe human chondrodysplasia with progressive spinal involvement. *Proc Natl Acad Sci U S A*. 2004;101:10155–60.

42. Baasanjav S, Al-Gazali L, Hashiguchi T, Mizumoto S, Fischer B, Horn D, Seelow D, Ali BR, Aziz SA, Langer R, et al. Faulty initiation of proteoglycan synthesis causes cardiac and joint defects. *Am J Hum Genet.* 2011;89:15–27.
43. Strisciuglio P, Sebastio G, Andria G, Maione S, Raia V. Severe cardiac anomalies in sibs with Larsen syndrome. *J Med Genet.* 1983;20:422–4.
44. Faden M, Al-Zahrani F, Arafah D, Alkuraya FS. Mutation of CANT1 causes Desbuquois dysplasia. *Am J Med Genet.* 2010;152A:1157–60.
45. Faivre L, Le Merrer M, Zerres K, Ben Hariz M, Scheffer D, Young ID, Maroteaux P, Munnich A, Cormier-Daire V. Clinical and genetic heterogeneity in Desbuquois dysplasia. *Am J Med Genet.* 2004;128A:29–32.
46. Laccone F, Schoner K, Krabichler B, Kluge B, Schwerdtfeger R, Schulze B, Zschocke J, Rehder H. Desbuquois dysplasia type I and fetal hydrops due to novel mutations in the CANT1 gene. *Eur J Hum Genet.* 2011;19:1133–7.
47. Nishimura G, Hong HS, Kawame H, Sato S, Cai G, Ozono K. A mild variant of Desbuquois dysplasia. *Eur J Pediatr.* 1999;158:479–83.
48. Kim OH, Nishimura G, Song HR, Matsui Y, Sakazume S, Yamada M, Narumi Y, Alanay Y, Unger S, Cho TJ, et al. A variant of Desbuquois dysplasia characterized by advanced carpal bone age, short metacarpals, and elongated phalanges: report of seven cases. *Am J Med Genet.* 2010;152A:875–85.
49. Furuichi T, Dai J, Cho TJ, Sakazume S, Ikema M, Matsui Y, Baynam G, Nagai T, Miyake N, Matsumoto N, et al. CANT1 mutation is also responsible for Desbuquois dysplasia, type 2 and Kim variant. *J Med Genet.* 2011;48:32–7.
50. Huber C, Oules B, Bertoli M, Chami M, Fradin M, Alanay Y, Al-Gazali LI, Ausems MG, Bitoun P, Cavalcanti DP, et al. Identification of CANT1 mutations in Desbuquois dysplasia. *Am J Hum Genet.* 2009;85:706–10.
51. Nizon M, Alanay Y, Tuysuz B, Kiper PO, Genevieve D, Sillence D, Huber C, Munnich A, Cormier-Daire V. IMPAD1 mutations in two Catel-Manzke like patients. *Am J Med Genet.* 2012;158A:2183–7.
52. Vissers LE, Lausch E, Unger S, Campos-Xavier AB, Gilissen C, Rossi A, Del Rosario M, Venselaar H, Knoll U, Nampoothiri S, et al. Chondrodysplasia and abnormal joint development associated with mutations in IMPAD1, encoding the Golgi-resident nucleotide phosphatase, gPAPP. *Am J Hum Genet.* 2011;88:608–15.
53. Bonaventure J, Lasselin C, Mellier J, Cohen-Solal L, Maroteaux P. Linkage studies of four fibrillar collagen genes in three pedigrees with Larsen-like syndrome. *J Med Genet.* 1992;29:465–70.
54. Weinstein SL. Natural history of congenital hip dislocation (DDH) and hip dysplasia. *Clin Orthop Relat Res.* 1987;62–76.
55. Record RG, Edwards JH. Environmental influences related to the aetiology of congenital dislocation of the hip. *Br J Prev Soc Med.* 1958;12:8–22.
56. Wynne-Davies R. Acetabular dysplasia and familial joint laxity: two etiological factors in congenital dislocation of the hip. A review of 589 patients and their families. *J Bone Joint Surg Br.* 1970;52:704–16.
57. Carter CO, Wilkinson JA. Genetic and environmental factors in the etiology of congenital dislocation of the hip. *Clin Orthop Relat Res.* 1964;33:119–28.
58. Carter C, Wilkinson J. Persistent joint laxity and congenital dislocation of the hip. *J Bone Joint Surg Br.* 1964;46:40–5.
59. Mabuchi A, Nakamura S, Takatori Y, Ikegawa S. Familial osteoarthritis of the hip joint associated with acetabular dysplasia maps to chromosome 13q. *Am J Hum Genet.* 2006;79:163–8.
60. Sollazzo V, Bertolani G, Calzolari E, Atti G, Scapoli C. A two-locus model for non-syndromic congenital dysplasia of the hip (DDH). *Ann Hum Genet.* 2000;64:51–9.
61. Roby P, Eyre S, Worthington J, Ramesar R, Cilliers H, Beighton P, Grant M, Wallis G. Autosomal dominant (Beukes) premature degenerative osteoarthropathy of the hip joint maps to an 11-cM region on chromosome 4q35. *Am J Hum Genet.* 1999;64:904–8.

62. Cilliers HJ, Beighton P. Beukes familial hip dysplasia: an autosomal dominant entity. *Am J Med Genet.* 1990;36:386–90.
63. Nagchowdhuri PS, Andrews KN, Robart S, Capehart AA. Versican knockdown reduces interzone area during early stages of chick synovial joint development. *Anat Rec (Hoboken).* 2012;295:397–409.
64. Choocheep K, Hatano S, Takagi H, Watanabe H, Kimata K, Kongtawelert P, Watanabe H. Versican facilitates chondrocyte differentiation and regulates joint morphogenesis. *J Biol Chem.* 2010;285:21114–25.

# Chapter 4

## DMP-1 in Postnatal Bone Development

Shuxian Lin and Jerry Jian Q. Feng

**Abstract** Dentin matrix protein 1 (DMP1) was cloned from a rat dentin cDNA library 30 years ago. Initially, this non-collagenous matrix protein was thought to be dentin specific and attracted little interest in most scientific disciplines, except for the dental research area. In the last three decades, great progress has been made in the following four areas: (1) Gene expression studies show that DMP1 is widely expressed in both non-mineralized tissues (such as brain, kidney, salivary gland, and cancer tissues) and all mineralized tissues; it is highly expressed in osteocytes; (2) Protein chemistry studies confirm that full-length DMP1 is a precursor that is cleaved into two distinct forms: the C-terminal and N-terminal fragments; (3) Functional studies revealed that DMP1 is essential to the maturation of osteocytes and mineralization via local and systemic mechanisms; and (4) Genetic research identified DMP1 mutations in humans, leading to the discovery of a novel disease: autosomal recessive hypophosphatemic rickets. Importantly, the regulation of phosphate homeostasis by DMP1 through FGF23, a potent hormone that is released from bone and targeted in the kidneys, contributes to a new concept that connects bone with kidney and recognizes the osteocyte as an endocrine cell.

**Keywords** Dentin matrix protein 1 · Osteocyte · Bone · Phosphate homeostasis · Hypophosphatemic rickets

### Introduction

The extracellular matrix (ECM) serves many functions including providing support, regulating intercellular communication, along with sequestering a wide range of cellular growth factors and acts as a local depot for them, etc. The ECM of bone

---

J. J. Q. Feng (✉) · S. Lin  
Biomedical Sciences, Baylor College of Dentistry, TX A&M, 3302 Gaston Ave,  
Dallas, TX 75246, USA  
e-mail: jfeng@bcd.tamhsc.edu

S. Lin  
e-mail: shuxian.lin@hotmail.com

© Springer Science+Business Media New York 2015  
C. A. Wise, J. J. Rios (eds.), *Molecular Genetics of Pediatric Orthopaedic Disorders*,  
DOI 10.1007/978-1-4939-2169-0\_4

and dentin contains a large amount of minerals and numerous non-collagenous proteins (NCPs). One of the categories of NCPs is termed the “Small Integrin-Binding Ligand, N-linked Glycoprotein (SIBLINGs) family” based on the similarities of the intron/exon properties, conserved protein biochemical properties (such as unstructured and acidic), and specific peptide motifs (e.g., phosphorylation and integrin-binding arginine-glycin-aspartic acid (RGD)). There are five members in this SIBLINGs family: dentin matrix protein 1 (DMP1), bone sialoprotein (BSP), osteopontin (OPN), enamelin, matrix extracellular phosphoglycoprotein (MEPE), and dentin sialophosphoprotein (DSPP)[1]. DMP1 was originally identified by cDNA cloning from the rat dentin matrix [2] and was initially believed to be dentin-specific but was later observed in bone matrices at a much higher level [3, 4]. Studies suggested that DMP1 begins its expression at E15.5 and resides mainly in osteoblasts during embryonic development. However, DMP1 is predominantly expressed in the osteocytes during postnatal development [4, 5].

The *Dmp1* gene is mapped to the long (q) arm of chromosome 4 at position 21 (4q21) in humans and to 5q21 in mice. *Dmp1* is encoded by 6 exons with 80% of its coding information in exon 6. There are two promoter control domains: a proximal one located between the -2.4 kb and the +4 kb region, and a distal one between the -2.4 and -9.6 kb region. The proximal domain controls the early stages of DMP1 expression, and the distal domain controls the later stages [6]. AP-1, JunB, Runx2, Msx 1/2, Tcf/Lef, C/EBP, and YY-1 are essential transcription factors for bone and tooth tissue-specific regulation. The potential response elements for these transcription factors have been identified in the mouse *Dmp1* promoters [7].

DMP1 protein contains an unusually large number of acidic domains that are rich in Ser, Glu, and Asp; many of the Ser are in the consensus motif for potential phosphorylation via casein kinases I and II. Data obtained from protein chemistry studies on DMP1 isolated from rat bones showed that a full-length DMP1 molecule contains an average of 53 phosphate groups. This number indicates a potentially high calcium ion-binding capacity, a property considered necessary for a protein to participate in mineralization [8]. Studies suggested that the full-length DMP1 protein is likely a precursor that will be processed into 37-kDa N-terminal and 57-kDa C-terminal fragments (Fig. 4.1a). Extensive sequencing of tryptic peptides derived from DMP1 fragments and compared with the cDNA-deduced sequence has confirmed that rat DMP1 is proteolytically cleaved at four bonds: Phe<sup>173</sup>-Asp<sup>174</sup>, Ser<sup>180</sup>-Asp<sup>181</sup>, Ser<sup>217</sup>-Asp<sup>218</sup>, and Gln<sup>221</sup>-Asp<sup>222</sup>, among which Ser<sup>180</sup>-Asp<sup>181</sup> is the key cleavage site [8]. One group of candidate enzyme(s) responsible for DMP1 processing is bone morphogenetic protein 1 (BMP-1)/tolloid-like metalloproteinase [9], which is widely expressed in mesenchymal-derived tissues (including bone and cartilage) and has also been shown to cleave other protein precursors such as collagens [10]. Phosphate analysis indicated that DMP1 is highly phosphorylated: its C-terminal fragment contains 41 phosphate groups with a RGD tripeptide located in its central region, while the N-terminal fragment possesses only 12 phosphate groups. The C-terminal is currently considered to be the key functional domain, based on both *in vitro* and *in vivo* studies [11, 12] (Fig. 4.1a).

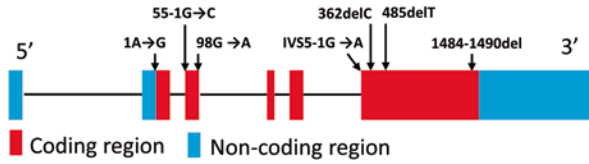


**Fig. 4.1** Schematic structure of DMP1 protein, gene and ARHR mutations. **a** Schematic structure of the human *DMP1* gene and ARHR mutations. *DMP1* is composed of six exons. Because of the recessive nature of this disease, there are only 7 variable mutations reported in the literature (see text for details). **b** Schematic structure of Full-length DMP1 protein: DMP1 signal peptide, MKTVILLVFLWGLSCAL, 37-kDa N-terminal fragment, a main cleavage site at peptide bond Ser196-Asp197, and the 57-kDa C-terminal fragment

## Dmp1 Mutation/Deletion Leads to Autosomal Recessive Hypophosphatemia

DMP1 is mainly expressed in mineralized tissues and plays an important role during osteogenesis [13], although some *in vivo* animal studies showed that DMP1 may also have potential functions in non-mineralized tissues such as in brain [14], kidney [15] and salivary tissues [16]. For example, DMP1 is thought to actively promote and control the mineralization of collagen fibers and crystal growth within osteoids and predentin when these tissues are converted to mature bone and dentin [13]. In addition, DMP1 regulates and supports the maturation of osteoblasts to osteocytes and pre-odontoblasts to odontoblasts [17]. Importantly, *DMP1* mutations in humans or deletion in mice lead to autosomal recessive hypophosphatemic rickets (ARHR)/osteomalacia [18]. It is noteworthy that, unlike other genetic disease cases in which human mutations are identified first and then animal studies such as gene knockouts are performed, it is the *Dmp1* null mouse research results [19, 20] that triggered searches for *DMP1* mutations in humans.

### *Autosomal Recessive Hypophosphatemia*

Rickets is the softening of bones in children because of a deficiency or impaired metabolism of vitamin D, phosphorus, or calcium. This disease not only interrupts child development but also can potentially lead to fractures and disturbance of normal ossification. Rickets due to nutrition deficiency is more common in children in developing countries. The adult equivalent of rickets is known as “osteomalacia”, a disease characterized by inadequate or delayed mineralization of osteoids in mature cortical and spongy bones. Hypophosphatemic rickets/osteomalacia is a group of disorders characterized by hypophosphatemia, which mainly results from disorders of renal phosphate wasting (Unlike the situation with calcium, there is no rickets due to phosphorus deficiency, since one’s daily diet is rich in this element). There are several inherited gene mutations responsible for deficiencies in reabsorption

in the renal tubule, which results in hypophosphatemia. For example, mutations in the *PHEX* gene (encoding phosphate regulating gene with homologies to endopeptidases on the X chromosome) lead to x-linked dominant hypophosphatemic (XLH) rickets [21], *FGF23* (encoding fibroblast growth factor 23) mutations result in autosomal dominant hypophosphatemic rickets (ADHR) [22], and homozygous inactivating mutations in *DMP1* cause autosomal recessive hypophosphatemic rickets (ARHR)/osteomalacia [18, 23, 25]. Comparisons of patients having XLH, the most common hypophosphatemic rickets, there are fewer than ten cases of kindred ARHR have been identified worldwide due to the autosomal recessive nature of the *DMP1* mutations [18, 23–26]. Molecular genetic analysis of these cases revealed the following changes: (1) the deletion of nucleotides 1484–1490 in exon 6 (1484–1490del) resulting in a frameshift that replaced the 18 conserved C-terminal residues with 33 unrelated residues, or another deletion in the same exon leading to a frameshift replacing 335 conserved amino acids with 53 unrelated ones; (2) a mutation in the start codon (1A→G) causing a methionine to valine change (M1V); (3) a homozygous 1-bp deletion in exon 6 (362delC) led to the placement of a premature stop codon after 120 unrelated amino acids; (4) a biallelic nucleotide substitution at nucleotide 98 in exon 3 (98G→A) introduced a premature termination codon (PTC) at codon 33, which replaced the wild type tryptophan residue (W33X); and (5) a mutation at the splice acceptor junction of exon 6 (IVS5–1G→A) or intron 2 (55–1G→G) is predicted to alter pre-mRNA splicing, which results in a shift in the open-reading frame if the final message is stable (Fig. 4.1b).

Considering the reported cases, the primary clinical symptoms of ARHR include: lower limb deformities (bowed legs or knock-knees), waddling gait, short stature or stunted growth, tooth abscesses or early loss of teeth, bone and muscle pain, biochemical abnormalities (hypophosphatemia with normal levels of serum calcium and parathyroid hormone). More severely afflicted patients may also suffer from nerve deafness, facial and dental abnormalities, learning disabilities, joint pain, and contracture and immobilization of the spine. Patients diagnosed with ARHR display symptoms in their early childhood that are likely to have a wide spectrum of severity, depending on the site and size of the mutations and the severity and chronicity of the associated phosphate depletion [27] (see Table 4.1).

As with the human patients, *Dmp1* null mice do not have apparent abnormalities during prenatal bone development, but severely impaired after birth presented as a chondrodysplasia-like phenotype that characterized by short and widened long bones with flared and irregular metaphyses, and malformed ossification centers with delayed development during postnatal growth [20]. In accordance with human patients, *Dmp1* null animals display significantly lower serum phosphorus level than the wild type controls, which is due to the increased urinary phosphate excretion. In addition to human patients, *Dmp1* null mice also significantly increase their serum PTH level [12, 17, 18]. Bone histological studies demonstrated that the *Dmp1* null mice displayed severe osteomalacia, which show as a significant reduction in bone mineralization together with increased osteoid and more porous cortical bone, compared to wild type littermates. Under higher-magnification back-scattered scanning

**Table 4.1** Characteristics of ARHP patients and mice models

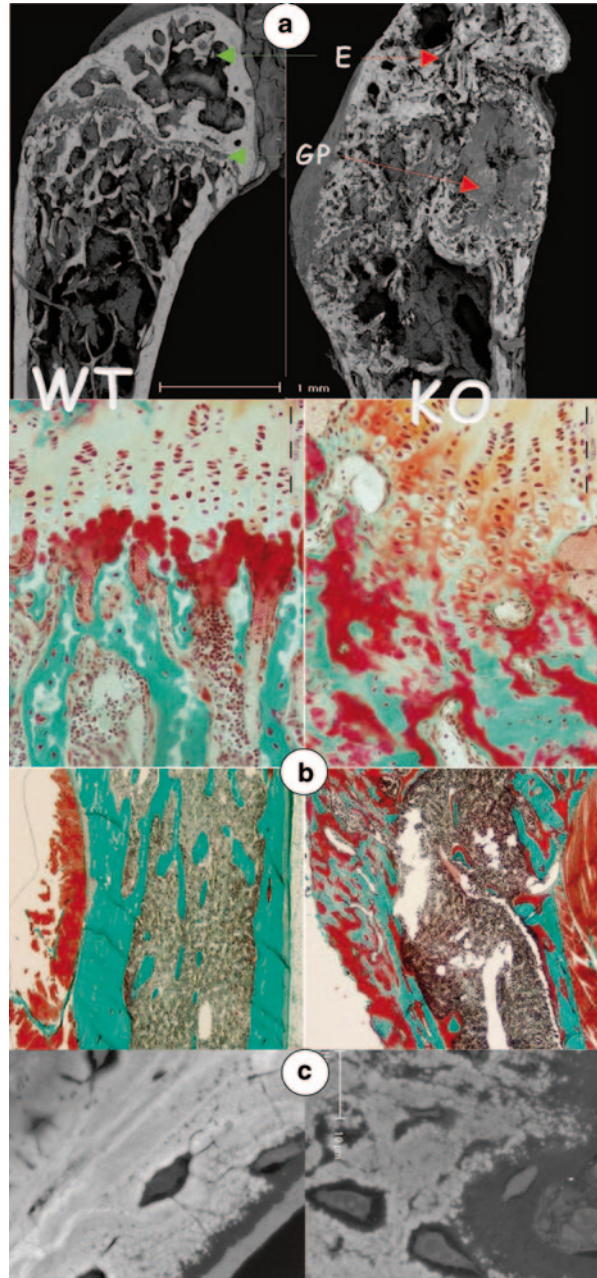
Aspects	Characteristic features	
<i>Clinical</i>	Figure	Short stature or growth retardation
	Posture	Waddling gait, immobilization of the spine, kyphosis
	Craniofacial	Facial abnormalities, tooth abscesses or early loss
	Limb	Genu varum or knock-knees
	Symptom	Bone and muscle pain, joint pain, contracture, enthesopathy, nerve deafness, learning disabilities
<i>Skeletal</i>	Craniofacial	Enlarged dental pulp chambers and thin dentin, thick calvarium and skull base, skeletal malocclusion
	Spine	Disappearance of intervertebral disks and disk space, ossification of the longitudinal ligament
	Joint	Loss of articular cartilage, narrowed joint space, osteophytes
	Limb	Short, broad, bowing, ossification of tendon attachments, pathological bone fractures
	Chest	Rachitic rosaries, narrow chest with wide clavicles
<i>Biochemistries</i>	Increase	FGF23, ALP
	Decrease	P <sub>i</sub> , TmP/GFR
	Normal	Ca

electron microscopic (SEM) images, the minerals, which are normally found to be evenly distributed around the osteocyte lacunae, were either absent or sparsely located in regions surrounding the *Dmp1* null osteocytes. Scanning transmission electron microscopic images indicated a much lower content of mineral, calcium, and phosphorus in the *Dmp1* null mineralized matrix (Fig. 4.2a, b, c) [12, 17, 18]. These observations suggested that genetic removal of *Dmp1* (in mice) and loss-function of *DMP1* mutation (in human ARHR kindreds) concurrently lead to independently altered skeletal mineralization and disturbed phosphate homeostasis.

### ***Osteocyte Maturation Defects in Dmp1 Null Mice***

An early transfection study of MC3T3-E1 cells that expressed excessive DMP1, displayed accelerated differentiation of osteoblasts and an earlier onset of mineralization, suggesting that DMP1 plays an important role during osteoblast differentiation, as well as osteocyte maturation and function [28]. It was later reported that patients with *DMP1* mutations or mice with *Dmp1* deletion did not display any gross abnormalities during the embryonic period or at birth [29]. However, they generally appeared to have the ARHP phenotype during their early postnatal development stage when DMP1 is highly produced by osteocytes and secreted into the mineral matrix. Further analysis indicated that *Dmp1* deletion leads to defects primarily in osteocytes [12, 17, 18], cells that account for more than 95% of bone cells.

**Fig. 4.2** Defective osteocytes are responsible for abnormal bone formation in the *Dmp1* knockout (KO) mice (*right panels*). **a** Backscattered scanning electron microscopic (BSEM) images revealed the expanded and poorly organized growth plate (GP) in the *Dmp1* KO femur, and severe defects in mineralization as reflected by discontinuous mineral content in the cortical bone region; **b** The Goldner stain showed sharp increases in osteoid areas (*red*) but greatly reduced mature bone (*green*) in the KO bone; and **c** BSEM images revealed that the mineral was evenly distributed surrounding the osteocyte lacunae in the control bone (*left, white*); however, the mineral content was either missing, or sparsely located in regions surrounding the *Dmp1* KO osteocytes



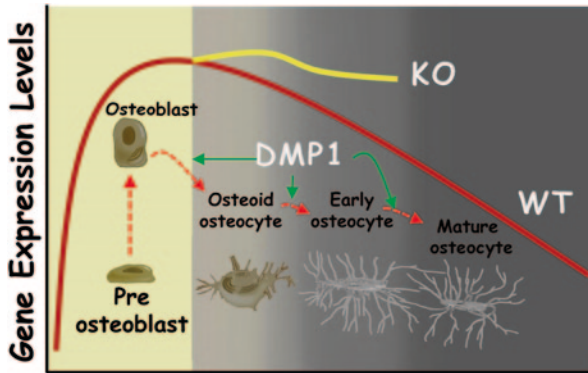


**Fig. 4.3** Roles of DMP1 in control of osteocyte maturation. The gene expression levels are high during differentiation of osteoblasts from preosteoblasts, whereas the gene expression levels are gradually reduced during osteocyte maturation from osteoid osteocyte-early osteocyte and then mature osteocytes. DMP1 is one of key players during this process. The loss of *Dmp1* in mice or *DMP1* mutations in humans will disrupt normal osteoblast to osteocyte maturation. As a result, these immature osteoblast-like osteocytes express high levels of many osteoblast markers (RunX2, OSX, Col I, ALP, BSP, and OCN) and early osteocyte markers such as E11 in bone matrices

The osteocytes reside in lacunae within the mineralized bone matrix and send their dendritic processes (ranging from 40 to 100 per cell) through tiny tunnels called “canaliculi” to form the osteocyte lacunocanalicular network [30]. As the osteocytes mature, numerous cellular projections form and elongate. Next, their cell volume and ultrastructure, such as the endoplasmic reticulum and the Golgi apparatus, are reduced, and a well-organized lacunocanalicular system is built up [30]. Compared to the well-established smooth inner wall of the lacunae and canaliculi, *Dmp1* null osteocytes display bulky and coarse microstructural features, as well as abnormally enlarged and round-shaped osteocytes accompanied by a reduction in dendrite numbers [12, 17, 18]. A number of studies have consistently suggested the key pathological cause responsible for the ARHP phenotype in *Dmp1* null mice is the maturational and functional defects of the osteocytes [12, 17, 18].

There is general agreement that dramatic decreases in protein expression and metabolic activity occur during the maturation of osteoblasts into osteocytes [31]. However, the analysis of *Dmp1* null mice showed sharp increases of osteoblastic marker expression levels, such as runt-related transcription factor 2 (RunX2), osterix (OSX), Col I, alkaline phosphatase (ALP), bone sialoprotein (BSP), and osteocalcin (OCN). In addition, the early osteocyte marker E11/gp38 is widely and increasingly expressed throughout the whole cortical bone layer in the *Dmp1* null mice. In contrast, sclerostin (SOST), mainly expressed in mature osteocytes, is greatly reduced. These studies indicated that osteocyte differentiation is likely regulated by DMP1 [12, 18, 19]. In addition, there is strong evidence showing that the osteocytes, the terminal differentiated cells, regain the ability to divide and proliferate in the *Dmp1* mice [11, 12, 17, 18, 20] (see Fig. 4.3 for the working hypothesis).

## **Dmp1 Regulates Osteocyte Biology and Bone Development**

As previously mentioned, DMP1 is essential for osteogenesis by regulating the maturational process of osteoblasts to osteocytes and bone mineralization during postnatal development. As a key regulator, DMP1 performs several functions in osteocyte biology and bone development as described below.

### ***DMP1 Directly Promotes Hydroxyapatite Formation In Vitro***

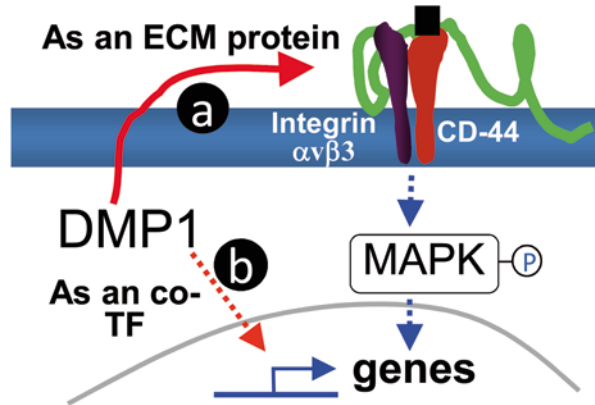
The initial finding linking DMP1 with mineralization was based on the close association of the DMP1 expression and the *in vitro* “bone nodule” formation in primary rat calvarial cell cultures [4]. Soon after, He and colleagues reported that the specific acidic clusters in DMP1 molecules can provide the molecular design necessary for controlling the formation of oriented calcium phosphate crystals, and that the self-assembly of acidic clusters into a beta-sheet template of DMP1 is likely required for the role of DMP1 in biomineral induction [32]. Gajjeraman et al. also showed that both full-length recombinant DMP1 and native DMP1 C-terminal fragments isolated from rat bone accelerated the nucleation of hydroxyapatite in the presence of type I collagen, whereas the N-terminal domain of DMP1 (amino acid residues 1–334) inhibited hydroxyapatite nucleation [33]. Further analysis of these three DMP1 fragments within the mineralized tissues [N-terminal, C-terminal, and a chondroitin-sulfate-linked N-terminal fragment (DMP1-PG)] implies that both the C-terminal and N-terminal fragments are promoters of hydroxyapatite formation and growth, while DMP1-PG is an inhibitor [34]. These findings appear controversial although they indicate that distinct forms of DMP1 may work collectively to control the mineralization process in a different manner. However, the direct role of DMP1 in mineralization described above is mainly based on *in vitro* culture studies with little *in vivo* evidence.

### ***DMP1 Signaling***

#### **DMP1 Signals via Cell Surface Integrin**

*In vitro* studies have shown that DMP1 promotes cell attachment through its RGD motif in a cell- and tissue-specific manner, suggesting a possible role for this protein in specific cell types to activate signaling pathways. This speculation is strengthened by the observation that exogenous DMP1 added to the exposed dental pulp may act as a morphogen trigger and/or promoter of the differentiation of undifferentiated ectomesenchymal cells in the pulp toward the odontoblast lineage. A further *in vitro* analysis demonstrated that either the full-length DMP1 or the 57-kDa fragment can activate phosphorylated extracellular signal-regulated kinase (p-ERK),

**Fig. 4.4** Proposed Models for DMP1 control genes critical for osteogenesis. DMP1 either acts as an extracellular matrix (ECM) protein that binds to integrin  $\alpha v \beta 3$ /CD-44 via its RGD domain and activates the MAPK signaling pathway (a), or as a co-transcriptional factor (TF) that targets the nucleus (b). The end results are that the genes critical for mineralization are activated



with the effect of the 57-kDa fragment lasting longer than that of the full-length protein [35]. More recently, two separate studies confirmed that matrix DMP1 has the ability to activate the mitogen activated protein kinase (MAPK) pathways via interaction with cell surface  $\alpha v \beta 3$  integrin. This interaction stimulates the activation of its downstream effectors, namely as extracellular signal-related kinases (ERK1/2) and Jun N-terminal kinases (JNK1/2). These kinases later lead to the nuclear phosphorylation of c-Jun and ATF2, which shown as transcriptional factors that involved in regulating osteoblastic gene expression. [36, 37] (Fig. 4.4a).

### DMP1 Works as a Transcriptional Factor

As mentioned above, DMP1 is generally considered to be an extracellular matrix protein, but recently studies suggest there is a bi-functional role for DMP1 that it may also works as a transcriptional factor. *In vitro* studies showed the expression of DMP1 in the nuclei of several cell lines: MC3T3-E1, C3H10T1/2, and 17IIA11 [38, 39]. These studies suggest that DMP1 could function in the nucleus, possibly as a transcriptional factor. Moreover, Narayanan et al. reported a functional nuclear localization signal (NLS) peptide at the carboxyl terminal of DMP1 and proposed that this signal peptide could bring DMP1 into the nucleus [38]. They then found a specific domain in the N-terminal of DMP1 that interacted with the glucose-regulated protein -78 (GRP -78) receptor leading to the internalization and nuclear localization of full-length DMP1 [40]. Recently, Siyam et al. reported finding two DMP1 subpopulations in non-synchronized cells: one in the nucleus and one in the cytoplasm [39]. Nevertheless, this transcriptional factor theory is mainly supported by *in vitro* cell line studies with little *in vivo* evidence. Importantly, Lu and colleagues reported that the 57 kDa C-terminal fragment of DMP1 is sufficient to fully rescue the rachitic abnormalities found in the *Dmp1* null mice, suggesting that the putative N-terminal signal sequence is dispensable [12]. Thus, more *in vivo* studies are required to support this transcriptional factor theory (Fig. 4.4b).

## ***Pathophysiologic Regulation***

Recent findings showed that osteocytes embedded in the mineralized bone matrix are far more important than previously described in the literature. These studies imply that osteocytes are multifunctional cells that connect to themselves, to cells on the bone surface and to the vasculature, and they play a key regulatory role in bone and mineral homeostasis under normal and pathological conditions during postnatal development [31]. As a crucial protein mainly produced by osteocytes, DMP1 is responsible for the pathophysiologic development of the heritable disorders of rickets and osteomalacia by impacting the regulatory effect of osteocytes [27].

### **Regulating the Axis of FGF23-Renal Phosphorus Reabsorption-Serum Phosphorus Level**

Prior studies demonstrated that serum FGF23, which is released from bone, targets the kidneys and decreases the expression of the sodium/phosphate cotransporters: NaPi-IIa and NaPi-IIc. These co-transporters are required for renal phosphate reabsorption, and a decrease in co-transporter expression will lead to an increase of the urinary excretion of phosphate and a decrease of serum phosphate levels [41]. Additionally, FGF23 also down-regulates the production of 1- $\alpha$  hydroxylase, resulting in a decreased conversion of 25(OH)D to the active vitamin D metabolite, 1,25(OH)<sub>2</sub>D. This reduced production leads to a decreased expression of NaPi-IIb, a third sodium/phosphate co-transporter, and therefore affects phosphate absorption in the intestine [42]. It is generally agreed that the defect in functional axis of the FGF23 renal and intestinal phosphorus reabsorption is the key systematic pathological mechanism responsible for the development of inherited hypophosphatemic rickets/osteomalacia. Studies of *Dmp1* null mice and *DMPI* mutations in patients showed that FGF23 is significantly up-regulated in osteocytes, which is released into circulation through the connection between osteocytes and vessels, leading to an increase of FGF23 in serum and in subsequent hypophosphatemia [18]. Specifically, *in situ* hybridization (measuring mRNA levels) or immunohistochemistry (measuring protein levels), revealed that the FGF23 level in control osteocytes was much lower than that in osteoblasts, indicating differential regulatory mechanisms for FGF23 in bone cells of healthy versus disease conditions. The discovery of elevated level of FGF23 in the *Dmp1* null osteocytes indicates that bone is an endocrine organ regulating phosphate homeostasis [43] (Fig. 4.5).

### **Canonical Wnt/ $\beta$ -Catenin Pathway**

In addition to controlling FGF23 levels, DMP1 may regulate hypophosphatemic rachitic/osteomalacic disorder via the canonical Wnt/ $\beta$ -catenin signaling pathway. In normal bone development, the canonical Wnt/ $\beta$ -catenin pathway is required for

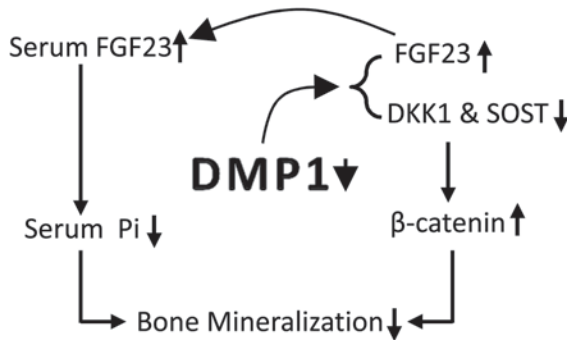


**Fig. 4.5** Working hypothesis on mineralization defects in ARHR. In ARHR, the abnormal renal phosphate wasting and bone mineralization occur as a consequence of a DMP1 mutation that limits the production of the DMP1 protein. These phenotypic characteristics result from the same abnormal biomolecular events due to the deficient *Dmp1* KO mice, in which the ectopic expressed FGF23 from osteocytes targets the kidneys and leads to P waste. In addition, the immature osteocytes fail to produce enough DKK1 and SOST, resulting in increased activity of  $\beta$ -catenin. Both low Pi in circulates and high  $\beta$ -catenin in local cells are responsible for bone mineralization defect

osteogenesis and bone remodeling via regulation of early osteoblast lineage [44]. However, recent studies have indicated that a high level of  $\beta$ -catenin may cause bone defects in rickets [45]. This pathological change is likely due to a dramatic decrease in the expression levels of SOST (a potent inhibitor of the Wnt/ $\beta$ -catenin pathway[46]) in the *Dmp1*-KO osteocytes. In addition, the expression level of DKK1, another antagonist of the Wnt signaling pathway [47], is low in *Dmp1* null mice. As a result, the canonical Wnt/ $\beta$ -catenin signaling is abnormally up-regulated in *Dmp1* null mice. A pilot study by Lin et al. showed that normalization of the  $\beta$ -catenin level by overexpressing DKK1 significantly improved the osteomalacia phenotype of *Dmp1* null mice (Lin et al. unpublished) (Fig. 4.5).

## Summary

DMP1 was cloned 20 years ago [2]. Since then, research has significantly advanced our understanding of this molecule, including gene regulation, biochemical characterization, cell/tissue localization and function, as well as identification of DMP1 mutations in ARHR patients. It is now clear that the full-length DMP1 is not biologically active and is cleaved into the 37 kDa N-terminal and the 57 kDa C-terminal fragments. The latter is the key functional form of DMP1. There is strong evidence that DMP1, highly expressed in dentin and bone, is critical for mineralization, although the direct role of DMP1 on the formation of hydroxyapatite is largely based on the *in vitro* non-cell model with little *in vivo* evidence. The development of different forms of *Dmp1* transgenic mouse models such as conventional and condi-

tional null mice, the full-length and the C-terminal forms of over-expressed *Dmp1* mice, and the *Dmp1* point mutation models have started to reveal the *in vivo* functions of DMP1 in bone and teeth during development [12, 29, 35, 48]. Because DMP1 controls the maturation of both odontoblasts and osteoblasts, defects in this process result in sharp changes in dentin morphologies (such as dentin tubules) and bone (especially the osteocyte-canalicular system). Finally, the observation of abnormal FGF23 production in *Dmp1* null osteocytes led directly to the discovery of DMP1 mutations in human patients with hypophosphatemia. Altogether, the accumulated data from different laboratories strongly support the notion that DMP1 is a key player in the control of osteocyte and bone biology.

### Acknowledgments

This study was supported by NIH grants to JQF (DE018486), and Shuxian Lin is partially supported by National Science Foundation of China. There is no conflict of interest.

### References

1. Fisher LW, Fedarko NS. Six genes expressed in bones and teeth encode the current members of the SIBLING family of proteins. *Connect Tissue Res.* 2003;44(Suppl 1):33–40.
2. George A, Sabsay B, Simonian PA, Veis A. Characterization of a novel dentin matrix acidic phosphoprotein. Implications for induction of biomineralization. *J Biol Chem.* 1993;268(17):12624–30.
3. D'Souza RN, Cavender A, Sunavala G, Alvarez J, Ohshima T, Kulkarni AB, MacDougall M. Gene expression patterns of murine dentin matrix protein 1 (*Dmp1*) and dentin sialophosphoprotein (DSPP) suggest distinct developmental functions *in vivo*. *J Bone Miner Res.* 1997;12(12):2040–9.
4. Fen JQ, Zhang J, Dallas SL, Lu Y, Chen S, Tan X, Owen M, Harris SE, MacDougall M. Dentin matrix protein 1, a target molecule for *Cbfa1* in bone, is a unique bone marker gene. *J Bone Miner Res.* 2002;17(10):1822–31.
5. Toyosawa S, Shintani S, Fujiwara T, Ooshima T, Sato A, Ijuhin N, Komori T. Dentin matrix protein 1 is predominantly expressed in chicken and rat osteocytes but not in osteoblasts. *J Bone Miner Res.* 2001;16(11):2017–26.
6. Lu Y, Zhang S, Xie Y, Pi Y, Feng JQ. Differential regulation of dentin matrix protein 1 expression during odontogenesis. *Cells Tissues Organs.* 2005;181(3–4):241–7.
7. Narayanan K, Ramachandran A, Hao J, George A. Transcriptional regulation of dentin matrix protein 1 (DMP1) by AP-1 (c-fos/c-jun) factors. *Connect Tissue Res.* 2002;43(2–3):365–71.
8. Qin C, Brunn JC, Cook RG, Orkiszewski RS, Malone JP, Veis A, Butler WT. Evidence for the proteolytic processing of dentin matrix protein 1. Identification and characterization of processed fragments and cleavage sites. *J Biol Chem.* 2003;278(36):34700–8.
9. Steiglitz BM, Ayala M, Narayanan K, George A, Greenspan DS. Bone morphogenetic protein – 1/Tolloid-like proteinases process dentin matrix protein-1. *J Biol Chem.* 2004;279(2):980–6.
10. Scott IC, Blitz IL, Pappano WN, Imamura Y, Clark TG, Steiglitz BM, Thomas CL, Maas SA, Takahara K, Cho KW, Greenspan DS. Mammalian BMP-1/Tolloid-related metalloproteinases, including novel family member mammalian Tolloid-like 2, have differential enzymatic

- activities and distributions of expression relevant to patterning and skeletogenesis. *Dev Biol.* 1999;213(2):283–300.
11. Lu Y, Qin C, Xie Y, Bonewald LF, Feng JQ. Studies of the DMP1 57-kDa functional domain both in vivo and in vitro. *Cells Tissues Organs.* 2009;189(1–4):175–85.
  12. Lu Y, Yuan B, Qin C, Cao Z, Xie Y, Dallas SL, McKee MD, Drezner MK, Bonewald LF, Feng JQ. The biological function of DMP-1 in osteocyte maturation is mediated by its 57-kDa C-terminal fragment. *J Bone Miner Res.* 2011;26(2):331–40.
  13. Qin C, D'Souza R, Feng JQ. Dentin matrix protein 1 (DMP1): new and important roles for biomineralization and phosphate homeostasis. *J Dent Res.* 2007;86(12):1134–41.
  14. Lv K, Huang H, Lu Y, Qin C, Li Z, Feng JQ. Circling behavior developed in *Dmp1* null mice is due to bone defects in the vestibular apparatus. *Int J Biol Sci.* 2010;6(6):537–45.
  15. Rangiani A, Cao Z, Sun Y, Lu Y, Gao T, Yuan B, Rodgers A, Qin C, Kuro OM, Feng JQ. Protective roles of DMP1 in high phosphate homeostasis. *PLoS One.* 2012;7(8):e42329.
  16. Ogbureke KU, Fisher LW. Expression of SIBLINGs and their partner MMPs in salivary glands. *J Dent Res.* 2004;83(9):664–70.
  17. Zhang R, Lu Y, Ye L, Yuan B, Yu S, Qin C, Xie Y, Gao T, Drezner MK, Bonewald LF, Feng JQ. Unique roles of phosphorus in endochondral bone formation and osteocyte maturation. *J Bone Miner Res.* 2011;26(5):1047–56.
  18. Feng JQ, Ward LM, Liu S, Lu Y, Xie Y, Yuan B, Yu X, Rauch F, Davis SI, Zhang S, Rios H, Drezner MK, Quarles LD, Bonewald LF, White KE. Loss of DMP1 causes rickets and osteomalacia and identifies a role for osteocytes in mineral metabolism. *Nat Genet.* 2006;38(11):1310–5.
  19. Ye L, MacDougall M, Zhang S, Xie Y, Zhang J, Li Z, Lu Y, Mishina Y, Feng JQ. Deletion of dentin matrix protein-1 leads to a partial failure of maturation of predentin into dentin, hypomineralization, and expanded cavities of pulp and root canal during postnatal tooth development. *J Biol Chem.* 2004;279(18):19141–8.
  20. Ye L, Mishina Y, Chen D, Huang H, Dallas SL, Dallas MR, Sivakumar P, Kunieda T, Tsutsui TW, Boskey A, Bonewald LF, Feng JQ. *Dmp1*-deficient mice display severe defects in cartilage formation responsible for a chondrodysplasia-like phenotype. *J Biol Chem.* 2005;280(7):6197–203.
  21. A gene (PEX) with homologies to endopeptidases is mutated in patients with X-linked hypophosphatemic rickets. The HYP Consortium. *Nat Genet.* 1995;11(2):130–6.
  22. The ADHR Consortium. Autosomal dominant hypophosphataemic rickets is associated with mutations in *FGF23*. *Nat Genet.* 2000;26(3):345–8.
  23. Lorenz-Depiereux B, Bastepe M, Benet-Pages A, Amyere M, Wagenstaller J, Muller-Barth U, Badenhoop K, Kaiser SM, Rittmaster RS, Shlossberg AH, Olivares JL, Loris C, Ramos FJ, Glorieux F, Vikkula M, Juppner H, Strom TM. DMP1 mutations in autosomal recessive hypophosphatemia implicate a bone matrix protein in the regulation of phosphate homeostasis. *Nat Genet.* 2006;38(11):1248–50.
  24. Makitie O, Pereira RC, Kaitila I, Turan S, Bastepe M, Laine T, Kroger H, Cole WG, Juppner H. Long-term clinical outcome and carrier phenotype in autosomal recessive hypophosphatemia caused by a novel DMP1 mutation. *J Bone Miner Res.* 2010;25(10):2165–74.
  25. Turan S, Aydin C, Bereket A, Akcay T, Guran T, Yarlioglu BA, Bastepe M, Juppner H. Identification of a novel dentin matrix protein-1 (DMP-1) mutation and dental anomalies in a kindred with autosomal recessive hypophosphatemia. *Bone.* 2010;46(2):402–9.
  26. Koshida R, Yamaguchi H, Yamasaki K, Tsuchimochi W, Yonekawa T, Nakazato M. A novel nonsense mutation in the DMP1 gene in a Japanese family with autosomal recessive hypophosphatemic rickets. *J Bone Miner Metab.* 2010;28(5):585–90.
  27. Feng JQ, Clinkenbeard EL, Yuan B, White KE, Drezner MK. Osteocyte regulation of phosphate homeostasis and bone mineralization underlies the pathophysiology of the heritable disorders of rickets and osteomalacia. *Bone.* 2013;54(2):213–21.
  28. Narayanan K, Srinivas R, Ramachandran A, Hao J, Quinn B, George A. Differentiation of embryonic mesenchymal cells to odontoblast-like cells by overexpression of dentin matrix protein 1. *Proc Natl Acad Sci U S A.* 2001;98(8):4516–21.

29. Feng JQ, Huang H, Lu Y, Ye L, Xie Y, Tsutsui TW, Kumieda T, Castranio T, Scott G, Bonewald LB, Mishina Y. The Dentin matrix protein 1 (Dmp1) is specifically expressed in mineralized, but not soft, tissues during development. *J Dent Res.* 2003;82(10):776–80.
30. Harris SS, Wood MJ, Dawson-Hughes B. Bone mineral density of the total body and forearm in premenopausal black and white women. *Bone.* 1995;16(4 Suppl):311S–15S.
31. Dallas SL, Prideaux M, Bonewald LF. The Osteocyte: an endocrine cell and more. *Endocr Rev.* 2013;34(5):658–90.
32. He G, Dahl T, Veis A, George A. Nucleation of apatite crystals in vitro by self-assembled dentin matrix protein 1. *Nat Mater.* 2003;2(8):552–8.
33. Gajjerman S, Narayanan K, Hao J, Qin C, George A. Matrix macromolecules in hard tissues control the nucleation and hierarchical assembly of hydroxyapatite. *J Biol Chem.* 2007;282(2):1193–204.
34. Gericke A, Qin C, Sun Y, Redfern R, Redfern D, Fujimoto Y, Taleb H, Butler WT, Boskey AL. Different forms of DMP1 play distinct roles in mineralization. *J Dent Res.* 2010;89(4):355–9.
35. Jiang B, Cao Z, Lu Y, Janik C, Lauziere S, Xie Y, Poliard A, Qin C, Ward LM, Feng JQ. DMP1 C-terminal mutant mice recapture the human ARHR tooth phenotype. *J Bone Miner Res.* 2010;25(10):2155–64.
36. Wu H, Teng PN, Jayaraman T, Onishi S, Li J, Bannon L, Huang H, Close J, Sfeir C. Dentin matrix protein 1 (DMP1) signals via cell surface integrin. *J Biol Chem.* 2011;286(34):29462–9.
37. Eapen A, Ramachandran A, Pratap J, George A. Activation of the ERK1/2 mitogen-activated protein kinase cascade by dentin matrix protein 1 promotes osteoblast differentiation. *Cell Tissue Organ.* 2011;194(2–4):255–64.
38. Narayanan K, Ramachandran A, Hao J, He G, Park KW, Cho M, George A. Dual functional roles of dentin matrix protein 1. Implications in biomineralization and gene transcription by activation of intracellular Ca<sup>2+</sup> + store. *J Biol Chem.* 2003;278(19):17500–8.
39. Siyam A, Wang S, Qin C, Mues G, Stevens R, D'Souza RN, Lu Y. Nuclear localization of DMP1 proteins suggests a role in intracellular signaling. *Biochem Biophys Res Commun.* 2012;424(3):641–6.
40. Ravindran S, Narayanan K, Eapen AS, Hao J, Ramachandran A, Blond S, George A. Endoplasmic reticulum chaperone protein GRP-78 mediates endocytosis of dentin matrix protein 1. *J Biol Chem.* 2008;283(44):29658–70.
41. Gattineni J, Bates C, Twombly K, Dwarakanath V, Robinson ML, Goetz R, Mohammadi M, Baum M. FGF23 decreases renal NaPi-2a and NaPi-2c expression and induces hypophosphatemia in vivo predominantly via FGF receptor 1. *Am J Physiol Renal Physiol.* 2009;297(2):F282–91.
42. Nashiki K, Taketani Y, Takeichi T, Sawada N, Yamamoto H, Ichikawa M, Arai H, Miyamoto K, Takeda E. Role of membrane microdomains in PTH-mediated down-regulation of NaPi-2a in opossum kidney cells. *Kidney Int.* 2005;68(3):1137–47.
43. Quarles LD. Role of FGF23 in vitamin D and phosphate metabolism: implications in chronic kidney disease. *Exp Cell Res.* 2012;318(9):1040–8.
44. Liu F, Kohlmeier S, Wang CY. Wnt signaling and skeletal development. *Cellular signalling.* 2008;20(6):999–1009.
45. Zhang R, Chen FM, Zhao SL, Xiao MZ, Smith AJ, Feng JQ. Expression of dentine sialoprophosphoprotein in mouse nasal cartilage. *Arch Oral Biol.* 2012;57:607–13.
46. Ke HZ, Richards WG, Li X, Ominsky MS. Sclerostin and dickkopf-1 as therapeutic targets in bone diseases. *Endocr Rev.* 2012;33(5):747–83.
47. Li J, Sarosi I, Cattley RC, Pretorius J, Asuncion F, Grisanti M, Morony S, Adamu S, Geng Z, Qiu W, Kostenuik P, Lacey DL, Simonet WS, Bolon B, Qian X, Shalhoub V, Ominsky MS, Zhu Ke H, Li X, Richards WG. Dkk1-mediated inhibition of Wnt signaling in bone results in osteopenia. *Bone.* 2006;39(4):754–66.
48. Sun Y, Prasad M, Gao T, Wang X, Zhu Q, D'Souza R, Feng JQ, Qin C. Failure to process dentin matrix protein 1 (DMP1) into fragments leads to its loss of function in osteogenesis. *J Biol Chem.* 2010;285(41):31713–22.

# Chapter 5

## The Genetic Architecture of Idiopathic Scoliosis

Carol A. Wise

**Abstract** Idiopathic scoliosis (IS) is the most common pediatric spinal deformity, affecting 2–3% of school age children worldwide. This disease is typically classified by age at onset, with the great majority occurring around the time of the adolescent growth spurt, so-called AIS. AIS can progress rapidly, threatening pain, deformity, and pulmonary dysfunction. Heritability of AIS is high, with genetic factors likely explaining over 80% of disease risk. Population studies have consistently found that AIS is best explained by a polygenic inheritance model, in which many genetic risk factors combine to cause the disease. Population studies have associated AIS with candidate genes, including the *LBX1* homeobox transcription factor, and the G protein-coupled receptor *GPR126*. AIS candidate genes thus far identified function in muscle and nerve specification in early development, suggesting neuromuscular disease origins, but their role in later human development and growth of the axial spine is an unexplored area of developmental biology. Animal models that can address these issues will become a valuable resource for the AIS research community. Likewise continued gene discovery efforts, aided by next-generation genomic platforms, are a priority for the field and will provide the tools for biological investigations of AIS pathogenesis.

**Keywords** Idiopathic scoliosis · Genetics · Next-generation genomics · Neuromuscular system · Zebrafish modeling

### Introduction

Art and literature dating back to the beginnings of modern history have depicted the human struggle with scoliosis. The word itself is derived from the Greek “skolio-sis” or “crooked”, attributed to Galen in first century Greece [1]. Today scoliosis

---

C. A. Wise (✉)

Sarah M. and Charles E. Seay Center for Musculoskeletal Research,  
Texas Scottish Rite Hospital for Children, 2222 Welborn St, Dallas TX 75219, USA  
e-mail: carol.wise@tsrh.org

Departments of Orthopaedic Surgery, Pediatrics, and McDermott Center for Human Growth and Development, University of Texas Southwestern Medical Center, Dallas TX 75235, USA

© Springer Science+Business Media New York 2015

C. A. Wise, J. J. Rios (eds.), *Molecular Genetics of Pediatric Orthopaedic Disorders*,  
DOI 10.1007/978-1-4939-2169-0\_5

is clinically defined as a rotational deformity of the spine with lateral deviation of the spine from the vertical of at least  $10^\circ$ . This measurement is known as the “Cobb angle” and is taken from standing spinal radiographs (Fig. 5.1). Although scoliosis is a common deformity in many congenital disorders, about 80% of the time it appears to be an isolated, or “idiopathic” problem in an otherwise healthy child. Thus, a diagnosis of idiopathic scoliosis is reached only after excluding the various common causes of scoliosis. The differential diagnosis of idiopathic scoliosis includes developmental neurologic conditions, such as spinal cord anomalies (tethered cord, syringomyelia) or spina bifida; other heritable neuromuscular disorders that may involve scoliosis, such as neurofibromatosis, Charcot-Marie-Tooth syndrome, the muscular dystrophies, and spinal muscular atrophy; and disorders of connective tissue, such as Ehlers-Danlos or Marfan syndrome. Many of these disorders may be quickly excluded by clinical examination, supported by imaging and/or genetic testing. Structural scoliosis caused by leg length discrepancy or vertebral segmentation anomalies may be excluded by physical examination and radiography [2, 3]. A diagnosis of “idiopathic” scoliosis is typically described by age at onset. Traditionally, idiopathic scoliosis is described as “infantile” (0–3 years of age), “juvenile” (JIS; 4–8 years of age), or “adolescent” (AIS; 10 years and older). Many prefer a simpler classification of “late onset” (6 years of age or older) and “early onset” (up to 6 years of age), as it is more descriptive of the natural history of early

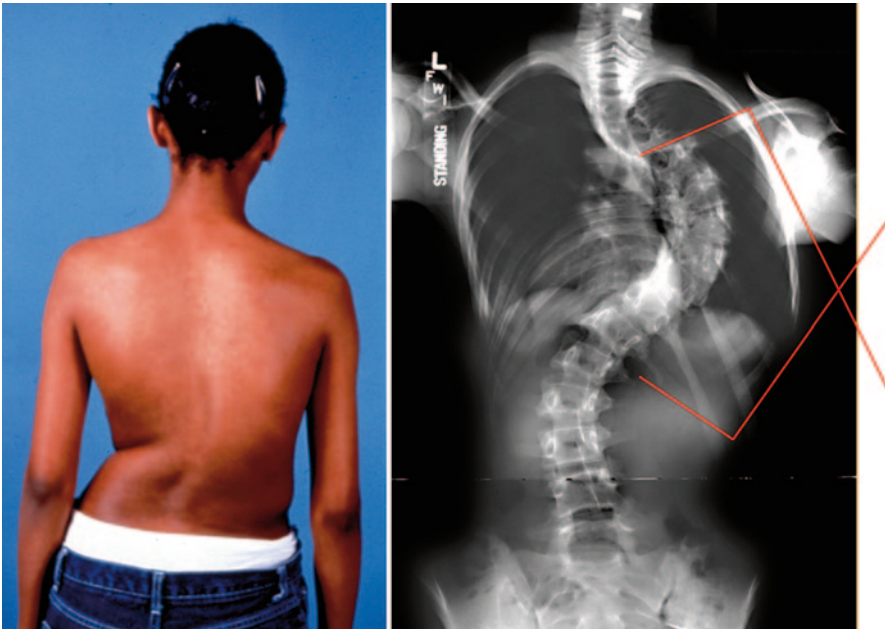


**Fig. 5.1 Patient with idiopathic scoliosis.** Curvature of the spine to the *right* with shoulder imbalance is evident in the picture on the *left*. Standing postero-anterior spinal radiograph reveals severe thoracic curvature measuring  $>70^\circ$  by the Cobb angle method

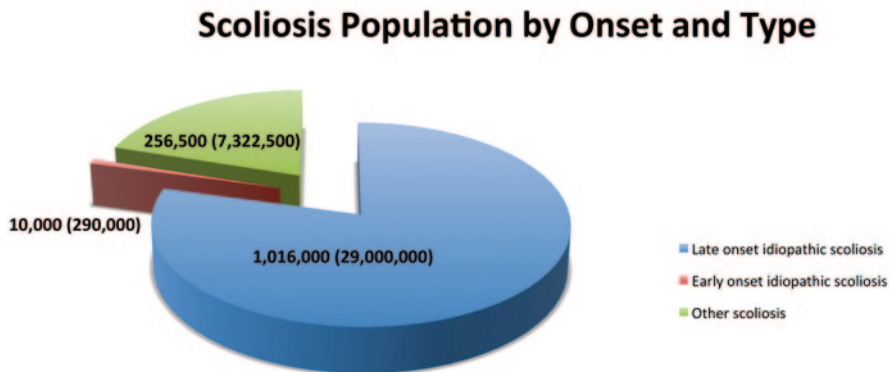


**Fig. 5.2 Scoliosis populations.** Pie chart depicts type of scoliosis (idiopathic shown in *blue* and *brown*, congenital shown in *green*) and proportion of each. The estimated numbers of scoliosis patients are given for the United States, with worldwide estimates in parentheses

spinal growth. However the two systems have led to some semantic confusion [4]. Here we use the traditional terminology and focus on AIS, by far the most common form of idiopathic scoliosis.

Adolescent idiopathic scoliosis is coincident with the pre-pubertal growth spurt and affects ~2% of the pediatric population, or about 29 million children worldwide (Fig. 5.2). Most AIS patients have non-progressive curves; that is to say, the deformity will not worsen appreciably. About 0.4% of these children however will require active treatment to control progression, usually by bracing or surgery [3]. If left untreated, the natural history of progressive AIS is possible chest wall compromise with concomitant lung restriction, pain, deformity, and possible spinal osteoarthritis [1, 3]. Risk factors for progression in an affected child are well-documented. Female patients, and skeletally immature patients who present with large curves have a greater risk of progression, but additional predictive markers are highly sought [3]. Certain curve patterns, e.g. in the thoracic region, are also more likely to progress in severity and therefore must be monitored carefully. The potential for rapid, progressive deformity is significant enough that many professional health organizations recommend school screening programs, although their efficacy remains controversial [5]. The child who has AIS and is at risk of progression typically will be treated by bracing, with the goal of slowing or halting progression of the deformity. Although there is some evidence that bracing can be effective [3, 6], some deformities will continue to worsen, warranting surgery. Today surgery typically involves fixation with instrumentation and spinal fusion [2]. Although outcomes and safety in AIS treatment have benefited from recent advances in surgical and bracing techniques, the methods conceptually have remained the same for decades [3, 6].

As described in this chapter, although AIS is genetically heterogeneous, it bears several distinct features. For one, the location of spinal deformity in AIS patients (unlike infantile IS or syndromic scoliosis) usually involves vertebrae in the thoracic region [7]. In fact curve patterns in AIS appear to mirror spinal growth at this

particular developmental stage in humans, which is known to be at its most rapid, particularly in the thoracic region [8]. Remarkably, greater than 90% of thoracic curves are right-sided [2]. Girls are much more likely to have progressive deformity, leading some to the notion that AIS is a “female disease”. It is important to emphasize, however, that males comprise ~12–17% of progressive cases [9]. Perhaps the most notorious of these was King Richard III of England, described by his acquaintance Thomas More as having “...croke backed, his left shoulder much higher than his right...”, a description borne out as scoliosis by his recently unearthed skeleton [10].

Less invasive interventions to halt or prevent scoliotic deformity altogether are clearly desirable. However until recently, etiologic understanding of the disease has lagged despite decades of clinical research. The reasons for this center on the complexity of the problem: the architecture of the spine itself (is AIS a problem of muscle, nerve, bone, or connective tissues?), the complex genetic underpinnings of AIS as described below, and lack of genetically-defined animal models that faithfully recapitulate the AIS phenotype. Recent advances in genomic technologies are fortunately proving to be powerful tools for deconstructing the causes of AIS in human patients. As outlined in this chapter, recent genetic discoveries have yielded new insights into AIS disease mechanisms. Here we describe the genetic underpinnings of AIS, and the progress in understanding AIS pathogenesis derived from gene discovery research. We also discuss emerging genetic investigations of AIS in humans and animal models, and the prospects for future molecular interventions.

## **Epidemiology and Inheritance—How Common and “Genetic” is AIS?**

The prevalence of AIS is similar across all the major ancestral groups (summarized in Table 5.1), although some early studies found otherwise, likely reflecting differences in disease definition or diagnostic screening methods (e.g. physical examination versus radiography) [11–17]. Intra- and inter-observer error of 5° is generally accepted for measuring the Cobb angle, hence small curves are more likely to be false positives. If the standard scoliosis definition (>10 degree Cobb angle method from standing lateral radiographs) is applied, most studies report prevalence of AIS in the range of 2–3% of school age children. Consequently AIS does not generally cluster within any particular geographic region, nor is it evident that any population or ethnic group has been spared from AIS. Indeed, there is increasing evidence for genetic risk factors shared between ancestral groups as described later in this chapter.

Genetic influences in AIS have been postulated for almost a century (reviewed in 7) [18]. Twin studies have consistently shown higher concordance in monozygotes compared to dizygotes, pointing to heritable factors [19, 20]. (Lack of full concordance in identical (monozygotic) twins reminds us of complex issues that are still poorly understood for genetic disorders, including reduced penetrance and possible environmental effects.) AIS sibling risk and heritability estimates also support

**Table 5.1** Published prevalence and heritability estimates for idiopathic scoliosis

(1) Country	Populations	Age group (years)	Minimum Cobb angle (degrees)	Prevalence	Inheritance (heritability)	Reference
USA	Black, white	> 14	> 10 <sup>a</sup>	Black: 2.1% White: 1.9%		[11]
Canada		12–14	5 10	4.5% 2.0%		[12]
Sweden			≥ 10	Girls: 3.2% Boys: 0.5%		[13]
England		10–14	≥ 10	2.8%		[16]
Japan		Junior high school	≥ 15	Girls: 1.77% Boys: 0.25%		[14]
Greece		9–14	≥ 10	1.7%		[15]
USA	Boston (various ethnicities)	Families			Multifactorial	[22]
USA	Utah	Families	> 10		Mixed polygenic/recessive (96%)	[23]
China	Chinese females	Families	≥ 20		Mixed polygenic/recessive (87.5 +/- 11.1%)	[21]

<sup>a</sup> Measured from chest X rays

significant genetic contributions. One study of AIS compared 415 Chinese index patients and found a sibling recurrence risk of 17.7% and estimated a heritability of 87.5% [21]. It is interesting to note that these results closely mirror an original recurrence risk estimate from a study of Caucasian cases 50 years prior [22]. A separate study of 100 U.S. Intermountain West probands with severe scoliosis (defined as requiring surgical correction) found an even higher recurrence risk of 33% in first-degree female relatives. The latter study also suggested that the location of the scoliotic deformity on the spine may be more heritable than its pattern or severity [23]. At the population level, AIS inheritance is consistent with several to many mutations contributing greater than 80% of disease risk [21–23]. However Mendelian (single gene) inheritance patterns including autosomal dominant, recessive, and X-linked dominant also have been described in AIS families [18, 24]. Accordingly both family- and population-based methods have been used in AIS gene discovery as described later in this chapter. Considering a multi- or poly-genic inheritance model, the preponderance of progressive AIS in females suggests that genetic loading may be greatest in affected males. In other words, males may require more risk mutations, or mutations with greater effect sizes, before they manifest disease. This phenomenon is known as the Carter effect [25], and recent data support this model in AIS inheritance [26]. It is also interesting to speculate that sexual dimorphism in AIS may be a function of gender-specific gene regulation, as has been described for other diseases such as liver cancer [27].

As with other complex disorders, there is considerable uncertainty in predicting individual genetic risk of developing AIS. For families with history of presumed AIS, care must be given to ensure that there is no underlying syndrome or known Mendelian disorder. Otherwise it is appropriate to advise patients with familial AIS that their recurrence risk is increased, but that quantifying the absolute risk is difficult [28].

## **AIS: A Disease of Bone, Muscle, or Nerve?**

Neuropathologic mechanisms have long been proposed for AIS due to the association of scoliosis with neurologic/neuromuscular diseases. In laboratory animals, experimental models of scoliosis have been produced by surgically-created small brain lesions. One of the better-described methods involves removal of the pineal gland from chickens, fish, or bipedal rats, reportedly yielding scoliosis that resembles AIS [29–31]. Several investigations of AIS patients have suggested co-existing deficits in oculo-vestibular (visual/hearing) and proprioceptive function [32–36]. How primary alterations in the nervous system can effect spinal curvature is not altogether obvious, but presumably involves crosstalk with muscle/bone/connective tissue. Indeed we now understand that sensory innervation may affect bone homeostasis; for example, nerve-specific knockout of the axon guidance gene *Sema3A* produces low bone mass phenotypes in animal models [37]. It is interesting that several studies have found decreased bone mass in girls with AIS [38, 39]. One

study found that osteopenia of the femoral neck was a prognostic indicator of curve progression, with an odds ratio of 2.3 [40]. Whether such a mechanism of nerve/bone crosstalk functions in skeletal growth and AIS will be important to consider in future hypothesis-driven studies. Other morphologic studies of AIS spinal structures have revealed some disarrangement of fibers of the ligamentum flavum in AIS patients compared to controls [41]; a separate study found decreased glycosaminoglycan content in the intervertebral discs of AIS patients [42]. Histochemical analyses of paraspinous muscles surrounding the scoliotic curve have shown relative hypertrophy and increased electromyographic signaling of type I fibers on the convexity of the curve in AIS patients. This was explained as most likely a compensatory response to curve progression [42, 43].

## Identifying AIS Genes in Humans—Mapping Susceptibility Loci

AIS research in humans, consistent with most disease gene discovery efforts, has benefited from hypothesis-free, genome-wide methods that map the location of genetic risk factors in the genome relative to fixed markers [44]. One such method, linkage mapping, relies on identifying chromosomal loci that co-segregate with disease in families. Another method, association mapping, identifies polymorphic loci shared or transmitted more frequently to AIS cases (i.e. populations) compared to controls. Here we describe the results of both family- and population-based studies of AIS.

*Family-Based Studies* As noted, both family- and population-based methods have identified genomic regions harboring putative AIS disease mutations. Table 5.2 lists five familial risk loci as given in the Online Mendelian Inheritance in Man (OMIM). Three loci, OS1, OS2, and OS5 (OMIM numbers 181800, 607354, and 612239) were mapped to chromosomes 19p13.3, 17p11, and 17q25-qter by linkage mapping in single East Asian (Han Chinese), European (Italian), and European (British) families [45–47]. Two additional loci IS3 (OMIM 608765), and IS4 (OMIM 612238) were each identified in family-based studies using independent cohorts and methods. IS3 was originally mapped to chromosome 8q12 by linkage mapping in a cohort of 52 families analyzed by model-free methods [48]. In similar fashion, IS4 was mapped to 9q31-q34 in a family with dominantly inherited AIS; moreover a suggestive linkage to this region was previously reported in a study of 202 affected sibling pair families [47, 49]. Consequently IS4 locus is potentially the first and only independently replicated AIS linkage. These studies underscore that AIS is genetically heterogeneous even between families. Indeed, one study suggested genetic heterogeneity even within a single family [50] (Table 5.2). One candidate gene, *CHD7* encoding the chromodomain helicase DNA binding protein 7 transcription factor, has been proposed from linkage studies. Loss-of-function *CHD7* mutations are well described in the CHARGE syndrome of multiple developmental

**Table 5.2 Susceptibility loci in idiopathic scoliosis.** Regions in the human genome providing statistically significant evidence of harboring an AIS risk factor are denoted by their OMIM locus number (column one) where applicable. The markers shown are those that provided most significant evidence in the region

Locus	Region	Marker	Mapping method	LOD score	P value (odds ratio)	Candidate gene	Reference
IS1	19p13.3	D19S216	Genome-wide linkage in seven families	3.63	–	–	[45]
IS2	17p11.2	D17S799	Genome-wide linkage in extended family	3.20	–	–	[46]
IS3	8q12.1	D8S1136 rs1038351	Targeted linkage association across <i>CHD7</i>	2.77	0.0002 (GRR=3.1)	<i>CHD7</i>	[48]
IS4	9q31.2-34.2	D9S2157 D9S915	Genome-wide linkage in extended family genome-wide linkage in affected sibling pair families <sup>a</sup>	3.64 –	0.0005	– –	[47, 49]
IS5	17q25.3	AAT095	Genome-wide linkage in two families	4.08	–	–	[47]
–	5q13.3 3q12.1	D5S2003 D3S2462	Genome-wide linkage	3.01	–	–	
–	10q24.31	rs11190870	GWAS	–	1.24x10 <sup>-19</sup> (1.56)	<i>LBX1</i>	
–	6q24.1	rs6570507	GWAS	–	1.27x10 <sup>-14</sup> (1.27)	<i>GPR126</i>	

<sup>a</sup> This analysis used non-parametric methods; all other linkage analyses used parametric, two-point methods

anomalies that can include scoliosis [51, 52]. Tests of association produced significant results for common single nucleotide polymorphisms (SNPs) within a *CHD7* intron, but how this gene region might be causal is unclear [48].

*Population-Based Studies* Genome-wide association studies (GWAS) typically involve genotyping a high density of common SNPs ( $\geq 350,000$ ) that span the genome. Subsequent statistical comparisons of genotyped SNP allele frequencies between cases and controls may yield associated haplotypes that tag common disease loci. GWAS are proving effective for mapping common susceptibility loci in large cohorts of sporadic AIS. The Catalog of Published Genome-Wide Association Studies (<http://www.genome.gov/gwastudies/>) currently lists two studies (Table 5.2). The first GWAS of AIS utilized 419 families of various ethnicities, in a trio design that is robust to the effects of population substructure. This mostly non-Hispanic white cohort yielded strongest signals near the *CHL1* gene encoding close homolog of L1, a cell adhesion protein involved in axon guidance [53]. The second study of 1033 East Asian (Japanese) cases and 1473 matched controls yielded strongest signals on chromosome 10q24.1 near the *LBX1* gene. *LBX1* encodes the Ladybird homeobox 1 protein involved in muscle and nerve specification [54]. This association was subsequently replicated in independent East Asian cohorts, and a larger combined analysis from multiple ethnic groups (i.e. mostly East Asian and non-Hispanic white) has provided further evidence for this susceptibility locus (Table 5.2). Thus, *LBX1* is the first identified major AIS susceptibility locus. More recently, an expanded East Asian study yielded significant association with SNPs in the *GPR126* gene encoding G-protein coupled receptor 126. This association was replicated in both East Asian and non-Hispanic white cohorts but is still untested in other ethnic groups. It is interesting that SNPs in *GPR126* also have been associated with sitting height in humans [55]. Thus population studies have implicated several genes in multiple ethnic groups, although further study is clearly needed in under-represented minorities.

*Chromosomal Breakpoint Mapping* Many chromosomal alterations with phenotypes that include scoliosis have been reported, although most do not appear to recapitulate idiopathic forms, i.e., without obvious vertebral anomalies or co-existing diagnoses. One family segregating a pericentric inversion of chromosome 8 with idiopathic scoliosis has been reported [56]. Using methods of chromosomal breakpoint mapping, Bashiardes et al. found that one end of this inversion disrupted the 8q11.2 gene encoding gamma-1-syntrophin (*SNTG1*), while the other end of the inversion occurred in a gene-free region of 8p23. Subsequent analysis of the *SNTG1* gene in 152 additional AIS patients revealed an apparent mutation in DNA samples from three unrelated patients. These changes were not detected in screens of 480 healthy control individuals. These results suggested that rare mutations in *SNTG1* could occur in a small percentage of idiopathic scoliosis patients and left open the possibility that other nearby genes could be important in AIS. While chromosomal breakpoint mapping is still a powerful method for pinpointing disease genes, the majority of AIS cases are cytogenetically normal and not amenable to study by this method.

## Candidate Genes and AIS Etiology

What have genetic mapping and association studies revealed about AIS biology? It is important to emphasize that, at this stage, candidate genes have been implicated because of their proximity to associated SNPs, rather than by any direct demonstrations of causality. Nevertheless, AIS candidate genes (Table 5.2) underscore potentially important disease pathways as illustrated in Fig. 5.3.

***LBX1*** *LBX1* is the vertebrate ortholog of Ladybird Late (*lbl*) homeobox gene originally discovered in the fruitfly *Drosophila melanogaster* [57, 58]. In the fly, *lbl* participates in segmentation and cell specification of heart and muscle precursors. Targeted inactivation in the mouse has shown that this gene is necessary for lateral migration of muscle precursors into the limbs [59]. Further, loss of *LBX1* causes loss of dorsal association neurons, cells of the dorsal spinal cord that relay somatosensory information, and disruption of dorsal horn innervation by nociceptive afferent neurons along with an increase in dorsal commissural neurons [60, 61].

***GPR126*** *GPR126* is a member of the adhesion G protein-coupled receptor (GPCR) family that functions in cell adhesion and migration [62]. In zebrafish, *gpr126* is required for Schwann cell myelination, an effect that could be overcome by elevating cAMP levels with forskolin. Originally characterized as an orphan receptor, these data suggested that GPR126 signals through G proteins [63]. GPR126 studies in other vertebrates reveal a potential role in both bone and nerve development. Mouse *Gpr126*<sup>-/-</sup> null mutants fail to grow, and also have severe neurologic deficits, displaying hypomyelinating peripheral neuropathy [64, 65]. In humans common variants in this gene are also associated with overall height and trunk length as noted, implying that a GPR126 signaling pathway somehow regulates appropriate truncal growth in three dimensions.

**Other Genes** Neurologic mechanisms are also suggested by the *CHL1* gene that was highlighted in the first AIS GWAS [53]. *CHL1* encodes an immunoglobulin-class neural cell adhesion protein that participates in commissural axon guidance, i.e. axon crossing at the midline of the corticospinal tract. Deficiencies in commissural axon guidance mechanisms are known to cause scoliosis, as evidenced by the Mendelian disorder *horizontal gaze palsy with progressive scoliosis* (HGPPS, MIM #607313). This disease is caused by recessively inherited mutations in the *ROBO3* gene encoding a transmembrane receptor controlling axon guidance in the same functional and molecular class as *CHL1* [60]. Remarkably, HGPPS patients exhibit only severe scoliosis and absent horizontal eye movement clinically. Imaging studies in these patients confirm that motor and sensory axonal projections do not properly cross within the corticospinal tract of the hind-brain, consistent with their clinical presentation secondary to lesions in *ROBO3*-mediated axon guidance.

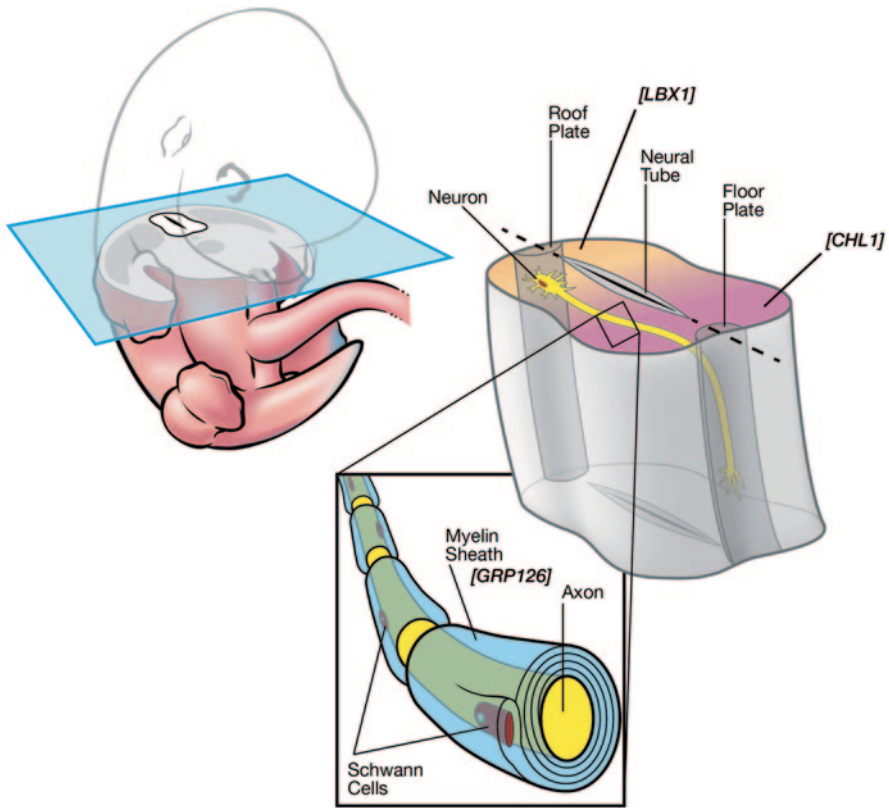


**Fig. 5.3 AIS candidate genes and functions.** A transverse section of developing spinal cord in mouse E12.5 is depicted. *LBX1* and *CHL1* are expressed in roof plate (shaded yellow) and floor plate (shaded magenta) of developing spinal cord, respectively. *GRP126* is expressed in the myelin sheath surrounding axons

## Quantitative Analyses: Do Genetic Factors Influence Disease Course?

Genetic factors exert quantitative effects on various complex traits, such as plasma levels of HDL cholesterol, or blood pressure [66, 67]. Quantitative effects are central issues in AIS as well, i.e. what is the risk of severe scoliosis, and how fast will it progress, in a given patient? Genetic risk factors are hypothesized, but identifying them first requires objective, standardized outcome measures. “Severity” is typically measured as the Cobb angle of the major curve, but what constitutes “mild”, “moderate”, or “severe” deformity? This measure varies between first diagnosis and skeletal maturity, so time is also a co-variate to consider. Severity at the time of surgical intervention is necessarily a surrogate final endpoint in many patients. Happily, statistical models are developed that can consider AIS curve measurement/surgical intervention endpoints. The rate of AIS curve progression is more

easily measured as increase in Cobb angle over time. Survival analysis methods with longitudinal data may facilitate the identification of input variables predicts differing times to “severe” curvature [68]. In these methods, input variables may include, for example, SNP genotypes, gender, ethnicity, and initial measures of age, curve magnitude, curve pattern, Risser sign, with outcome variable being curve magnitude at a later time point. In this way it may be possible to identify combinations of genotypes and phenotypes that classify progressive AIS. In fact a genetic test predicting the likelihood of curve non-progression in idiopathic scoliosis is commercially available [69]. At present the true efficacy of this test, and its applicability to general AIS populations are unknown.

## **AIS Genetics: Ongoing and Future Research**

As noted, genetic discoveries to date are estimated to explain about 1 % of the trait variance for AIS. In other words, the great majority of genetic risk responsible for AIS awaits discovery. It is clear that genomic methods will continue to bear new insights into AIS etiology. As noted, more AIS genes/disease mutations and epigenetic factors await discovery and exploration. Systems for modeling the disease in animals are needed, not only to understand the physiologic origins of disease but also as a vehicle for therapeutic testing.

*Genomic Studies* Current work such as GWAS has focused on copy-neutral changes in the DNA sequences that correlate with disease. The contribution of copy number variation (CNV), defined as contiguous losses or gains of DNA sequence, would seem worthy of exploration, given that a number of Mendelian disorders such as Charcot-Marie-Tooth disease, Smith-Magenis syndrome, spinal muscular atrophy, Di George syndrome etc. are associated with scoliosis and CNV [70–72]. Methods to detect CNV include array comparative genomic hybridization (CGH) and quantitative analysis of chip-based SNP genotyping; the latter is often discovered initially from the SNP microarrays used in GWAS [73, 74].

Additional GWAS with sufficient power to detect new AIS risk loci are clearly warranted, but the design of such studies is a challenge. Several tactics may help in this regard: (1) performing screens of much larger cohorts, on the orders of ten of thousands of cases, (2) utilizing more informative genotyping platforms, and (3) reducing genetic heterogeneity in the screened cohorts. The first goal, studies of larger cohorts, is largely an effort to overcome the “signal-to-noise” problem posed by genetic heterogeneity. Research consortia that can combine large datasets productively are key. The first such group, the International Consortium for Scoliosis Genetics (ICSG), formed in 2012 for this purpose and subsequently produced the first AIS large scale genetic meta-analysis, a study of the chromosome 10 *LBX1* locus in multiple cohorts (manuscript submitted). Ongoing consortium efforts also will include genome-wide meta-analysis of existing datasets and organizational efforts to support the creation of much larger cohorts, on the order of >10,000 patients. We can anticipate that large consortium-driven cohorts will also enable

studies of under-represented ethnic/ancestral groups. Fortunately, genotyping platforms continue to improve in both chemistry and in density and content of markers [75]. The ultimate genotyping platform, whole genome sequencing, is not feasible for most studies due to costs and the extensive analyses and data storage that this would involve. An alternative “hybrid” approach has been developed that involves inferring genotypes from lower-coverage, whole-genome sequencing [76]. This method is proving superior to standard GWAS of common variants for providing information for less common variants that may confer larger effects on disease [77, 78]. Well-powered genetic studies in richly phenotyped cohorts should yield better AIS classification schemes. Consequently prospective, detailed, and standardized phenotyping of existing cohorts is a key goal in the AIS research community represented by ICSG.

As described in this chapter, most AIS genetic research has centered on discovery of common risk factors. Rare variants, that is, mutations that are individually rare in patient populations, may collectively contribute significantly to the overall disease burden but will have been missed by traditional GWAS or even modifications as described above [79–81]. Such mutations are predicted to be important in AIS as well. Extended families with AIS are certain to prove useful in this endeavor, but appropriate validation in additional cohorts will be warranted [50, 82]. It is worth noting that rare variants may contribute considerable risk to individual patients and may prove to be valuable in disease prediction [83].

*Epigenetics* Another contribution to the genetic architecture of AIS in fact may be epigenetic, that is, alterations to the genome that do not involve changes in the DNA sequence itself. Two mechanisms, DNA methylation and histone modifications, are primarily associated with epigenetic consequences. Variations in either phenomena are expected to alter gene expression and may consequently confer specific phenotypes. For example, DNA methylation patterns are known to vary between males and females, leading to sex-specific imprinting of impacted genes. Two relevant diseases caused by effects on imprinting are Angelmann/Prader Willi and maternal uniparental disomy chromosome 14, both of which can involve progressive scoliosis [84]. As these disorders may be caused by alterations in sex-specific methylation, it is reasonable to speculate that other epigenetic changes could figure in AIS.

*Disease Modeling in Animals* The path from gene discovery to molecular intervention is unpredictable. However it is intriguing to consider the possibilities suggested by extant data, for example, for the AIS candidate gene *GPR126*. Although it is important to remember that the nature of *GPR126* association with AIS is unclear at present (i.e. how does it provoke disease?), nevertheless the prospect of a small molecule intervention such as forskolin is evocative. Zebrafish in fact may prove quite useful to AIS studies. Zebrafish are also amenable to large scale forward and reverse genetic screens, and targeted mutagenesis; it also has a short reproductive cycle (2–3 days), and spinal structures that are visualized fairly easily. Indeed recent gene targeting studies have yielded zebrafish strains that appear to recapitulate idiopathic scoliosis [85] (Fig. 5.4). It is worth noting that ease of drug screening through the gills is proving useful in zebrafish models of other disorders such as Duchenne’s muscular dystrophy [86]. Thus forward and reverse genetics, that is, from zebrafish

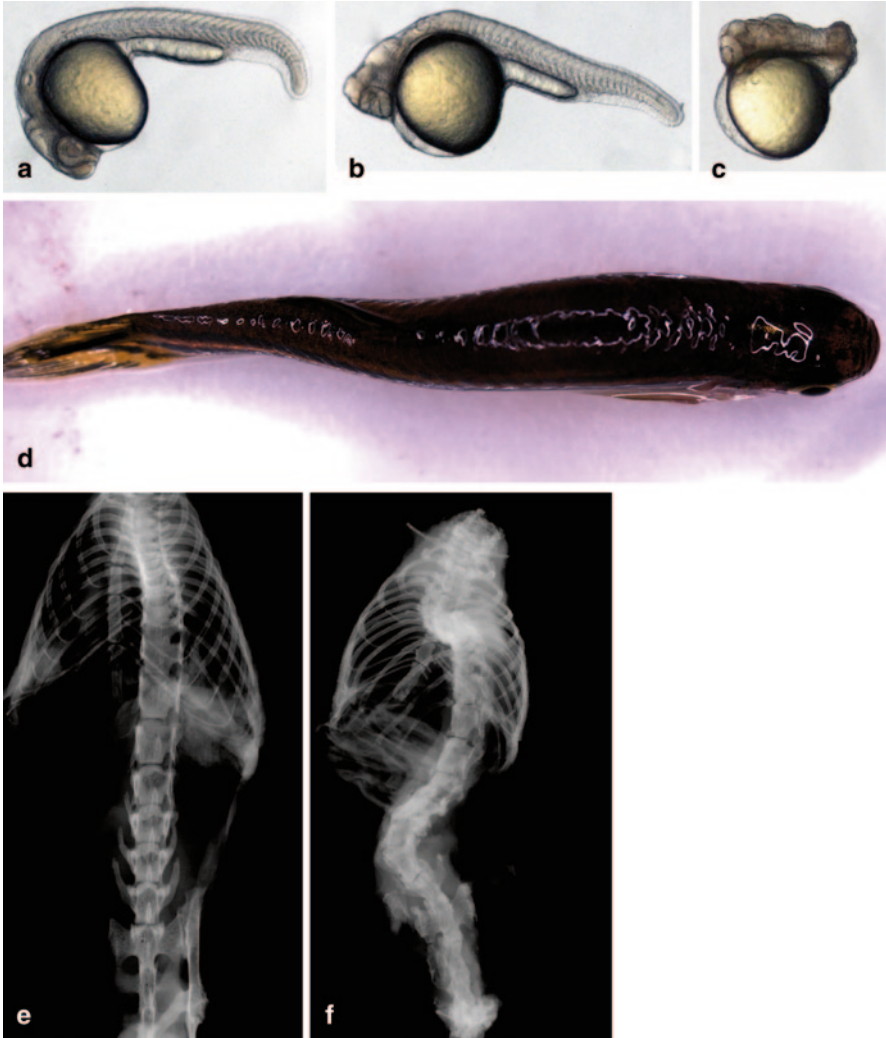


**Fig. 5.4** Animal models of “idiopathic” scoliosis. A wild type 24 h zebrafish embryo (a) is elongated compared to 24 h embryos in with mild (b) and severe (c) *Ptk7* overexpression. A *ptk7* mutant strain is shown in an adult fish (d) (see reference [75]). A normal control mouse (e) is shown alongside a conditional mutant of the SHP2 gene (f) (see reference [77])

screens to humans and vice versa, may prove quite powerful in the next few years of AIS gene discovery and analysis. Likewise conditional mouse mutants may also recapitulate idiopathic scoliosis, for example as described for a Shp-2 (encoding src homology protein 2) knockout [87].

## Summary

Adolescent idiopathic scoliosis, or AIS, is one of the most common diagnoses in pediatric orthopaedic practice. Despite centuries of treatment and decades of study, underlying AIS pathogenesis is poorly understood due largely to lack of naturally-occurring, genetically-defined model systems. Consequently, and because of its significant heritability, genetic studies of AIS in human populations have been the most fruitful approach to the question of disease etiologies. Recent GWAS have yielded associations implicating candidate genes that suggest neuromuscular disease origins. Next-generation genomic technologies are enabling the creation of defined conditional AIS mutations in animal model systems that will facilitate hypothesis testing. These discoveries and tools set the stage for exciting new insights into AIS pathogenesis and for the prospect of pharmaceutical interventions.

**Acknowledgments** We thank Drs. Brian Ciruna and Nobuhiro Kamiya for kindly contributing images of genetically engineered zebrafish and mice, respectively. We also thank patients, other individuals, and families who have participated in the studies described here.

## References

1. Scoliosis. In: Herring J, editor. Tachdjian's Pediatric Orthopaedics. 5th edn. Philadelphia: Elsevier-Saunders; 2014.
2. Herring JA. Tachdjian's pediatric orthopaedics. Philadelphia: WB Saunders; 2008.
3. Hresko MT. Clinical practice. Idiopathic scoliosis in adolescents. *N Engl J Med*. 2013;368(9):834–41.
4. Akbarnia BA. Management themes in early onset scoliosis. *J Bone Joint Surg Am*. 2007;89 Suppl 1:42–54.
5. Richards BS, Vitale MG. Screening for idiopathic scoliosis in adolescents. An information statement. *J Bone Joint Surg Am*. 2008;90(1):195–8.
6. Katz DE, Herring JA, Browne RH, Kelly DM, Birch JG. Brace wear control of curve progression in adolescent idiopathic scoliosis. *J Bone Joint Surg Am*. 2010;92(6):1343–52.
7. Lonstein JE, Carlson JM. The prediction of curve progression in untreated idiopathic scoliosis during growth. *J Bone Joint Surg Am*. 1984;66(7):1061–71.
8. Akbarnia GMB. Idiopathic scoliosis: infantile and juvenile. In: Thompson GH, editor. *The growing spine: management of spinal disorders in young children*. New York: Springer-Verlag; 2011. pp. 199–212.
9. Karol LAM, Johnston CE II MD, Browne RH PhD, Madison M PhD. Progression of the curve in boys who have idiopathic scoliosis. *J Bone Joint Surg Am*. 1993;75-A(12):1804–10.
10. [http://www.richardiii.net/2\\_4\\_0\\_riii\\_appearance.php](http://www.richardiii.net/2_4_0_riii_appearance.php) - description. Feb 14, 2014.
11. Shands AR Jr, Eisberg HB. The incidence of scoliosis in the state of Delaware; a study of 50,000 minifilms of the chest made during a survey for tuberculosis. *J Bone Joint Surg Am*. 1955;37-A(6):1243–9.
12. Rogala EJ, Drummond DS, Gurr J. Scoliosis: incidence and nature history. A prospective epidemiological study. *J Bone Joint Surg Am*. 1978;60(2):173–6.
13. Willner S, Uden A. A prospective prevalence study of scoliosis in Southern Sweden. *Acta Orthop Scand*. 1982;53(2):233–7.

14. Ohtsuka Y, Yamagata M, Arai S, Kitahara H, Minami S. School screening for scoliosis by the Chiba University Medical School screening program. Results of 1.24 million students over an 8-year period. *Spine (Phila Pa 1976)*. 1988;13(11):1251–7.
15. Soucacos PN, Soucacos PK, Zacharis KC, Beris AE, Xenakis TA. School-screening for scoliosis. A prospective epidemiological study in northwestern and central Greece. *J Bone Joint Surg Am*. 1997;79(10):1498–503.
16. Dickson RA. Scoliosis in the community. *Br Med J*. 1983;286(6365):615–8.
17. Horton WA. Common skeletal deformities. In: Rimoin DL, Connor JM, Pyeritz RE, Korf BR, editor. *Emery and Rimoin's principles and practice of medical genetics*. 4th edn. London: Churchill Livingstone; 2002. pp. 4236–44.
18. Sharma S, Wise C. Current understanding of genetic factors in idiopathic scoliosis. In: Kusumi K and Dunwoodie S, editor. *The genetics and development of scoliosis*. New York: Springer; 2010. pp. 167–90.
19. Kimberly L, Kesling M, Reinker KA MD. Scoliosis in twins: a meta-analysis of the literature and report of six cases. *Spine*. 1997;22(17):2009–15.
20. Andersen MO, Thomsen K, Kyvik KO. Adolescent idiopathic scoliosis in twins: a population-based survey. *Spine (Phila Pa 1976)*. 2007;32(8):927–30.
21. Tang NL, Yeung HY, Hung VW, Di Liao C, Lam TP, Yeung HM et al. Genetic epidemiology and heritability of AIS: a study of 415 Chinese female patients. *J Orthop Res*. 2012;30(9):1464–9.
22. Riseborough EJ, Wynne-Davies R. A genetic survey of idiopathic scoliosis in Boston, Massachusetts. *J Bone Joint Surg Am*. 1973;55(5):974–82.
23. Ward K, Ogilvie J, Argyle V, Nelson L, Meade M, Braun J et al. Polygenic inheritance of adolescent idiopathic scoliosis: a study of extended families in Utah. *Am J Med Genet A*. 2010;152A(5):1178–88.
24. Raggio CL, Giampietro PF, Dobrin S, Zhao C, Dorshorst D, Ghebranious N et al. A novel locus for adolescent idiopathic scoliosis on chromosome 12p. *J Orthop Res*. 2009;27(10):1366–72.
25. Carter CO, Evans KA. Inheritance of congenital pyloric stenosis. *J Med Genet*. 1969;6(3):233–54.
26. Kruse LM, Buchan JG, Gurnett CA, Dobbs MB. Polygenic threshold model with sex dimorphism in adolescent idiopathic scoliosis: the Carter effect. *J Bone Joint Surg Am*. 2012;94(16):1485–91.
27. Li Z, Tuteja G, Schug J, Kaestner KH. Foxa1 and Foxa2 are essential for sexual dimorphism in liver cancer. *Cell*. 2012;148(1–2):72–83.
28. Pyeritz RE. Common disorders of connective tissue. In: King RA, Rotter JI, Motulsky AG, editor. *Genetic basis of common diseases*. Oxford: Oxford University Press; 2002. pp. 638–45.
29. Machida M, Dubouset J, Imamura Y, Iwaya T, Yamada T, Kimura J. An experimental study in chickens for the pathogenesis of idiopathic scoliosis. *Spine (Phila Pa 1976)*. 1993;18(12):1609–15.
30. Machida M, Miyashita Y, Murai I, Dubouset J, Yamada T, Kimura J. Role of serotonin for scoliotic deformity in pinealectomized chicken. *Spine (Phila Pa 1976)*. 1997;22(12):1297–301.
31. Fjellidal PG, Grotmol S, Kryvi H, Gjerdet NR, Taranger GL, Hansen T et al. Pinealectomy induces malformation of the spine and reduces the mechanical strength of the vertebrae in Atlantic salmon, *Salmo salar*. *J Pineal Res*. 2004;36(2):132–9.
32. Guo X, Chau WW, Hui-Chan CW, Cheung CS, Tsang WW, Cheng JC. Balance control in adolescents with idiopathic scoliosis and disturbed somatosensory function. *Spine*. 2006;31(14):E437–40.
33. Lonstein JE. Adolescent idiopathic scoliosis. *Lancet*. 1994;344(8934):1407–12.
34. Mallau S, Bollini G, Jouve JL, Assaiante C. Locomotor skills and balance strategies in adolescents idiopathic scoliosis. *Spine*. 2007;32(1):E14–22.

35. Rousie D, Hache JC, Pellerin P, Deroubaix JP, Van Tichelen P, Berthoz A. Oculomotor, postural, and perceptual asymmetries associated with a common cause. Craniofacial asymmetries and asymmetries in vestibular organ anatomy. *Ann N Y Acad Sci.* 1999;871:439–46.
36. Wiener-Vacher SR, Mazda K. Asymmetric otolith vestibulo-ocular responses in children with idiopathic scoliosis. *J Pediatr.* 1998;132(6):1028–32.
37. Fukuda T, Takeda S, Xu R, Ochi H, Sunamura S, Sato T et al. Sema3A regulates bone-mass accrual through sensory innervations. *Nature.* 2013;497(7450):490–3.
38. Cheng JC, Guo X, Sher AH. Persistent osteopenia in adolescent idiopathic scoliosis. A longitudinal follow up study. *Spine (Phila Pa 1976).* 1999;24(12):1218–22.
39. Lee WT, Cheung CS, Tse YK, Guo X, Qin L, Lam TP et al. Association of osteopenia with curve severity in adolescent idiopathic scoliosis: a study of 919 girls. *Osteoporos Int.* 2005;16(12):1924–32.
40. Hung VW, Qin L, Cheung CS, Lam TP, Ng BK, Tse YK et al. Osteopenia: a new prognostic factor of curve progression in adolescent idiopathic scoliosis. *J Bone Joint Surg Am.* 2005;87(12):2709–16.
41. Hadley-Miller N, Mims B, Milewicz DM. The potential role of the elastic fiber system in adolescent idiopathic scoliosis. *J Bone Joint Surg Am.* 1994;76(8):1193–206.
42. Lowe TG, Edgar M, Margulies JY, Miller NH, Raso VJ, Reinker KA et al. Etiology of idiopathic scoliosis: current trends in research. *J Bone Joint Surg Am.* 2000;82-A(8):1157–68.
43. Lonstein JE. Adolescent idiopathic scoliosis. *Lancet.* 1994;344:1407–12.
44. Altshuler D, Daly MJ, Lander ES. Genetic mapping in human disease. *Science.* 2008;322(5903):881–8.
45. Chan V, Fong GC, Luk KD, Yip B, Lee MK, Wong MS et al. A genetic locus for adolescent idiopathic scoliosis linked to chromosome 19p13.3. *Am J Hum Genet.* 2002;71(2):401–6.
46. Salehi LB, Mangino M, De Serio S, De Cicco D, Capon F, Semprini S et al. Assignment of a locus for autosomal dominant idiopathic scoliosis (IS) to human chromosome 17p11. *Hum Genet.* 2002;111(4–5):401–4.
47. Ocaña L, Zhao C, Reed JA, Ebenezer ND, Brice G, Morley T et al. Assignment of two loci for autosomal dominant adolescent idiopathic scoliosis to chromosomes 9q31.2–q34.2 and 17q25.3–qtel. *J Med Genet.* 2008;45(2):87–92.
48. Gao X, Gordon D, Zhang D, Browne R, Helms C, Gillum J et al. CHD7 gene polymorphisms are associated with susceptibility to idiopathic scoliosis. *Am J Hum Genet.* 2007;80(5):957–65.
49. Miller NH, Justice CM, Marosy B, Doheny KF, Pugh E, Zhang J et al. Identification of candidate regions for familial idiopathic scoliosis. *Spine (Phila Pa 1976).* 2005;30(10):1181–7.
50. Edery P, Margaritte-Jeannin P, Biot B, Labalme A, Bernard JC, Chastang J et al. New disease gene location and high genetic heterogeneity in idiopathic scoliosis. *Eur J Hum Genet.* 2011;19(8):865–9.
51. Vissers LE, van Ravenswaaij CM, Admiraal R, Hurst JA, de Vries BB, Janssen IM et al. Mutations in a new member of the chromodomain gene family cause CHARGE syndrome. *Nat Genet.* 2004;36(9):955–7.
52. Doyle C, Blake K. Scoliosis in CHARGE: a prospective survey and two case reports. *Am J Med Genet A.* 2005;133A(3):340–3.
53. Sharma S, Gao X, Londono D, Devroy SE, Mauldin KN, Frankel JT et al. Genome-wide association studies of adolescent idiopathic scoliosis suggest candidate susceptibility genes. *Hum Mol Genet.* 2011;20(7):1456–66.
54. Takahashi Y, Kou I, Takahashi A, Johnson TA, Kono K, Kawakami N et al. A genome-wide association study identifies common variants near LBX1 associated with adolescent idiopathic scoliosis. *Nat Genet.* 2011;43(12):1237–40.
55. Kou I, Takahashi Y, Johnson TA, Takahashi A, Guo L, Dai J et al. Genetic variants in GPR126 are associated with adolescent idiopathic scoliosis. *Nat Genet.* 2013;45(6):676–9.
56. Bashiardes S, Veile R, Allen M, Wise CA, Dobbs M, Morcuende JA et al. SNTG1, the gene encoding gamma1-syntrophin: a candidate gene for idiopathic scoliosis. *Hum Genet.* 2004;115(1):81–9.

57. Jagla K, Frasch M, Jagla T, Dretzen G, Bellard F, Bellard M. ladybird, a new component of the cardiogenic pathway in *Drosophila* required for diversification of heart precursors. *Development*. 1997;124(18):3471–9.
58. Jagla K, Jagla T, Heitzler P, Dretzen G, Bellard F, Bellard M. ladybird, a tandem of homeobox genes that maintain late wingless expression in terminal and dorsal epidermis of the *Drosophila* embryo. *Development*. 1997;124(1):91–100.
59. Gross MK, Moran-Rivard L, Velasquez T, Nakatsu MN, Jagla K, Goulding M. Lbx1 is required for muscle precursor migration along a lateral pathway into the limb. *Development*. 2000;127(2):413–24.
60. Gross MK, Dottori M, Goulding M. Lbx1 specifies somatosensory association interneurons in the dorsal spinal cord. *Neuron*. 2002;34(4):535–49.
61. Muller T, Brohmann H, Pierani A, Heppenstall PA, Lewin GR, Jessell TM et al. The homeodomain factor *lbx1* distinguishes two major programs of neuronal differentiation in the dorsal spinal cord. *Neuron*. 2002;34(4):551–62.
62. Langenhan T, Aust G, Hamann J. Sticky signaling—adhesion class g protein-coupled receptors take the stage. *Sci Signal*. 2013;6(276):re3.
63. Monk KR, Naylor SG, Glenn TD, Mercurio S, Perlin JR, Dominguez C et al. A G protein-coupled receptor is essential for Schwann cells to initiate myelination. *Science*. 2009;325(5946):1402–5.
64. Monk KR, Oshima K, Jors S, Heller S, Talbot WS. Gpr126 is essential for peripheral nerve development and myelination in mammals. *Development*. 2011;138(13):2673–80.
65. Waller-Evans H, Promel S, Langenhan T, Dixon J, Zahn D, Colledge WH et al. The orphan adhesion-GPCR GPR126 is required for embryonic development in the mouse. *PLoS One*. 2010;5(11):e14047.
66. Cohen JC, Kiss RS, Pertsemlidis A, Marcel YL, McPherson R, Hobbs HH. Multiple rare alleles contribute to low plasma levels of HDL cholesterol. *Science*. 2004;305(5685):869–72.
67. Ji W, Foo JN, O’Roak BJ, Zhao H, Larson MG, Simon DB et al. Rare independent mutations in renal salt handling genes contribute to blood pressure variation. *Nat Genet*. 2008;40(5):592–9.
68. Londono D, Chen KM, Musolf A, Wang R, Shen T, Brandon J et al. A novel method for analyzing genetic association with longitudinal phenotypes. *Stat Appl Genet Mol Biol*. 2013;12(2):241–61.
69. Ward K, Ogilvie JW, Singleton MV, Chettier R, Engler G, Nelson LM. Validation of DNA-based prognostic testing to predict spinal curve progression in adolescent idiopathic scoliosis. *Spine (Phila Pa 1976)*. 2010;35(25):E1455–64.
70. Wise CA, Garcia CA, Davis SN, Heju Z, Pentao L, Patel PI et al. Molecular analyses of unrelated Charcot-Marie-Tooth (CMT) disease patients suggest a high frequency of the CMT1A duplication. *Am J Hum Genet*. 1993;53(4):853–63.
71. Greenberg F, Guzzetta V, Montes de Oca-Luna R, Magenis RE, Smith AC, Richter SF et al. Molecular analysis of the Smith-Magenis syndrome: a possible contiguous-gene syndrome associated with del(17)(p11.2). *Am J Hum Genet*. 1991;49(6):1207–18.
72. Sucato DJ. Spine deformity in spinal muscular atrophy. *J Bone Joint Surg Am*. 2007;89 Suppl 1:148–54.
73. Pinkel D, Albertson DG. Array comparative genomic hybridization and its applications in cancer. *Nat Genet*. 2005;37 Suppl:S11–7.
74. Sebat J, Lakshmi B, Troge J, Alexander J, Young J, Lundin P et al. Large-scale copy number polymorphism in the human genome. *Science*. 2004;305(5683):525–8.
75. Jiang L, Willner D, Danoy P, Xu H, Brown MA. Comparison of the performance of two commercial genome-wide association study genotyping platforms in Han Chinese samples. *G3 (Bethesda)*. 2013;3(1):23–9.
76. Pasaniuc B, Rohland N, McLaren PJ, Garimella K, Zaitlen N, Li H et al. Extremely low-coverage sequencing and imputation increases power for genome-wide association studies. *Nat Genet*. 2012;44(6):631–5.

77. Morrison AC, Voorman A, Johnson AD, Liu X, Yu J, Li A et al. Whole-genome sequence-based analysis of high-density lipoprotein cholesterol. *Nat Genet.* 2013;45(8):899–901.
78. Jonsson T, Atwal JK, Steinberg S, Snaedal J, Jonsson PV, Bjornsson S et al. A mutation in APP protects against Alzheimer’s disease and age-related cognitive decline. *Nature.* 2012;488(7409):96–9.
79. Ng SB, Turner EH, Robertson PD, Flygare SD, Bigham AW, Lee C et al. Targeted capture and massively parallel sequencing of 12 human exomes. *Nature.* 2009;461(7261):272–6.
80. Iyengar SK, Elston RC. The genetic basis of complex traits: rare variants or “common gene, common disease”? *Methods Mol Biol.* 2007;376:71–84.
81. Gibson G. Rare and common variants: twenty arguments. *Nat Rev Genet.* 2011;13(2):135–45.
82. Asimit J, Zeggini E. Rare variant association analysis methods for complex traits. *Annu Rev Genet.* 2010;44:293–308.
83. Antonarakis SE, Chakravarti A, Cohen JC, Hardy J. Mendelian disorders and multifactorial traits: the big divide or one for all? *Nat Rev Genet.* 2010;11(5):380–4.
84. Temple IK, Cockwell A, Hassold T, Pettay D, Jacobs P. Maternal uniparental disomy for chromosome 14. *J Med Genet.* 1991;28(8):511–4.
85. Hayes M, Naito M, Daulat A, Angers S, Ciruna B. Ptk7 promotes non-canonical Wnt/PCP-mediated morphogenesis and inhibits Wnt/beta-catenin-dependent cell fate decisions during vertebrate development. *Development.* 2013;140(8):1807–18.
86. Kawahara G, Karpf JA, Myers JA, Alexander MS, Guyon JR, Kunkel LM. Drug screening in a zebrafish model of Duchenne muscular dystrophy. *Proc Natl Acad Sci U S A.* 2011;108(13):5331–6.
87. Kim HK, Aruwajoye O, Sucato D, Richards BS, Feng GS, Chen D et al. Induction of SHP2 deficiency in chondrocytes causes severe scoliosis and Kyphosis in mice. *Spine (Phila Pa 1976).* 2013;38(21):E1307–12.

## Chapter 6

# Insights into the Genetics of Clubfoot

Katelyn S. Weymouth, Susan H. Blanton and Jacqueline T. Hecht

**Abstract** Clubfoot, a common complex birth defect, affects 135,000 newborns each year worldwide. While tremendous strides have been made in treatment with the Ponsetti nonsurgical method, the post-treatment foot generally remains small with hypoplastic calf musculature. Even though clubfoot has been studied for more than 100 years, only a few contributing factors have been identified. Prenatal tobacco smoke exposure is the only consistently associated environmental factor and confers an increased risk in a dose dependent manner. Moreover, maternal smoking and a family history of clubfoot increases the risk 20-fold confirming that genetic factors play a role. Genetic studies have shown that variation in *TBX4* and *PITX1* cause syndromic forms of clubfoot; however, there is no evidence that variation in these genes contribute to nonsyndromic clubfoot. Recent work suggests that variants in the regulatory regions of muscle-specific genes play a role by subtly affecting gene expression and it is hypothesized that variation in the expression of multiple genes is necessary for clubfoot development. This mechanism is consistent with the multifactorial model first proposed for clubfoot over 50 years ago. Confirmation of this work should enable identification of unique gene risk signatures that will aid in genetic counseling. Next generation approaches should speed gene identification in clubfoot.

**Keywords** Clubfoot · *TBX4* · *PITX1* · Muscle · Genes next generation sequencing

---

K. S. Weymouth (✉)

Department of Pediatrics, University of Texas Health Science Center—Medical School,  
6431 Fannin St. MSB 3.031, Houston, TX 77020, USA  
e-mail: ksweymouth@gmail.com; Katelyn.s.weymouth@uth.tmc.edu

S. H. Blanton

Department of Human Genetics, University of Miami, 1501 NW 10th Ave BRB-406,  
Miami, FL 33136, USA  
e-mail: sblanton@med.miami.edu

J. T. Hecht

Department of Pediatrics, University of Texas Health Science Center—Medical School  
and School of Dentistry, 6431 Fannin St, Ste 3.136, Houston, TX 77020, USA  
e-mail: Jacqueline.t.hecht@uth.tmc.edu

© Springer Science+Business Media New York 2015

C. A. Wise, J. J. Rios (eds.), *Molecular Genetics of Pediatric Orthopaedic Disorders*,  
DOI 10.1007/978-1-4939-2169-0\_6

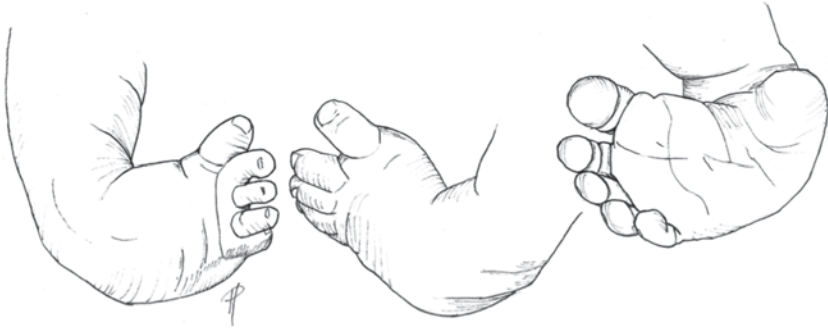


**Fig. 6.1** Dorsal and plantar views of clubfoot

## Introduction

Idiopathic congenital talipes equinovarus or isolated clubfoot is one of the most common, congenital musculoskeletal anomalies. It is characterized by forefoot adductus, hindfoot varus and ankle equinus, which presents as rigid inward turning of the foot towards the midline of the body resembling a persistently contracted foot (Fig. 6.1) [1]. Calf muscle hypoplasia is present at birth and remains even after corrective treatment.

## Treatment

The two most common nonsurgical approaches in current use are the Ponseti and Montpellier (French or functional) methods, which both promote the progressive stretching of the muscles and tendons to avoid the use of the surgical soft tissue release procedure [2, 3]. Treatment by both methods ideally begins within the first few weeks after birth. The Ponseti method involves serial manipulation, casting and bracing, along with clipping of the Achilles tendon (when necessary) to obtain a corrected foot [3–5]. In contrast, the Montpellier method involves daily manipulations of the clubfoot and uses adhesive taping to maintain the correction achieved with stretching [5]. The Montpellier method requires more parental participation but allows more flexibility in the foot, whereas the Ponseti method is less time consuming but more restrictive with foot movement because of the casting and bracing. However, while these conservative treatments have improved outcomes, they do not always produce a plantar grade foot and surgery is then needed. Because of the advances with these nonsurgical treatments, untreated clubfoot is rarely seen in developed countries.

**Table 6.1** Birth rates of clubfoot

Population	Incidence/1000 live births
Australia: Aboriginal [22]	3.49
Australia: Caucasians [22]	1.11
Belgium [21]	1.6
Denmark [20]	1.2
Hawaii [19]	6.8
India [18]	0.9
Japan [17]	0.87
Malawi [16]	2
Papua New Guinea [15]	2.7
Sweden [14]	1.4
Uganda [13]	1.2
US [12]	1.29

## Epidemiology

Twenty to twenty-five percent of clubfoot cases are associated with a syndrome such as Distal Arthrogryposis (DA), congenital myotonic dystrophy, myelomeningocele, amniotic band sequence, Trisomy 18 and Chromosome 22q11 deletion [6–9]. The remaining 75–80% of cases are isolated, having no other visible malformations. The birth prevalence of isolated clubfoot ranges from 1/700–1000 but varies by ethnicity from a high of 6.8/1000 in Hawaii to a low of 0.87/1000 in Japan (Table 6.1) [10–24]. Bilateral involvement is found in half of all cases, while in the unilateral cases, the right foot is affected more often than the left [22, 25]. Interestingly, males are affected twice as frequently as females [25, 26]. Clubfoot is a complex birth defect in which both genetic and environmental factors, presumably in combination as well as separately, contribute to the etiology [27].

## The Role of Environmental Factors in Clubfoot

Many environmental factors have been suggested to contribute to clubfoot but few have been consistently identified. Seasonal variation has been observed in some studies with higher birth prevalence in winter (December–March), while other studies have found no correlation [12, 28–31]. Similarly, sulfonamides and abortifacient agents have been inconsistently identified [32, 33]. While maternal folic acid supplementation decreases the birth prevalence of neural tube defects, only a small reduction in isolated clubfoot has been found on a population basis [24, 34]. There is little evidence to suggest that folic acid deficiency contributes to clubfoot.

Maternal smoking is the only environmental factor consistently associated with clubfoot [10, 35–39]. Mothers who smoke during pregnancy have an increased risk

of having a child with clubfoot and this risk increases in a dose-dependent pattern (Relative Risk: 1.3–2.2) [37–39]. Maternal smoking during pregnancy and a positive family history of clubfoot increased the risk of clubfoot [10, 38].

## Genetic Epidemiology of Clubfoot

Evidence for a genetic etiology for clubfoot comes from studies showing (1) aggregation of clubfoot in families, (2) increased risk with number of affected siblings, (3) heritability for clubfoot of 72%, and (4) higher concordance in monozygotic than dizygotic twins (32.5 vs. 2.9%) [15, 40–42]. Segregation analyses from different populations support a multifactorial/oligogenic model in which variation in multiple genes influenced by environmental factors play a causal role [17, 24, 41, 43–46]. It is now well accepted that genetic variation contributes to clubfoot, however the mechanism(s) remain to be defined. The generally accepted model is that of multifactorial inheritance with a threshold effect [47].

## Genes and Environment: Tobacco Metabolism and Clubfoot

Cigarette smoke consists of more than 4000 chemical compounds that are metabolized through the xenobiotic metabolism [48]. The identification of maternal smoking as a risk factor suggests that variants in genes involved in xenobiotic metabolism may contribute to clubfoot. Biotransformation through this pathway can detoxify a compound or it can create a more toxic/reactive intermediate metabolite that can create adducts. Adducts can bind DNA or proteins altering transcription and replication that could affect normal development [49]. N-acetyltransferase (*NAT*) genes are obvious candidate genes because they acetylate toxins including free radicals found in cigarette smoke. Variants in *NAT1* and *NAT2* were genotyped in a clubfoot dataset composed of both multiplex families (family history of clubfoot) and simplex (no family history) trios [50]. More slow acetylators were found in cases suggesting a potential link between clubfoot risk and slow acetylation [50].

Given the importance of this pathway, eight xenobiotic metabolizing genes, including *NAT1* and *NAT2* were interrogated in a subsequent study [51]. rs1048943/*CYP1A1* was significantly associated with nonHispanic white (NHW) multiplex families ( $p=0.009$ ) [51]. It was hypothesized that the presence of variation in multiple genes in this pathway would increase the risk over variation in a single gene. Indeed, the allelic combination comprised of rs105740/*EPHX1* and rs1799929/*NAT2* was found to be associated with clubfoot ( $p=0.007$ ). In addition, evidence for maternal and fetal genotypic effects were found for two SNPs in

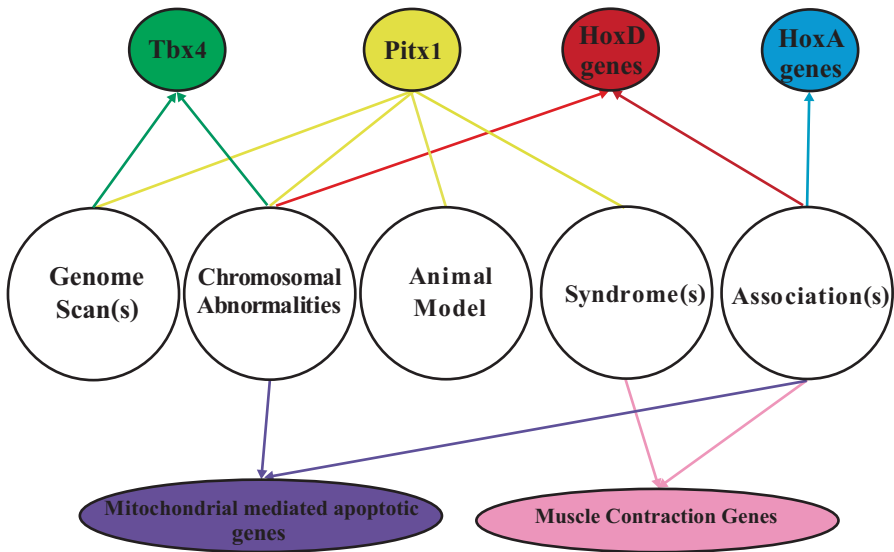


**Fig. 6.2** Methods used to identify clubfoot genes and identified genes

*CYP1A2*. A significant maternal genotypic effect was found for rs11854147/*CYP1A2* with a relative risk of 1.24 (95% CI: 1.04–1.44,  $p=0.03$ ) and a significant fetal genotypic effect for rs2470890/*CYP1A2* with a relative risk of 1.33 (95% CI: 1.13–1.54,  $p=0.01$ ) [51]. These findings suggest that xenobiotic metabolism genes are unlikely to play a major role in clubfoot; however, perturbation of this pathway may play a contributory role.

## Other Approaches to Gene Identification in Clubfoot

Given that there is a genetic component to clubfoot, studies have focused on identifying the clubfoot genes mainly using genome scans and candidate gene approaches. In brief, genome-wide scans utilize polymorphic markers such as SNPs and copy number variants (CNVs) spanning the genome to identify linked and/or associated variants/regions with the phenotype of interest. In contrast, the candidate gene approach uses prior knowledge to identify genes for consideration. In addition to genes in the xenobiotic pathway, genetic investigations of clubfoot have included analysis of genes that (1) play a biological role in hindlimb development, (2) cause a clubfoot phenotype when altered in an animal model and/or (3) are deleted, duplicated or mutated in a syndrome that has multiple malformations including clubfoot (Fig. 6.2). The following sections discuss the potential clubfoot genes and variants that have been identified.

## Hindlimb Development

Hindlimb morphogenesis is a multifaceted process involving cell proliferation, migration, patterning and programmed cell death, all of which are regulated by numerous factors such as growth and transcription factors and signaling molecules [52–57]. Hindlimb development begins between the fourth and fifth week of gestation with swelling along the lateral plate mesoderm. By the middle of the fifth week, the limb bud becomes pronounced and it is the regulation of three major axes: proximal-distal (PD, from knee to digits), anterior-posterior (AP, from the big toe to the little toe) and dorsal-ventral (DV, from the top of the foot to the bottom of the foot) that transforms the limb bud into a mature limb. Chondrification begins by the end of the sixth week; osteogenesis begins in the seventh week and is present in all the long bones by the twelfth week. Myoblasts aggregate and form large muscle masses in each limb bud differentiating into dorsal and ventral components as the long bone forms. As development progresses through week 6 and 7, programmed cell death occurs removing the interdigital webbing and freeing the individual toes [52]. During the final stages of limb development in weeks 8–11, the foot begins to rotate from an inward apposing position to a plantar position [58]. This complex process is regulated by a large number of genes which when perturbed could contribute to a clubfoot.

### PITX1

Evidence for a role of *PITX1*, paired-like homeodomain 1, has recently been reported [59]. *PITX1*, a bicoid-related homeodomain transcription factor, was first identified in a genome-wide linkage study (5q31: LOD: 3.31) in a five-generation clubfoot family with nine affected individuals [59]. A single missense mutation (E310K) in *PITX1* segregated with the clubfoot and was not present in 500 controls [59]. The mutation is located in a highly conserved homeodomain and reduces wild-type *PITX1* activity in a dose-dependent manner suggesting a dominant-negative effect on transcription [59]. Although this was the first evidence for a hindlimb-specific gene variant in clubfoot, members of this family had other lower-limb malformations including patellar hypoplasia, oblique talus, preaxial polydactyly suggesting that the mutation causes a syndromic form of clubfoot. This is further supported by the identification of *PITX1* deletions in three other individuals with isolated lower-limb malformations including polydactyly [60].

Another study provides additional evidence for a role of *PITX1* in isolated clubfoot. A copy number analysis of 40 familial clubfoot probands identified a 241 kb microdeletion involving *PITX1* in one individual [61]. The authors suggested *PITX1* haploinsufficiency as a cause for isolated clubfoot and cited support based on decreased *PITX1* activity from the E310K/*PITX1* mutation [59, 62]. Additional supporting evidence for a role of *PITX1* haploinsufficiency comes from the *Pitx1* haploinsufficient mouse; approximately 8.9% of these mice have a clubfoot-like

phenotype [61]. This is the first animal model to closely mimic human clubfoot. However, the *Pitx1* haploinsufficient mouse does differ from the human clubfoot in a number of ways: (1) females are affected more often than males, the opposite of the human condition, (2) there is peroneal artery hypoplasia, and (3) the tibial and fibular bone volumes are reduced. Nevertheless, the role of *PITX1* in isolated clubfoot remains intriguing. Other families may provide more etiologic and phenotypic information.

## TBX4

T-box transcription factor 4, *TBX4*, a direct transcriptional target of *PITX1* has been implicated in clubfoot [63]. Like *PITX1*, *TBX4* is also specifically expressed in the hindlimb and involved in limb muscle and tendon patterning [64, 65]. One study screened 66 familial clubfoot probands for genomic copy-number variants and found a 17q23.1q23.2 microduplication in three probands. The microduplication segregated in the families but showed reduced penetrance. Individuals with the microduplication also had mild short stature, developmental hip dysplasia and subtle skeletal abnormalities such as short wide feet. While the authors suggest that the 17q23.1q23.2 microduplication is a common cause for familial isolated clubfoot, only a few families were identified. A second study identified only one multiplex family out of 605 clubfoot families with a small 350 kb 17q23.1q23.2 microduplication [66]. This microduplication segregated with the clubfeet and the short, wide feet, once again supporting variable expressivity with this microduplication [66]. Therefore, the role of *TBX4* in the etiology of isolated clubfoot remains to be elucidated but appears to cause a syndromic form of clubfoot. Even more intriguing is the possible interactive role of genetic variants in the *TBX4-PITX1* pathway, which should be thoroughly interrogated.

## Muscle Contraction Genes

Clubfoot can occur as part of a number of Mendelian syndromes, which suggests that variation in the genes underlying these disorders could have an etiologic role in the isolated form. This is the paradigm that led to the identification of genetic variation in *IRF6* and nonsyndromic cleft lip and palate [67]. The Distal Arthrogryposis (DA) syndromes, for example, are characterized by congenital joint contractures and many include clubfoot [68]. Currently, there are nine different types of DA and clubfoot occurs in four. Mutations in muscle contraction genes, *MYH3*, *TNNT3*, *TNNI2*, *TPM2*, *MYBPC1* and *TPM8*, cause DA1, DA2A, DA2B and DA7 [68]. One study sequenced the exons of *MYH3*, *TNNT3* and *TPM2* in 20 clubfoot probands from multiplex clubfoot families [69]. While rare exonic variants were identified, none segregated in all affecteds in each family. The authors suggested

that these genes do not contribute to clubfoot, however the regulatory regions were not sequenced [69]. Similarly, sequencing of the exons, splice sites and predicted promoters of embryonic and perinatal myosin genes, *MYH2*, 3, 7 and 8 did not find any associations [70].

A more recent study interrogated fifteen muscle contraction genes in 224 families with a family history of clubfoot and 357 families with no family history and included upstream and downstream genomic regions in order to capture variation in the regulatory regions [71]. Several positive associations were found in the single SNP, haplotype and gene-gene interaction analyses for both the nonHispanic white (NHW) and Hispanic groups. Interestingly, the most significant associations involved SNPs located in potential regulatory regions, in *TPM1* and *TPM2* [71]. A follow-up study addressed the functional implications of these variants [72]. The *TPM2* SNPs, rs2025126 and rs2145925, altered nuclear protein binding and changed promoter activity in C2C12 mouse muscle cells. Interestingly, while the rs4075583/*TPM1* alternative allele showed an alteration in nuclear protein binding it did not affect promoter activity. However, when rs4075583 was analyzed in the context of a ~1.7 kb eight SNP haplotype, varying degrees of promoter activity were observed depending on allelic combination. Promoter activity was decreased when rs4075583 alternate allele was present in the haplotype [72]. These results suggest the importance of transcriptional regulation in muscle contraction genes as a mechanism for clubfoot.

## Homeobox A and D Genes

In order to identify chromosomal regions/genes that contribute to human malformations, Brewer et al. combined clinical reports to identify chromosomal abnormalities, deletions and duplications, in syndromic clubfoot [8, 9]. For clubfoot, this included six large chromosomal deletion regions (2q31-33, 3q23-24, 4p16-14, 7p22, 13q33-34 and 18q22-23) and two duplication regions (6q21-27 and 10p15-11) [8, 9]. Interrogation of the 2q31-33 deletion region identified associations with variations in *CASP8*, *CASP10* and *CFLAR* [73, 74]. These genes are involved in the mitochondrial-mediated apoptotic pathway which is consistent with the key role that apoptosis plays in limb and muscle development. In a follow-up study, interrogation of five additional mitochondrial-mediated apoptotic genes (*CASP9*, *CASP3*, *APAF1*, *BCL2* and *BID*) identified suggestive associations between variation in each gene and clubfoot [75].

Also present in the 2q31-33 deletion region is the Homeobox gene cluster D (*HOXD*). Genes in the *HOXD* cluster direct limb and muscle patterning during development. This cluster is functionally redundant with the Homeobox A gene cluster (*HOXA*) located on chromosome 7p15; this region was not identified in the report of Brewer et al. [76–78]. Mutations in both *HOXA* and *HOXD* have been associated with syndromes that involve limb abnormalities but not clubfoot [79, 80]. The *HOXA* genes are also known to regulate the synchronized development of

muscles, tendons and cartilages [78]. Interrogation of these genes in the clubfoot nonHispanic and Hispanic multiplex and simplex families identified associations with SNPs in both gene clusters [74]. One SNP, rs3801776, located in the basal promoter of *HOXA9*, gave the strongest association with clubfoot in both discovery and validation clubfoot groups ( $p=0.004$  and  $p=0.03$ , respectively) [74]. The ancestral allele of rs3801776 created a nuclear protein binding site that increased promoter activity [72]. These results suggest that perturbation in genes involved in limb and muscle patterning and development play a role in clubfoot. Again, the association was with regulatory SNPs suggesting that gene expression plays an important role in clubfoot.

## Summary

Clubfoot is a well-recognized birth anomaly for which etiologic insights are only now being identified. Genome-wide linkage studies are only successful if there are sufficient numbers of large families to overcome any heterogeneity issues. While multiplex clubfoot families do exist, and it has been suggested that clubfoot fits a single major gene model [46, 81, 82], most families have only 2 or 3 affected individuals. Moreover, extensive heterogeneity would be expected given the complexity of hindlimb development. As a result, most linkage studies of clubfoot have not been successful [81, 83]. Evidence for involvement of *PITX1* and *TBX4*, both hindlimb-specific genes, have been found in only a few clubfoot families/cases and not confirmed in association studies, suggesting that variation in these genes is not involved in the majority of cases of clubfoot [27, 66]. Genome-wide associations studies are most successful when the disease in question is due to common variation and the dataset is sufficiently large. Lack of a large dataset can be circumvented to some extent by focusing on candidate genes. This approach has led to the identification of associations between clubfoot and variation in several genes, including *HOXA9* and the muscle contraction genes *TPM1* and *TPM2*. While potential mechanisms have been described for clubfoot for these genes, independent verification is still needed. Given the paucity of large families or the lack of large datasets, clubfoot genetic studies should benefit from next-generation approaches, such as whole exome and genome sequencing. Families can be examined individually and in concert with other families to identify genes and pathways, which appear to underlie the development of clubfoot. Results of these studies will then require verification in animal models and functional studies. The challenge is great but the payoff is also large as it will provide insight into biological mechanisms causing clubfoot, and in some cases families may benefit from personalized recurrence risk information.

**Acknowledgements** We thank Hilary Page ([www.hilarypage.com](http://www.hilarypage.com)) for the depiction of clubfoot in Fig. 6.1. Parts of the work described in this chapter were supported by grants from NIH (R01-HD043342) and Shriners Hospital for Children.

## References

1. Bohm M. Embryologic origin of clubfoot. *J Bone Joint Surg.* 1929;11:229–59.
2. Hulme A. The management of congenital talipes equinovarus. *Early Hum Dev.* 2005;81:797–802.
3. Laaveg SJ, Ponseti IV. Long-term results of treatment of congenital club foot. *J Bone Joint Surg Am.* 1980;62:23–31.
4. Ponseti IV. Treatment of congenital club foot. *J Bone Joint Surg Am.* 1992;74:448–54.
5. Fromental-Ramain C, et al. Hoxa-13 and Hoxd-13 play a crucial role in the patterning of the limb autopod. *Development.* 1996;122:2997–3011.
6. Gurnett CA, Boehm S, Connolly A, Reimschisel T, Dobbs MB. Impact of congenital talipes equinovarus etiology on treatment outcomes. *Dev Med Child Neurol.* 2008;50:498–502.
7. Gurnett MB, DaCA. Genetics of clubfoot. *J Pediatr Orthop B.* 2011;21:7–9.
8. Brewer C, Holloway S, Zawalynski P, Schinzel A, FitzPatrick D. A chromosomal deletion map of human malformations. *Am J Hum Genet.* 1998;63:1153–9.
9. Brewer C, Holloway S, Zawalynski P, Schinzel A, FitzPatrick D. A chromosomal duplication map of malformations: regions of suspected haplo- and triplolethality-and tolerance of segmental aneuploidy-in humans. *Am J Hum Genet.* 1999;64:1702–8.
10. Parker SE, et al. Multistate study of the epidemiology of clubfoot. *Birth Defects Res A Clin Mol Teratol.* 2009;85:897–904.
11. Pirani S, et al. Towards effective Ponseti clubfoot care: the Uganda sustainable clubfoot care project. *Clin Orthop Relat Res.* 2009;467:1154–63.
12. Wallander H, Hovelius L, Michaelsson K. Incidence of congenital clubfoot in Sweden. *Acta Orthop.* 2006;77:847–52.
13. Culverwell AD, Tapping CR. Congenital talipes equinovarus in Papua New Guinea: a difficult yet potentially manageable situation. *Int Orthop.* 2009;33:521–6.
14. Mkandawire NC, Kaunda E. Incidence and patterns of congenital talipes equinovarus (clubfoot) deformity at Queen Elizabeth Central Hospital, Banter, Malawi. *East and Cent Afr J Surg.* 2004;9:28–31.
15. Yamamoto H. A clinical, genetic and epidemiologic study of congenital club foot. *Jinrui Idengaku Zasshi.* 1979;24:37–44.
16. Mittal RL, Sekhon AS, Singh G, Thakral H. The prevalence of congenital orthopaedic anomalies in a rural community. *Int Orthop.* 1993;17:11–2.
17. Ching GH, Chung CS, Nemechek RW. Genetic and epidemiological studies of clubfoot in Hawaii: ascertainment and incidence. *Am J Hum Genet.* 1969;21:566–80.
18. Krogsgaard MR, et al. Increasing incidence of club foot with higher population density: incidence and geographical variation in Denmark over a 16-year period-an epidemiological study of 936,525 births. *Acta Orthop.* 2006;77:839–46.
19. Paton RW, Fox AE, Foster A, Fehily M. Incidence and aetiology of talipes equino-varus with recent population changes. *Acta Orthop Belg.* 2010;76:86–9.
20. Carey M, Bower C, Mylvaganam A, Rouse I. Talipes equinovarus in Western Australia. *Paediatr Perinat Epidemiol.* 2003;17:187–94.
21. Chung CS, Nemechek RW, Larsen IJ, Ching GH. Genetic and epidemiological studies of clubfoot in Hawaii. General and medical considerations. *Hum Hered.* 1969;19:321–42.
22. Lochmiller C, Johnston D, Scott A, Risman M, Hecht JT. Genetic epidemiology study of idiopathic talipes equinovarus. *Am J Med Genet.* 1998;79:90–6.
23. Beals RK. Club foot in the Maori: a genetic study of 50 kindreds. *N Z Med J.* 1978;88:144–6.
24. Moorthi RN, et al. Idiopathic talipes equinovarus (ITEV) (clubfeet) in Texas. *Am J Med Genet A.* 2005;132:376–80.
25. Cardy AH, Sharp L, Torrance N, Hennekam RC, Miedzybrodzka Z. Is there evidence for aetiologically distinct subgroups of idiopathic congenital talipes equinovarus? A case-only study and pedigree analysis. *PLoS One.* 2011;6:e17895.
26. Dietz F. The genetics of idiopathic clubfoot. *Clin Orthop Relat Res.* 2002;401: 39–48.

27. Dobbs MB, Gurnett CA. Genetics of clubfoot. *J Pediatr Orthop B*. 2012;21:7–9.
28. Barker SL, Macnicol MF. Seasonal distribution of idiopathic talipes equinovarus in Scotland. *J Pediatr Orthop B*. 2002;11:129–33.
29. Loder RT, et al. Lack of seasonal variation in idiopathic talipes equinovarus. *J Bone Joint Surg Am*. 2006;88:496–502.
30. Pryor GA, Villar RN, Ronen A, Scott PM. Seasonal variation in the incidence of congenital talipes equinovarus. *J Bone Joint Surg Br*. 1991;73:632–4.
31. Pavone V, et al. Congenital talipes equinovarus: an epidemiological study in Sicily. *Acta Orthop*. 2012;83:294–8.
32. Heydanus R, Ledward RS. Failed mifepristone termination of pregnancy and talipes equinovarus: coincidence? *J Obstet Gynaecol*. 1995;15:211.
33. Czeizel AE, Puho E, Sorensen HT, Olsen J. Possible association between different congenital abnormalities and use of different sulfonamides during pregnancy. *Congenit Anom (Kyoto)*. 2004;44:79–86.
34. Ulrich M, et al. The influence of folic acid supplement on the outcome of pregnancies in the county of Funen in Denmark. Part III. Congenital anomalies. An observational study. *Eur J Obstet Gynecol Reprod Biol*. 1999;87:115–8; (discussion 103–4).
35. Hackshaw A, Rodeck C, Boniface S. Maternal smoking in pregnancy and birth defects: a systematic review based on 173,687 malformed cases and 11.7 million controls. *Hum Reprod Update*. 2011;17:589–604.
36. Niemann S, et al. Homozygous WNT3 mutation causes tetra-amelia in a large consanguineous family. *Am J Hum Genet*. 2004;74:558–63.
37. Honein MA, Paulozzi LJ, Moore CA. Family history, maternal smoking, and clubfoot: an indication of a gene-environment interaction. *Am J Epidemiol*. 2000;152:658–65.
38. Skelly AC, Holt VL, Mosca VS, Alderman BW. Talipes equinovarus and maternal smoking: a population-based case-control study in Washington state. *Teratology*. 2002;66:91–100.
39. Dickinson KC, Meyer RE, Kotch J. Maternal smoking and the risk for clubfoot in infants. *Birth Defects Res A Clin Mol Teratol*. 2008;82:86–91.
40. Idelberger K. Die Ergebnisse der Zwillingforschung beim angeborenen Klumpfuß. *Verh Deutsch Orthopd Ges*. 1939;33:272–6.
41. Barker S, Chesney D, Miedzbrodzka Z, Maffulli N. Genetics and epidemiology of idiopathic congenital talipes equinovarus. *J Pediatr Orthop*. 2003;23:265–72.
42. Strach E. Club-foot through the centuries. *Prog Pediatr Surg*. 1986;20:215–237.
43. Yang HY, Chung CS, Nemecek RW. A genetic analysis of clubfoot in Hawaii. *Genet Epidemiol*. 1987;4:299–306.
44. Wynne-Davies R. Family studies and the cause of congenital club foot. Talipes equinovarus, talipes calcaneo-valgus and metatarsus varus. *J Bone Joint Surg Br*. 1964;46:445–63.
45. Wynne-Davies R. Family studies and aetiology of club foot. *J Med Genet*. 1965;2:227–32.
46. de Andrade M, et al. Segregation analysis of idiopathic talipes equinovarus in a Texan population. *Am J Med Genet*. 1998;79:97–102.
47. Kruse LM, Dobbs MB, Gurnett CA. Polygenic threshold model with sex dimorphism in clubfoot inheritance: the Carter effect. *J Bone Joint Surg Am*. 2008;90:2688–94.
48. Kitamura M, Kasai A. Cigarette smoke as a trigger for the dioxin receptor-mediated signaling pathway. *Cancer Lett*. 2007;252:184–94.
49. Czekaj P, Wiaderkiewicz A, Florek E, Wiaderkiewicz R. Tobacco smoke-dependent changes in cytochrome P450 1A1, 1A2, and 2E1 protein expressions in fetuses, newborns, pregnant rats, and human placenta. *Arch Toxicol*. 2005;79:13–24.
50. Hecht JT, et al. NAT2 variation and idiopathic talipes equinovarus (clubfoot). *Am J Med Genet A*. 2007;143A:2285–91.
51. Sommer A, et al. Smoking, the xenobiotic pathway, and clubfoot. *Birth Defects Res A Clin Mol Teratol*. 2011;91:20–8.
52. Zuzarte-Luis V, Hurler JM. Programmed cell death in the developing limb. *Int J Dev Biol*. 2002;46:871–6.

53. Capdevila J, Izpisua Belmonte JC. Patterning mechanisms controlling vertebrate limb development. *Annu Rev Cell Dev Biol.* 2001;17:87–132.
54. Duboc V, Logan MP. Building limb morphology through integration of signalling modules. *Curr Opin Genet Dev.* 2009;19:497–503.
55. Logan M. Finger or toe: the molecular basis of limb identity. *Development.* 2003;130:6401–10.
56. Yang Y. Growth and patterning in the limb: signaling gradients make the decision. *Sci Signal.* 2009;2:pe3.
57. Duboc V, Logan MP. Regulation of limb bud initiation and limb-type morphology. *Dev Dyn.* 2011;240:1017–27.
58. Bareither D. Prenatal development of the foot and ankle. *J Am Podiatr Med Assoc.* 1995;85:753–64.
59. Gurnett CA, et al. Asymmetric lower-limb malformations in individuals with homeobox PITX1 gene mutation. *Am J Hum Genet.* 2008;83:616–22.
60. Klopocki E, et al. Deletions in PITX1 cause a spectrum of lower-limb malformations including mirror-image polydactyly. *Eur J Hum Genet.* 2012;20:705–8.
61. Alvarado DM, et al. Pitx1 haploinsufficiency causes clubfoot in humans and a clubfoot-like phenotype in mice. *Hum Mol Genet.* 2011;20:3943–52.
62. Alvarado DM, et al. Familial isolated clubfoot is associated with recurrent chromosome 17q23.1q23.2 microduplications containing TBX4. *Am J Hum Genet.* 2010;87:154–60.
63. Logan M, Tabin CJ. Role of Pitx1 upstream of Tbx4 in specification of hindlimb identity. *Science.* 1999;283:1736–9.
64. Rodriguez-Esteban C, et al. The T-box genes Tbx4 and Tbx5 regulate limb outgrowth and identity. *Nature.* 1999;398:814–8.
65. Hasson P, et al. Tbx4 and tbx5 acting in connective tissue are required for limb muscle and tendon patterning. *Dev Cell.* 2010;18:148–56.
66. Lu W, et al. Studies of TBX4 and chromosome 17q23.1q23.2: an uncommon cause of non-syndromic clubfoot. *Am J Med Genet A.* 2012;158A:1620–7.
67. Rahimov F, et al. Disruption of an AP-2alpha binding site in an IRF6 enhancer is associated with cleft lip. *Nat Genet.* 2008;40:1341–7.
68. Bamshad M, Jorde LB, Carey JC. A revised and extended classification of the distal arthrogyposes. *Am J Med Genet.* 1996;65:277–81.
69. Gurnett CA, Alaei F, Desruisseau D, Boehm S, Dobbs MB. Skeletal muscle contractile gene (TNNT3, MYH3, TPM2) mutations not found in vertical talus or clubfoot. *Clin Orthop Relat Res.* 2009;467(5):1195–200.
70. Shyy W, Wang K, Sheffield VC, Morcuende JA. Evaluation of embryonic and perinatal myosin gene mutations and the etiology of congenital idiopathic clubfoot. *J Pediatr Orthop.* 2010;30:231–4.
71. Weymouth KS, et al. Variants in genes that encode muscle contractile proteins influence risk for isolated clubfoot. *Am J Med Genet A.* 2011;155A:2170–9.
72. Weymouth KS, Patel CV, Savill SA, Hecht JT. Variation in *HOXA9*, *TPM1* and *TPM2* contributes to clubfoot. *Clin Orthop Relat Res.* 2013 (in preparation).
73. Heck AL, Bray MS, Scott A, Blanton SH, Hecht JT. Variation in *CASP10* gene is associated with idiopathic talipes equinovarus. *J Pediatr Orthop.* 2005;25:598–602.
74. Ester AR, et al. Altered transmission of HOX and apoptotic SNPs identify a potential common pathway for clubfoot. *Am J Med Genet A.* 2009;149A:2745–52.
75. Ester AR, Tyerman G, Wise CA, Blanton SH, Hecht JT. Apoptotic gene analysis in idiopathic talipes equinovarus (clubfoot). *Clin Orthop Relat Res.* 2007;462:32–7.
76. McGinnis W, Krumlauf R. Homeobox genes and axial patterning. *Cell.* 1992;68:283–302.
77. Mark M, Rijli FM, Chambon P. Homeobox genes in embryogenesis and pathogenesis. *Pediatr Res.* 1997;42:421–9.
78. Houghton L, Rosenthal N. Regulation of a muscle-specific transgene by persistent expression of Hox genes in postnatal murine limb muscle. *Dev Dyn.* 1999;216:385–97.

79. Dobbs MB, et al. HOXD10 M319K mutation in a family with isolated congenital vertical talus. *J Orthop Res.* 2006;24:448–53.
80. Shrimpton AE, et al. A HOX gene mutation in a family with isolated congenital vertical talus and Charcot–Marie–Tooth disease. *Am J Hum Genet.* 2004;75:92–6.
81. Rebbeck TR, Dietz FR, Murray JC, Buetow KH. A single-gene explanation for the probability of having idiopathic talipes equinovarus. *Am J Hum Genet.* 1993;53:1051–63.
82. Wang JH, Palmer RM, Chung CS. The role of major gene in clubfoot. *Am J Hum Genet.* 1988;42:772–6.
83. Bonafe L, et al. DTDST mutations are not a frequent cause of idiopathic talipes equinovarus (club foot). *J Med Genet.* 2002;39:e20.

## Chapter 7

# Classification and Etiologic Dissection of Vertebral Segmentation Anomalies

Peter D. Turnpenny

**Abstract** Congenital segmentation defects of the vertebrae (SDV) often give rise to early onset or congenital scoliosis (CS) and cover a multitude of diverse radiological and developmental phenotypes with various formation and segmentation anomalies. Single or multiple vertebrae may be affected and any spinal region involved. Anomalies of rib formation and alignment are commonly associated, and other organ systems may be involved as part of an underlying syndrome. In general, our understanding of the causation of this hugely diverse group of malformation conditions is poor but progress has been made through studying relatively rare families demonstrating mendelian inheritance. This group is dominated by the family of conditions known as the ‘spondylocostal dysostoses’ (SCD), where segmentation anomalies occur throughout the vertebral column. Four Notch signaling pathway genes are now linked to autosomal recessive (AR) SCD, types 1–4, and one to autosomal dominant (AD) SCD—type 5. SCD1 is caused by mutated delta-like 3 (*DLL3*) at chromosome 19q13.1; SCD2, and the severe spondylo*thoracic* dysostosis (STD), is due to mutated mesoderm posterior 2 (*MESP2*) at 15q26; SCD3 is due to mutated *LFNG* O-fucosylpeptide 3-beta-N-acetylglucosaminyltransferase (*LFNG*) at 7p22; and SCD4 is due to mutated hairy and enhancer of split 7 (*HES7*) gene at 17p13.2. SCD5, following autosomal dominant (AD) inheritance, is due to mutated *T-box 6* (*TBX6*) at 16p11.2. Klippel-Feil syndrome (KFS), characterised by fusion of the cervical vertebrae, also embraces much diversity. KFS1 and KFS3 are AD forms and due to mutated *GDF6* (8p22.1) and *GDF3* (12p13.3) respectively. KFS2 is AR and due to mutated *MEOX1* (17q21). Vertebral segmentation anomalies are a variable feature of a wide variety of rare syndromes but for a high proportion of the diverse radiological and developmentally aberrant phenotypes seen in clinical practice the underlying cause is unknown. Further progress will depend on identifying causative genes in familial cases of CS/SDV, or cohorts of subjects with similar phenotypes, using next generation DNA sequencing. Several classifications for SDV, CS and KFS have been proposed and they are described.

---

P. D. Turnpenny (✉)  
Clinical Genetics, Royal Devon & Exeter Hospital, Gladstone Road,  
Exeter EX1 2ED, UK  
e-mail: peter.turnpenny@nhs.net

© Springer Science+Business Media New York 2015  
C. A. Wise, J. J. Rios (eds.), *Molecular Genetics of Pediatric Orthopaedic Disorders*,  
DOI 10.1007/978-1-4939-2169-0\_7

**Keywords** Segmentation defects of the vertebrae (SDV) · Spondylocostal dysostosis · Spondylothoracic dysostosis · Jarcho-Levin syndrome · Klippel-Feil syndrome · Notch signaling pathway · Somitogenesis

## Introduction

Prior to the molecular genetic era analyses were often undertaken as epidemiological studies, leading to the assembly of empiric data that would allow analysis of possible inheritance patterns and recurrence risks for the purpose of genetic counselling. In 134 infants with idiopathic scoliosis, and their first degree relatives, Wynne-Davies [1] found approximately 3% of parents and 3% of siblings had the same, or a similar, deformity. Congenital heart disease occurred in 2.5% (population incidence is ~6/1000 live births) and intellectual disability in 13%, strongly suggesting an admixture of syndromic forms of CS. Genitourinary abnormalities were reported by Vitko et al. [2] in 37 of 85 (43%) patients with CS, and Erol et al. [3] studied 81 patients with different forms of CS and SDV, 39 of whom were prospectively recruited, and 15 (38%) were found to have multi-organ/syndromic associations, many of which fitted loosely into the oculo-auriculo-vertebral (OAV) (or Goldenhar) spectrum. Purkiss et al. [4] studied 237 cases of congenital scoliosis and identified 49 where two or more family members had either congenital or idiopathic scoliosis, suggesting a much higher recurrence rate of 20.7%. There was also a history of idiopathic scoliosis in 17.3% of the families. Maisenbacher et al. [5] reported that 10% of congenital scoliosis cases described having first degree relatives with idiopathic scoliosis. These risk data are diverse and there is a need for more studies with clearer phenotypic stratification.

Table 7.1 lists rare syndromes that may include CS and/or SDV, along with the genetic basis, if known (possible associations also listed [6, 7]). Most are rare and, where the genetic basis of these rare syndromes with segmentation anomalies is known, the mechanisms leading to abnormal vertebral formation are usually not elucidated. The most commonly encountered diagnostic groups in clinical practice are OAV/Goldenhar spectrum, VATER or VACTERL (*V*ertebral, *A*nal, *C*ardiac, *T*racheo-*E*sophageal, *R*enal and *L*imb) association, MURCS (*M*ullerian duct, *R*enal aplasia, *C*ervicothoracic *S*omite dysplasia) association, and Maternal Diabetes syndrome. The pathogenesis of these broad clinical groups is also poorly understood. Any case series presenting to the spinal surgeon and/or paediatrician/geneticist will demonstrate enormous radiological and structural heterogeneity, and a syndromic or genetic diagnosis will be at best vague (including the OAV/VACTERL/MURCS associations) and at worst completely elusive. Table 7.1 highlights that young (and not so young) patients presenting with CS/SDV should be examined and investigated very thoroughly for additional anomalies and a syndrome diagnosis considered. Referral to a clinical geneticist should therefore be part of the patient care pathway.

Although CS is frequently associated with SDV this is not always so and CS may occur in the absence of segmentation anomalies, though abnormalities of

**Table 7.1** Some syndromes and disorders that include segmentation defects of the vertebrae

Syndromes/disorders	OMIM	Gene
Acrofacial dysostosis <sup>a</sup>	263750	
Alagille syndrome	118450	<i>JAG1, NOTCH2</i>
Anhalt <sup>a</sup>	601344	
Atelosteogenesis III	108721	<i>FLNB</i>
Campomelic dysplasia	211970	<i>SOX9</i>
Casamassima-Morton-Nance <sup>a</sup>	271520	
Caudal regression <sup>a</sup>	182940	
Cerebro-facio-thoracic dysplasia <sup>a</sup>	213980	
CHARGE syndrome	214800	<i>CHD7</i>
‘Chromosomal’		
Currarino	176450	<i>HLXB9</i>
Atelosteogenesis, type II (de la Chapelle syndrome)	256050	<i>SLC26A2</i>
DiGeorge/deletion 22q11.2/velocardiofacial syndrome	188400	
Dysspondylochondromatosis <sup>a</sup>		
Femoral hypoplasia-unusual facies <sup>a</sup>	134780	
Fibrodysplasia ossificans progressiva	135100	<i>ACVRI</i>
Fryns-Moerman <sup>a</sup>		
Goldenhar/OAV Spectrum <sup>a</sup>	164210	
Holmes-Schimke <sup>a</sup>		
Incontinentia pigmenti	308310	<i>IKBKG</i>
Kabuki syndrome	147920	<i>MLL2</i>
McKusick-Kaufman syndrome	236700	<i>MKKS</i>
KBG syndrome	148050	<i>ANKRD11</i>
Klippel-Feil <sup>a</sup>	148900	<i>GDF6, GDF3, MEOX1, PAX1<sup>b</sup></i>
Larsen syndrome	150250	<i>FLNB</i>
Lower mesodermal agenesis <sup>a</sup>		
Maternal diabetes mellitus <sup>a</sup>		
MURCS association <sup>a</sup>	601076	
Multiple pterygium syndrome	265000	<i>CHRNA3</i>
OEIS syndrome <sup>a</sup>	258040	
Phaver <sup>a</sup>	261575	
RAPADILINO syndrome ( <i>RECQL4</i> -related disorders)	266280	<i>RECQL4</i>

**Table 7.1** (continued)

Syndromes/disorders	OMIM	Gene
Robinow ( <i>ROR2</i> -related disorders)	180700	<i>ROR2</i>
Rolland-Desbuquois <sup>a</sup>	224400	
Rokitansky sequence <sup>a</sup>	277000	<i>WNT4</i> <sup>b</sup>
Silverman-Handmaker type of dyssegmental dysplasia (DDSH)	224410	<i>HSPG2</i>
Simpson-Golabi-Behmel syndrome	312870	<i>GPC3</i>
Sirenomelia <sup>a</sup>	182940	
Spondylorpotarsal synostosis	272460	<i>FLNB</i>
Thakker-Donnai <sup>a</sup>	227255	
Toriello <sup>a</sup>		
Urioste <sup>a</sup>		
VATER/VACTERL <sup>a</sup>	192350	
Verloove-Vanhorick <sup>a</sup>	215850	
Wildervanck <sup>a</sup>	314600	
Zimmer <sup>a</sup>	301090	

<sup>a</sup> Underlying cause not known

<sup>b</sup> Possible associations reported: *PAX1* [6]; *WNT4* [7]

vertebral *formation* may be present. In cases of this kind a diagnosis of one of the skeletal dysplasias should be considered, though a precise radiological diagnosis may require follow-up skeletal surveys as the child grows. A clinical genetics opinion with a view to genetic testing may be very helpful and examples include: congenital contractural arachnodactyly (*aka* Beals syndrome), which is autosomal dominant and due to mutations in *FBN2*; chondrodysplasia punctata, Conradi-Hünemann type (*aka* Happel syndrome), which is X-linked and due to mutations in the *EBP* gene; diastrophic dysplasia, which is autosomal recessive and due to mutations in the sulphate transporter gene *SLC26A2* (*aka* *DTDST*); and spondylometaphyseal dysplasia, Kozłowski type, which is autosomal dominant and due to mutations in *TRPV4*.

## Spondylocostal Dysostosis, Somitogenesis, and the Notch Signaling Pathway

The main progress in understanding the genetic basis of SDV has come through the study of somitogenesis in animal models, mainly mouse but also chick. Animals with specific gene knockouts are generated and multiple gene expression assays

undertaken to help elucidate the developmental pathways. Somitogenesis is the sequential process whereby paired blocks of paraxial mesoderm are patterned and laid down on either side of the midline from the presomitic mesoderm (PSM) to form somites, a process that takes place between days 20–32 of human embryonic development, proceeding in a rostro-caudal direction. In mouse, a pair of somites is formed every 1–3 h, whilst in humans the process is estimated to take 6–12 h based on cell culture models and analysis of staged anatomical collections [8, 9]. Somites ultimately give rise to four substructures—sclerotome, which forms the axial skeleton and ribs; dermatome, which forms the dermis; myotome, which forms the axial musculature and syndetome, which forms the tendons [10, 11]. Somitogenesis begins shortly after gastrulation and continues until the pre-programmed number of somite blocks is formed. In man 31 blocks of paired tissue are formed but the number is species-specific. The establishment of somite boundaries takes place as a result of very finely tuned molecular processes determined by activation and negative feedback interactions between components of the Notch, Wnt and FGF signaling pathways [12, 13] (Fig. 7.1). In the rostral third of the PSM formation of segmental boundaries is subject to levels of the factor FGF8, which is produced in the caudal region of the embryo [14] and which probably maintains cells in an immature state until levels fall below a threshold, allowing boundary formation. Somites already harbour specification toward their eventual vertebral identity, a process regulated by the Hox family of transcription factors [15], which also display oscillatory expression in the mouse during somitogenesis [16].

The Wnt signalling pathway also displays oscillatory expression in a different temporal phase from Notch pathway genes, and plays a key role in the segmentation clock [17–19]. The mediators of the determination front and the segmentation clock (Notch, FGF, Wnt) are required for forming the somite boundary and specify rostro-caudal patterning of presumptive somites, for which *Mesp2* is crucial [20]. *Mesp2* is expressed caudal to the somite which is forming and this domain is set where Notch signalling is active, FGF signalling is absent, and the transcription factor *Tbx6* is expressed. Precise periodicity in the establishment of somite blocks is mediated by several so-called ‘cycling’, or ‘oscillatory’, genes, two of which, *LFNG* and *HES7*, are implicated in human SCD.

Somites themselves, having formed, are subsequently partitioned into rostral and caudal compartments, with vertebrae formed from the caudal compartment of one somite and the adjacent rostral compartment of the next, a phenomenon that is known as ‘resegmentation’ [21–24]. An understanding of the molecular biology of somitogenesis in animal models, in combination with finding patients and families with specific forms, or patterns, of segmentation anomalies, has led to the most definitive progress in understanding the causes of rare mendelian forms of SDV. Ongoing research is identifying more cycling genes and pathways involved in the regulation of somitogenesis.

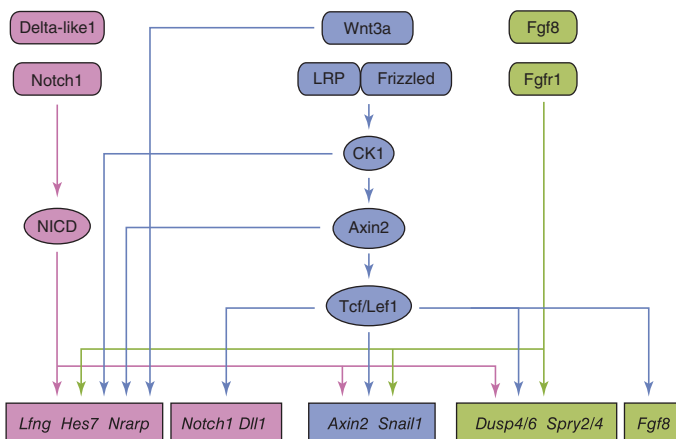
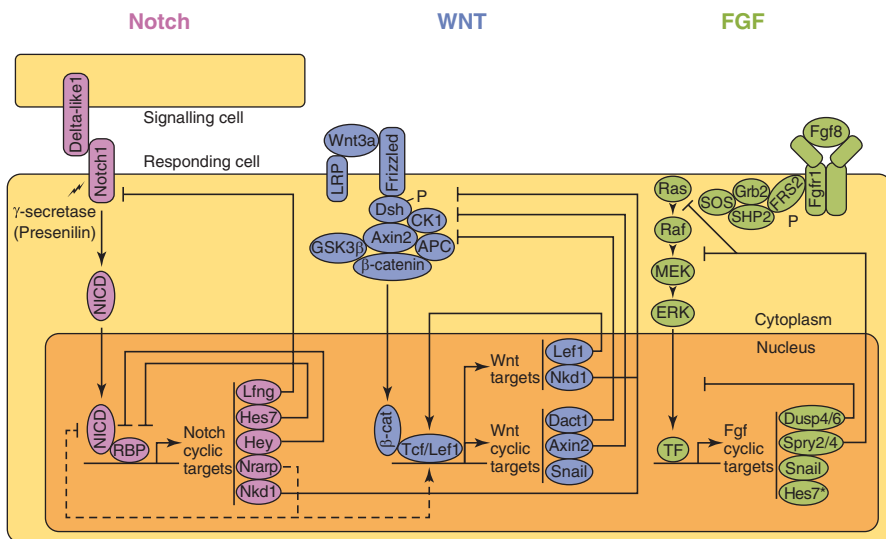


**Fig. 7.1** The putative relationships between the *Notch*, *Wnt* and *FGF* pathways in somitogenesis. (Adapted from Gibb et al. [13] ©Elsevier)

## Varied Use of Clinical Terminology

### *Spondylocostal Dysostosis*

In clinical practice the use of terms for vertebral segmentation abnormalities has been inconsistent and confusing. ‘Spondylocostal dysostosis’ (SCD) continues to be applied to a wide variety of radiological phenotypes where abnormal segmentation is evident together with rib involvement. For this review I use our preferred definition

**Table 7.2** Proposed definitions for the terms spondylocostal dysostosis (SCD) and spondylothoracic dysostosis (STD) (ICVAS)

Features	Spondylocostal Dysostosis (SCD)	Spondylothoracic Dysostosis (STD)
General	No major asymmetry to chest shape	Chest shape symmetrical, with ribs fanning out in a ‘crab-like’ appearance
	Mild, non-progressive scoliosis	Mild, non-progressive scoliosis, or no scoliosis
	Multiple SDV (MSDV) $\geq 10$ contiguous segments	Generalised SDV (GSDV)
	Absence of a bar	Regularly aligned ribs, fused posteriorly at the costovertebral origins, but no points of intercostal fusion
	Mal-aligned ribs with intercostal points of fusion	
Specific, descriptive	‘Pebble beach’ appearance of vertebrae in early childhood radiographs (Fig. 7.3)	‘Tramline’ appearance of prominent vertebral pedicles in early childhood radiographs, not seen in SCD (Fig. 7.6)
		‘Sickle cell’ appearance of vertebrae on transverse imaging [49]

**Table 7.3** Genes causing generalised SDV, i.e. ‘spondylocostal dysostosis’ according to the definition proposed in Table 7.2

SCD	Gene symbol	Chromosomal locus	Protein name
SCD type 1	<i>DLL3</i>	19q13	Delta-like protein 3
SCD type 2 and STD	<i>MESP2</i>	15q26.1	Mesoderm posterior protein 2
SCD type 3	<i>LFNG</i>	7p22	Beta-1,3-N-acetylglucosaminyltransferase lunatic fringe
SCD type 4	<i>HES7</i>	17p13.2	Transcription factor HES-7
SCD type 5	<i>TBX6</i>	16p11.2	T-box6 protein

as given in Table 7.2. This restricts use of the term to *generalised* SDV, which defines the mendelian forms of SCD thus far identified, as summarised in Table 7.3. This is usually a short trunk, short stature condition with multiple/generalised SDV accompanied by rib fusions and/or mal-alignment. A mild, non-progressive kyphoscoliosis is present, usually without additional organ abnormalities. Five Notch signalling pathway genes are now linked to this group, four demonstrating autosomal recessive (AR) inheritance and one autosomal dominant (AD), as described below.

A number of attempts have been made to classify SDV. The scheme proposed by Mortier et al. [25] combines phenotype and inheritance pattern (Table 7.4). The scheme proposed by Takikawa et al. [26] allows a very broad definition of SCD (Table 7.5), and both these schemes identify Jarcho-Levin Syndrome (JLS) with a ‘crab-like’ chest. McMaster and Singh’s [27] surgical approach to classification (1999) distinguishes between formation and segmentation errors (Table 7.6). As with McMaster’s scheme, Aburakawa’s [28] classification scheme for vertebral abnormalities (1996), which includes vertebral morphology (Table 7.7), does not attempt to identify phenotypic patterns of malformation based on assessment of the spine as a whole. The use of a limited number of terms in these classification schemes neither reflects the great diversity of radiological SDV phenotypes seen in clinical practice nor incorporates knowledge from molecular genetics. Furthermore, the diversity of SDV is not captured within the classification of osteochondrodysplasias [29, 30]. A new scheme for classification and reporting from the International Consortium for Vertebral Anomalies and Scoliosis (ICVAS) is described later.

### ***Klippel-Feil Syndrome***

The term Klippel-Feil anomaly or syndromes (KFS) has a more specific application, even though the phenotypes within the general category are diverse. KFS refers to vertebral fusion or segmentation errors involving the cervical region and has been the subject of several classifications (Table 7.8) [31, 32]. Clarke et al. [33] (Table 7.9) proposed a further, detailed classification combining modes of inheritance. To these clinical classifications must now be added a classification based on the recently discovered gene associations with rare forms of KFS [34–36] (Table 7.10). The *Pax1* gene has been shown to be active during sclerotome formation and differentiation and mutations were identified in the mouse *undulated*, suggesting that sclerotome condensation is a *Pax1*-dependent process [37]. Two studies on patient cohorts with KFS were subsequently undertaken [6, 38] but despite some gene variants being identified in a small number the same variants were either detected in an asymptomatic parent or did not occur in a conserved region of the gene. Overall, the role of *PAX1* in KFS remains to be elucidated.

## **The Genetics and Clinical Description of SCD Sub-types**

### ***SCD1***

Autozygosity mapping was used to identify a locus for AR SCD at chromosome 19q13.1 in a large Arab–Israeli kindred first reported in 1991 [39, 40]. The region is syntenic with murine chromosome 7 harbouring the *Dll3* gene, which is truncated in the pudgy mouse [41]. *Dll3*-null mice show disruption of the cyclical somitogenesis

**Table 7.4** Classification of SDV according to Mortier et al. [25]

Nomenclature	Definition
Jarcho-Levin syndrome	Autosomal recessive
	Symmetrical crab-like chest, lethal
Spondylothoracic dysostosis	Autosomal recessive
	Intrafamilial variability, severe/lethal
	Associated anomalies uncommon
Spondylocostal dysostosis	Autosomal dominant
	Benign
Heterogeneous group	Sporadic
	Associated anomalies common

**Table 7.5** Classification/definition of SDV according to Takikawa et al. [26]

Nomenclature	Definition
Jarcho-Levin syndrome	Symmetrical crab-like chest
Spondylocostal dysostosis	$\geq 2$ vertebral anomalies associated with rib anomalies (fusion and/or absence)

**Table 7.6** Classification (surgical/anatomical) of vertebral segmentation abnormalities causing congenital kyphosis/kyphoscoliosis, according to McMaster and Singh [27]

Type	Anatomical deformity	Anomalies
I	Anterior failure of vertebral body formation	Posterolateral quadrant vertebrae
		Single vertebra
		Two adjacent vertebrae
		Posterior hemivertebrae
		Single vertebra
		Two adjacent vertebrae
		Butterfly (sagittal cleft) vertebrae
		Anterior or anterolateral wedged vertebrae
		Single vertebra
		Two adjacent vertebrae
II	Anterior failure of vertebral body segmentation	Anterior unsegmented bar
		Anterolateral unsegmented bar
III	Mixed	Anterolateral unsegmented bar contralateral posterolateral quadrant vertebrae
IV	Unclassifiable	

**Table 7.7** Aburakawa Classification of vertebral segmentation abnormalities [26, 28] (modified North American classification). Note that hemivertebrae are seen in Types B to F, and L

<b>Failure of formation</b>	
<i>Type I</i>	
A. Double pedicle	
B. Semi segmented	
C. Incarcerated	
<i>Type II</i>	
D. Non incarcerated, no lateral shift	
E. Non incarcerated, plus lateral shift	
<i>Type III</i>	
F. Multiple	
<i>Type IV</i>	
G. Wedge	
H. Butterfly	
<b>Failure of segmentation</b>	
I. Unilateral Bar	
J. Complete block	
K. Wedge (plus narrow disc)	
<b>Mixed</b>	
L. Unilateral bar plus hemivertebra	
M. Unclassifiable	

**Table 7.8** Classification of Klippel-Feil anomaly, referring to segmentation defects or fusion of the cervical vertebrae, according to Feil [31] and Thomsen et al. [32]

Type	Site	Anomaly
I	Cervical and upper thoracic	Massive fusion with synostosis
II	Cervical	One or two interspaces only, hemivertebrae, occipito-atlantoid fusion
III	Cervical and lower thoracic or lumbar	Fusion

clock within the PSM [42]. Human *DLL3* was therefore the obvious candidate for *SCD1* in 3 separate families where affected individuals were homozygous for mutations [43]. The organization of human *DLL3* is almost identical to mouse *Dll3*, excepting the terminal exon, which corresponds to a fusion of mouse exons 9 and 10, resulting in a human protein of 32 additional amino acids. There is variability in the size of the mouse and human introns. The gene is sequentially ordered with a signal sequence (SS), the delta-serrate-lag (DSL) domain, 6 highly conserved epidermal growth factor (EGF) repeats, and a transmembrane<sup>TM</sup> region (Fig. 7.2). More than 30 *DLL3* mutations have now been identified and most of these published [44, 45]. Approximately 75% of positive cases have protein truncation nonsense mutations (the rest being missense) and parental consanguinity is seen in the same proportion of cases.

**Table 7.9** Classification of Klippel-Feil anomaly according to Clarke et al. [33]. (Adapted from original publication)

Class	Vertebral fusions	Inheritance	Possible anomalies
KF1	Only class with C1 fusions C1 fusion not dominant Variable expression of other fusions	Recessive	Very short neck; heart; urogenital; craniofacial; hearing; limb; digital; ocular defects Variable expression
KF2	C2-3 fusion dominant C2-3 most rostral fusion Cervical, thoracic and lumbar fusion variable within a family	Dominant	Craniofacial; hearing; otolaryngeal; skeletal and limb defects Variable expression
KF3	Isolated cervical fusions Variable position Any cervical fusion except C1	Recessive or reduced penetrance	Craniofacial Facial dysmorphology Variable expression
KF4	Fusion of cervical vertebrae, data limited	Possible X-linked Predominantly females	Hearing and ocular anomalies—abducens palsy with retraction bulbi <i>aka</i> Wildervanck syndrome

**Table 7.10** Genes associated with Klippel-Feil syndrome (KFS) [34–36]

KFS	Gene symbol	Chromosomal locus	Encodes	Inheritance
KFS1	<i>GDF6</i> [ <i>aka</i> cartilage-derived morphogenetic protein 2 ( <i>CDMP2</i> )]	8q22.1	A member of the bone morphogenetic protein family	AD
KFS2	<i>MEOX1</i>	17q21.31	Homeodomain-containing protein	AR
KFS3	<i>GDF3</i>	12p13.1	A member of the bone morphogenetic protein family	AD

There is a general consistency in the abnormal form and shape of the vertebrae in the different regions, from cervical to lumbar. The radiological appearances in childhood are of vertebrae that are circular or ovoid on A-P projection, and they have smooth outlines. To this appearance the term ‘pebble beach sign’ has been applied [45] (Fig. 7.3). Stature is affected to a variable degree, with some affected subjects achieving a final adult height that is only about 15 cm less than their predicted height on the basis of arm span measurements (assuming arm length is unaffected). Final adult stature is more severely affected in some cases and in the large family reported by Turnpenny et al. [39], a range of severity was evident. We know of two patients with slightly milder phenotypes due to missense mutations C309R and G404C, both with less dramatic vertebral segmentation abnormalities, even though the whole spine was involved (unpublished data). The milder phenotype

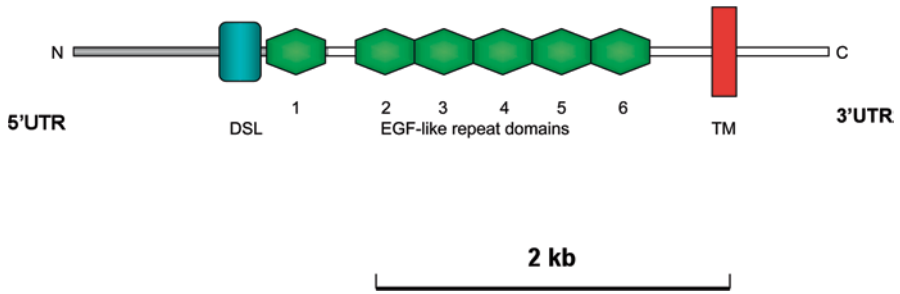
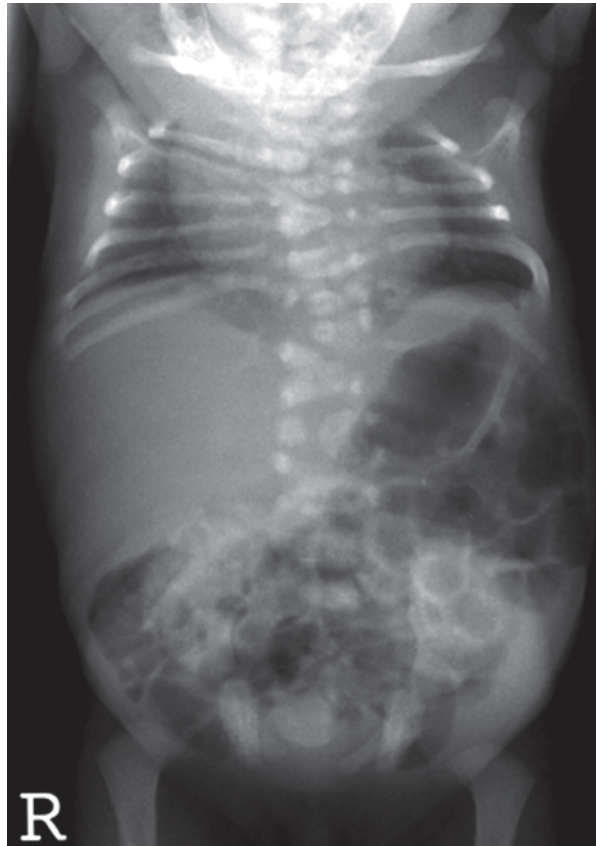


**Fig. 7.2** The organization of the *DLL3* gene. *DSL* delta-serrate-lag domain, *EGF* epidermal growth factor domain(s), *SS* starter sequence, *TM* transmembrane domain

**Fig. 7.3** The radiological phenotype of SCD1 due to mutated *DLL3*. This shows segmentation abnormalities throughout the vertebral column and the variable ovoid appearance of multiple vertebrae—the ‘pebble beach’ sign. The ribs are mal-aligned with points of fusion along their length. (Reproduced from Turnpenny et al. [46])



may be due to the position of these residues within the EGF domains. It seems likely that some missense mutations, though not all, may give rise to milder phenotypes. There is no clear, consistent evidence for organ abnormalities beyond the spine in subjects with SCD1. Learning difficulties or intellectual disability is not a feature, and although affected individuals have mild scoliotic curves from an early stage,

these appear to remain stable throughout life in the majority of cases and spinal surgery is usually not required.

## ***SCD2***

A genome-wide scanning was used to identify linkage to 15q21.3–15q26.1 in a consanguineous family with two affected children who neither had *DLL3* mutations nor demonstrated linkage to 19q13.1. This region harbors the somitogenesis gene *MESP2*, and sequencing identified a 4-bp (AGGC) duplication, frameshift mutation for which the affected subjects were homozygous and the parents heterozygous [47]. The mutation was not found in 68 normal ethnically matched control chromosomes. *MESP2* encodes a basic helix-loop-helix (bHLH) transcription factor, a protein of 397 amino acids. Human *MESP2* protein shares 58.1% identity with mouse *Mesp2*. Human *MESP2* amino terminus contains a bHLH region encompassing 51 amino acids, which is divided into an 11-residue basic domain, a 13-residue helix I domain, an 11-residue loop domain, and a 16-residue helix II domain. The loop region is conserved between mouse and human *MesP1* and *MesP2*. In addition, both *MesP1* and *MesP2* contain a unique CPXCP motif immediately carboxy-terminal to the bHLH domain. The amino- and carboxy-terminal domains are separated in human *MESP2* by a GQ repeat region, which is also present in human *MESP1* (2 repeats), but have expanded in human *MESP2* (13 repeats). Mouse *Mesp1* and *Mesp2* do not contain any GQ repeats but they do contain a couple of QX repeats in the same region (Fig. 7.4). In cases designated SCD2 the mutations identified do not appear to give rise to nonsense mediated decay of the derivative protein, in contrast to the effect of mutations in STD (see below), the more severe phenotype due to mutated *MESP2*.

Only one family with SCD due to a mutation in *MESP2*, demonstrating AR inheritance, has been published [47] and, therefore, the phenotype is based on minimal data. However, a second affected family with the same mutation and a very similar radiological phenotype was presented at an international meeting in 2005 (Bonafé et al.). Subsequent haplotype analysis failed to show evidence for a common ancestry for the two families (unpublished data), so the particular 4-bp duplication mutation is recurrent. A further case was found to be a compound heterozygote for *MESP2* mutations (Fig. 7.5). The radiological phenotype is similar to, but distinguishable from, that of SCD1, and the ribs are more normally aligned. Segmentation defects appear more severe in the thoracic vertebrae compared to the lumbar vertebrae, which are relatively spared. Stature is affected to a small degree and no additional organ abnormalities have been reported.

## ***STD—Spondylothoracic Dysostosis***

Mutated *MESP2* is also the cause of STD [48], a severe form of SDV with marked shortening of the spine, reduced thoracic volume, and in some cases life-threatening

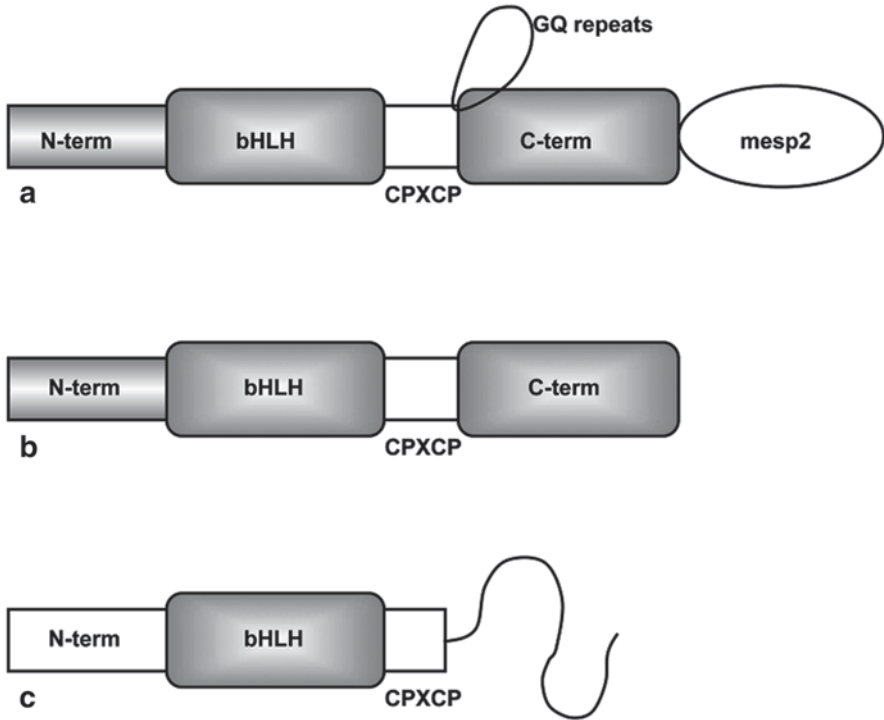


**Fig. 7.4** Comparison of Mesoderm posterior 2: **a** *MESP2* and **b** *MESP1* (adjacent to *MESP2* at 15q26 in man). Both sequences clearly contain a basic helix–loop–helix (*bHLH*) domain. The length of the loop region is conserved between *MESP1* and *MESP2*. In addition, *MESP1* and *MESP2* contain a unique CPXCP motif immediately C-terminal to the bHLH domain. *MESP1* and *MESP2* also share a C-terminal region that is likely to adopt a similar fold. *MESP2* sequences contain a unique region at the C-terminus. The GQ repeats, which are located between the CPXCP motif and the shared C-terminal domain, are also found in human *MESP1* (only two repeats) but have expanded in human *MESP2* (13 repeats). Although lacking GQ repeats, the mouse sequences have two QX repeats in the same region: mouse *MESP1* QSQS; mouse *MESP2* QAQM. **c** Human *MESP2* frameshift mutant

respiratory insufficiency. The mutations are of the type that give rise to nonsense-mediated decay (unpublished data).

There are two very useful radiological features that help distinguish SCD type 1 from STD (and to some extent SCD2). Firstly, in SCD points of fusion of the ribs along their length are usually apparent, whereas in STD the ribs are fused *posteriorly* and fan out laterally ('crab-like' appearance) without points of fusion along their length. Secondly, in fetal life and early childhood multiple rounded hemivertebrae characterizes SCD1 (*DLL3* gene)—the 'pebble beach sign' [45]—and the vertebral pedicles are poorly visualised because they are not yet ossified. By contrast, in *MESP2*-associated SCD and STD, the vertebral pedicles are visible radiologically in fetal life and early childhood. Indeed, they are often neatly arranged and aligned,

**Fig. 7.5** The radiological phenotype of SCD2 due to mutated *MESP2*. This shows segmentation abnormalities throughout the vertebral column with the thoracic region most severely disrupted. (Reproduced from Turnpenny et al. [46])



bordering multiple hemivertebrae between (Fig. 7.6). This is sometimes referred to as the ‘tramline sign’. STD has been well delineated and described by Cornier et al. [49]. Most reported cases are Puerto Rican but, although rare, it has been seen globally.

### ***SCD3***

A candidate gene approach was used to identify *LFNG* as the genetic cause of SCD in an individual in whom no mutation could be found in *DLL3* or *MESP2* [50] (Fig. 7.7). *LFNG*—Lunatic fringe—encodes a glycosyltransferase (fucose-specific  $\beta$

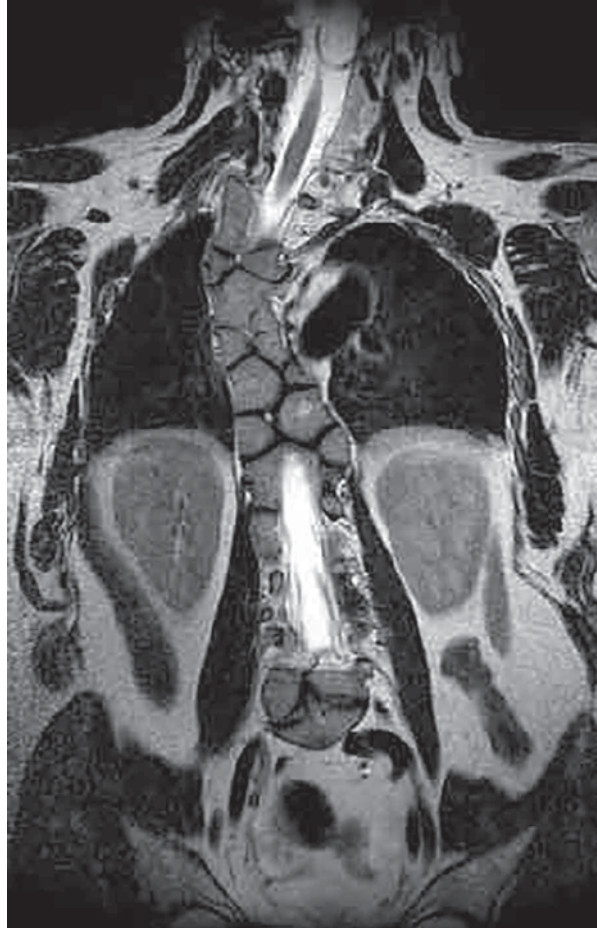
**Fig. 7.6** The radiological phenotype of STD due to mutated *MESP2*. This shows marked shortening of the spine, generalised segmentation defects, a ‘crab-like’ fanning out of the ribs from their posterior costovertebral origins, and well aligned ribs. The vertebral pedicles are ossified at this early stage of like (in contrast to *SCD1*), sometimes called the ‘tramline’ sign. (Reproduced courtesy of eLS)



1,3 N-acetylglucosamine) that post-translationally modifies the Notch family of cell surface receptors, a key step in the regulation of this signaling pathway [51], and is one of the ‘cycling’ genes whose wave of expression in the PSM, in a caudal-rostral direction, is crucial to the establishment of the next somite boundary. *LFNG* was sequenced as its expression is severely disregulated in mouse embryos that lack *Dll3* [52, 53] (the phenotypes of *Dll3* and *Lfng* null mutant mice are very similar), and is associated with the Notch signalling pathway (like *DLL3* and *MESP2*). In the affected case a missense mutation (c.564C→A) was detected that resulted in the substitution of leucine for phenylalanine (F188L). The proband’s consanguineous parents, of Lebanese Arab origin, were normal and heterozygous for the mutant allele. Functional assays showed that F188L did not localize to the Golgi apparatus as the wild-type *LFNG* protein, and that F188L lacked transferase activity.

In this, so far unique, case of *SCD3* the segmentation disruption was severe compared to *SCD1* and *SCD2*, giving rise to marked truncal shortening and apparently normal limb length—arm span 186.5 cm and adult height 155 cm, lower segment 92.5 cm. Multiple vertebral ossification centres in the thoracic spine, with very angular shapes were apparent. The affected case also demonstrated a minor form of distal arthrogyriposis in the upper limbs, and it is not known whether this was part of the condition or secondary to peripheral nerve entrapment.

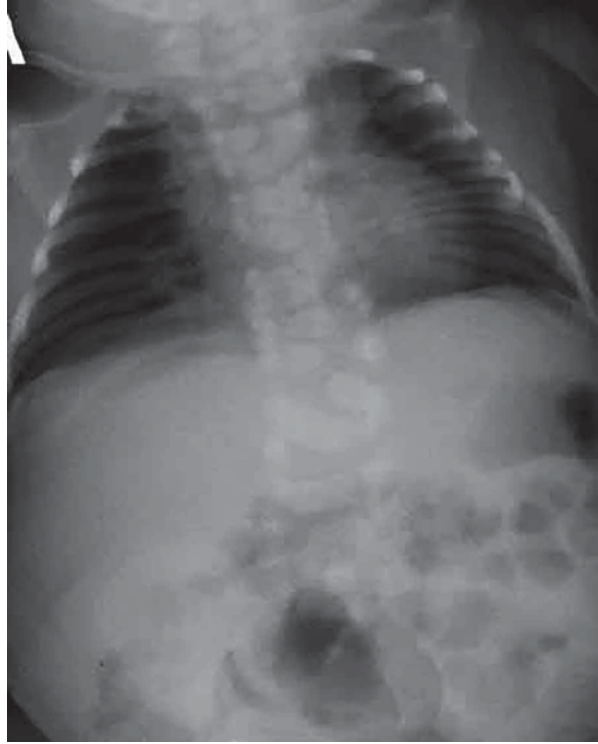
**Fig. 7.7** The radiological phenotype of SCD3 due to mutated *LFNG*. This shows severe shortening of the thoracic spine in particular. (Reproduced from Sparrow et al. [49] ©Elsevier)



### ***SCD4***

In humans the first identified case of SCD due to a mutation in *HES7* was found to be homozygous for a C>T nucleotide transition in exon 2, resulting in an arginine to tryptophan amino acid substitution [54]. Subsequently a family demonstrating compound heterozygosity for *HES7* mutations was identified [55]. *HES7* encodes a bHLH-Orange domain transcriptional repressor protein that is both a direct target of the Notch signalling pathway, and part of a negative feedback mechanism required to attenuate Notch signalling [56]. Like *LFNG*, *HES7* is a cycling gene; it is expressed in the PSM in an oscillatory pattern [57], which is achieved by an autoregulatory loop. Once translated, Hes proteins act on their own promoters to repress transcription and, due to the short half-life of Hes proteins, autorepression is relieved, which allows a new wave of transcription and translation every 90–120 min in the mouse. Hes7-null mice display severe multiple SDV phenotypes [58].

**Fig. 7.8** The radiological phenotype of SCD4 due to mutated *HES7*. This shows segmentation abnormalities throughout the vertebral column and the appearance resembles that of SCD2/STD. (Reproduced with permission from Sparrow et al. [54] ©Oxford University Press)



To date, the pattern of SDV in SCD4 lies somewhere between SCD1 and mild STD, with ribs appearing to show fusion posteriorly and fanning out in a crab-like fashion (Fig. 7.8). The first reported patient was homozygous for a *HES7* mutation and also had a lumbar myelomeningocele neural tube defect [54], whilst there were no associated malformations in the second reported family [55], where SCD occurred only in subjects who were compound heterozygotes for *HES7* mutations. The findings in a large extended, inbred kindred is [59], in which some affected individuals have midline developmental defects besides generalised SDV.

### ***SCD5—Autosomal Dominant***

Only one genetic cause of AD SCD has thus far been identified, namely mutated *TBX6* [60], in a three-generation Macedonian family previously shown not have a mutation in *DLL3*, *MESP2*, *LFNG* and *HES7* [61]. Exome capture and next-generation sequencing were used to identify a stop loss mutation in *TBX6* that segregated with the phenotype in two generations, and the family demonstrated a generalised pattern of SDV without any additional malformations (Fig. 7.9).

The *TBX6*, or T-box6, gene encodes a putative DNA-binding protein expressed in somite precursor cells, indicating that it is implicated in the specification of the

**Fig. 7.9** The radiological phenotype of SCD5 due to mutated *TBX6*. This shows segmentation abnormalities throughout the vertebral column in an adult. The pattern is similar to that seen in an adult with SCD1. (Reproduced courtesy of eLS, 2014)



paraxial mesoderm. Studies in mouse demonstrate that the *Tbx6* protein is directly bound to the *Mesp2* gene, mediates Notch signalling, and subsequent *Mesp2* transcription in the PSM [62]. Functional studies in this reported family [60] demonstrated a deleterious effect on the transcriptional activation activity of the *TBX6* protein, probably secondary to haploinsufficiency.

## A New Classification and Radiological Reporting System for SDV

Currently, the use of nomenclature to describe CS/SDV is inconsistent and confusing, even though some authors have recognized the existence of different entities and applied a rational distinction in the use of terms [63, 64]. Unfortunately this applies to the eponym *Jarcho-Levin* syndrome (JLS), which is used so widely that it no longer serves any useful specific purpose. Its use is therefore discouraged. *Klippel-Feil* anomaly or syndrome, is long established and more specific in application (see above), and therefore retains some usefulness. It is suggested that the terms SCD and STD be reserved for specific phenotypes (Tables 7.2 and 7.3). Strictly speaking, these are dysostoses, not dysplasias, because they are due to errors of segmentation or formation early in morphogenesis, rather than an ongoing abnormality of chondro-osseous tissues during pre- and postnatal life.

Experience indicates that the widely used terms Jarcho-Levin syndrome (JLS) [65–70], costovertebral syndrome [71–73], spondylocostal dysostosis (SCD, or SCDO according to OMIM nomenclature) [74, 75], and spondylothoracic dysplasia (STD) [76–78] are used interchangeably and indiscriminately [26, 79, 80]. In 1938 Jarcho and Levin [81] reported two siblings with short trunks, multiple SDV (M-SDV), and abnormally aligned ribs with points of fusion. Since then JLS has been widely and indiscriminately applied. Furthermore, in recent years many authors have equated JLS with the distinctive phenotype of a severely shortened spine and a ‘crab-like’ appearance of the ribs for which the preferred term today is STD [48, 49], first suggested by Moseley and Bonforte [76]. Berdon et al. [82] have clarified the historical record. The incidence of STD is relatively high in Puerto Ricans compared to elsewhere because of a founder effect *MESP2* mutation [49]. The ethnicity of the siblings reported by Jarcho and Levin [81] was ‘colored’, they did not manifest the distinctive crab-like appearance, and their phenotype was closer to either SCD2 or SCD4, as previously described. A further example illustrating inconsistency is the rare eponymous entity with marked diversity in the few reported cases, namely Casamassima-Morton-Nance (CMN) syndrome [83]. This combines SDV with urogenital anomalies, apparently following autosomal recessive inheritance. However, subsequent reports [84, 85] demonstrated a different SDV phenotype from the cases of Casamassima et al. [83] and consistency across all three reports, based on the SDV phenotype, is lacking.

The newly proposed classification and reporting system for SDV conditions is illustrated in Fig. 7.10 and was developed by a working group of the International Consortium for Vertebral Anomalies and Scoliosis (ICVAS). The goal was to produce a classification system for SDV that provides simple, uniform terminology, and can be applied both to man and animal models. The system takes account of these conditions being either syndromic or non-syndromic. The numerous examples of syndromes and associations are outlined in Table 7.1. Non-syndromic conditions include most cases of mendelian SCD and STD (as defined in this paper), whereby the malformation is usually restricted to the spine. There are many examples with single, or multiple, SDV with limited regional involvement, associated

Figure 7. ICVAS clinical classification algorithm.  
 SDV: Segmentation Defect(s) of the Vertebrae; M: Multiple; S: Single; R: Regional;  
 G: Generalised; U: Undefined

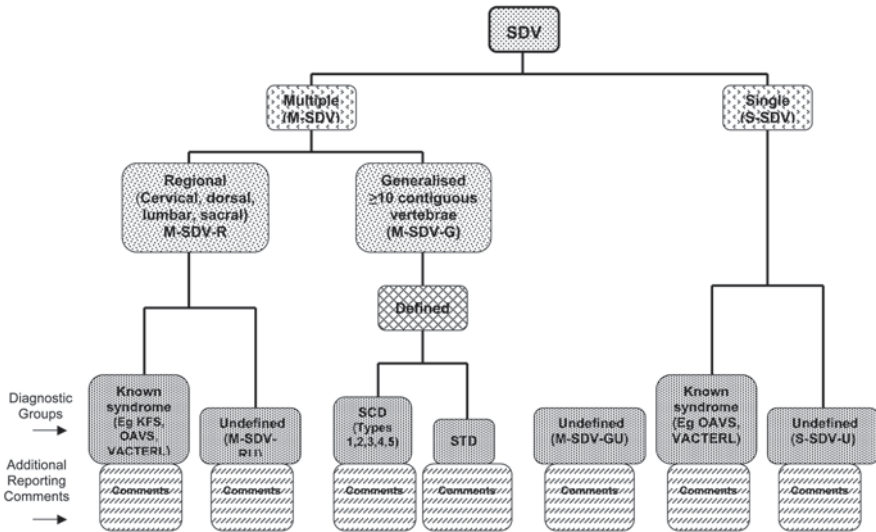


Fig. 7.10 The classification algorithm for SDV proposed by ICVAS, the International Consortium for Vertebral Anomalies and Scoliosis. By this scheme any patient can be placed within one of seven basic categories, with provision for further description of the specific findings in any individual

kyphoscoliosis, and cases classified as KFS (without other associations). As a generalisation, these conditions are caused by defective genetic determination of somitogenesis, and/or non-intrinsic disruption of normal segmentation and/or formation of vertebrae. In the proposed scheme (Fig. 7.10) conditions essentially fall into one of seven categories. This simplification allows for uniformity between observers. For example, a case with limited thoracic spine involvement that might previously have been diagnosed as JLS or SCD, would now be classified and reported as an ‘undefined regional (thoracic) M-SDV’. In any particular case, once placed within one of the seven categories, further detailed descriptions of the position and effects of the segmentation anomalies can be added. Where appropriate, therefore, the ICVAS scheme incorporates existing terminology. This greatly reduces confusion that might be generated by indiscriminate use of the terms JLS or SCD. In cases where at least ten vertebral segments are affected but non-contiguously, we suggest this be designated a ‘multi-regional’ form of M-SDV rather than ‘generalized’. This group of phenotypes appears to be diverse, and further delineation will only be possible with advances in our understanding of causation.

The usefulness of correlating a detailed clinical examination with radiological findings has been well described previously [3]. The system has been piloted [86] and allows for a more precise characterization of the radiological phenotype compared to the indiscriminate use of a small number of terms, including eponyms. Furthermore, the system incorporates assessment of radiographic patterns of the spine

as a whole, in addition to malformations of individual vertebrae. A consistent use of terminology using this system will lead to improved diagnostic consensus and better stratification of patient cohorts for testing of novel gene candidates and evaluation of natural history. Adoption of the ICVAS classification system in clinical practice is recommended, although it is recognised that patient management often depends on additional assessments, e.g. respiratory function, in cases with restricted lung capacity and/or associated kyphoscoliosis, as well as monitoring changes over time. It is also recognised that the system will evolve over time as the identification of new genes brings clarity to the causation of different conditions, and groups of conditions, with CS and SDV. Indeed, this is already the case with new gene discoveries for both SCD (type 5) and KFS.

## References

1. Wynne-Davies R. Infantile idiopathic scoliosis. Causative factors, particularly in the first six months of life. *J Bone Joint Surg Br.* 1975;57:138–41.
2. Vitko RJ, Cass AS, Winter RB. Anomalies of the genitourinary tract associated with congenital scoliosis and congenital kyphosis. *J Urol.* 1972;108:655–9.
3. Erol B, Tracy MR, Dormans JP, Zachai EH, Tonnesen M, O'Brien ML, Turnpenny PD, Kusumi K. Congenital scoliosis and vertebral malformations: characterization of segmental defects for genetic analysis. *J Pediatr Orthop.* 2004;24:674–82.
4. Purkiss SB, Driscoll B, Cole WG, Alman B. Idiopathic scoliosis in families of children with congenital scoliosis. *Clin Orthop Relat Res.* 2002;401:27–31.
5. Maisenbacher MK, Han JS, O'Brien ML, Tracy MR, Erol B, Schaffer AA, Dormans JP, Zachai EH, Kusumi K. Molecular analysis of congenital scoliosis: a candidate gene approach. *Hum Genet.* 2005;116(5):416–9.
6. McGaughran J, Oates A, Donnai D, Read AP, Tassabehji M. Mutations in PAX1 may be associated with Klippel-Feil syndrome. *Eur J Hum Genet.* 2003;11:468–74.
7. Philibert P, Biason-Lauber A, Rouzier R, Pienkowski C, Paris F, Konrad D, Schoenle E, Sultan C. Identification and functional analysis of a new WNT4 gene mutation among 28 adolescent girls with primary amenorrhea and müllerian duct abnormalities: a French collaborative study. *J Clin Endocrinol Metab.* 2008;93(3):895–900.
8. William DA, Saitta B, Gibson JD, Traas J, Markov V, Gonzalez DM, Sewell W, Anderson DM, Pratt SC, Rappaport E, Kusumi K. Identification of oscillatory genes in somitogenesis from functional genomic analysis of a human mesenchymal stem cell model. *Dev Biol.* 2007;305:172–86.
9. Eckalbar WL, Fisher RE, Rawls A, Kusumi K. Scoliosis and segmentation defects of the vertebrae. *Wiley Interdiscip Rev Dev Biol.* 2012;1(3):401–23.
10. Keynes RJ, Stern CD. Mechanisms of vertebrate segmentation. *Development.* 1988;103:413–29.
11. Brent AE, Schweitzer R, Tabin CJ. A somitic compartment of tendon progenitors. *Cell.* 2003;113(2):235–48.
12. Dequéant M-L, Pourquié O. Segmental patterning of the vertebrate embryonic axis. *Nat Rev Genet.* 2008;9:370–82.
13. Gibb S, Maroto M, Dale JK. The segmentation clock mechanism moves up a notch. *Trends Cell Biol.* 2010;20:593–600.
14. Dubrulle J, McGrew MJ, Pourquié O. FGF signaling controls somite boundary position and regulates segmentation clock control of spatiotemporal Hox gene activation. *Cell.* 2001;106:219–32.

15. Krumlauf R. Hox genes in vertebrate development. *Cell*. 1994;78:191–201.
16. Zákány J, Kmita M, Alarcon P, de la P JL, Duboule D. Localized and transient transcription of Hox genes suggests a link between patterning and the segmentation clock. *Cell*. 2001;106(2):207–17.
17. Aulehla A, Wehrle C, Brand-Saberi B, Kemler R, Gossler A, Kanzler B, Herrmann BG. Wnt3a plays a major role in the segmentation clock controlling somitogenesis. *Dev Cell*. 2003;4:395–406.
18. Aulehla A, Herrmann B. Segmentation in vertebrates: clock and gradient finally joined. *Genes Dev*. 2004;18:2060–7.
19. Hofmann M, Schuster-Gossler K, Watabe-Rudolph M, Aulehla A, Herrmann BG, Gossler A. WNT signaling, in synergy with T/TBX6, controls Notch signaling by regulating Dll1 expression in the presomitic mesoderm of mouse embryos. *Genes Dev*. 2004;18(22):2712–7.
20. Saga Y. The mechanism of somite formation in mice. *Curr Opin Genet Dev*. 2012;22:331–8.
21. Remak R. Untersuchungen über die entwicklung der Wirbeltiere. Berlin: Reimer; 1850.
22. Bagnall KM, Higgins SJ, Sanders EJ. The contribution made by cells from a single somite to tissues within a body segment and assessment of their integration with similar cells from adjacent segments. *Development*. 1989;107(4):931–43.
23. Ewan KB, Everett AW. Evidence for resegmentation in the formation of the vertebral column using the novel approach of retroviral-mediated gene transfer. *Exp Cell Res*. 1992;198(2):315–20.
24. Goldstein RS, Kalcheim C. Determination of epithelial half-somites in skeletal morphogenesis. *Development*. 1992;116:441–5.
25. Mortier GR, Lachman RS, Bocian M, Rimoin DL. Multiple vertebral segmentation defects: analysis of 26 new patients and review of the literature. *Am J Med Genet*. 1996;61:310–9.
26. Takikawa K, Haga N, Maruyama T, Nakatomi A, Kondoh T, Makita Y, Hata A, Kawabata H, Ikegawa S. Spine and rib abnormalities and stature in spondylocostal dysostosis. *Spine*. 2006;31:E192–7.
27. McMaster MJ, Singh H. Natural history of congenital kyphosis and congenital kyphoscoliosis. A study of one hundred and twelve patients. *J Bone Joint Surg Am*. 1999;81:1367–83.
28. Aburakawa K, Harada M, Otake S. Clinical evaluations of the treatment of congenital scoliosis. *Orthop Surg Trauma*. 1996;39:55–62.
29. Offiah AC, Hall CM. Radiological diagnosis of the constitutional disorders of bone. As easy as A, B, C? *Pediatr Radiol*. 2003;33:153–61.
30. Superti-Furga A, Unger S. Nosology and classification of genetic skeletal disorders: 2006 revision. *Am J Med Genet*. 2007;143:1–18.
31. Feil A. L'absence et la diminution des vertebres cervicales. Thesis, Librairie Litteraire et Medicale, 1919, Paris.
32. Thomsen M, Schneider U, Weber M, Johannisson R, Niethard F. Scoliosis and congenital anomalies associated with Klippel-Feil syndrome types I-III. *Spine*. 1997;22:396–401.
33. Clarke RA, Catalan G, Diwan AD, Kearsley JH. Heterogeneity in Klippel-Feil syndrome: a new classification. *Pediatr Radiol*. 1998;28:967–74.
34. Tassabehji M, Fang ZM, Hilton EN, McGaughran J, Zhao Z, de Bock CE, Howard E, Malass M, Donnai D, Diwan A, Manson FDC, Murrell D, Clarke RA. Mutations in GDF6 are associated with vertebral segmentation defects in Klippel-Feil syndrome. *Hum Mutat*. 2008;29:1017–27.
35. Mohamed JY, Faqeih E, Alsiddiky A, Alshammari MJ, Ibrahim NA, Alkuraya FS. Mutations in MEOX1, encoding mesenchyme homeobox 1, cause Klippel-Feil anomaly. *Am J Hum Genet*. 2013;92:157–61.
36. Ye M, Berry-Wynne KM, Asai-Coakwell M, Sundaresan P, Footz T, French CR, Abitbol M, Fleisch VC, Corbett N, Allison WT, Drummond G, Walter MA, Underhill TM, Waskiewicz AJ, Lehmann OJ. Mutation of the bone morphogenetic protein GDF3 causes ocular and skeletal anomalies. *Hum Molec Genet*. 2010;19:287–98.
37. Balling R, Deutsch U, Gruss P. Undulated, a mutation affecting the development of the mouse skeleton, has a point mutation in the paired box of Pax 1. *Cell*. 1988;55:531–5.

38. Giampietro PF, Raggio CL, Reynolds CE, Shukla SK, McPherson E, Ghebranious N, Jacobsen FS, Kumar V, Faciszewski T, Pauli RM, Rasmussen K, Burmester JK, Zaleski C, Merchant S, David D, Weber JL, Glurich I, Blank RD. An analysis of PAX1 in the development of vertebral malformations. *Clin Genet.* 2005;68:448–53.
39. Turnpenny PD, Thwaites RJ, Boulos FN. Evidence for variable gene expression in a large inbred kindred with autosomal recessive spondylocostal dysostosis. *J Med Genet.* 1991;28:27–33.
40. Turnpenny PD, Bulman MP, Frayling TM, Abu-Nasra TK, Garrett C, Hattersley AT, Ellard S. A gene for autosomal recessive spondylocostal dysostosis maps to 19q13.1-q13.3. *Am J Hum Genet.* 1999;65:175–82.
41. Kusumi K, Sun ES, Kerrebrock AW, Bronson RT, Chi DC, Bulotsky MS, Spencer JB, Birren BW, Frankel WN, Lander ES. The mouse pudgy mutation disrupts *Delta* homolog *Dll3* and initiation of early somite boundaries. *Nature Genet.* 1998;19:274–8.
42. Dunwoodie SL, Clements M, Sparrow DB, Bedington RSP. Axial skeletal defects caused by mutation in the spondylocostal dysplasia/pudgy gene *Dll3* are associated with disruption of the segmentation clock within the presomitic mesoderm. *Development.* 2002;129:1795–806.
43. Bulman MP, Kusumi K, Frayling TM, McKeown C, Garrett C, Lander ES, Krumlauf R, Hattersley AT, Ellard S, Turnpenny PD. Mutations in the human *Delta* homologue, *DLL3*, cause axial skeletal defects in spondylocostal dysostosis. *Nature Genet.* 2000;24:438–41.
44. Bonafé L, Giunta C, Gassner M, Steinmann B, Superti-Furga A. A cluster of autosomal recessive spondylocostal dysostosis caused by three newly identified *DLL3* mutations segregating in a small village. *Clin Genet.* 2003;64:28–35.
45. Turnpenny PD, Whittock N, Duncan J, Dunwoodie S, Kusumi K, Ellard S. Novel mutations in *DLL3*, a somitogenesis gene encoding a ligand for the Notch signaling pathway, cause a consistent pattern of abnormal vertebral segmentation in spondylocostal dysostosis. *J Med Genet.* 2003;40:333–9.
46. Turnpenny PD, Young E, (International Consortium for Vertebral Anomalies and Scoliosis) ICVAS. Spondylocostal Dysostosis, Autosomal Recessive. In: Pagon RA, Bird TC, Dolan CR, Stephens K, editors. *Gene Reviews* [Internet]. Seattle: University of Washington; 2013. (1993–2014, 2009 Aug 25).
47. Whittock NV, Sparrow DB, Wouters MA, Sillence D, Ellard S, Dunwoodie SL, Turnpenny PD. Mutated *MESP2* causes spondylocostal dysostosis in humans. *Am J Hum Genet.* 2004;74:1249–54.
48. Cornier AS, Staehling-Hampton K, Delventhal KM, Saga Y, Caubet JF, Sasaki N, Ellard S, Young E, Ramirez E, Carlo SE, Torres J, Emans JB, Turnpenny PD, Pourquié O. Mutations in the *MESP2* gene cause spondylothoracic dysostosis/Jarcho-Levin syndrome. *Am J Hum Genet.* 2008;82:1334–41.
49. Cornier AS, Ramírez N, Arroyo S, Acevedo J, García L, Carlo S, Korf B. Phenotype characterisation and natural history of spondylothoracic dysplasia syndrome: a series of 27 new cases. *Am J Med Genet.* 2004;128A:120–6.
50. Sparrow DB, Chapman G, Wouters MA, Whittock NV, Ellard S, Fatkin D, Turnpenny PD, Kusumi K, Sillence D, Dunwoodie SL. Mutation of the LUNATIC FRINGE gene in humans causes spondylocostal dysostosis with a severe vertebral phenotype. *Am J Hum Genet.* 2006;78:28–37.
51. Haines N, Irvine KD. Glycosylation regulates Notch signaling. *Nat Rev Mol Cell Biol.* 2003;4:786–97.
52. Evrard YA, Lun Y, Aulehla A, Gan L, Johnson RL. *Lunatic fringe* is an essential mediator of somite segmentation and patterning. *Nature.* 1998;394:377–81.
53. Zhang N, Gridley T. Defects in somite formation in lunatic fringe-deficient mice. *Nature.* 1998;394:374–7.
54. Sparrow DB, Guillén-Navarro E, Fatkin D, Dunwoodie SL. Mutation of Hairy-and-Enhancer-of-Split-7 in humans causes spondylocostal dysostosis. *Hum Mol Genet.* 2008;17:3761–6.

55. Sparrow DB, Sillence D, Wouters MA, Turnpenny PD, Dunwoodie SL. Two novel missense mutations in HAIRY-AND-ENHANCER-OF-SPLIT-7 in a family with spondylocostal dysostosis. *Eur J Hum Genet.* 2010;18:674–9.
56. Kageyama R, Niwa Y, Isomura A, González A, Harima Y. Oscillatory gene expression and somitogenesis. *Wiley Interdiscip Rev Dev Biol.* 2012;1:629–41.
57. Bessho Y, Miyoshi G, Sakata R, Kageyama R. *Hes7*: a bHLH-type repressor gene regulated by notch and expressed in the presomitic mesoderm. *Genes Cells.* 2001;6:175–85.
58. Bessho Y, Sakata R, Komatsu S, Shiota K, Yamada S, Kageyama R. Dynamic expression and essential functions of *Hes7* in somite segmentation. *Genes Dev.* 2001;15:2642–7.
59. Sparrow DB, Faqeih EA, Sallout B, Alswaid A, Ababneh F, Al-Sayed M, Rukban H, Eyaid WM, Kageyama R, Ellard S, Turnpenny PD, Dunwoodie SL. Mutation of *HES7* in a large extended family with spondylocostal dysostosis and dextrocardia with situs inversus. *Am J Med Genet A.* 2013;161(9):2244–49.
60. Sparrow DB, McInerney-Leo A, Gucev ZS, Gardiner B, Marshall M, Leo PJ, Chapman DL, Tasic V, Shishko A, Brown MA, Duncan EL, Dunwoodie SL. Autosomal dominant spondylocostal dysostosis is caused by mutation in *TBX6*. *Hum Mol Genet.* 2013;22(8):1625–31.
61. Gucev ZS, Tasic V, Pop-Jordanova N, Sparrow DB, Dunwoodie SL, Ellard S, Young E, Turnpenny PD. Autosomal dominant spondylocostal dysostosis in three generations of a Macedonian family: negative mutation analysis of *DLL3*, *MESP2*, *HES7*, and *LFNG*. *Am J Med Genet.* 2010;152A:1378–82.
62. Yasuhiko Y, Haraguchi S, Kitajima S, Takahashi Y, Kanno J, Saga Y. *Tbx6*-mediated Notch signaling controls somite-specific *Mesp2* expression. *Proc Natl Acad Sci U S A.* 2006;103:3651–6.
63. Aymé S, Preus M. Spondylocostal/spondylothoracic dysostosis: the clinical basis for prognosticating and genetic counselling. *Am J Med Genet.* 1986;24:599–606.
64. Roberts AP, Conner AN, Tolmie JL, Connor JM. Spondylothoracic and spondylocostal dysostosis. *J Bone Joint Surg.* 1988;70B:123–6.
65. Perez-Comas A, Garcia-Castro JM. Occipito-facial-cervicothoracic-abdomino-digital dysplasia: Jarcho Levin syndrome of vertebral anomalies. *J Pediatr.* 1974;85:388–91.
66. Karnes PS, Day D, Berry SA, Pierpont ME. Jarcho-Levin syndrome: four new cases and classification of subtypes. *Am J Med Genet.* 1991;40(3):264–70.
67. Martínez-Frías ML, Urioste M. Segmentation anomalies of the vertebrae and ribs: a developmental field defect: Epidemiologic evidence. *Am J Med Genet.* 1994;49:36–44.
68. Rastogi D, Rosenzweig EB, Koumbourlis A. Pulmonary hypertension in Jarcho Levin syndrome. *Am J Med Genet.* 2002;107:250–2.
69. Bannykh SI, Emery SC, Gerber J-K, Jones KL, Benirschke K, Masliah E. Aberrant *Pax1* and *Pax9* expression in Jarcho Levin syndrome: report of 2 caucasian siblings and literature review. *Am J Med Genet.* 2003;120A:241–6.
70. Cornier AS, Ramirez N, Carlo S, Reiss A. Controversies surrounding Jarcho-Levin syndrome. *Current Opinion Pediatr.* 2003;15:614–20.
71. Cantú JM, Urrusti J, Rosales G, Rojas A. Evidence for autosomal recessive inheritance of costovertebral dysplasia. *Clin Genet.* 1971;2:149–54.
72. Bartsocas CS, Kiossoglou KA, Papas CV, Xanthou-Tsingoglou M, Anagnostakis DE, Daskalopoulou HD. Costovertebral dysplasia. *Birth Defects Orig Artic Ser.* 1974;X(9):221–6.
73. David TJ, Glass A. Hereditary costovertebral dysplasia with malignant cerebral tumour. *J Med Genet.* 1983;20:441–4.
74. Rimoin DL, Fletcher BD, McKusick VA. Spondylocostal dysplasia. *Am J Med Genet.* 1968;45:948–53.
75. Silengo MC, Cavallaro S, Francheschini P. Recessive spondylocostal dysostosis: two new cases. *Clin Genet.* 1978;13:289–94.
76. Moseley JE, Bonforte RJ. Spondylothoracic dysplasia—a syndrome of congenital anomalies. *Am J Roentgenol.* 1969;106:166–9.
77. Pochaczewsky R, Ratner H, Perles D, Kassner G, Naysan P. Spondylothoracic dysplasia. *Radiology.* 1971;98:53–8.

78. Solomon L, Jimenez B, Reiner L. Spondylothoracic dysostosis. *Arch Pathol Lab Med.* 1978;102:201–5.
79. Kozlowski K. Spondylo-costal dysplasia. *Fortschr Röntgenstr.* 1984;140:204–9.
80. Ohashi H, Sugio Y, Kajii T. Spondylocostal dysostosis: report of three patients. *Jpn J Hum Genet.* 1987;32:299–303.
81. Jarcho S, Levin PM. Hereditary malformation of the vertebral bodies. *Bull Johns Hopkins Hosp.* 1938;62:216–26.
82. Berdon WE, Lampl BS, Cornier AS, Ramirez N, Turnpenny PD, Vitale MG, Seimon LP, Cowles RA. Clinical and radiological distinction between spondylothoracic dysostosis (Lavy-Moseley syndrome) and spondylocostal dysostosis (Jarcho-Levin syndrome). *Pediatr Radiol.* 2011;41(3):384–8.
83. Casamassima AC, Morton CC, Nance WE, Kodroff M, Caldwell R, Kelly T, Wolf B. Spondylocostal dysostosis associated with anal and urogenital anomalies in a Mennonite sibship. *Am J Med Genet.* 1981;8:117–27.
84. Daikha-Dahmane F, Hutten Y, Morvan J, Szpiro-Tapia S, Nessmann C, Eydoux P. Fetus with Casamassima-Morton-Nance syndrome and an inherited (6;9) balanced translocation. *Am J Med Genet.* 1998;80:514–7.
85. Poor MA, Alberti O Jr, Griscom NT, Driscoll SG, Holmes LB. Nonskeletal malformations in one of three siblings with Jarcho-Levin syndrome of vertebral anomalies. *J Pediatr.* 1983;103:270–2.
86. Offiah A, Alman B, Cornier AS, Giampietro PF, Tassy O, Wade A, Turnpenny P. Pilot assessment of a radiologic classification system for segmentation defects of the vertebrae. *Am J Med Genet.* 2010;152A:1357–71.

# Chapter 8

## Genetic and Environmental Interaction in Malformation of the Vertebral Column

Sally L. Dunwoodie and Duncan B. Sparrow

**Abstract** Congenital vertebral defects occur with an incidence of 0.5–1 per 1000 live births, and can arise from incorrect formation of the vertebral precursors during early embryogenesis (dysostoses), or from ongoing abnormalities of bone and/or cartilage formation during pre- and postnatal life (dysplasias). Much progress has been made over the last 13 years into understanding the genetic etiologies of many cases of congenital vertebral defects. In particular, many vertebral dysostoses are caused by mutation of components of the Notch signaling pathway; whereas vertebral dysplasias may be caused by mutations in components of other signaling pathways. In addition to genetic causes, for the past 200 years experimental and epidemiological evidence has been accumulating that perturbation of the environment of the developing embryo can also result in vertebral defects. Of course neither genetic nor environmental factors are likely to act in isolation, and the interaction of these factors is likely to affect the penetrance and expressivity of vertebral defects. Recently we have uncovered the first mechanistic insights into how the interaction of genetic and environmental factors can increase the incidence and severity of congenital vertebral defects.

**Keywords** Spondylocostal dysostosis · Spondylothoracic dysostosis · Congenital scoliosis · Somitogenesis · Klippel-Feil syndrome · Notch signaling pathway · FGF signaling pathway · Sclerotome

### Abbreviations

SCDO Spondylocostal dysostosis  
STD Spondylothoracic dysostosis  
KFS Klippel-Feil syndrome  
SNP Small nucleotide polymorphism

---

D. B. Sparrow (✉) · S. L. Dunwoodie  
Developmental and Stem Cell Biology, Victor Chang Cardiac Research Institute,  
405 Liverpool Street, Darlinghurst, Sydney, NSW 2010, Australia  
e-mail: d.sparrow@victorchang.edu.au

S. L. Dunwoodie  
e-mail: s.dunwoodie@victorchang.edu.au

© Springer Science+Business Media New York 2015  
C. A. Wise, J. J. Rios (eds.), *Molecular Genetics of Pediatric Orthopaedic Disorders*,  
DOI 10.1007/978-1-4939-2169-0\_8

DLL3	Delta-like 3 ( <i>Drosophila</i> )
MESP2	Mesoderm posterior 2 homolog (mouse)
LFNG	LFNG O-fucosylpeptide 3-beta-N-acetylglucosaminyltransferase
HES7	Hairy and enhancer of split 7 ( <i>Drosophila</i> )
TBX6	T-box 6
MEOX1	Mesenchyme homeobox 1
GDF3	Growth differentiation factor 3
GDF6	Growth differentiation factor 6
GXE	Gene-environment interaction
E	Embryonic day
PSM	Presomitic mesoderm

The vertebral column is an essential component of the skeleton, providing both structural support and protection for the spinal cord. In humans, congenital vertebral defects occur with an incidence of 0.5–1 per 1000 live births [1]. These can arise from incorrect formation of the vertebral precursors during early embryogenesis (dysostoses), or from ongoing abnormalities of bone and/or cartilage formation during pre- and postnatal life (dysplasias). These can present with a large variety of forms, with variation in not only the phenotype and number of affected vertebrae but also the locations of affected vertebrae within the spinal column. Vertebral defects can occur in isolation (non-syndromic), or in combination with malformation of other organs (syndromic). Unsurprisingly there is also a large degree of variation in the clinical terms used to describe individual cases. To overcome these difficulties, a standardized nomenclature has been developed by the International Consortium for Vertebral Anomalies and Scoliosis (ICVAS; [www.icvas.org](http://www.icvas.org); [41, 61]. This system first divides cases into those with “Multiple” or “Single” affected regions/vertebrae. “Multiple” cases are divided into “Regional” (cervical, dorsal lumbar or sacral) or “Generalized” ( $\geq 10$  contiguous malformed vertebrae; Fig. 8.1a). In addition, some severe cases may be classified as “Multi-regional” if they have multiple but non-contiguous affected vertebrae. “Single” cases are milder, and include cases of congenital scoliosis (Fig. 8.1b).

## The Developmental Origins of Vertebral Defects

The axial skeleton develops from precursor tissues called somites. These are blocks of mesodermal tissue that develop along the axis of the embryo in a regular repeated process of segmentation from an unsegmented precursor tissue, the presomitic mesoderm (PSM, summarized in Fig. 8.2). Vertebral defects can arise either from a disruption of the segmentation process, or from a failure of the correct differentiation of the somite. Somite formation or somitogenesis occurs via a complex interplay of FGF, WNT, Notch and retinoic acid signal transduction pathways [42]. Failure of this process in both humans and mice can result in a variety of phenotypes including

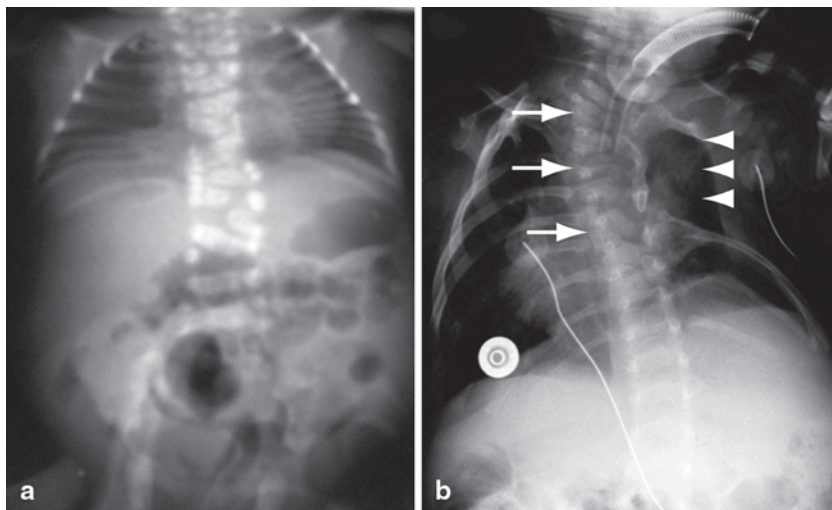


**Fig. 8.1** Radiographs showing (a) a case of SCDO with severe vertebral segmentation anomalies throughout the vertebral column (adapted from [51] with permission from Oxford University Press); and (b) a case of congenital scoliosis with a few vertebral and rib anomalies and marked scoliosis. *Arrows* indicate malformed vertebrae and *arrowheads* indicate missing ribs. (Adapted from [54] with permission from Elsevier)

vertebral fusion, hemi-vertebrae, and proximal fusions or bifurcations of the ribs. These can be considered as “dysostoses”. Mature somites consist of two cellular compartments [11]. Firstly, cells derived from the sclerotome form the vertebrae and ribs, with a subgroup of cells within this domain going on to form the tendons (syndetome). Secondly, the dermomyotome consists of two populations of cells: cells from the dermatome form the dermis of the trunk, and cells from the myotome form the axial musculature. Rib and vertebral defects can also arise from a failure of sclerotome differentiation. However the phenotypes generated by such disruption are subtly different to those generated by segmentation defects. For example, the vertebral spinal processes fail to fuse medially, instead fusing in a rostral-caudal direction, and rib fusions and bifurcations generally occur distally [32, 48, 67]. These can be considered as “dysplasias”.

### **Autosomal Recessively Inherited Severe Non-Syndromic Multiple Contiguous Vertebral Defects**

Over the past 13 years it has become apparent that congenital vertebral defects can arise from simple genetic deficiencies, from maternal or embryonic exposure to environmental teratogens, or a combination of both factors. These etiological

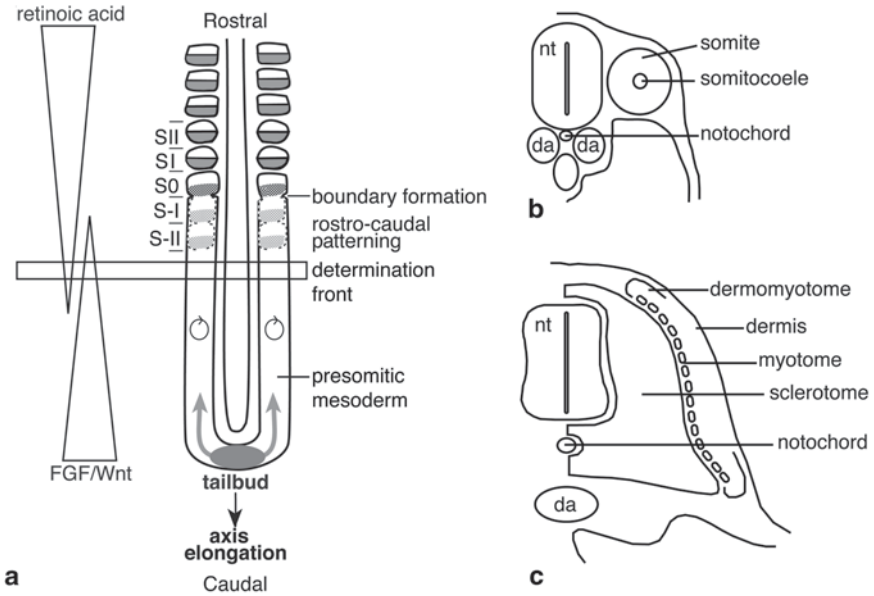


**Fig. 8.2** Somitogenesis in mouse. **a** Schematic representation of somite formation and rostral-caudal patterning in mouse. A dorsal view of a midgestation mouse embryo showing the production of presomitic mesoderm from the tail bud, resulting in elongation of the embryonic axis. FGF and Wnt signaling gradients emanate from the tail bud, while a retinoic acid signaling gradient derives from the somites. These opposing gradients set the position of the determination front: cells rostral to this front become competent to form somites. Notch1 signaling oscillates (circle with arrow) between on and off states in PSM cells, giving the impression that a wave of activity sweeps rostrally. This wave stalls in the region of the next forming somite, forming a sharp band of cells undergoing signaling (*S-I*). Rostral-caudal polarity is established in presumptive somites (*S-II*, *S-I*) and a boundary forms (between *S0* and *S-I*), defining the formation of a nascent epithelial somite. Rostral-caudal polarity is maintained as somites mature and differentiate along their dorsoventral axis to form dermomyotome and sclerotome. **b** Cross-sectional view of a newly formed epithelial somite. **c** Cross-sectional view of a mature somite after dorsoventral compartmentalization and differentiation. The dermomyotome has largely differentiated into the dermis and the myotome. The sclerotome has expanded and moved ventrally to surround the neural tube and notochord. S-I and S-II, segmented somites; S0, next somite to form; S-I and S-II, prospective somites; *nt* neural tube; *da* dorsal aorta. (Figure and legend reproduced from [54] with kind permission from Springer Science and Business Media)

insights have come from a combination of human molecular genetics and animal studies. The most significant advances in identifying the genetic etiologies of human congenital vertebral malformations have resulted from studying familial cases with clear autosomal recessive inheritance patterns (Table 8.1). This is in a large part due to genetic mapping and candidate gene sequencing of consanguineous cases. In such cases, the causative mutation has been inherited by both parents from a recent common ancestor, and is therefore relatively easy to identify. In addition,

**Table 8.1** Summary of human vertebral malformation syndromes with known etiology

Disease name	Inheritance	OMIM	Gene	References
SCDO1	AR	277300	<i>DLL3</i>	[6, 7, 49, 60, 61]
SCDO2/STD	AR	608681	<i>MESP2</i>	[14, 66]
SCDO3	AR	609813	<i>LFNG</i>	[50]
SCDO4	AR	613686	<i>HES7</i>	[51, 52, 55]
SCDO5	AD	122600	<i>TBX6</i>	[56]
KFS2	AR	214300	<i>MEOX1</i>	[38]
KFS1	AD	118100	<i>GDF6</i>	[3, 57]
KFS3	AD	613702	<i>GDF3</i>	[68]
Congenital scoliosis	AD	Na	<i>MESP2</i> <i>HES7</i>	[54]

many of details of the underlying genetic pathways and molecular mechanisms of vertebral formation have now been uncovered using a variety of animal model systems. These studies have identified a large number of candidate genes for causing vertebral defects (reviewed in [53]), and this has accelerated the discovery of the genetic bases of many human cases of vertebral defects. One particular disorder, spondylocostal dysostosis (SCDO), has been intensely investigated. Cases of SCDO have abnormal segmentation of nearly all vertebrae with associated abnormal ribs. However, even though the vertebral defects are severe, the rightward and leftward curves tend to cancel each other out resulting in a mild degree of non-progressive scoliosis without a major asymmetry of the thorax. The phenotype can result in compromised respiratory function in neonates due to the reduced capacity of the thorax, respiratory complications in children, and an increased incidence of inguinal hernia in males. However, despite the dramatic vertebral phenotype, SCDO cases rarely have any neurological affects. Below we outline the genetically-defined subclasses of SCDO.

### ***SCDO1 (OMIM 277300)***

Although severe non-syndromic multiple contiguous vertebral defects had been described in the literature as early as 1938 [30], it was not until the end of the twentieth century that the first insights into their genetic etiology were made, arising from the combined efforts of three groups. Turnpenny and colleagues approached the problem by using the then relatively new method of homozygosity mapping [34] on three large consanguineous families to map the SCDO critical region in these families to a 7.8 cM region of chromosome 19 [7, 59]. Simultaneously, Kusumi and colleagues were investigating a recessive mouse mutant *pudgy* that had come from an X-ray mutagenesis screen at the Oak Ridge National Laboratory prior to 1961. This mouse line had a rib and vertebral phenotype very similar to that seen in

human cases of SCDO, and a combination of classical genetic mapping and BAC transgenic rescue methods narrowed the *pudgy* critical region to a 159 kb region containing eight genes [33]. One of these was *Dll3* encoding the *delta-like 3* protein, a gene that had been shown by Dunwoodie and colleagues the previous year to be expressed in the vertebral precursor tissues [18]. Sequence analysis of *Dll3* in the mutant mice revealed a frameshift mutation that was not present in the parental mouse strain. Kusumi and Turnpenny then collaborated to demonstrate that in humans *DLL3* lay in the SCDO critical region on chromosome 19, and that each of the three families used for homozygosity mapping had different deleterious mutations in *DLL3* [7]. This discovery was quickly translated to clinical practice, and routine sequencing of *DLL3* in SCDO cases by clinical services is now standard in many countries internationally. Around 70% of SCDO cases have homozygous mutations in *DLL3*, and up to 40 distinct mutations have been identified [62], making this the most important gene causing SCDO.

### ***SCDO2 (OMIM 608681)***

Investigation of a small consanguineous family, also with an autosomal recessive inheritance pattern, resulted in the discovery of the second SCDO-associated gene [66]. The proband had extensive vertebral defects throughout the spine, however the phenotype was distinct from that of SCDO1 in that the ribs were well aligned. Homozygosity mapping of two affected siblings, their parents and an unaffected sibling detected a 36.6 Mb region on chromosome 15. This region contained more than 50 genes, including an excellent candidate *MESP2* encoding *mesoderm posterior 2* homolog protein. Mouse embryos homozygous for a targeted null allele of *Mesp2* show very similar vertebral and rib malformations to homozygous *pudgy* mice [44]. Sequence analysis of *MESP2* in the family detected a 4 bp insertion that segregated with disease. This mutation causes a frameshift and premature truncation of the MESP2 protein, however it is not predicted to cause nonsense-mediated decay of the transcript. MESP2 is a transcription factor required for formation of the vertebral precursors (somites). When tested in an *in vitro* transcription activation assay, the mutant MESP2 protein was significantly less active than the wildtype protein [55]. Taken together, these data provide good evidence that mutation of *MESP2* is causative of the vertebral phenotype in this family.

Interestingly, mutation of *MESP2* causes another human congenital vertebral segmentation abnormality, spondylothoracic dysostosis (STD), that is phenotypically distinct from SCDO [4]. Typically in STD, the thoracic spine and the ribs are most affected, with the latter being fused posteriorly creating a fan-like or “crab” configuration. This results in a severe reduction of respiratory function, and 75% of cases die in infancy. In addition, many cases have fusion of all cervical vertebrae, as well as that of C1 to the skull, preventing the head from being turned. STD is particularly prevalent in Puerto Rico, most likely due to a founder effect. Cornier and colleagues [14] used a candidate gene sequencing approach to determine the ge-

netic cause of STD. They sequenced five genes (*DLL3*; *LFNG*; *MESP2*; *HES7*; and *PSENI*) in a large cohort of patients with congenital vertebral defects. In patients with STD they identified three mutations in *MESP2* predicted to either produce non-functional proteins and/or to be susceptible to nonsense-mediated RNA decay (NMD). An *in vitro* transcription assay was used to confirm the deleterious nature of these mutations.

Despite being caused by mutation of the same gene, SCDO2 and STD clearly have different phenotypes. This is especially apparent in the ribcage. It has been suggested that these phenotypic differences might be the result of different types of *MESP2* mutation (P. Turnpenny, personal communication). It is also apparent that there are clear phenotypic differences between SCDO1 and SCDO2 in humans. Likewise, comparisons of *Mesp2* and *Dll3* homozygous null mouse embryos show differences at the molecular level in somite patterning. *Mesp2* null embryos lack specification of the rostral half of the mature somite [44], whereas *Dll3* null embryos express markers of both rostral and caudal somite identity, but lack the correct spatial separation of the two [19]. The rostral and caudal compartment of the mature somite give rise to different parts of the mature vertebra, this may explain the phenotypic differences seen in human cases of SCDO1 and SCDO2.

### ***SCDO3 (OMIM 609813)***

A third SCDO causative gene was identified in a consanguineous case of SCDO with a severely disorganized spine including malformations throughout the cervical, thoracic and lumbar spine [50]. There were no mutations detected in *DLL3* or *MESP2*, and so a candidate gene sequencing approach was used to identify the causative mutation. *LFNG*, encoding the *LFNG O-fucosylpeptide 3-beta-N-acetylglucosaminyltransferase* protein, was chosen for sequencing because mouse embryos carrying homozygous null mutations of *Lfng* have a similar vertebral and rib phenotype to that of *Dll3* and *Mesp2* homozygous null mutants [20, 69]. A homozygous single nucleotide change predicted to cause a non-synonymous F188L amino acid change was present in the affected individual, and both parents were heterozygous carriers for the variant. The functional consequences of this sequence alteration were tested in a series of *in vitro* assays, showing that the variant was likely to be highly deleterious to protein function. To our knowledge only one other mutation in *LFNG* has been discovered (Bonafe, unpublished data), and therefore mutation of *LFNG* is likely to be the least common cause of SCDO.

### ***SCDO4 (OMIM 613686)***

Advances in molecular genetic techniques have greatly facilitated homozygosity mapping of disease loci in offspring of consanguineous unions. First SNP arrays,

and now whole-exome sequencing, have allowed much more rapid identification of new loci causing genetic diseases. We investigated a single affected individual with consanguineous parents who had multiple and contiguous vertebral segmentation defects mainly involving the thoracic spine and ribs, but also affecting the cervical and lumbar regions. The patient also had Chiari II malformation, lumbosacral myelomeningocele, ectopic stenotic anus and talipes. We used SNP array technology to map a single large “homozygous-by-descent” region unique to the affected individual [51]. This region of 10.1 Mb contained 201 genes, of which two (*HES7* and *DVL2*) were possible candidates on the basis of the skeletal phenotype of homozygous null mouse embryos for these genes [5]. Sequence analysis revealed a homozygous non-synonymous change in the proband at a highly evolutionarily conserved residue in the DNA-binding domain of *HES7* encoding *hairy and enhancer of split 7*. The functional consequences of this nucleotide variation were tested in two *in vitro* assays, showing that this significantly reduced the transcriptional repression activity of the protein.

Three more deleterious mutations in *HES7* have now been reported [51, 52, 55]. Closer analysis of the phenotypes of all ten reported cases suggests that there are two additional phenotypes associated with homozygous deleterious mutations in *HES7* that have not been reported in any SCDO cases involving mutation of *DLL3*, *MESP2* or *LFNG* [56]. Firstly, three of the ten cases had neural tube defects including myelomeningocele, spina bifida occulta and/or Chiari type II malformation. Secondly, four of the ten cases had dextrocardia with *situs inversus*. Neural tube malformations have been reported in patients with SCDO with no reported molecular diagnosis [8, 13, 23, 46] and three of these patients were also reported as having laterality defects [8, 13, 23, 46]. Thus it is possible that these are also cases involving *HES7* mutation.

## **Autosomal Dominantly Inherited Severe Non-Syndromic Multiple Contiguous Vertebral Defects**

Autosomal dominantly inherited SCDO cases are much more rare than the autosomal recessive forms, possibly representing less than 10% of total cases [39]. To date the genetic lesion for an autosomal dominant form of SCDO has only been identified in a single family [56] (Table 8.1).

### ***SCDO5 (OMIM 122600)***

We investigated a family with affected individuals in three consecutive generations. All individuals had multiple generalized contiguous vertebral malformations throughout the spine, including hemivertebra and fused vertebral blocks, however the ribs were relatively unaffected [24]. Sequence analysis of *DLL3*, *MESP2*, *LFNG*

and *HES7* was negative. We used whole-exome sequencing of three affected and two unaffected individuals to identify the causative mutation in the cases [56]. After filtering, six potentially disease-causative variants remained, one of which was in *TBX6*. Studies in mouse have shown that this transcription factor is an important element of the somitogenesis machinery, and mouse embryos homozygous for null or hypomorphic alleles of *Tbx6* have SCDO-like phenotypes [9, 64, 65]. The mutation was confirmed by Sanger sequencing to segregate with the vertebral phenotype, and an *in vitro* functional assay revealed a statistically significant impairment of the transcriptional activation activity of Tbx6 protein.

Although it appears clear that *TBX6* is haploinsufficient in this family, and results in a severe vertebral phenotype, it is puzzling that *Tbx6* haploinsufficiency does not produce a SCDO-like phenotype in mouse. This may be due to unknown genetic modifier genes, but can only be resolved when more human cases of *TBX6* mutation are reported.

## Multiple Regional Vertebral Defects

The next most severe class of vertebral defects comprises those cases restricted to one or more regions of the spine. The most common of these is Klippel-Feil syndrome (KFS), which is a general term used to refer to vertebral defects that are mostly limited to the cervical region [58]. Cases present with a short neck with limited movement due to fusions of the neck vertebrae, which can vary considerably in their number and location. Additionally, other skeletal defects are sometimes associated with KFS including Sprengel's deformity (one scapula higher than the other) and presence of omo-vertebral bones (a bony connection from the scapula to a cervical vertebra). A significant proportion of KFS cases have two other phenotypes: deafness and a low posterior hairline. In familial cases, both autosomal dominant and autosomal recessive inheritance patterns have been described (Table 8.1).

### Autosomal Recessive KFS2 (OMIM 214300)

A large consanguineous family with five affected individuals was investigated. The index case had a short immobile neck with C2-C3 fusion, Sprengel's deformity and a low posterior hairline. In this family a single 16.1 Mb region containing 477 genes was identified by homozygosity mapping following SNP array genotyping, and was confirmed by classical linkage analysis [38]. Candidate gene sequencing revealed a single base deletion in the *MEOX1* gene that segregated completely with disease. This deletion was predicted to cause a frameshift and introduce a premature termination codon. *MEOX1* was also sequenced in an unrelated consanguineous family with two affected individuals. Both cases had a short neck with severely limited mo-

bility due to cervical vertebral fusion, a low posterior hairline, scoliosis due to deformity of the thoracic spine between T2 and T11 and the presence of omo-vertebral bones. In addition they had craniofacial defects including micrognathia, cleft palate (in one case only) and congenital ptosis. A different single base change in *MEOXI* was detected that was also predicted to cause a premature termination codon. Both premature stop codons were demonstrated to trigger NMD in affected individuals. *MEOXI* is an excellent candidate for being the causative gene in these cases, because targeted deletion of *Meox1* causes similar skeletal phenotypes in mouse [48]. Mouse embryos lacking *Meox1* have entirely remodeled cranio-cervical joints such that the skull rests on the axis, rather than the atlas, and the spine is often partially fused to the skull. In addition they have variably penetrant vertebral defects, particularly in the lumbar and sacral regions, as well as occasional rib defects. However, unlike the other mouse models of vertebral malformation mentioned above, mutation of *Meox1* appears to have no effect on somitogenesis. Expression patterns and levels of segmentation genes such as *Mesp2*, *Lfng*, *Dll1*, *Dll3* and *EphA4* are normal in the presomitic mesoderm [36, 48]. Instead these mutants have reduced cellular proliferation in the caudal somitic compartment of the most rostral somites. Therefore the vertebral and rib fusions are likely to be a result of impaired sclerotomal formation and differentiation. This may be a consequence of downregulation of the *Meox1* direct target genes *Tbx18*, *Uncx* and *Bapx1* [48]. Interestingly, the reduction in somitic cell proliferation is reduced as development proceeds, and by E12.5 proliferation has returned to normal. This may explain why the cervical vertebrae are the most affected in *Meox1* mutants in both mice and humans. In conclusion, it would appear that, in contrast to SCDO/STD, KFS is a dysplasia with ongoing abnormalities of bone and/or cartilage formation during pre- and postnatal life.

### **Autosomal Dominant KFS1 (OMIM 118100)**

The first insights into the etiology of autosomal dominant KFS came from studies of a large four-generation family. All affected individuals had C2-3 vertebral fusions, with a variable rate of more caudal vertebral fusions. In addition, affected individuals had restricted limb joint flexibility, moderate hearing impairment and severe vocal impairment. Cytogenetic analysis revealed an inversion on the long arm of chromosome 8 that segregated completely with affected status [12]. The breakpoints were either side of the *GDF6* locus, and the proximal breakpoint was suggested as lying in a *GDF6* regulatory region [40, 57].

Growth/differentiation factor 6 (*GDF6*) is a member of bone morphogenetic protein (BMP) family sub-class of the transforming growth factor  $\beta$  (TGF- $\beta$ ) superfamily of secreted growth factors that have important roles in embryonic development. Candidate gene sequencing of *GDF6* in an unrelated family and two “sporadic” cases of KFS revealed heterozygous non-synonymous coding variants in *GDF6*. In a second study, *GDF6* was selected as a candidate gene for causing eye and/

or vertebral defects on the basis of human linkage mapping of human syndromes including either vertebral or eye phenotypes [3]. *GDF6* was sequenced in a very large cohort of cases, and seven potentially deleterious heterozygous base changes identified. Four of these were associated with solely ocular phenotypes, two with skeletal phenotypes, and the last with either phenotype. Lastly a third study found more heterozygous non-synonymous coding variants in human cases of mostly ocular, but also vertebral defects [16].

The association of *GDF6* with ocular defects is well supported by studies in mouse, *Xenopus laevis* and fish. *Gdf6* heterozygous null mouse embryos have variable and asymmetric ocular defects [3]; in the X-ray-induced mouse mutant *total cataract with microphthalmia (Tcm)*, the genetic defect has been mapped to a 1.3 Mb region on mouse chromosome 4 containing six genes including *Gdf6* [63]; *Xenopus laevis* morpholino knockdown results in eye and neural defects [26, 57]; and in zebrafish, homozygous null *gdf6a* mutants and morpholino knockdown of *gdfa* results in ocular defects [3, 16]. By contrast, the association of mutation of *GDF6* with vertebral defects is less clear. In the mouse embryo, *Gdf6* is expressed in the developing skeletal condensations of a subset of joints, namely elbow, carpal joints, ankle, a restricted portion of the knee, and the vertebral joints. However, *Gdf6* homozygous null embryos do not have vertebral defects [45]. Instead they have fusions between specific bones in the wrists and ankles, consistent with *Gdf6* having a role in early joint specification or segmentation. They also have disrupted formation and growth of cartilage and ligament structures, including the coronal sutures between bones in the skull, and the cartilage of the middle ear. This suggests that *Gdf6* also is required for cartilage development and proliferation. Furthermore, *Gdf6* heterozygous null mouse embryos do not have vertebral defects (although only two embryos were analysed, [3]. In *Xenopus laevis* and zebrafish, skeletal defects, defined as bent axes, have only been observed in morpholino knockdown experiments but not in naturally-occurring mutants, suggesting that these phenotypes could be the result of morpholino toxicity or off-target effects. Finally, many of the heterozygous missense variants associated in these studies with human skeletal defects are present within the general population with a significantly higher frequency than KFS itself (Exome variant server; EVS; [evs.gs.washington.edu](http://evs.gs.washington.edu)). These reservations highlight the general difficulty of conclusively proving the causative nature of observed heterozygous sequence changes in cases of autosomal dominantly inherited phenotypes.

### **Autosomal Dominant KFS3 (OMIM 613702)**

The Lehman group extended their analysis of human cases of developmental ocular defects including microphthalmia (reduced ocular size), anophthalmia (absent eyes) and colobomata (ocular fissure closure defects) [68]. They investigated a three-generation family with variable ocular and vertebral defects including cervical ver-

tebral fusions, mild lumbar and thoracic scoliosis, and rudimentary 12th ribs. They selected *Growth/differentiation factor 3 (GDF3)*, a member of the same group of secreted growth factors as GDF6, as a candidate gene for sequence analysis. Affected individuals were all heterozygous for a non-synonymous coding variant in this gene. Interestingly, members of an unrelated family carrying the same mutation had ocular but not vertebral defects. Three other potentially deleterious coding variants in *GDF3* were found in cases with ocular defects, however none of these had apparent vertebral defects. As with *KFS1*, the functional evidence supporting the conclusion that mutation of *GDF3* causes the vertebral defects is weak. Knockdown of the zebrafish homologue of *GDF3 (dvr1)* does result in eye and axial skeletal defects. However, in two independent mouse lines, although about one third of *Gdf3* homozygous null embryos die at or prior to gastrulation, the remaining two-thirds are born [2, 10, 47]. These mice are physically indistinguishable from wild type littermates, with no vertebral or eye defects reported. The only reported phenotype for these mice is a resistance to developing obesity when fed on a high fat diet [47]. Finally, the *GDF3* variant present in the family with vertebral defects is relatively common on EVS (R266C; present in 22/12984 exomes). Therefore it remains to be conclusively established whether these heterozygous variants in *GDF3* are causal for eye or vertebral defects in humans.

## Single Vertebral Defects

Only one or two malformed vertebrae present at birth can result in a sideways curve in the spine termed congenital scoliosis. This scoliosis is usually non-progressive, and as such is distinct from progressive forms of scoliosis that may arise as a result of neuro-muscular problems [21, 37]. Congenital scoliosis arises from a failure of segmentation or formation of the vertebral precursors during weeks 3–6 of gestation. There is some evidence for a simple genetic cause of congenital scoliosis, with a few cases reported to carry heterozygous potentially deleterious coding variants in *DLL3*, *MESP2* and *HES7* [7, 35, 54]. In the case of *MESP2* and *HES7*, *in vitro* studies demonstrated that the *MESP2* and *HES7* variant proteins were functionally impaired. It remains to be seen what proportion of individuals carrying deleterious mutations in Notch pathway genes actually have congenital scoliosis. It appears that it is extremely rare for individuals heterozygous for deleterious mutations in the most commonly mutated gene in SCDO, *DLL3*, to have overt congenital scoliosis (P.D. Turnpenney personal communication). Likewise a survey of 100 Chinese cases of congenital scoliosis revealed no sequence alterations in *MESP2*, *HES7* or *DUSP6* [43]. However it is likely that, with the advent of whole-exome sequencing technology, the genetic basis of a higher proportion of congenital scoliosis cases will be elucidated in the near future.

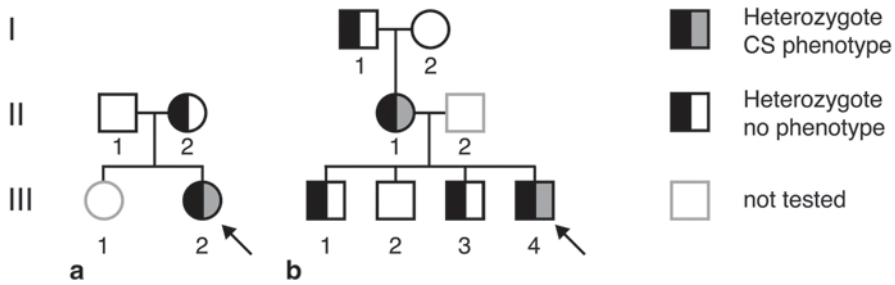


**Fig. 8.3** Pedigrees of two families with congenital scoliosis that carry deleterious mutations in *MESP2* (a) and *HES7* (b). Probands indicated by arrows, presence of congenital scoliosis phenotype indicated by gray shading, and mutant alleles indicated by black shading. Individuals that were not genotyped are indicated by gray boxes. (Figure adapted from [54] with permission from Elsevier)

## Environmental Influences on the Etiology of Vertebral Defects

In addition to a genetic etiology, perturbation of the environment of the developing embryo can cause specific defects, including vertebral. For example, there is ample epidemiological evidence that environmental factors such as maternal smoking or diabetes increases the risk of congenital malformations [15, 25]. However, since somite formation in humans occurs between weeks 3–5, it is difficult to prove that vertebral defects present at birth are the result of teratogenic environmental exposure at a time when the mother may have been unaware of her pregnancy. Therefore, analysis of the majority of environmental risk factors contributing to vertebral defects has been limited to animal model systems. Indeed, such animal experimentation was first reported almost 200 years ago [22]. These experiments have provided evidence for such diverse agents as retinoic acid, valproic acid, maternal diabetes, embryonic hypoxia, carbon monoxide, arsenic, ethanol, hyperthermia, maternal zinc-deficient diet, organophosphate pesticides, inhibition of nitric oxide production and boric acid to act as potential environmental teratogens [1, 27]. Of course neither genetic nor environmental factors are likely to act in isolation, and the interaction of these factors (gene-environment interaction, “GXE”) is likely to affect the penetrance (the proportion of mutation carriers that have defects) and expressivity (the precise phenotype of mutation carriers) of vertebral defects. This hypothesis is supported by twin studies. For example, in the majority of reported cases of monozygotic twins with congenital scoliosis, only one twin is affected [31]. Where both twins are affected, the location and severity of the vertebral defects are different. Our study of congenital scoliosis provides the first experimental evidence supporting this hypothesis [54]. We investigated two families with multiple individuals showing mild vertebral

defects with variable penetrance (Fig. 8.3). Candidate gene sequencing revealed that these families carried deleterious alleles of *MESP2* and *HES7*, respectively. In both families, all affected individuals were heterozygous for the mutant allele, conversely not all heterozygotes showed vertebral defects. We also investigated the skeletal phenotypes of mouse lines carrying null alleles for *Mesp2* and *Hes7*. Approximately 50% of the *Hes7* heterozygous E14.5 mouse embryos, and 10% of the *Mesp2* heterozygous embryos had vertebral defects. Thus in both humans and mice, individuals heterozygous for deleterious mutations in the Notch pathway genes *MESP2* and *HES7* have congenital scoliosis with low penetrance (Fig. 8.4a). We hypothesized that the penetrance and expressivity of congenital scoliosis was affected by an environmental factor, and selected acute gestational embryonic hypoxia as a potential environmental factor. Studies beginning in the early nineteenth century have shown that reducing the oxygen levels available to the vertebrate embryo can induce gross structural abnormalities, including vertebral defects very similar to those seen in *Hes7* heterozygous mice [22, 29]. This is relevant to human pregnancy, since intrauterine hypoxia can be caused by many environmental factors [28]. We demonstrated that maternal exposure to extreme hypoxia (5.5% oxygen) for 8 h at the time when the vertebral precursor tissues (somites) are forming (E 9.5) induces severe vertebral defects in approximately 90% of embryos (analysed at E14.5 when vertebral formation can first be assessed easily). However, when mothers were exposed to mild hypoxia (8% oxygen) for 8 h at E9.5, only about 15% of embryos showed vertebral defects at E14.5, and these were very mild (Fig. 8.4b). We next combined our genetic and environmental models to demonstrate that mouse embryos heterozygous for null mutants in the Notch signaling pathway genes *Mesp2*, *Hes7*, *Dll1* and *Notch1* (but not *Dll3*) showed increased penetrance and severity of vertebral defects when exposed *in utero* exposure to mild hypoxia compared to the effects of either genetic or environmental factor alone (Fig. 8.4c). Lastly we investigated the underlying molecular mechanism by which embryonic hypoxia causes vertebral defects. Here we discovered that hypoxia appeared to interrupt FGF signaling in the PSM. This resulted in a loss of the cyclical activation of Notch signaling required for somite formation, and consequently a loss of somite segmentation (Fig. 8.4d, e).

## Concluding Remarks

In the last 13 years researchers have made significant progress into understanding the genetic factors underlying human congenital vertebral defects, with causative mutations in at least eight genes having been identified to date (Table 8.1). These advances have been aided to a large extent by parallel studies of knockout mouse

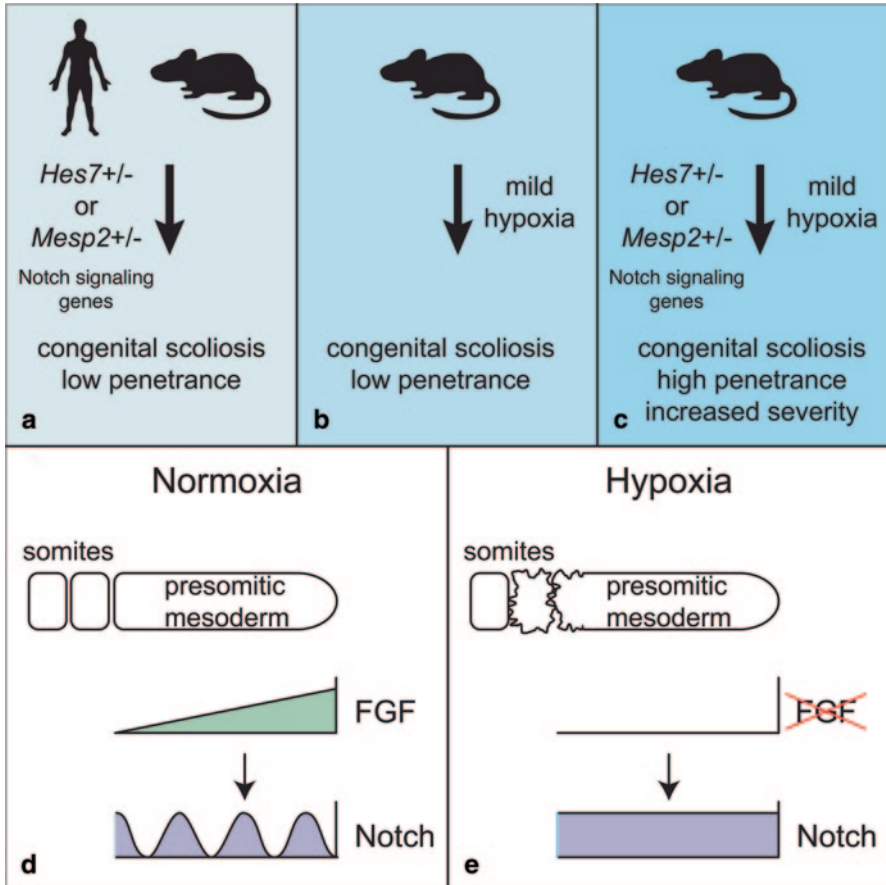


**Fig. 8.4** **a** Heterozygous mutations in Notch pathway genes *Hes7* and *Mesp2* can cause mild vertebral defects in humans and mice. **b** *In utero* exposure of mouse embryos to moderate levels of hypoxia can induce mild vertebral defects. **c** A combination of heterozygous mutation of *Hes7* or *Mesp2* and *in utero* exposure of mouse embryos to moderate hypoxia causes vertebral defects with increased penetrance and severity. **d** In normoxic conditions *FGF* signaling is present in a gradient in the PSM, and cyclical activation of Notch signaling occurs. Correct somite segmentation requires the cyclical activation of Notch signaling. **e** Hypoxia reduces the overall levels of *FGF* signaling in the PSM, and cyclical activation of Notch signaling ceases. This results in abnormal somite segmentation. (Figure reproduced from [54] with permission from Elsevier)

models. Such models have been crucial in dissecting the genetic and signaling pathways required for the formation and patterning of the vertebral precursor tissues (somites) in the developing embryo. This knowledge has identified a number of candidate genes for vertebral defects in humans, which have been investigated by classical and modern genetic means. Interestingly, the majority of disease-

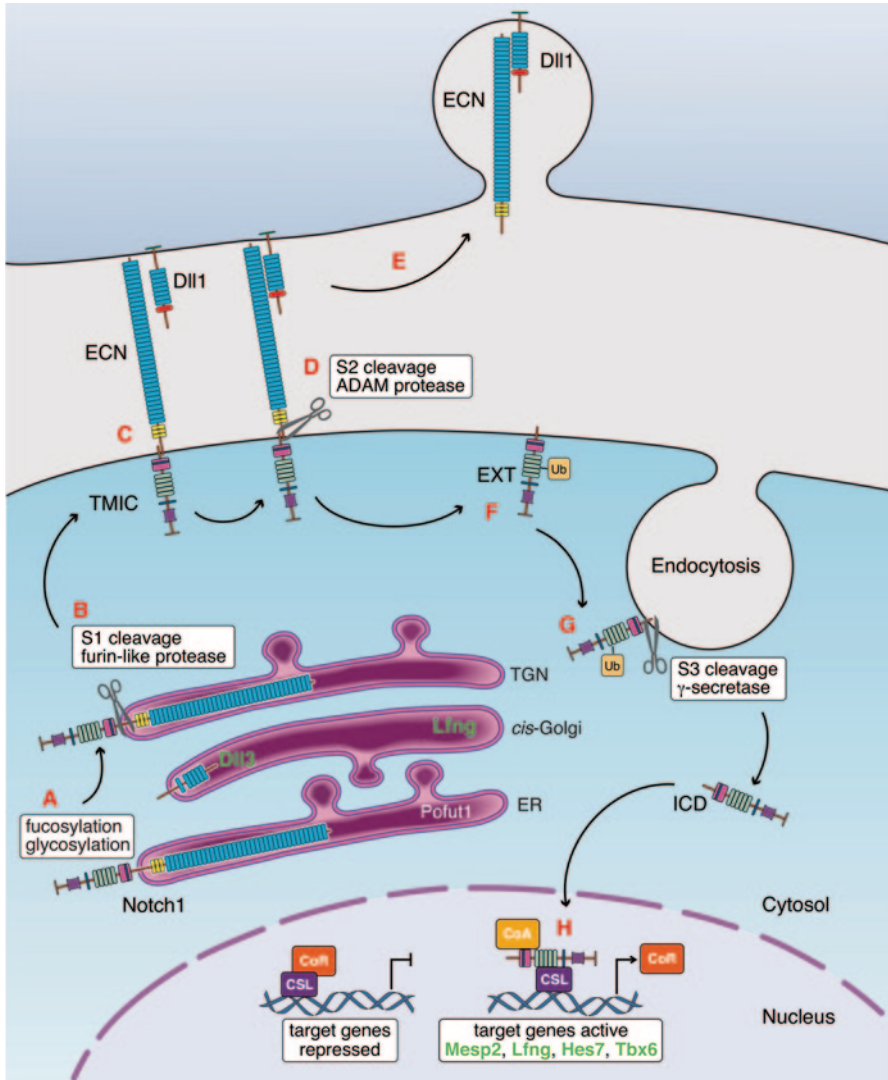


**Fig. 8.5** Notch signaling in mammalian somitogenesis. The *Notch1* receptor is synthesized as a single polypeptide: (a) specific EGF-like repeats are modified by O-fucosylation in the endoplasmic reticulum (ER) by protein O-fucosyltransferase 1 (*Pofut1*). As *Notch1* passes through the Golgi, (b) N-glycosylation occurs on O-fucose by Lunatic fringe (*Lfng*) and (c) *Notch1* is S1-cleaved by a Furin-like convertase. The ligand *Dll3* is localized to the *cis*-Golgi and acts as a negative regulator of Notch signaling. The *Notch1* heterodimer consisting of N-terminal extracellular truncation (TMIC) and C-terminal transmembrane and intracellular domain (ECN) traffics to the cell surface. The DSL ligand *Dll1*, ubiquitylated (Ub) by Mindbomb 1 (*Mib1*), is on the surface of the signal-sending cell. *Dll1* binds *Notch1* ECN in *trans*, and this activates S2-cleavage by the ADAM protease TACE (d). (E) *Dll1* and *Notch1* ECN are released and endocytosed into

causing genes in humans discovered to date are Notch-associated: *DLL3* is an inhibitory ligand; *LFNG* glycosylates the Notch receptor; and the *LFNG*, *MESP2*, *HES7* and *TBX6* genes are direct transcriptional targets of the activated pathway (Fig. 8.5). Furthermore, the *HES7* protein also inhibits Notch signaling, creating a negative feedback loop. It remains to be seen if this reflects the central importance of this signaling pathway in somitogenesis, or is the result of ascertainment bias. Advances in technology have dramatically increased the rate of discoveries. However the advent of whole exome sequencing (with affordable whole genome sequencing on the horizon) has created a new problem: the identification of many potentially damaging heterozygous gene and regulatory variants in each individual, only one or two of which are likely to be the cause of the vertebral defects. This will necessitate sequencing of multiple affected and unaffected members of each family, and will further increase the importance of functional studies in animal models and *in vitro* systems to verify the pathogenicity of variants. Our recent findings regarding environmental influences on vertebral formation add another level of complexity, and in the long term may provide the basis for therapeutic intervention to minimize the severity and/or penetrance of vertebral defects in families with a clear genetic basis. These are exciting times for clinical genetics and important times for individuals with congenital malformation and their families.

---

the signal-sending cell. (f) The membrane anchored Notch1 extracellular truncation (*EXT*) may undergo ubiquitylation (*Ub*) facilitating endocytosis. (g) *Notch1 EXT* undergoes S3-cleavage in the transmembrane domain. This is mediated by the gamma-secretase complex and it releases *Notch1 ICD*. (h) *Notch1 ICD* enters the nucleus and binds the DNA-binding protein CSL/Rbpj, and this triggers the release of corepressor (*CoR*) proteins and histone deacetylases, and facilitates the binding of Mastermind and coactivators (*CoA*) such as histone acetylases, which facilitate transcription of target genes such as *Lfng*, *Mesp2*, *Hes7* and *Tbx6*. Notch signalling components and targets mutated in human cases of vertebral malformation are indicated in green lettering. (Figure and legend adapted from [17] with permission from Elsevier)

## References

1. Alexander PG, Tuan RS. Role of environmental factors in axial skeletal dysmorphogenesis. *Birth Defects Res C Embryo Today*. 2010;90:118–32.
2. Andersson O, Bertolino P, Ibanez CF. Distinct and cooperative roles of mammalian Vg1 homologs GDF1 and GDF3 during early embryonic development. *Dev Biol*. 2007;311:500–11.
3. Asai-Coakwell M, French CR, Ye M, Garcha K, Bigot K, Perera AG, et al. Incomplete penetrance and phenotypic variability characterize Gdf6-attributable oculo-skeletal phenotypes. *Hum Mol Genet*. 2009;18:1110–21.
4. Berdon WE, Lampl BS, Cornier AS, Ramirez N, Turnpenny PD, Vitale MG, et al. Clinical and radiological distinction between spondylothoracic dysostosis (Lavy-Moseley syndrome) and spondylocostal dysostosis (Jarcho-Levin syndrome). *Pediatr Radiol*. 2011;41:384–8.
5. Bessho Y, Sakata R, Komatsu S, Shiota K, Yamada S, Kageyama R. Dynamic expression and essential functions of Hes7 in somite segmentation. *Genes Dev*. 2001;15:2642–7.
6. Bonafe L, Giunta C, Gassner M, Steinmann B, Superti-Furga A. A cluster of autosomal recessive spondylocostal dysostosis caused by three newly identified DLL3 mutations segregating in a small village. *Clin Genet*. 2003;64:28–35.
7. Bulman MP, Kusumi K, Frayling TM, McKeown C, Garrett C, Lander ES, et al. Mutations in the human delta homologue, DLL3, cause axial skeletal defects in spondylocostal dysostosis. *Nat Genet*. 2000;24:438–41.
8. Cetinkaya M, Ozkan H, Koksall N, Yazici Z, Yalcinkaya U. Spondylocostal dysostosis associated with diaphragmatic hernia and neural tube defects. *Clin Dysmorphol*. 2008;17:151–4.
9. Chapman DL, Papaioannou VE. Three neural tubes in mouse embryos with mutations in the T-box gene Tbx6. *Nature*. 1998;391:695–7.
10. Chen C, Ware SM, Sato A, Houston-Hawkins DE, Habas R, Matzuk MM, et al. The Vg1-related protein Gdf3 acts in a Nodal signaling pathway in the pre-gastrulation mouse embryo. *Development* 2006;133:319–29.
11. Christ B, Huang R, Scaal M. Amniote somite derivatives. *Dev Dyn*. 2007;236:2382–96.
12. Clarke RA, Singh S, McKenzie H, Kearsley JH, Yip MY. Familial Klippel-Feil syndrome and paracentric inversion inv(8)(q22.2q23.3). *Am J Hum Genet*. 1995;57:1364–70.
13. Cogulu O, Gunduz C, Karaca E, Onay H, Superti-Furga A, Ozkinay F. Duane anomaly, meningomyelocele, dextroposition of heart and localized vertebrocostal alterations with associated anomalies in a girl. *Genet Couns*. 2007;18:77–83.
14. Cornier AS, Staehling-Hampton K, Delventhal KM, Saga Y, Caubet JF, Sasaki N, et al. Mutations in the MESP2 gene cause spondylothoracic dysostosis/Jarcho-Levin syndrome. *Am J Hum Genet*. 2008;82:1334–41.
15. Correa A, Gilboa SM, Besser LM, Botto LD, Moore CA, Hobbs CA, et al. Diabetes mellitus and birth defects. *Am J Obstet Gynecol*. 2008;199:237 e1–9.
16. den Hollander AI, Biyanwila J, Kovach P, Bardakjian T, Traboulsi EI, Ragge NK, et al. Genetic defects of GDF6 in the zebrafish out of sight mutant and in human eye developmental anomalies. *BMC Genet*. 2010;11:102.
17. Dunwoodie SL. The role of Notch in patterning the human vertebral column. *Curr Opin Genet Dev*. 2009;19:329–37.
18. Dunwoodie SL, Henrique D, Harrison SM, Beddington RS. Mouse Dll3: a novel divergent Delta gene which may complement the function of other Delta homologues during early pattern formation in the mouse embryo. *Development*. 1997;124:3065–76.
19. Dunwoodie SL, Clements M, Sparrow DB, Sa X, Conlon RA, Beddington RS. Axial skeletal defects caused by mutation in the spondylocostal dysplasia/pudgy gene Dll3 are associated with disruption of the segmentation clock within the presomitic mesoderm. *Development*. 2002;129:1795–806.
20. Evrard YA, Lun Y, Aulehla A, Gan L, Johnson RL. Lunatic fringe is an essential mediator of somite segmentation and patterning. *Nature*. 1998;394:377–81.

21. Ferrari A, Ferrara C, Balugani M, Sassi S. Severe scoliosis in neurodevelopmental disabilities: clinical signs and therapeutic proposals. *Eur J Phys Rehabil Med.* 2010;46:563–80.
22. Geoffroy Saint Hilaire E. Différents états de pesanteur des oeufs au commencement et a la fin de l'incubation. *J Complement des Sci Medicales.* 1820;7:271.
23. Giacoia GP, Say B. Spondylocostal dysplasia and neural tube defects. *J Med Genet.* 1991;28:51–3.
24. Gucev ZS, Tasic V, Pop-Jordanova N, Sparrow DB, Dunwoodie SL, Ellard S, et al. Autosomal dominant spondylocostal dysostosis in three generations of a Macedonian family: negative mutation analysis of DLL3, MESP2, HES7, and LFNG. *Am J Med Genet A.* 2010;152A:1378–82.
25. Hackshaw A, Rodeck C, Boniface S. Maternal smoking in pregnancy and birth defects: a systematic review based on 173 687 malformed cases and 11.7 million controls. *Hum Reprod Update.* 2011;17:589–604.
26. Hanel ML, Hensey C. Eye and neural defects associated with loss of GDF6. *BMC Dev Biol.* 2006;6:43.
27. Hesemann J, Lauer E, Ziska S, Noonan K, Nemeth B, Scott-Schwoerer J, et al. Analysis of maternal risk factors associated with congenital vertebral malformations. *Spine (Phila Pa 1976).* 2013;38:E293–8.
28. Hutter D, Kingdom J, Jaeggi E. Causes and mechanisms of intrauterine hypoxia and its impact on the fetal cardiovascular system: a review. *Int J Pediatr.* 2010;2010:401323.
29. Ingalls TH, Curley FJ, Prindle RA. Experimental production of congenital anomalies; timing and degree of anoxia as factors causing fetal deaths and congenital anomalies in the mouse. *N Engl J Med.* 1952;247:758–68.
30. Jarcho S, Levin PM. Hereditary malformation of the vertebral bodies. *Bull Johns Hopkins Hosp.* 1938;62:216–26.
31. Kaspiris A, Grivas TB, Weiss HR. Congenital scoliosis in monozygotic twins: case report and review of possible factors contributing to its development. *Scoliosis.* 2008;3:17.
32. Kraut N, Snider L, Chen CM, Tapscott SJ, Groudine M. Requirement of the mouse *I-mfa* gene for placental development and skeletal patterning. *EMBO J.* 1998;17:6276–88.
33. Kusumi K, Sun ES, Kerrebrock AW, Bronson RT, Chi DC, Bulotsky MS, et al. The mouse pudgy mutation disrupts Delta homologue *Dll3* and initiation of early somite boundaries. *Nat Genet.* 1998;19:274–8.
34. Lander ES, Botstein D. Homozygosity mapping: a way to map human recessive traits with the DNA of inbred children. *Science.* 1987;236:1567–70.
35. Maisenbacher MK, Han JS, O'Brien M L, Tracy MR, Erol B, Schaffer AA, et al. Molecular analysis of congenital scoliosis: a candidate gene approach. *Hum Genet.* 2005;116:416–9.
36. Mankoo BS, Skuntz S, Harrigan I, Grigorieva E, Candia A, Wright CV, et al. The concerted action of *Meox* homeobox genes is required upstream of genetic pathways essential for the formation, patterning and differentiation of somites. *Development.* 2003;130:4655–64.
37. Marks DS, Qaimkhani SA. The natural history of congenital scoliosis and kyphosis. *Spine (Phila Pa 1976).* 2009;34:1751–5.
38. Mohamed JY, Faqieh E, Alsiddiky A, Alshammari MJ, Ibrahim NA, Alkuraya FS. Mutations in *MEOX1*, encoding mesenchyme homeobox 1, cause Klippel-Feil anomaly. *Am J Hum Genet.* 2013;92:157–61.
39. Mortier GR, Lachman RS, Bocian M, Rimoin DL. Multiple vertebral segmentation defects: analysis of 26 new patients and review of the literature. *Am J Med Genet.* 1996;61:310–9.
40. Mortlock DP, Guenther C, Kingsley DM. A general approach for identifying distant regulatory elements applied to the *Gdf6* gene. *Genome Res.* 2003;13:2069–81.
41. Offiah A, Alman B, Cornier AS, Giampietro PF, Tassy O, Wade A, et al. Pilot assessment of a radiologic classification system for segmentation defects of the vertebrae. *Am J Med Genet A.* 2010;152A:1357–71.
42. Pourquie O. Vertebrate segmentation: from cyclic gene networks to scoliosis. *Cell.* 2011;145:650–63.

43. Qiu XS, Zhou S, Jiang H, Ji ML, Ding Q, Lv F, et al. Mutation analysis of MESP2, HES7 and DUSP6 gene exons in patients with congenital scoliosis. *Stud Health Technol Inform.* 2012;176:52–5.
44. Saga Y, Hata N, Koseki H, Taketo MM. *Mesp2*: a novel mouse gene expressed in the presegmented mesoderm and essential for segmentation initiation. *Genes Dev.* 1997;11:1827–39.
45. Settle SH, Jr, Rountree RB, Sinha A, Thacker A, Higgins K, Kingsley DM. Multiple joint and skeletal patterning defects caused by single and double mutations in the mouse *Gdf6* and *Gdf5* genes. *Dev Biol.* 2003;254:116–30.
46. Sharma AK, Phadke SR. Another case of spondylocostal dysplasia and severe anomalies: a diagnostic and counseling dilemma. *Am J Med Genet.* 1994;50:383–4.
47. Shen JJ, Huang L, Li L, Jorgez C, Matzuk MM, Brown CW. Deficiency of growth differentiation factor 3 protects against diet-induced obesity by selectively acting on white adipose. *Mol Endocrinol.* 2009;23:113–23.
48. Skuntz S, Mankoo B, Nguyen MT, Hustert E, Nakayama A, Tournier-Lasserre E, et al. Lack of the mesodermal homeodomain protein MEOX1 disrupts sclerotome polarity and leads to a remodeling of the cranio-cervical joints of the axial skeleton. *Dev Biol.* 2009;332:383–95.
49. Sparrow DB, Clements M, Withington SL, Scott AN, Novotny J, Sillence D, et al. Diverse requirements for Notch signalling in mammals. *Int J Dev Biol.* 2002;46:365–74.
50. Sparrow DB, Chapman G, Wouters MA, Whittock NV, Ellard S, Fatkin D, et al. Mutation of the LUNATIC FRINGE gene in humans causes spondylocostal dysostosis with a severe vertebral phenotype. *Am J Hum Genet.* 2006;78:28–37.
51. Sparrow DB, Guillen-Navarro E, Fatkin D, Dunwoodie SL. Mutation of hairy-and-enhancer-of-split-7 in humans causes spondylocostal dysostosis. *Hum Mol Genet.* 2008;17:3761–6.
52. Sparrow DB, Sillence D, Wouters MA, Turnpenny PD, Dunwoodie SL. Two novel missense mutations in hairy-and-enhancer-of-split-7 in a family with spondylocostal dysostosis. *Eur J Hum Genet.* 2010;18:674–9.
53. Sparrow DB, Chapman G, Dunwoodie SL. The mouse notches up another success: understanding the causes of human vertebral malformation. *Mamm Genome.* 2011;22:362–76.
54. Sparrow DB, Chapman G, Smith AJ, Mattar MZ, Major JA, O'Reilly VC, et al. A mechanism for gene-environment interaction in the etiology of congenital scoliosis. *Cell.* 2012;149:295–306.
55. Sparrow DB, Faqeih EA, Sallout B, Alswaid A, Ababneh F, Al-Sayed M, et al. Mutation of HES7 in a large extended family with spondylocostal dysostosis and dextrocardia with situs inversus. *Am J Med Genet A.* 2013a;161A:2244–9.
56. Sparrow DB, McInerney-Leo A, Gucev ZS, Gardiner B, Marshall M, Leo PJ, et al. Autosomal dominant spondylocostal dysostosis is caused by mutation in TBX6. *Hum Mol Genet.* 2013b;22:1625–31.
57. Tassabehji M, Fang ZM, Hilton EN, McGaughran J, Zhao Z, de Bock CE, et al. Mutations in GDF6 are associated with vertebral segmentation defects in Klippel-Feil syndrome. *Hum Mutat.* 2008;29:1017–27.
58. Tracy MR, Dormans JP, Kusumi K. Klippel-Feil syndrome: clinical features and current understanding of etiology. *Clin Orthop Relat Res.* 2004;424:183–90.
59. Turnpenny PD, Bulman MP, Frayling TM, Abu-Nasra TK, Garrett C, Hattersley AT, et al. A gene for autosomal recessive spondylocostal dysostosis maps to 19q13.1-q13.3. *Am J Hum Genet.* 1999;65:175–82.
60. Turnpenny PD, Whittock N, Duncan J, Dunwoodie S, Kusumi K, Ellard S. Novel mutations in DLL3, a somitogenesis gene encoding a ligand for the Notch signalling pathway, cause a consistent pattern of abnormal vertebral segmentation in spondylocostal dysostosis. *J Med Genet.* 2003;40:333–9.
61. Turnpenny PD, Alman B, Cornier AS, Giampietro PF, Offiah A, Tassy O, et al. Abnormal vertebral segmentation and the notch signaling pathway in man. *Dev Dyn.* 2007;236:1456–74.

62. Turnpenny PD, Young E, Scoliosis IICfVAa. Spondylocostal dysostosis, autosomal recessive. In: Pagon RA, Bird T, Dolan CR, et al., editors. *Gene reviews*. (2010/03/20 (ed.)). Seattle: University of Washington; 1993-2014.
63. Wang KS, Zahn LE, Favor J, Huang KM, Stambolian D. Genetic and phenotypic analysis of *Tcm*, a mutation affecting early eye development. *Mamm Genome*. 2005;16:332–43.
64. Watabe-Rudolph M, Schlautmann N, Papaioannou VE, Gossler A. The mouse rib-vertebrae mutation is a hypomorphic *Tbx6* allele. *Mech Dev*. 2002;119:251–6.
65. White PH, Farkas DR, McFadden EE, Chapman DL. Defective somite patterning in mouse embryos with reduced levels of *Tbx6*. *Development*. 2003;130:1681–90.
66. Whittock NV, Sparrow DB, Wouters MA, Sillence D, Ellard S, Dunwoodie SL, et al. Mutated *MESP2* causes spondylocostal dysostosis in humans. *Am J Hum Genet*. 2004;74:1249–54.
67. Winnier GE, Hargett L, Hogan BL. The winged helix transcription factor *MFH1* is required for proliferation and patterning of paraxial mesoderm in the mouse embryo. *Genes Dev*. 1997;11:926–40.
68. Ye M, Berry-Wynne KM, Asai-Coakwell M, Sundaresan P, Footz T, French CR, et al. Mutation of the bone morphogenetic protein *GDF3* causes ocular and skeletal anomalies. *Hum Mol Genet*. 2010;19:287–98.
69. Zhang N, Gridley T. Defects in somite formation in lunatic fringe-deficient mice. *Nature*. 1998;394:374–7.

# Chapter 9

## Somatic Mutations in Overgrowth Syndromes

Jonathan J. Rios and Marybeth Ezaki

**Abstract** Human overgrowth syndromes are varied in their presentation and severity among patients. The etiology of these syndromes has long been associated with genetic phenomena associated with increased paternal or maternal age. Next generation genomic methods have expedited discovery of non-heritable mutations that cause overgrowth syndromes. Many of these somatic, tissue-specific mutations activate cancer-associated cell signaling pathways, leading to aberrant cell growth. Interestingly, although the different disorders have widely varied presentations—heretofore considered distinct syndromes—the genetic etiologies converge on similar mechanisms, which raises questions as to the proper classification and nomenclature of the different diagnoses. This chapter reviews multiple overgrowth syndromes and provides an in-depth explanation of the genetic mechanisms causing their varied presentations.

**Keywords** Somatic · Mosaic · Overgrowth · De novo · PIK3CA

### Introduction

We humans have always been intensely interested in variations in morphology of our species. Symmetry in form and size of the human body informs most of our daily lives from the sizes of our shoes to the manner in which we most readily access computer keyboards. While we celebrate the successes of athletes and beauty queens who have overcome the challenges of being born with less than fully formed limbs, we are less likely to embrace the beauty or accomplishments of a person who has an overgrowth of a limb. There is something frightening about uncontrolled

---

J. J. Rios (✉)

Sarah M. and Charles E. Seay Center for Musculoskeletal Research,  
Texas Scottish Rite Hospital for Children, 2222 Welborn Street, Dallas, TX 75219, USA  
e-mail: Jonathan.Rios@tsrh.org

M. Ezaki

Department of Orthopaedics, Texas Scottish Rite Hospital for Children,  
2222 Welborn Street, Dallas, TX 75219, USA  
e-mail: Marybeth.Ezaki@tsrh.org

© Springer Science+Business Media New York 2015

C. A. Wise, J. J. Rios (eds.), *Molecular Genetics of Pediatric Orthopaedic Disorders*,  
DOI 10.1007/978-1-4939-2169-0\_9

growth. Overgrowth conditions have long been recognized and considered mysterious, concerning both causation and treatment options.

Accounts imparting the mysticism of overgrowth syndromes can be observed throughout Western culture. The New York Academy of Medicine's "Foundations: The Monstrous in Antiquity and the Middle Ages" reviews the ancient fascination with human malformation [1]. Natural and supernatural explanations for rare conditions have been debated for centuries. The birth of such "monsters" was propagandized as a harbinger of evil and imminent destruction of a conflicting belief system. During recent centuries these individuals were often relegated to circuses and freak shows. The 1932 film *Freaks*, directed and produced by Tod Browning, is a voyeuristic peek into the lives of carnival performers [2]. While it was intended to be a horror show, the depiction of the mundane, back-stage life of these differently formed people elicited sympathy and transformed the "normal" people into the monsters for exploiting the "freaks." Another review of society's perspective of human variation is illustrated in LeRoi's *Mutants*, a sensitive discussion of attitudes toward, and their effects on, involved individuals [3]. These perspectives prove that society has only a limited understanding of how and why these conditions arise.

As scientists, our curiosity about these natural occurrences, combined with a propensity for natural (rather than supernatural) explanations, has fueled our search for the scientific understanding of human anomalies. Clues into the causes of a number of conditions have been recognized, but only recently has the convergence of disciplines given us the key to fully understand, and potentially treat, certain human diseases. In this chapter, we focus specifically on newly-elucidated genetic mechanisms causing orthopedic-related overgrowth syndromes.

## The Basics of Human Genetics

The human genome is diploid in nature, meaning every cell has two copies of the genome. Each copy of an individual's genome is inherited from his or her parents, one copy from the mother and one copy from the father. Thus, mutations in genes are passed from parent to child. The same is true for cells undergoing normal cell division; the genome of a cell is replicated and split evenly so the daughter cell receives the same genetic information as its parent cell. However, for many reasons, both genetic and environmental, this is an imperfect process. The human genome is dynamic and is therefore capable of spontaneously developing mutations.

*De novo* mutations are mutations in a person's genome that are not inherited from either parent; they occur for the first time in the individual's genome due to intrinsic (errors in DNA replication) or extrinsic (environmental influences, such as smoking) factors. In part, the consequence of pathogenic *de novo* mutations depends on the timing at which the mutation occurs (Fig. 9.1). *De novo* mutations may arise in the sperm or egg cells prior to fertilization or they may occur any time after birth. They may be present in every cell in a child or the child may be mosaic, where some cells carry the mutation while other cells do not. Additionally, *de novo* mutations may be benign with no effect on human health or survival, while others may cause disease.

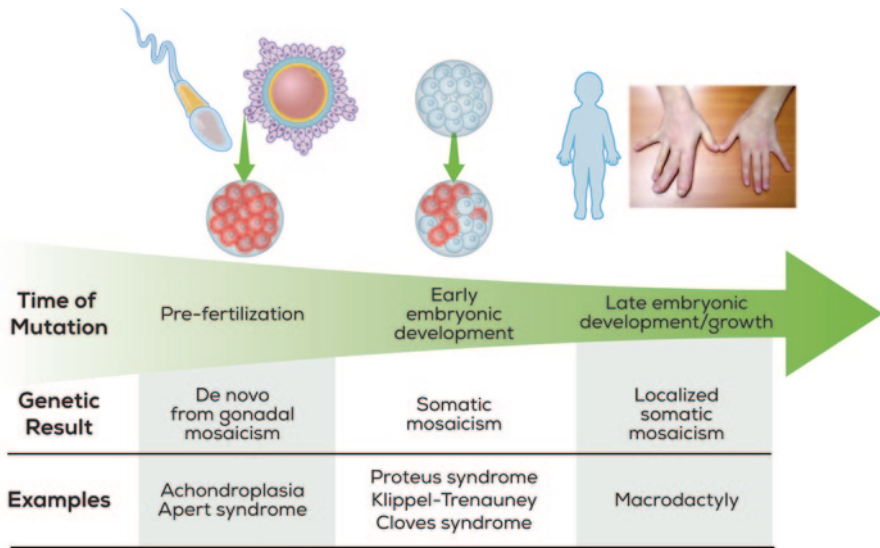


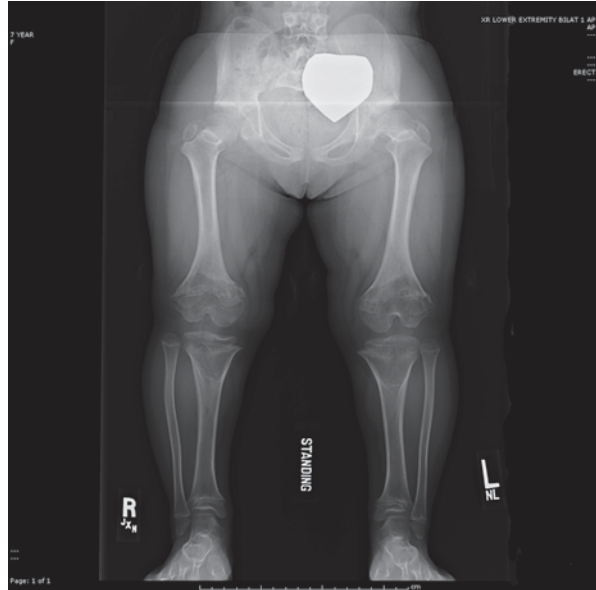
**Fig. 9.1** Timing and Genetic Consequence of *de novo* Mutations. *De novo* mutation may occur at any time during embryonic development, ranging from prior to fertilization to after birth. Mutations occurring prior to fertilization result in parental gonadal mosaicism; every cell in the developing embryo will contain the mutation (shown with red color). Mutations occurring during early embryonic development will result in somatic mosaicism in the developing embryo. The timing of the *de novo* mutation will, in part, dictate the extent to which the mutation occurs in the embryo/child. Examples for each are shown below

### Timing of *De Novo* Mutations

As noted, *de novo* mutations may occur randomly and their timing affects development in the child (Fig. 9.1). In general, every cell in a person’s body carries the identical genetic content. However, the term *genetic mosaicism* describes the accumulation of *de novo* mutations resulting in different cells carrying a slightly different genetic content (ie. one cell carries *de novo* mutations while other cells do not) [4]. *Gonadal mosaicism* occurs when the germ cells (sperm and egg cells) contain *de novo* mutations prior to fertilization. When a sperm cell contains a *de novo* mutation, it is genetically different from all other cells, a phenomenon commonly associated with advanced paternal age. If this sperm cell fertilizes an egg, every cell of the offspring will contain that same mutation. These mutations are easily identified during genetic analysis, as they are present in blood samples from the child but not from either parent.

If *de novo* mutations occur after fertilization, either during embryonic development or after birth, the child will be mosaic (also called *somatic mosaicism*). In this scenario, the child (not the parent) is mosaic. As cells divide, cells with the *de novo* mutation give rise to mutated cells, while the other cells are normal. Ultimately, the proportion of mutant cells in the child is determined, in part, by the timing of the original mutational event. Events during early embryonic development will yield

**Fig. 9.2** Achondroplasia. Lower limb length is 15 in (37.6 cm) in this 8 year-old child. Note the abnormal joint shape and growth plates



more cells in the patient that carry the mutation, while mutations that occur later in development or even after birth will result in fewer mutant cells that may be localized to a particular tissue, organ, or structure. For example, cancers arise from somatic mutations occurring after birth and are often localized to a particular tissue or organ [5, 6]. Genetic analyses that compare DNA from ‘affected’ and ‘normal’ tissues are required to identify these somatic mosaic *de novo* mutations.

## De Novo Mutations in Orthopaedic Disorders

Mutations associated with paternal age effects are thought to arise due to replication errors during spermatogenesis. During this process, male germ cells continuously divide, and as the number of DNA replications increases, so does the risk of error and *de novo* mutation. Achondroplasia is one of several hallmark disorders described as having a paternal age effect; Wilhelm Weinberg in 1912 first described an increased incidence of achondroplasia among ‘last-born’ children. As observed in 1912, and again later by Lionel Penrose in 1955, the incidence of achondroplasia increases with paternal age but in an accelerated, non-linear rate [7]. Achondroplasia (Fig. 9.2) is a form of disproportionate short-limb dwarfism caused by an abnormal three-dimensional configuration of the receptor for fibroblast growth factor 3 (*FGFR3*) [8–10]. Achondroplasia is caused most frequently by a spontaneous missense mutation (G380R) in the protein’s transmembrane domain that is subsequently transmitted in an autosomal dominant pattern [8–10]. In addition to

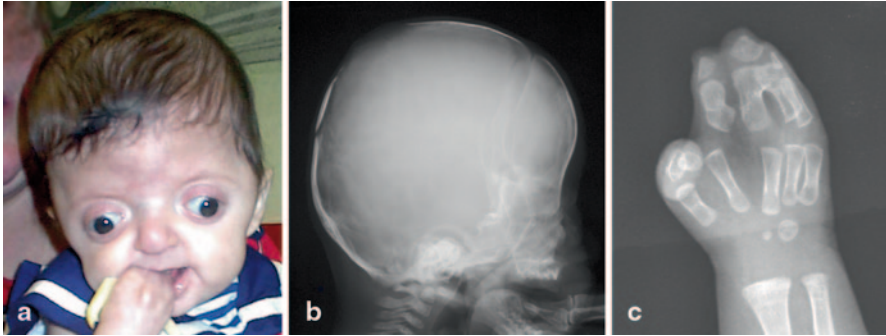


**Fig. 9.3** Child with apert syndrome. Children with apert syndrome have abnormal development of the face (a), skull (b) and hands (c)

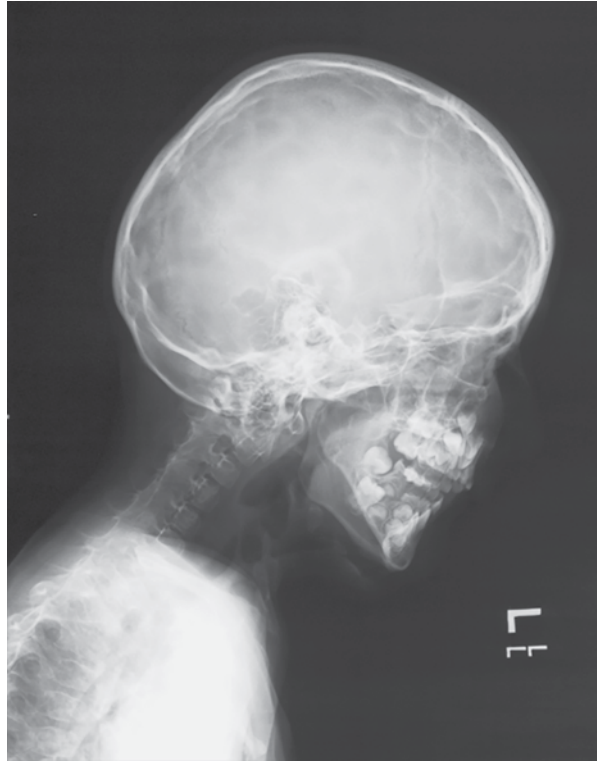
achondroplasia, other skeletal syndromes associated with advanced paternal age include craniofacial and skeletal dysplasias such as Apert syndrome (Fig. 9.3), Crouzon syndrome, Pfeiffer syndrome, and thanatophoric dwarfism [7]. All of these syndromes result from dominant missense mutations in *FGFR* genes [11]. Unlike advanced maternal age, known to be associated with chromosomal changes such as copy number variations or aneuploidy (trisomy 21 causing Down's Syndrome) [12], advanced paternal age is associated with sequence mutations [13].

It is worth noting that not all sporadic disorders are associated with age effects. *Krakov et al.* hypothesized that mutations in the *TRPV4* gene, which is known to cause autosomal dominant brachyolmia (ADB), may also cause spondylometaphyseal dysplasia Kozlowski type (SMDK) [14]; both disorders present with abnormal vertebral body development. After sequencing the gene in five sporadic patients, they identified a missense mutation (R594H) in four patients; this mutation was confirmed to be *de novo* in two patients. The final sporadic patient had a different *de novo* mutation (A716S). In another example, gene sequencing of sporadic patients with fibrodysplasia ossificans progressiva (FOP) (Fig. 9.4) identified a *de novo* missense mutation (R206H) in the *ACVRI* gene in a young patient [15]. The *ACVRI* gene was initially identified using genome-wide linkage analysis in multiple families with dominant inherited FOP [16]. In this study, the authors identified the R206H mutation inherited among all patients in seven families as well as in 32 patients with sporadic FOP.

## Mosaic Mutations

As noted, mutations that occur after fertilization, during early embryonic development, yield a pattern of somatic mosaicism. Thus, some cells in a patient may carry the mutation while other cells do not. Therefore, the disease is not systemic, but only occurs among the "affected" cells of the patient. The extent of the disease

**Fig. 9.4** Fibrodysplasia Ossificans Progressiva. Lateral skull and neck showing complete fusion of the posterior elements of the spine as well as characteristic soft tissue ossification in the anterior neck



is determined, in part, by the fraction of mutated cells expressing the mutant protein; consequently, the extent of mosaicism is expected to lead to great variability between patients. Mosaic mutations are best diagnosed using DNA from biopsies of affected tissue, and mosaic mutations are known to cause several disorders treated in orthopaedic clinics.

McCune Albright syndrome presents as a clinical association of fibrous dysplasia, precocious puberty and café-au-lait spots. It is caused by a somatic mutation in a critical enzyme that decreases GTPase activity and results in over production of cAMP. In turn, this increases proliferation of the involved cells, especially bone marrow stroma. Malignant degeneration has been reported but is not considered a high risk for this disease. This condition would be lethal if it were systemic (inherited) but is maintained as a disease because of its somatic mosaicism [17, 18].

Recently, the genetic cause of Ollier disease and Maffucci syndrome was identified. Both conditions are sporadic and present with multiple cartilaginous tumors during childhood; the skeletal severity depends on the extent and location of tumor formation (Fig. 9.5). When the enchondromatosis is associated with deep vascular lesions the condition is called Maffucci syndrome. Ollier's and Maffucci's diseases are known to be asymmetric in presentation and at times present with hemimelic involvement. Neither of these is transmitted genetically in a Mendelian fashion but

**Fig. 9.5** Ollier Disease.  
Radiograph of the hand of a  
patient with Ollier disease



both are known to involve dysregulation of normal enchondral ossification, which may result in malignant degeneration (Fig. 9.6). Maffucci recognized that some of his patients went on to develop cancers in the enchondromatous lesions that had been slowly growing since childhood [19]. As well, the extent of the affected bones varies between patients; ranging from single to several affected bones [20]. Based on their prior association with cartilaginous tumors, two isocitrate dehydrogenase genes (*IDH1* and *IDH2*) were sequenced in multiple lesions from many patients [21]. Nearly all the lesions harbored mutations in one of the two genes. Additionally, identical mutations were identified among multiple tumors from the same patient, suggesting the mutations were mosaic in the patient. The somatic mosaicism of mutations in these genes explains the wide phenotypic spectrum of the disease [21].

Similar to Ollier and Maffucci's syndrome, Proteus syndrome is another very rare sporadic disorder. Patients present with overgrowth affecting multiple body regions and various orthopaedic abnormalities. *Zhou et al.* wrote in 2001 that they suspected a mutation in the PTEN pathway to explain Proteus syndrome (PTEN negatively regulates the PI3K/AKT/MTOR pathway described below) [22]. They had identified genomic mutations in this pathway for other overgrowth and hamartoma syndromes such as Cowden and Bannayan-Riley-Ruvalcaba syndrome, which



**Fig. 9.6** Maffucci syndrome. Malignant degeneration of an enchondromatous/angioma in the **a** proximal tibia and **b** hands in an 8 year-old with Maffucci syndrome. Histology showed angiosarcoma

are hereditary [22]. SOLAMON (segmental overgrowth, lipomatosis, arteriovenous malformation and epidermal nevus) syndrome, another overgrowth condition, is also known to be associated with mutations in the PTEN pathway [23]. Whole-exome sequencing (WES) was performed using DNA extracted from “affected” overgrowth lesions from multiple patients and compared to DNA from blood (considered “normal”). This comparative analysis identified a somatic mutation in the *AKT1* gene that was specific to overgrowth tissue. Furthermore, *AKT1* mutations were identified in multiple patients [24].

The mosaic *AKT1* mutation in Proteus syndrome results in a gain-of-function effect, similar to the *de novo* mutations in the FGFR proteins associated with paternal age effects (described above). The Proteus mutation results in dysregulated activation of the AKT1 protein and upregulation of the PI3K/AKT/MTOR pathway. This pathway is well characterized for its involvement in various cancers and is associated with other overgrowth syndromes such as CLOVES (congenital, lipomatous overgrowth, vascular malformations, epidermal nevi and skeletal anomalies), fibroadipose hyperplasia and hemimegalencephaly [25–27].

Not all mosaic disease-causing mutations result in a gain-of-function effect. Neurofibromatosis type 1 (NF1) is caused by loss-of-function mutations that disrupt the *NF1* gene. Neurofibromin, the protein encoded by the *NF1* gene, is a negative regulator of cell signaling; thus, loss of neurofibromin causes an increase in cell signaling. NF1 is a relatively common disorder caused either by *de novo* mutations in sporadic cases or inherited from affected parents. However, NF1 is also caused by mosaic mutations, which result in a distinct “segmental” NF1 phenotype. In one patient with segmental NF1, extensive freckling and café-au-lait spots were localized to one side of the patient’s body with distinct borders. Only one copy of the *NF1* gene was present in a skin biopsy of one of the café-au-lait spots, but the normal two copies of the gene were present in samples from blood cells and a skin biopsy

**Fig. 9.7** Neurofibromatosis plexiform neurofibroma. Upper arm of a Neurofibromatosis patient with plexiform neurofibroma underlying skin changes



from an unaffected area of the same patient [28]. Thus, this patient was mosaic for the mutation, which manifested as a distinctly different (segmented) phenotypic presentation, compared to other NF1 patients with sporadic or inherited NF1. NF1 is also associated with both limb overgrowth and tumor formation (Fig. 9.7). Malignant degeneration is a known risk of this disease. The phenotypic variability in this disease spectrum has been attributed to the extent of DNA mutation [29]; the clinical spectrum of NF1 includes lesions in multiple organ systems. Central nervous system involvement, intracranial lesions, congenital pseudarthroses of long bones and limb overgrowth make surveillance for malignant degeneration worrisome.

## Somatic Mutations

Unlike mosaic mutations that may be widely distributed throughout the body, somatic *de novo* mutations generally present as single-site focal disorders rather than as multi-site disorders, such as Proteus syndrome. Recently, the genetic causes of several overgrowth syndromes have been elucidated using WES [24–27, 30, 31]. As with mosaic disorders, conclusive genetic analyses of somatic disorders require DNA tests of affected tissues. Interestingly, these studies revealed gain-of-function mutations in the same cancer-associated cell-signaling pathway as Proteus syndrome.

Although not an orthopaedic condition, a recent study of hemimegalencephaly nicely illustrated the power of WES to identify somatic *de novo* mutations [26]. Patients with hemimegalencephaly present with overgrowth of a single cerebral hemisphere; treatment involves surgical removal of diseased tissue. In this study, WES of affected brain tissue was compared to WES of blood DNA. Somatic *de novo* mutations were identified in multiple patients; all mutations were in genes involved in the PI3K/AKT/MTOR pathway, the same as with Proteus syndrome. As with mosaic mutation disorders, which require a biopsy of affected tissue, the number of “diseased” cells present in the biopsy determines the ability of genetic analyses, e.g. WES, to identify the disease-causing mutation. Ideally, the biopsy should contain a majority of, if not entirely comprising, diseased tissue such that the proportion of

**Fig. 9.8** Isolated macrodactyly. Image of the hand of a patient with localized Type 1 Macrodactyly. Overgrowth involves the thumb, index and middle fingers



affected cells is very high. In this study, multiple anatomic sites were tested within the patients. Biopsies of different sites of the affected brain tissue showed the wide variability in the fraction of cells of the biopsy carrying the mutation [26].

Isolated, or Type I, macrodactyly is a localized overgrowth of a finger, toe or a multiple digit distribution of a limb. Part of the pathologic anatomy is an enlarged peripheral nerve, and the manifestations are described as “nerve territory oriented.” The median nerve is most often involved, with gross findings including circumferential enlargement as well as elongation of the nerve (Fig. 9.8). Histologic findings are consistent with fibrofatty infiltration between the axonal bundles, thickening of the perineurial layers, and extensive adipose proliferation around and within the nerve. Special stains indicate that all tissues express abnormal markers for nerve proliferation [34, 35]. Because of the isolated nature of the overgrowth, WES was used to identify somatic *de novo* mutations present in the affected nerve tissue that were not present in WES from blood DNA [30]. The exome sequence of a single patient identified a *de novo* somatic mutation in the *PIK3CA* (PI3K) gene. Known gain-of-function activating mutations were subsequently identified in *PIK3CA* in additional patients with Type 1 macrodactyly. Additionally, analysis of cultured cells from the nerve of one macrodactyly patient confirmed, as in other localized overgrowth syndromes, the PI3K/AKT/MTOR pathway was activated [30].

## Summary

Whole-genome molecular genomics is a new science. It has been a very short journey from Gregor Mendel’s experiments with peas, to the discovery of chromosomes in 1959, to the present-day ability to literally unravel and read the base pair sequences that encode all of life. Two decades ago, genetic testing meant assessing chromosomes and, perhaps, counseling for risk of conditions known to have Men-

**Fig. 9.9** Vascular overgrowth. Enlarged upper arm and hand in a child with vascular component to the overgrowth



delian transmission patterns. Now, powerful advances in DNA analysis allow side-by-side genome-wide sequencing of DNA or RNA from affected and unaffected tissues. However, reading base pairs is only the beginning of genetic literacy as it applies to our patients. The majority of the human genome does not contain genes, and the function of these regions (e.g. gene regulation) are only now beginning to be understood [32]. Corresponding to each gene is a protein that plays a role in a cascade of cellular activity. Consequently, biology is non-linear and each transcribed substance likely fits into a tight cycle that is simultaneously regulating and being regulated.

Growth is modulated through pathways that control cell cycle and proliferation. Advances in tumor genetics opened the door to discovering mutations in conditions with abnormal growth of a tissue. Comparing overgrowth syndromes to tumors was an intuitive next step in the search for causality. In 1891, Humphry presciently compared macrodactyly to a tumour, noting that the cause was likely local and dependent upon:

an excess, a want of due restraint, of that developmental force by which the several organs and structures acquire and maintain their proper dimensions and relations to one another, and by which their relative growth at different periods of life and under different circumstances is determined. [33]

An important concept is that the precise timing, tissue affected, and location within the body at which a mutation occurs can explain the pleomorphism of overgrowth syndromes. A somatic mutation that occurs in a perineural location during the embryogenesis of a finger or toe will appear very different from one that occurs in pluripotential mesoderm at the onset of limb differentiation.

Genome sequencing of affected and constitutional DNA can identify even the most subtle differences in DNA base pairs. The resultant change in the protein can alter downstream function. If this occurs in a critical pathway, especially one that regulates cell proliferation, dysregulation of normal growth can result.

Overlap between the vascular malformations (Fig. 9.9) and an overgrowth syndrome makes the eponymous nomenclature of the past confusing. Clarification will likely be made on a genetic basis, but both the involved tissues/limbs and the extent of overgrowth will determine treatment [34]. The PI3K/AKT/MTOR pathway is commonly shared with many of these overgrowth conditions. Finally, it is worth

noting that the elucidation of molecular pathways involved gives hope that targeted medical treatments—as with rapamycin, for example—may effectively decelerate overgrowth, if not completely control it.

## References

1. <http://www.nyam.org/library/rare-book-room/exhibits/telling-of-wonders/>.
2. Browning T. Freaks. 1932.
3. LeRoi AM. Mutants. New York: Viking Penguin; 2003.
4. Biesecker LG, Spinner NB. A genomic view of mosaicism and human disease. *Nat Rev Genet.* 2013;14(5):307–20.
5. Sjoblom T, Jones S, Wood LD, Parsons DW, Lin J, Barber TD, Mandelker D, Leary RJ, Ptak J, Silliman N, et al. The consensus coding sequences of human breast and colorectal cancers. *Science.* 2006, 314(5797):268–74.
6. Wood LD, Parsons DW, Jones S, Lin J, Sjoblom T, Leary RJ, Shen D, Boca SM, Barber T, Ptak J, et al. The genomic landscapes of human breast and colorectal cancers. *Science.* 2007, 318(5853):1108–13.
7. Risch N, Reich EW, Wishnick MM, McCarthy JG. Spontaneous mutation and parental age in humans. *Am J Hum Genet.* 1987;41(2):218–48.
8. Shiang R, Thompson LM, Zhu YZ, Church DM, Fielder TJ, Bocian M, Winokur ST, Was-muth JJ. Mutations in the transmembrane domain of FGFR3 cause the most common genetic form of dwarfism, achondroplasia. *Cell.* 1994;78(2):335–42.
9. Rousseau F, Bonaventure J, Legeai-Mallet L, Pelet A, Rozet JM, Maroteaux P, Le Merrer M, Munnich A. Mutations in the gene encoding fibroblast growth factor receptor-3 in achondroplasia. *Nature.* 1994;371(6494):252–4.
10. Bellus GA, Hefferon TW, Ortiz de Luna RI, Hecht JT, Horton WA, Machado M, Kaitila I, McIntosh I, Francomano CA. Achondroplasia is defined by recurrent G380R mutations of FGFR3. *Am J Hum Genet.* 1995;56(2):368–73.
11. Muenke M, Schell U. Fibroblast-growth-factor receptor mutations in human skeletal disorders. *Trends Genet.* 1995;11(8):308–13.
12. Hassold T, Abruozzo M, Adkins K, Griffin D, Merrill M, Millie E, Saker D, Shen J, Zaragoza M. Human aneuploidy: incidence, origin, and etiology. *Environ Mol Mutagen.* 1996;28(3):167–75.
13. Crow JF. The origins, patterns and implications of human spontaneous mutation. *Nat Rev Genet.* 2000;1(1):40–7.
14. Krakow D, Vriens J, Camacho N, Luong P, Deixler H, Funari TL, Bacino CA, Irons MB, Holm IA, Sadler L, et al. Mutations in the gene encoding the calcium-permeable ion channel TRPV4 produce spondylometaphyseal dysplasia, Kozlowski type and metatropic dysplasia. *Am J Hum Genet.* 2009;84(3):307–15.
15. Lin GT, Chang HW, Liu CS, Huang PJ, Wang HC, Cheng YM. De novo 617G-A nucleotide mutation in the ACVR1 gene in a Taiwanese patient with fibrodysplasia ossificans progressiva. *J Hum Genet.* 2006;51(12):1083–6.
16. Shore EM, Xu M, Feldman GJ, Fenstermacher DA, Cho TJ, Choi IH, Connor JM, Delai P, Glaser DL, LeMerrer M, et al. A recurrent mutation in the BMP type I receptor ACVR1 causes inherited and sporadic fibrodysplasia ossificans progressiva. *Nat Genet.* 2006;38(5):525–7.
17. Chapurlat RD, Orcel P. Fibrous dysplasia of bone an McCune-ALbright syndrome. *Best Pract Res Clin Rheumatol.* 2008;22(1):55–69.
18. Happle R. The McCune-Albright syndrome: a lethal gene surviving by mosaicism. *Clin Genet.* 1986;29:321–4.

19. Maffucci A. Di un caso di Encondroma ed angioma multiplio. Contribuzione alla genesi embrionale dei tumori. *Mov Med Chir.* 1881;13:399–412.
20. Unni KK. Cartilaginous lesions of bone. *J Orthop Sci.* 2001;6(5):457–72.
21. Amary MF, Damato S, Halai D, Eskandarpour M, Berisha F, Bonar F, McCarthy S, Fantin VR, Straley KS, Lobo S, et al. Ollier disease and Maffucci syndrome are caused by somatic mosaic mutations of IDH1 and IDH2. *Nat Genet.* 2011;43(12):1262–5.
22. Zhou X, Hampel H, Thiele H, et al. Association of germline mutation in the PTEN tumour suppressor gene and proteus and proteus-like syndromes. *Lancet.* 2001;358:210–1.
23. Caux F, Plauchu H, Chibon F, et al. Segmental overgrowth, lipomatosis, arteriovenous malformation and epidermal nevus (SOLAMEN) syndrome is related to mosaic PTEN nullizygosity. *Eur J Hum Genet.* 2007;15:767–73.
24. Lindhurst MJ, Sapp JC, Teer JK, Johnston JJ, Finn EM, Peters K, Turner J, Cannons JL, Bick D, Blakemore L, et al. A mosaic activating mutation in AKT1 associated with the proteus syndrome. *New Engl J Med.* 2011;365(7):611–9.
25. Kurek KC, Luks VL, Ayturk UM, Alomari AI, Fishman SJ, Spencer SA, Mulliken JB, Bowen ME, Yamamoto GL, Kozakewich HP, et al. Somatic mosaic activating mutations in PIK3CA cause CLOVES syndrome. *Am J Hum Genet.* 2012;90(6):1108–15.
26. Lee JH, Huynh M, Silhavy JL, Kim S, Dixon-Salazar T, Heiberg A, Scott E, Bafna V, Hill KJ, Collazo A, et al. De novo somatic mutations in components of the PI3K-AKT3-mTOR pathway cause hemimegalencephaly. *Nat Genet.* 2012;44(8):941–5.
27. Lindhurst MJ, Parker VE, Payne F, Sapp JC, Rudge S, Harris J, Witkowski AM, Zhang Q, Groeneveld MP, Scott CE, et al. Mosaic overgrowth with fibroadipose hyperplasia is caused by somatic activating mutations in PIK3CA. *Nat Genet.* 2012;44(8):928–33.
28. Tinschert S, Naumann I, Stegmann E, Buske A, Kaufmann D, Thiel G, Jenne DE. Segmental neurofibromatosis is caused by somatic mutation of the neurofibromatosis type 1 (NF1) gene. *Eur J Hum Genet.* 2000;8(6):455–9.
29. Pasmant E, Vidaud M, Vidaud D, Wolkenstein P. Neurofibromatosis type 1: from genotype to phenotype. *J Med Genet.* 2012;49(8):483–9.
30. Rios JJ, Paria N, Burns DK, Israel BA, Cornelia R, Wise CA, Ezaki M. Somatic gain-of-function mutations in PIK3CA in patients with macrodactyly. *Hum Mol Genet.* 2013;22(3):444–51.
31. Riviere JB, Mirzaa GM, O’Roak BJ, Beddaoui M, Alcantara D, Conway RL, St-Onge J, Schwartzentruber JA, Gripp KW, Nikkel SM, et al. De novo germline and postzygotic mutations in AKT3, PIK3R2 and PIK3CA cause a spectrum of related megalencephaly syndromes. *Nat Genet.* 2012;44(8):934–40.
32. Bernstein BE, Birney E, Dunham I, Green ED, Gunter C, Snyder M. An integrated encyclopedia of DNA elements in the human genome. *Nature.* 2012;489(7414):57–74.
33. Humphry GM. Macrodactyly, and soem other forms of congenital overgrowth and their relation to tumours. *Trans Poyal Med Chir Soc Lond.* 1891;84:557–67.
34. Keppler-Noreuil K, Rios JJ, Parker VE, Semple RK, Lindhurst MH, Sapp JC, Alomari A, Ezaki M, Dobyns W, Biesecker LG. PIK3CA-related overgrowth spectrum (PROS): Diagnostic and testing eligibility criteria, differential diagnosis, and evaluation. *Am J Med Genet A.* 2015;167(2):287–95.

# Index

## B

Bone, 5, 18, 20–22, 27–34, 58, 60, 63, 66–68, 96

## C

Cartilage, 18–20, 23, 25, 27, 46, 49, 51, 58, 132, 140, 141  
Clubfoot, 41, 48, 92, 93–99  
    genetic epidemiology of, 94  
    idiopathic, 3  
Congenital multiple large joint dislocation, 40  
Congenital scoliosis, 106, 142–144  
Copy number variation (CNV), 1, 3, 5

## D

De novo, 43  
Dentin matrix protein 1 (DMP1), 57–61  
    signaling, 64, 65

## E

Ehlers Danlos syndrome (EDS) arthrochalasia type, 44, 45  
Exome, 122, 147

## F

FGF signaling pathway, 109

## G

Genetics, 108, 112, 134, 147  
Genotyping, 1, 2, 13, 139

## H

Hypophosphatemic rickets, 59, 60, 66

## I

Idiopathic scoliosis, 106

## J

Jarcho-Levin syndrome (JLS), 112, 124, 125  
Joint dislocation, 12, 39, 40, 46, 48, 51  
    congenital, 45, 47, 48, 50

## K

Klippel-Feil syndrome (KFS), 112, 139

## L

Larsen syndrome, 41, 42, 45  
Low bone mass, 20

## M

Microarray, 1, 3, 5  
Muscle, 3, 23, 27, 28, 30, 33–35, 40, 60, 96–99  
    limb, 97

## N

Neurofibromatosis type 1 (NF1), 18, 20, 21, 22, 27, 29–32  
Next-generation genomics, 1, 7  
    sequencing, 1, 7, 122  
Nf1Prx1, 23, 26–31, 33, 34  
Notch signaling pathway, 144

## O

Osteocyte, 61–63  
Overgrowth, 13

## P

Phosphate homeostasis, 61, 66  
PIK3CA, 13  
PITX1, 3, 96, 97, 99  
Proteoglycan synthesis, 46, 48, 49

**S**

Sclerotome, 109, 112, 133, 134  
Scoliosis, 32, 46, 49, 112, 124, 132, 140, 142  
    dystrophic, 32, 33  
    idiopathic, 106  
    non-dystrophic, 32  
Segmentation defects of the vertebrae (SDV),  
    111, 112, 117, 122, 124–126  
Somatic, 13, 18, 22, 42  
Somitogenesis, 108, 109, 117, 132, 139,  
    140, 147  
    cyclical, 112

Spondylocostal dysostosis (SCD), 108, 110,  
    112, 124, 135  
Spondylothoracic dysostosis (STD), 105, 136

**T**

T-box transcription factor 4 (TBX4), 3, 97, 99  
Tibial dysplasia, 22, 27, 30, 32